UNIVERSITY OF NOVA GORICA
GRADUATE SCHOOL

APPLICATION OF MULTIVARIATE STATISTICAL METHODS AND ARTIFICIAL NEURAL NETWORK FOR SEPARATION BEDROCK BACKGROUND AND INFLUENCE OF MINING AND METALLURGY ACTIVITIES ON DISTRIBUTION OF CHEMICAL ELEMENTS IN THE STAVNJA VALLEY (BOSNIA AND HERZEGOVINA)

Jasminka ALIJAGIĆ

Dissertation

Mentor: Dr. Robert Šajn

Nova Gorica, 2013

Vareš 111–41471

TABLE OF CONTENTS

LIST OF TABLES

LIST OF FIGURES

LIST OF APENDICES

1. INTRODUCTION

1.1. The research problem

The Stavnja river valley is known with intensive mining and metallurgical activities for more than 100 years. In municipality of Vareš, three abandoned iron ore deposits (Smreka, Brezik and Droškovec), abandoned lead, zinc and barite deposit Veovača and abandoned ironwork Vareš are located. City Breza is located in the southern part of the study area, known with brown coal mining. Assessment of trace metalsdistribution and contamination has been evaluaed using the total trace metal concentration is soil/sediment samples and attic dust. In order to achieve a spatial distribution of anthropogenic and geogenic elements various predicting modelling techniques have been applied.

Long period of ore mining and processing had left significant consequences on the whole valley. However,the valley had been selected as a study area because of several reasons. High concentrations of particular elements are released into environment not only by anthropogenic activities but also by natural erosion and weathering reactions of parental rocks what contribute to the environmental assessment complexity. The valley has a very interesting geology, which can be represented by isolated lithological units where the oldest are on the north and younger on the south. This regular layout is quite unique and makes this study area more engaging and challenging for the geochemical investigation. Here are essential two types of contamination, atmospherical and river transport, respectively. The valley of river Stavnja is very narrow, surrounded with steep hills and contamination is transported down to the river accumulating into alluvial sediments. Even the atmospheric particles have the direction N–S. Problem of contamination along the river can be demonstrated as anisotropic appearance between the layered (isotropic) lithological units. The problem is quite complicated, and being discussed for the last several decades. Some problems can be solved by using denser and more regular sampling grid, but in this study area is impossible due to the remained minefields. During the last war (1992–1995) the area has been place of intensive military operation, between three major ethnic groups in Bosnia and Herzegovina, making the sampling more difficult and very restricted. According the available maps about 5.7 km^2 or 5.5% of the study area is covered by remain minefields.

Because of study complexity such as the anthropogenic, geogenic, morphological impact as well as sampling restriction due to remained minefields, three various prediction methods of trace element concentrations have been developed. Following three predictive methods have been applied: the Segment Kriging, Polynomial Multiple Regression and Artificial Neural Network - Multilayer Perceptron. The spatial variability of soil trace elements is an important part of environmental supervision and ecosystem evaluation. Kriging has successfully been applied in investigating and mapping of hazardous soil trace elements around the world, but unfortunately in the narrow and long study area with complex geology, such as the Stavnja valley, this classical interpolation method is providing model of prediction with deficiencies so called “Bull eyes effect”. This problem arise mainly from the fact that the classical interpolation methods such as the kriging depends only from the chemical concentrations but not from another (geo) spatial data such as geological background (parental rocks and its chemistry), pedogenic processes, shape of study area, aspect, slope, altitude, climatic conditions, etc. For example the aspect or insolation is directly proportional to the land temperature and inversely proportional to the humidity of area. Important assumption is that contaminant concentrations change with distance and direction from the emission objects primarily influenced by atmospheric processes such as regional and local wind directions, daily temperatures, temperature inversions in lower areas and closed basins. This can be solved by introducing two new parameters: Distance and Azimuth.

Due to high cost and timeconsuming nature of soil sampling, research in developing methods for the creation of soil maps based in various prediction methods is becoming increasingly important. Development of linear and nonlinear predicton methods that use secondary attributes sourced from the DEM, land use, and remote sensing in combination with sparse and expensive soil measurements has been sharpening focus of research. Consequently, the potential for using such information to soil mapping at the within field extent is greater than ever before. Appling various modelling techniques for trace metal distributin in soil have been applied and compared among each other. As well the best combination of prediction method and secondary information has been selected. Each aforementioned applied modelling techniqueby itself helped us in reconstruction simultaneously different processes that influenced the entire study area.

1.2. The goals of doctoral dissertation

- Determination of concentration levels and spatial distribution of chemical elements in secondary materials (such as soil, river sediments and attic dust) along the Stavnja valley,

- Assessment of the natural background according to lithology and the proportion of influence of mining and metallurgy activities on distribution of chemical elements in secondary materials (soil, river sediments and attic dust) along the Stavnja valley,

- Identification of main geochemical associations and their spatial distribution by using multivariate statistical approach,

- To design the various models of trace metal dispersion around the major emitters, using linear and nonlinear predicting methods: Segmental Kriging (SK), Multiple Polynomial Regression (MPR), and Artificial Neural Network – Multilayer Perceptron (ANN-MP),

- Identification of optimal methodology for geochemical research in the area of former military operations (with remain minefields and/or suspected mined areas), according to the sampling material, sampling density, data processing and interpretation of results

2. THEORETICAL BACKGROUND

2.1. Contamination

Contamination is an undesirable change of physical, chemical, or biological feature of natural environment, which is caused by human activities and which is harmful for human beings. Contamination particles infiltrate very easily in soil, water, and atmosphere. There are two types of pollutants: biodegradable pollutants (e.g. organic sewage) and non-biodegradable pollutants (e.g. trace elements, pesticides, thermic contamination, photochemical smog, disposal of nuclear waste, etc).

An area of spot contamination is much more contaminated than areas met with diffuse contamination; anyway, consequences of this kind contamination are only local. Examples of spot contamination are traffic, industrial and energy activity, various dumps and dumps waste materials (Yaron et al., 1996). Contents of trace elements are very high and they decrease with distance (Mattigod and Page, 1983). Example of linear soil contamination is contamination alongside roads and railways. Intensity of contamination depends upon type and density of traffic, while meteorological factors influence scope of contamination in extant (dominant permanent winds) and relief.

The most frequent cause for soil contamination with trace elements is diffuse contamination, where soil is polluted over air, not only locally, but also in larger distance from source of contamination in the surroundings of industrial and urban centres. Trace elements are usually present in the air at low concentration, and they are less dangerous (Yaron et al., 1996). Different emissions of substances to the air in gaseous, liquid, or solid state are transported by the air and fall on the soil surface according to time circumstances, there because of constant contamination accumulate in soil.

2.2. Trace elements in soil

2.2.1. Soil physical, biological and chemical interactions

The soil as a physical, biological, and chemical filter is nature's purifying agent and place where pollutant sinks. However, in soil environments physical, biological, and chemical processes are not independents processes but rather interactive processes. These phrases signify the important role soils play in cleansing our environment of pollutants in terms of our food, surface water, and groundwater resources. There are several dynamic interactive processes, which in turn can be influenced by various biogeochemical factors that govern metal behaviour rendering the predictability of the fate and effects of trace elements in the environment rather cumbersome. These include abiotic and biotic processes and factors in heterogeneous environmental media. Therefore, a background understanding of the various biogeochemical processes, i.e., from the landscape to the molecular level, and relevant factors is in order (Adriano, 1986, 2001; Siegel, 2002).

Soil is product of weathering and may or may not contain organic matter but quite often contain air and water or soil is natural body that contain mineral particles, organic matter, living organisms, water and air, and include physical, chemical, and biological processes (Gerrard, 2000). Chemical weathering of bedrock and soil formation are important geological processes and play a critical role in maintaining terrestrial ecosystems. For example, the conversion of bedrock to soil not only provides habitat for the vast majority of terrestrial organisms, but also supplies nutrients available to primary producers for food production. In addition, chemical weathering acts as a buffer to acidification of catchments caused by acid precipitation at regional scales (Drever and Hurcomb, 1986; Johnson et al., 1981; Huang et al., 2013). In spite of the importance of chemical weathering and soil formation for natural

environment and for sustaining life on earth, our knowledge of many aspects of these processes is still limited. For example, accurate weathering and soil formation rates in natural environment and their quantitative dependences on environmental factors (such as the prevailing acid precipitation) are still poorly understood. However, this kind of information is indispensable for the understanding of the biogeochemical cycling and for the development of sustainable land use strategies. The rates at which weathering and soil formation proceed depend on the environmental factors, such as climate, vegetation, parent material, topography, and soil age. Although numerous studies have been performed to investigate the effect of various environmental factors on chemical weathering rates (White and Blum, 1995; Von Blanckenburg, 2005; Guicharnaud and Paton, 2006; Taylor et al., 2012), much of the literature isolated one predominant factor by assuming that other factors remain constant and did not assess the synergistic effects of several factors functioning together.

2.2.2. Distribution of trace elements in soil

Soils contain trace elements of various origin: lithogenic elements which are directly inherited from the lithosphere, pedogenic elements which are of lithogenic origin, but their concentration and distribution in soil layers and soil particles are changed due to pedogenic processes or anthropogenic elements which are all those deposed into soil as direct or indirect results of man's activities. The behaviour of trace elements in soil and in consequence their bioavailability differs as to their origin. However, regardless of the forms of the anthropogenic trace elements in soil, their phytoavailability is significantly higher than those of pedogenic origin (Kabata-Pendias and Pendias, 2001).

Trace elements are group of elements having specific gravities greater than 5 g/cm^3. To this group belong very toxic such as Pb, Cd, Hg, As and U, which have negative influence on living organisms. Among them, exist also elements that are essential for the organisms such as Cu, Mn, Fe, Zn, Co, Cr, Se, B and Mo (Baudo, 1987). Stumm and Morgan (1996) distinguish atmophile and lithophile trace elements. As, Pb and Cd, which are easier transported by air than by water, belong to the first group. Because of that, the main source of environmental contamination with these elements is air transportation. The main representatives of lithophile trace elements are Co, Cr and Mg, which are more likely transported by water than by air. For this reason, the main source of contamination with these elements is water transportation. Many properties such as pH, Eh, organic matter in soil, cation exchange processes, and part of clay minerals and oxides of Fe, Mn ad Al, affect the trace elements mobility. Most of the metals in upper layer of soil are present in adsorbed form. Simple ions are changed into solution, become mobile and accessible to the plants. Some of the trace elements are easily transported from surface to ground water (Kabata-Pendias and Pendias, 2001).

Anthropogenic contamination with trace elements is represented by industrial emissions, gaseous and dust material from thermal power plants, fumes from houses and transport emission. Smelters and mines are the biggest destructors of environment. Concentration of trace elements such as Cd, Cr, Cu, Hg, Mn, Pb and Zn exceed for several decades times the natural background. Mining and ore processing have a huge influence of environment because the metals are present in minerals in low concentrations, and after their processing left a big amount of waste, that still contain minute amount a trace elements and chemicals. Trace metal contamination as a consequence of mining, smelting and ironworking as well their toxic and harmful impact on human health has recently become a subject of many studies around the world (Hoskin et al., 2000; Budkovič et al., 2003; Borůvka et al., 2005; Chen et al., 2005; Moller et al., 2005; Wang et al., 2005; Bretzel and Calderisi, 2006; Stafilov et al., 2013).

2.2.3. Determining of critical values of trace elements in soil

European countries are using different methods for the determining of critical values and harmfulness of trace elements on living organisms. Referent points are commonly used for the determination of soil contamination. Those points represent possible unpolluted soil areas, which have similar physical, chemical, and biological properties and are situated on the same bedrocks as the area that is being studied. Soil contamination is easily and properly defined with examples of referent and polluted locations.

The Dutch Standards are environmental pollutant reference values (i.e., concentrations in environmental medium) used in environmental remediation, investigation and clean-up. Barring a few exceptions, the target values are underpinned by an environmental risk analysis wherever possible and apply to individual substances. In most cases, target values for the various substances are related to a national background concentration. The soil remediation intervention values indicate when the functional properties of the soil for humans, plants and animals is seriously impaired or threatened. They are representative of the level of contamination above which a serious case of soil contamination is deemed to exist. The target values for soil are listed below in Table 1 (Layla Resources Ltd, 2011).

Table 1: The Standard list

Metal	Target value (mg/kg)	Intervention value (mg/kg)
As	29	55
Ba	200	625
Cd	0.8	12
Cr	100	380
Co	20	240
Cu	36	190
Hg	0.3	10
Mo	10	200
Ni	35	210
Pb	85	530
Zn	140	720

2.3. Atmospheric transport

2.3.1. Definition of attic dust

The name dust is used in a variety of ways, and with different meanings. These range from the material that accumulates on the earth's surface, such as on streets and in living and working environments, to the particulate material suspended in the atmosphere. Atmospheric dust, or atmospheric particulate matter, originates from a wide variety of natural processes and anthropogenic activities, including volcanism, forest fires, rock/crust degassing, combustion of fossil fuels, agricultural practices, industrial manufacturing, and construction activities (Fergusson, 1992; Ozaki et aI., 2004; Tasdemir and Kural, 2005; Wilson and Pyatt, 2007). The discrete airborne particles that compose atmospheric dust consist of a complex mixture of metals, acids, biogenic material, and other organic and inorganic compounds that may represent health risks. Through several exposure routes (such as inhalation, skin contact, absorption in mucosal membranes of eyes and airways, swallowing and

ingestion) the particles may reach into humans, especially children (Cizdziel and Hodge, 2000; Molhave et al., 2000).

Many authors recognize the great importance of studying chemical compositions of atmospheric particles and their interaction between soils, street sediment, attic dust and household dust. Toxic metals are ubiquitous in environmental compartments as low natural concentrations, and they have been always present in a minute amount in our environment. There are so many sources for releasing dust into the environment. The most important human activities that emit significant amounts of toxic metals are transportation and industrial production. Mining activities, ore processing and the processing of waste are found as significant emitters of trace metals in the air, particularly an open pit metal mining. The open pits and ore tailings are quite often unprotected surfaces from which fine grain particles are carried away by wind or water. Transportation distance might be very long under favourable conditions. These elements get distributed among soils, air, surface dust and water. As metals cannot be degraded or decomposed, they are usually accumulated in the environments (Banerjee, 2003; Imperato et al., 2003; Pacyna et al., 2007; Agarval, 2009; Šajn et al., 2011). As a matter of fact, metal contamination has become a global environmental problem, owing to the large scale atmospheric transport. It is noticeable that humaninduced metals have been detected even in snow samples in Greenland and Antarctica (Gorlach and Boutron, 1992; Candelone et al., 1995; Hong et al., 1996; Boutron et al., 1998; Van de Velde et al., 2005; Hur et al., 2007).

2.3.2. Sources of trace elements in attic dust

In geochemical studies, the term "dust" usually refers to street dust and household dust. Household dust represents an important vector for the ingestion and consequent accumulation of toxic substances by humans, particularly by young children. Household dust has many internal and external sources, including garden soil, road dust, human hair and skin, carpet and clothing fibers, paint chips and fungi, resulting in a heterogeneous matrix of organic matter and inorganic and metallic particles. Trace elements, like Cd, Cu, Pb and Zn, exist in many of these sources and therefore exhibit considerable enrichment in the household environment relative to their crustal abundances (Culbard et al., 1988; Fergusson and Kim, 1991; Fergusson, 1992; Rasmussen, 2004). Toxic metals find their way into residential homes either as airborne dust (e.g., leaded gasoline emissions from motor vehicles) or through items used or activities carried out within the house (e.g., renovating or types of heating).

However, contaminated residential dust provides a critical link in the exposure pathway for most young children. Through their hand-to-mouth actions, many children are inadvertently ingesting the metal toxins. In some cases, a child may not exhibit conspicuous pica activity, yet he/she may still be ingesting over 50 mg of lead from traces of dust, dirt or soil (Mielke et al., 1989). In Birmingham, England, the daily uptake of lead for a two yearold was estimated to be 36 mg (Davies et al., 1990). Rasmussen et al. (2004) showed that ingestion of house dust is the main exposure pathway for Pb (69%) for children living in contaminated areas.

Atmospheric particles are tiny particles of solids or liquids suspended in air. These particles vary in size and density (Finlayson-Pitts and Pitts, 2000). Particles 0.005-0.1 μm in diameter are primary particles produced from high temperature combustion processes and gas condensation. Metals emitted by those processes into the atmosphere have high solubility and reactivity, especially under the low pH, and can be carried far away from the sources by the atmosphere. Such processes could contribute particle matter to the atmosphere, pedosphere and hydrosphere under certain dynamic conditions (Hršak et al., 2003; Avila and Rodrigo, 2004; Hou et al., 2005).

A particular type of household dust is attic dust. It represents dust deposited in the attics abandoned by inhabitants, so that tenant influence is minimized. The attic dust is derived predominantly from external sources, such as aerosols deposit and soil dusting, and less from household activities. While household dust is a material to which we are exposed daily, attic dust clearly shows the size and shape of the anomaly produced by atmospheric contamination (Šajn, 2005, 2006). The attic dust as sampling material has the advantage that its composition remains constant, i.e., chemically unchanged, with time. Investigations of attic dust chemistry therefore reveal the average historical state of the atmosphere (Šajn, 1999, 2003).

2.3.3. The historical record of atmospheric contamination

The use of undisturbed attic dust has the advantage of being a measurement, albeit indirect, of air contamination. An attic dust measurement provides an integrated measure based upon the above variables over time; it is, therefore, closer to the endpoint in the process continuum from sources to exposure and, ultimately, effects (Lioy, 1990). The use of attic dust was also successful in tracing plutonium aureole in Nevada, which was a result of atomic bomb experiments (Cizdziel et al., 1998; Cizdziel et al., 1999). Several investigations of attic dust as an important indicator of contamination have also been studied in West Balkan, mostly around contamination sources such as ironworks, smelters, mines, ore deposits, and waste dumps. Systematic studies were done all over Macedonia, especially around the places where mining and ore processing left significant consequences for the environment. Baseline data regarding trace metal levels have been established by comparing different sampling media: soil, attic dust, moss and lichen (Bačeva et al., 2011; Balabanova et al., 2010, 2011).

The use of undisturbed attic dust as a tool for reconstructing historical air contamination was evaluated in many geochemical studies in Slovenia. The first studies were mostly limited to individual industrial facilities, concerning health effects of particulate matter (Gspan and Hrašovec, 1993). According to the Slovenian Environment Agency, measurements of suspended particulate matter were performed in Ljubljana, Maribor in Celje during 90's at several monitoring sites. However, the first systematic study of soil, street sediment and attic dust wascompletedin 1999 for entire territory (Šajn, 1998, 1999, 2003). The chemical composition of selected urban deposits (household dust and attic dust) and their relation to spatial macrolocation (rural/urban environments), geological background, topsoil composition, dominant natural/anthropogenic factors and other influential factors have been described by Šajn at al., 2012. Attic dust was also used for tracing the mercury halo in the Idrija area (Gosar at al., 2002, 2006) and contamination of trace elements in Celje area (Šajn, 2005; Žibret, 2008; Žibret and Šajn, 2008b), Mežica area (Šajn at al., 2000; Šajn, 2006) and Litija area (Jemec and Šajn, 2007, Šajn and Gosar, 2007).

2.4. Impact of metal ore mining and processing

The impact of metal ore mining and processing are responsible for some of the largest releases of trace elements into the environment. This type of industry include several important source of trace elements from a) the mining and milling operations with problems of grinding, concentrating and transporting ores, and disposal of tailings along with mine and mill waste water and b) the smelterrefinery process with problems of concentrating, haulage, storage, sintering, atmospheric discharges and blowing dust (Dudka and Adriano, 1997; Singha et al., 2005; Navarro et al., 2008). The environmental concern in mining areas is primarily related to physical disturbance of the surrounding landscape, spilled mine tailings, emitted dust and acid mine drainage (AMD) transported into rivers. Excessive accumulation of trace elements in agricultural soils around mining areas,

resulting in elevated trace metal uptake by food crops, is of great concern because of potential health risk to the local inhabitants (McLaughlin et al., 1999; Adriano, 2001; Pruvot et al., 2006).

Most metals in the soil upper layers appear in adsorbed form. Free ions go over to solution, become mobile and accessible to plants. They can go over to surface and groundwater. Contamination of soil is strongly endangering vegetation. High share of toxic substances can appear in plants, and through nutritive cycle reach human being. Particles of household dust that do not fall down on soil can accumulate directly in human organism through inhaling or ingestion and cause poisoning (Fergusson, 1992). The consumption of plants produced in contaminated areas, as well as ingestion or inhalation of contaminated particles is two principal factors contributing to human exposure to metals. Potential health risks to humans and animals from consumption of crops can be due to trace metal uptake from contaminated soils via plant roots as well as direct deposition of contaminants from the atmosphere onto plant surfaces (McBride, 2003). Mining has some unique features such as natural background contamination (enrichment) associated with mineral deposits, industrial activities and contamination in the three-dimensional subsurface space, problem of long term remediation after mine closure, problem of secondary contaminated areas around mine sites, land use conflicts and abandoned mines. These problems require special tools to address the complexity of the environmental problems of mining related contamination (Jordan, 2009). Natural background contamination, often present in mining areas due to underlying mineralisation, adds to the complexity of the environmental assessment of contamination at mining sites. Knowledge of the mineralogy of trace metal bearing phases is important in understanding their stability, solubility, mobility, bioavailability and toxicity, modelling their future behaviour, and developing remediation strategies (Hudson-Edwards, 2003).

Mines produce large amounts of waste because the ore is only a small fraction of their total volume of the mined material. Even in highgrade ores is generally just a several percentage of their total mass. Mining itself affects relatively small areas but the tailings and waste rock deposits close to the mining area are important sources of contamination In many areas worldwide present and historical mining and smelting activities are causing a variety of environmental problems such as elevated metal concentrations in soils/sediments, dispersion of toxic metals in soil and water and ecological damage caused by extensive metal contamination (Ashton et al., 2001; Lee, 2003; Navarro et al., 2004; Gomes and Favas, 2006; Chopin and Alloway, 2007; Navarro et al., 2008;Jordan, 2009; García-Lorenzo et al., 2012).

On the territory of present day Bosnia and Herzegovina, mining and metallurgy are counted among the oldest forms of industry. The earliest recorded evidence of this dates back to the Neolithic Age, but major mineral exploration and mine development are began during Medieval times. Throughout Bosnia lead, copper, and silver mines have opened. The most important mines were situated in the middle Bosnia basin (Kamenica, Olovo, Dusina and Deževica) and in eastern Bosnia basin (Srebrenica and their surrounding). The mines attracted foreign entrepreneurs who established settlements, colonies, and caravan parks. Large natural resources – especially coalmines (Tuzla, Doboj, Banovići, Ugljevik, Gacko, Breza, Kakanj, Zenica, etc.), Fe mines (the Majdan Mountain, Vareš, Ljubija) Pb and Zn mines (Olovo, Vareš and Srebrenica) bauxite mines (Bužim, Jajce, Mostar and Vlasenica) led Bosnia to total prosperity. First ironworks, steelworks, and smelters were built during the Austro-Hungarian period. Between the two World Wars, the stagnation of industrial production is noticed; anyway, during the Communism, industrialization of Bosnia and Herzegovina increased. During the war in Bosnia from 1992 to 1995, most major mineral production facilities were damaged significantly, and pre-war levels of production had only recently been achieved by some producers. Aluminum producer, Aluminij d.d. Mostar and iron and steel producer, ArcelorMittal Zenica were the most economically important companies in the mineral industry in terms of the value of their output in last couple of years (Brininstool, 2007).

3. MATERIALS AND METHODS

3.1. Description of the study area

3.1.1. Geographical description of study area

The river Stavnja has a length about 35 km, located in the Central Bosnia and Herzegovina, northern from the capital Sarajevo (Figure 1). Approximately, in its valley live 30000 inhabitants, mostly settled in two small cities Vareš and Breza. The valley belongs to the temperate continental mountain climate zone, with cold winters and moderately warm summer. In general, autumn is warmer than spring.The Stavnja catchment area is large about 180 km^2, including only three bigger tributaries on left side, the Mala River, the Ponikva and the Žalja but the study area is large c. 104 km^2 (Figures 2 and 3). The river valley is a very narrow valley surrounded with steep hills with average width about 5 km. According to a north base line, the whole valley has an azimuth 17 degrees. The river Stavnja springs at 1080 m, but ends at 430 m. Most of the study area is covered by forest 57 km^2 or 55%. Meadows, pastures and cultivated land cover 37.4 km^2 or 36%, settlements 4.5 km^2, industrial zone 1.2 km^2, and open mine pits 3.6 km^2 (Figure 3).

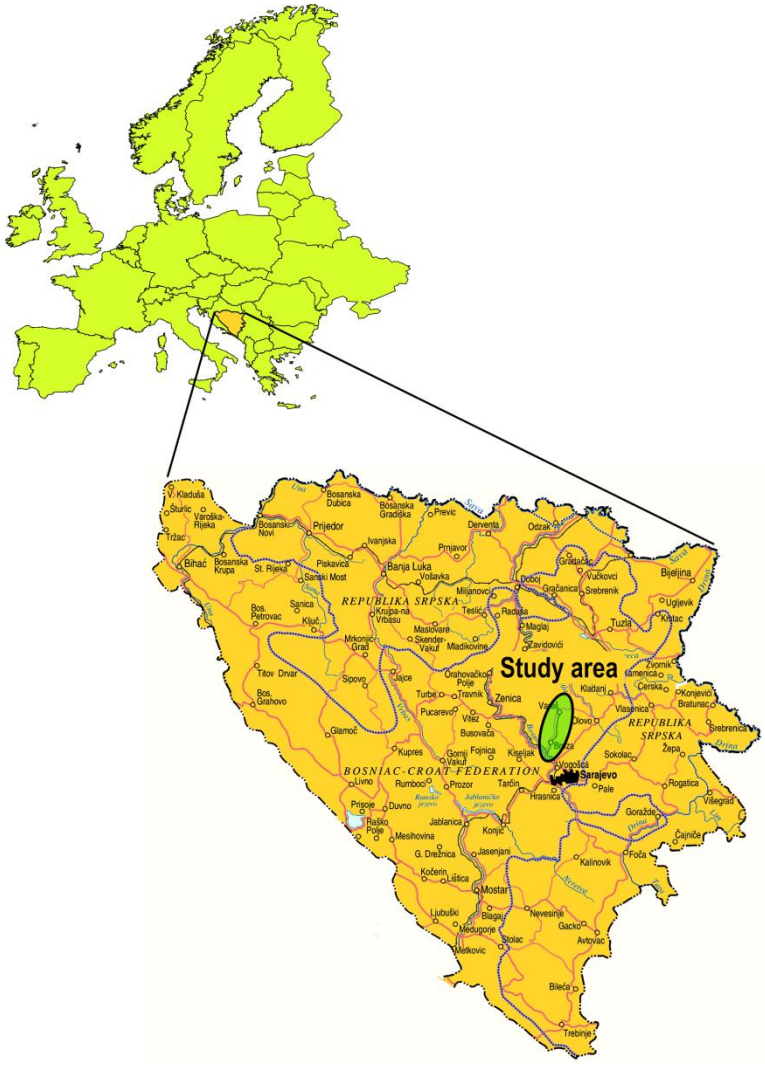

Figure 1: Location of study area

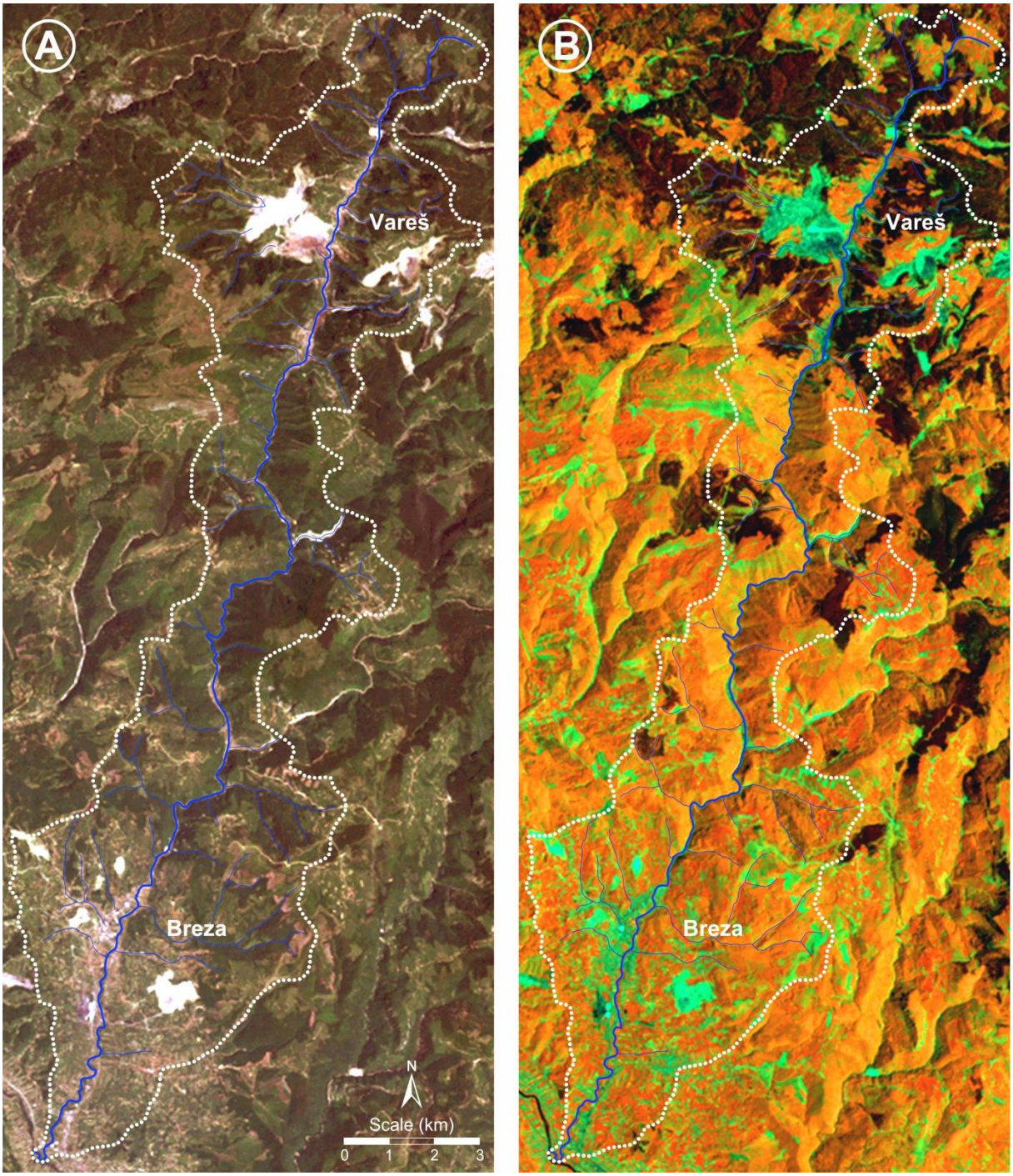

Figure 2: Landsat multispectral images. Set from 1990, before of civil war in B&H. A – Composite of visible bands (B1, B2 and B3); B – Composite of infrared bands (B4, B5 and B7)

The study area is rich with archaeological findings from different epochs. In the municipality of Vareš were found the remaining of metallurgical activities dating back to Bronze Age. On several surrounding locations are found remains of copper artefacts from prehistorically period, the mining tools and lamps from the Roman era. Ottoman government has been pried with this region because of craftsmen and their very qualitative products. With the arrival of Austrians all area had a biggest prosperity. Even Saxons moved in the new industrial area. In the town centre itself, there is an old stone arched bridge from Ottoman period, the oldest preserved Catholic Church of St. Michael in

Bosnia and Herzegovina. The church are among the oldest preserved in Bosnia and date back to 1643. The remaining of the medieval royal city and castle Bobovac is located close to Vareš. Ruins of Basilica from the 5th Centuryare preserved. In the city centre Breza. On several locations of the study area are preserved lots of monumental medieval tombstones.

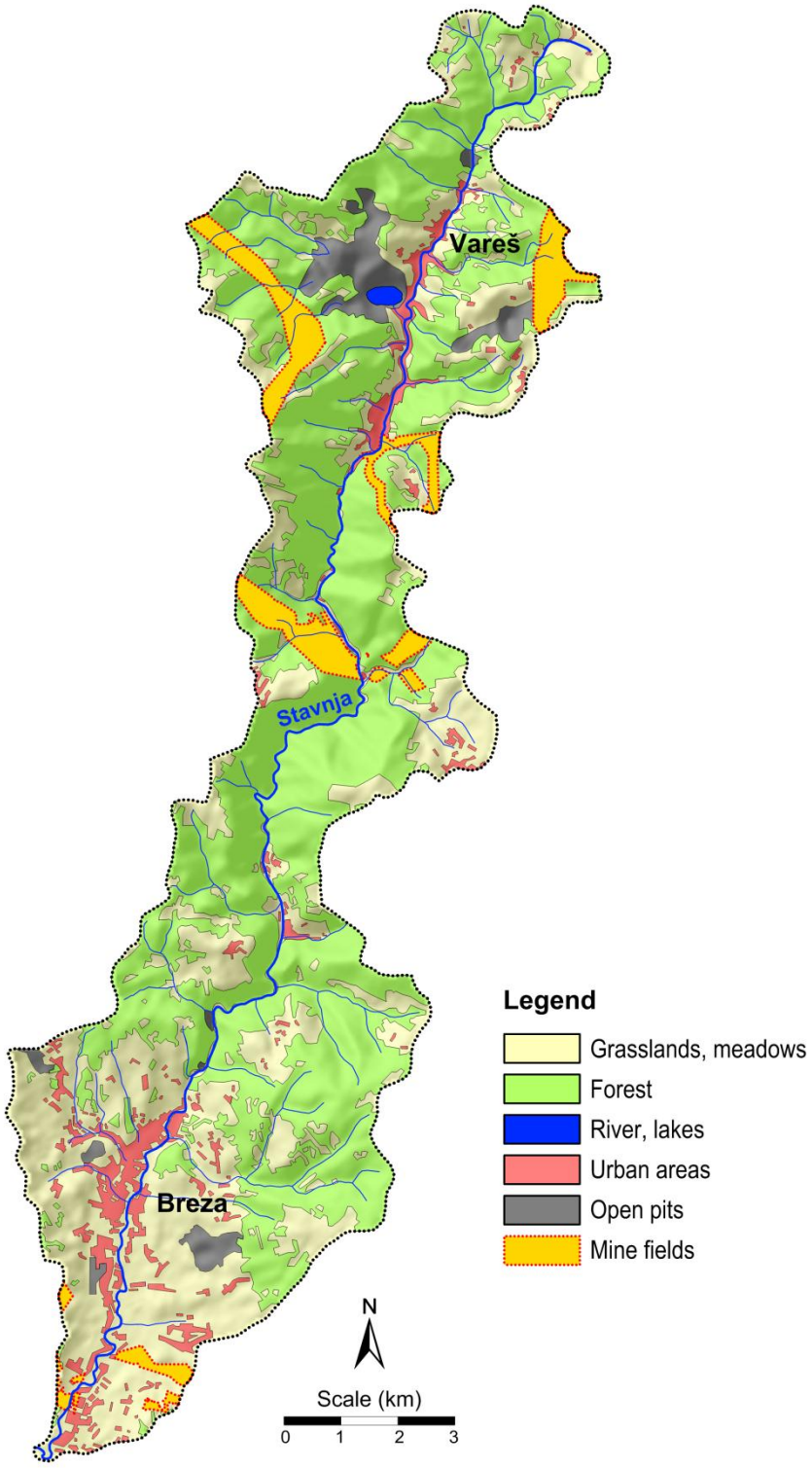

Figure 3: Land use map

Figure 4: The Iron open pits, Smreka (left) and Brezik (right)

Figure 5: Abandoned ironworks Vareš

In the region of Vareš municipality, mineral exploitation begun already in the Antique period but with arrival Austrians to Bosnia, Vareš admire revival in economy aspect. The iron ore deposits are conducted to the Triassic structures. The mine Vareš is the oldest and largest in Bosnia and Herzegovina, comprising of three areas of exploitation: Smreka, Droškovac and Brezik (Figure 4). The mining zones of aforementioned areas make one geological unit. In 1991, open pit's reserves and resources in the mentioned three Fe ore deposits have been deemed to 169 million tonnes. Beside the main iron ore minerals, hematite and siderite there are present various metal ore sulphides of Cu, Pb, Zn, As, Sb and Sn. Lead, zinc and barite Veovača open pit is situated about 10 km eastern of Vareš. Sulphide mineralization is associated with layers of barite and have volcanogenic – sedimentary genesis. Inside of these deposits hydrothermal processeshave formedsome minor

veinsriched with various minerals. Lead – zinc mineralization is basically associated to Droškovac iron deposit. Together with main minerals galena, sphalerite and barite are associated another minerals such as pyrite, marcasite, tetraedrite, antimonite, chalcopyrite, cinnabar, realgar, calcite, quartz, limonite, covelline, etc.Construction of the ironworks and metal foundry in Vareš begin in 1891.Until 1991,it was operated within one company called “Mine and Ironworks Vareš”. The ironworks have been the second largest ironworks in Bosnia and Herzegovina. All activities in the ironworks have ended in 1998, when two furnaces were overthrown because of disuse technology and unprofitability. Metal foundry still works but with much reduced capacity. The ironworks are situated in upper part of the valley, under the urban zone (Figure 5).

A town Breza with surrounding settlements is developed on river terraces of the river Stavnja. It is known with brown coal mining. This coal basin belongs to the Central Bosnian coal basin that lies along the river Bosna. Comparing to the mines and ironworks in municipality of Vareš where all industry is abandoned, this mine is still active (Figure 6).

Figure 6: Town Breza (left) and brown coal open pit (right)

3.1.2. Geological description of study area

Geology of the study area is taken from the Basic Geological Map, sheets Vareš (L 34-133) and Sarajevo (K 34-1), scale 1: 100,000 (Jovanović at al., 1977; Olujić et al., 1978; Pamić et al., 1978). The study area is a part of the Durmitor nappe. The most important geotectonic unit of Vareš metallogenic district belongs to the Central ophilote zone. Advanced rifting magmatism produced spilites, ophitic basalts and diabases, and scarce keratophyres, interlayered with Ladinian sedimentary rocks. Deposits related to magmatism include cinnabar deposits, Mn-oxide deposits, monomineralic and polymetalic barite deposits, and siderite–hematite deposits. The deposits are placed within a sigmoid shaped curved belt, 2 to 5 km wide and 25 km long (Palinkaš et al., 2008).

The outcropping stratigraphic sequence exposes rock formations spanning from the Upper Triassic to more recent times. Ten major lithological units have beenisolated (Figure 7). The river Stavnja perpendicularly crosses the lithological units, from the oldest one in the north to the youngest in south of the study area. The younger Quaternary layers are developed along present watercourse or something higher in gravel–conglomerate terraces.

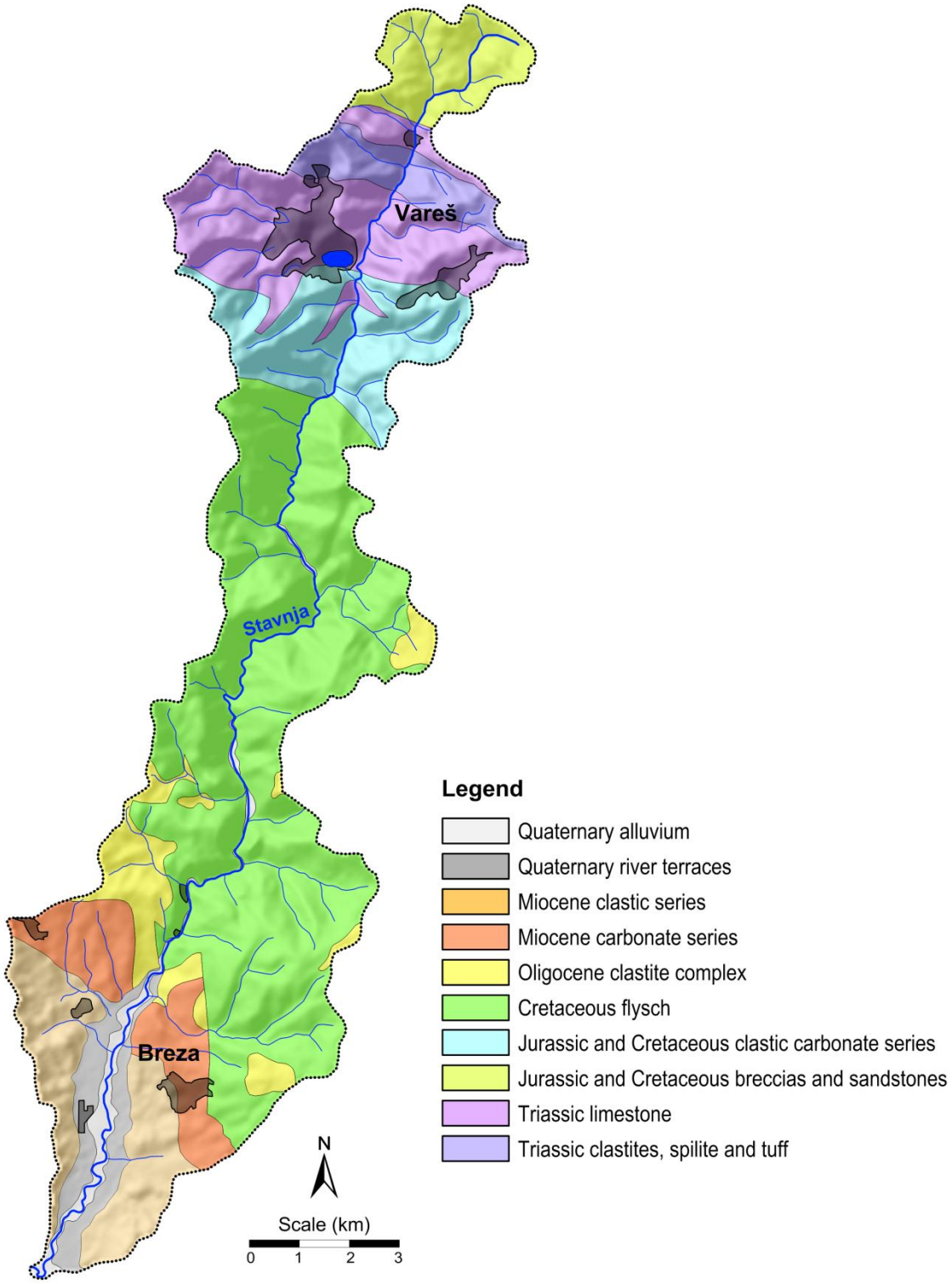

Figure 7: Map of isolated lithological units

The oldest Upper Triassic clastite rocks (T_1) in the study area are represented by slate, quartz–mica–chlorite schists, metasandstone, and chert. These rocks also include sandstone, subordinate shale and marly shale. Lower and Middle Triassic ($T_{2,3}$)is represented by massive and thick bedded limestone with chert noduls. There is a part with the Anisian limestones and dolomites, hematite and siderite shale. These are followed by crinoide limestone and dolomitic limestone. Same ages are

spilite and tuff (tuffaceous sandstone), which are found northern of Vareš. Unseparated volcanic sedimentary formations represent about 1000 m thick complex of rocks. Jurassic and Cretaceous clastic carbonate series (J,K) have direction NW–SE, represented by marly shale, limestone, sandstone, conglomerate, breccia, and chert. Jurassic and Cretaceous Pogari series is formed by breccias and sandstones (JK). Most of the study area is covered with flysch sediments. Turonian–Senonian flysch ($K_2^{2,3}$) is built-up of conglomerate, breccia, limestone, marle and siltstone. Cenomanian–Turonian flysh ($K_2^{1,2}$) is represented by limestone breccias, limestone, sandy limestone, shale, sandstone and chert (Pamić et al., 1978).

On the south of research area is found Oligo clastite complex (Ol). Those sediments are represented by variegated series (conglomerate, sandstone, limestone, marl, and clay) and sandstone conglomerate and limestone with coal beds. Older Miocene transitional zone ($^2M_2$) represented by thin-bedded marl and sandstone and roof limestone zone ($^1M_2$) includes sandy limestone with roof coal bed. The youngest sediments are Holocene ages represented by the Quaternary terraces (t) and Quaternary alluvium (a_1). Younger Quaternary layers are developed along present watercourse or something higher in gravel-conglomerate terraces (Pamić et al., 1978).

Vareš, siderite–hematite sedimentary exhalative (SEDEX) deposits, Smreka, Droškovac and Brezik, are locus typicus mineralisation of the Mid Triassic, advanced Tethyan rifting phase (Red Sea stage). The deposits contain hydrothermal, stratiform siderite–hematite–chert beds. The mineralisation form part of the Anisian and Ladinian sequences and displays a distinct vertical zoning, reflecting a gradual change of redox conditions in the depositional environment. The sequence starts with bituminous, thinly bedded shales with pyrite and base metal sulphides, overlain by barite and siderite, deposited under reducing conditions. Overlying clastics and oolithic limestone are succeeded by hematite shale, hematite ±chert beds, deposited in oxidizing environment. Major minerals are siderite, manganese rich hematite, barite, pyrite, marcasite, chalcopyrite, galena, sphalerite, tetrahedrite and Pb-sulphosalts. Veovača Pb, Zn, Ba deposit contains ore breccia or ore conglomerates with dm to msized clasts cemented by barite and Pb–Zn sulphides. Microcrystalline dark barite is accompanied with galena and sphalerite. Barite from the Veovačamine is typical for Triassic SEDEX deposits elsewhere in the Dinarides (Palinkaš et al., 2008).

3.2. Sampling design

Regarding the primary purpose of research, experience (Šajn, 2005, 2006; Alijagić, 2008; Alijagić and Šajn,2006, 2010; Stafilov et al., 2008a, 2008b) and some sampling difficulties (such as narrow gorge, inaccessible terrain and remained minefields), the sampling grid have been prepared so that the soil profiles were raised to the river flow transversely. In this way, changes of environmental chemisms according to distance from the source of contamination, a change in altitude, and a transport mode (atmospheric or water transport of trace elements) have been followed. According to the above issues, we have to design the sampling grid covering the geogenic distributions of elements, as well as anthropogenically induced anomalies caused by atmospheric and water transport.

The sampling grid was set up respecting a presence of the minefields as well. Whereas, the reliability of the mine maps is relatively low, we put special emphasis on integration and communication with residents. In many places, the sampling points were moved according to the suggestions of local residents. Researches from the Croatian Geological Survey have already faced such problems shareing with us their experience and providing a many useful suggestions. Even the area covered with the minefield is relatively small (5.5%), possibility of their encounters is much higher. At the same time, the sampling grid has been created so that all the main lithological units are covered. Various lithological units are enriched with various chemical elements, which during natural processes are

released into soil. Determination of parental material will help in reconstruction of the environmental chemism and baseline data regarding trace metal levelsin the study area. For this purpose,various sampling materials are collected such as automorphic (cambisol) and alluvial soils (fluvisol), river sediments and attic dust.

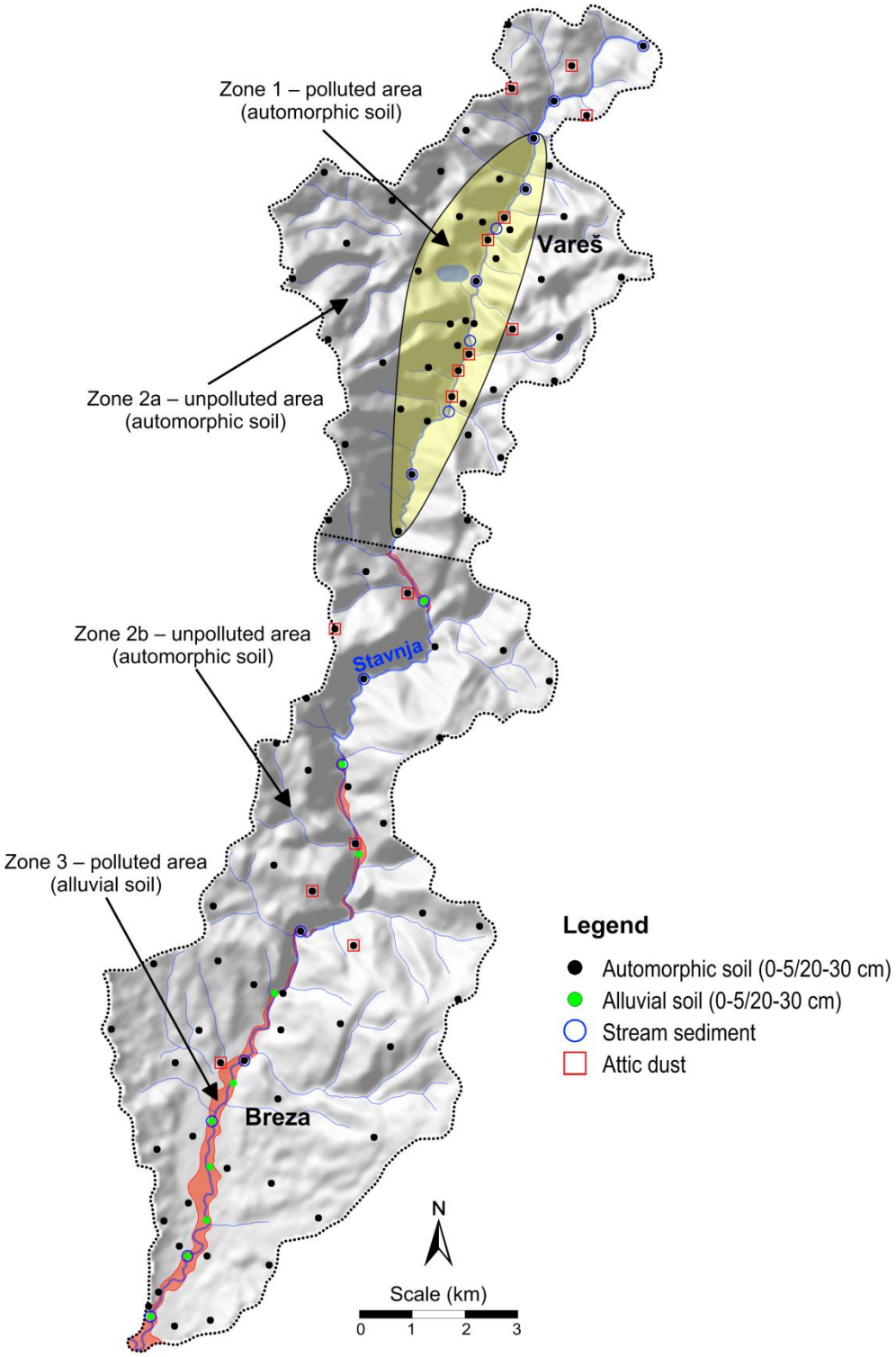

Figure 8: Samplingsiteswith determined zones

Sampling was performed into two phases. Inthe first phase of sampling (2009), the entire valley (c. 35 km) has been covered with 12 profile lines set to cross a river flow. In the area of former intensive mining operations as well, sampling grid has been sparse, but in urban and industrialized areas the sampling grid was denser (Figure 8). Second phase of sampling (2011) includes sampling on the edges of study area, and following lithological units: Triassic spilites and tuffs, Oligocene clastit complex, Miocene carbonate and clastites series, which are not covered well by sampling during the first phase. Some additional samples were collected on places where some anomalies occur, such as an Arsenic anomaly. Total number of soil samplingsites from both sampling phases is 111, attic dust 15, and river sediments 17.

The Figure 8 provides also the main determined zones. Zone 1 is concerned as a probably polluted area and it is located in the upper part of the Stavnja valley. There are collected only automorphic soil at 24 sampling sites. Those sampling locations are mainly situated in the industrial zone and represent the area with biggest expected influence on environment. This zone is marked with the ellipse. The Zone 2 is determined as unpolluted zone. This zone is divided into two zones, Zone 2a and Zone 2b, respectively. Zone 2a is located around the Zone 1, and there are collected soil samples at 27 sampling sites. Zone 2b is situated around the Zone 3, whit 50 sampling sites. The last zone is Zone 3, located in the lowest part of the Stavnja valley. This zone is concerned as contaminated zone, with high content of trace elements. In this zone, soil samples are collected solely at the alluvial plain, at 10 sampling sites.

From the geological view, 10 soil sampling sites are located on the Quaternary alluvium, 9 on the Quaternary river terraces, 8 on the Miocene clastic series, 5 on the Miocene carbonate series, 6 on the Oligocene clastite complex, 28 on the Cretaceous flysch, 16 on the Jurassic and Cretaceous clastic carbonate series, 6 on the Jurassic and Cretaceous breccias and sandstones, 19 on the Triassic limestone and 4 samples on the Triassic clastites, spilites and tuff.

3.3. Sampling materials

3.3.1. Soil

In geochemical studies, soils represent the most widespread sampling material for environmental assessment due to their availability and relatively undemanding sampling method. Disadvantage is only high variability of soil chemism, which can be dispatched by taking composite samples. According to mentioned sampling problem, one soil sample represents the composite material collected at the central sample point itself and at four points within the radius of 50 m around it. At each sampling point, topsoil (0-5 cm) and subsoil (20-30 cm) are collected and the mass of such a composite was about 1 kg (Borůvka et al., 2005; Chen et al., 2005; Salminen et al., 2005; Bretzel and Calderisi, 2006; Tembo et al., 2006; Alijagić, 2008). The distribution of elements that can reflect natural processes are indicated by elements that rarely or never participate in technogenic processes. Their contents usually change gradually across the landscape. Naturally caused chemism of soil is characteristic for deeper soil horizons. For the anthropogenic accumulation of chemical elements is characterized by explicit increase in concentration, appearing from the relatively low natural background. The anomalies occur close to industrial zones, mines, smelters and ironworks (Šajn, 2005; Alijagić and Šajn, 2006; Cappuyns et al., 2006; Stafilov et al., 2008a, 2008b). High concentrations of anthropogenically entered chemical elements are characterized mainly for surface soil horizon.

Figure 9: Sampling of automorphic soil

Figure 10: Sampling of alluvial soil

According to the sampling sites collected soil can be genetically divided into two main groups, the automorphic soil and alluvial soil, respectively. Automorphic soils (FAO, 2006) are defined as well drained soils. All automorphic soils belong to the Cambisol (type of developed soil), collected at meadow and pastures. Total number of collected cambisol topsoil (0-5 cm) and subsoil (20-30 cm) is 222 (Figures 8, 9 and 10).

Soils developed only on the youngest Quaternary material, alluvium are called fluvisol (FAO classification). Alluvial soils (fluvisol) are poorly drained soils, form because of the permanent or periodical presence of groundwater, precipitation, or floodwater in or on the soil profile. From the 10 sampling site are collected samples of alluvial sediments.

After sampling, each soil sample is described into separate inscription list. The inscription list contain following information: ID number, Sample label, Sampling material, Sample coordinates: Lon (WGS84), Lat (WGS84), and Altitude, Name of location, Year of sampling, Area, Land use, Lithology, Pollution, Soil Texture, Soil Structure, Soil Skeleton, Soil org. matter (Appendices A and B). The inscription lists and all samples are stored at Geological Survey of Slovenia.

3.3.2. River sediment

When it rains, soil and debris from the surrounding land are eroded and washed into streams. As the rivers move they are carrying soil, sand, and sediment along with them and deposit on the river bed. River sediments are contemporary materials that keep emerging, which means that their chemism reflects the current state of the environment. Concentrations of chemical elements are result of weathering constant. Active stream sediment represents the fine to mediumgrained bed load material (silty–clayey sandy), which is transported by running water (Salminen et al., 2005). Increased concentrations of trace elements represent the current transfer of trace elements as a result of leaching from abandoned (nonrecultivated) open pits, mining and smelting waste residues (Šajn, 2005, 2006). High concentrations of trace elements in river sediments are usually, a strong indicator of contamination of alluvial (flood) planes, which are important agriculture areas.

Figure 11: Sampling of stream sediments

In geochemical studies, river sediments are widespread sampling material that gives current assessment state of the environment. Sampling is more difficult compared to the soil. Local variability is abolished by taking composite samples (Kunwar et al., 2005). Each stream sediment sample comprises material taken from 5-10 points over a stream stretch of 250 - 500 m. Prior to stream water and stream sediment collection, it is important to identify the 250 - 500 m stream stretch where obvious signs of contamination can be avoided and suitable sediment can be collected from 5-10 different locations. Sites should be located at least 100 m upstream of roads and settlements. Stream sediment sampling should start from the water sampling point and the other subsamples should be collected up stream (Salminen et al., 2005). Along the river Stavnja at 17 localities the river sediments are collected (Figures 8 and 11).

3.3.3. Attic dust

Close to the selected soil sampling sites the old houses were chosen with intact attic carpentry. A particular type of household dust – the attic dust will be studied in this work. To avoid collecting particles of tiles, wood and other construction materials, the attic dust samples were brushed from parts of wooden constructions that were not in immediate contact with roof tiles or floors. Attic dust represents stable sampling material with very low variability with distance. Only problem with attic dust is extremely difficult sampling. Total number of collected samples is 15 (Figures 8 and 12).

The attic dust as sampling material has the advantage that its composition remains constant, i.e. chemically unchanged, with time. Investigations of attic dust chemistry therefore reveal the average historical state of the atmosphere. In previous geochemical studies the use of attic dust as a sampling medium was established (Cizdziel et al., 1999; Šajn, 2003, 2005, Žibret, 2008; Žibret and Šajn, 2008a, 2008b).

Figure 12: Sampling of attic dust

3.4. Sampling preparation and analyses

The samples (soil samples and river sediments) were air dried to begin with, and subsequently were completely dried in a fan drier at 40°C. The sample preparation have been done in several following steps: (1) Disintegration – manual grinding of solid samples using a ceramic mortar and pestle; (2) Homogenizing – breaking of samples down into smaller parts and blending to make them more uniform in texture and consistency; (3) Removing roots and/or rock fragments– manual separation of impurities; (4) Splitting – reducing the weight of samples to less than 0,5 kg after grinding or disintegration procedure; (5) Quartering – dividing of the disintegrated granular sample into subsamples with identical quality and quantity; (6) Sieving– dry manual passing of samples through a 2 mm nylon mesh and (7) Pulverizing mechanically breaking down the particles of dry samples (Salminen et al., 2005). The samples of attic dust were prepared for chemical analysis only by sieving through a 0.125 mm nylon mesh (Šajn, 2003, 2005).

All samples were analysed in at the ACME, Ltd. laboratory in Vancouver, Canada (ACME Labs, 2010, 2011). Determination of 36 chemical elements (Ag, Al, As, Au, B, Ba, Bi, Ca, Cd, Co, Cr, Cu, Fe, Ga, Hg, K, La, Mg, Mn, Mo, Na, Ni, P, Pb, S, Sb, Sc, Se, Sr, Th, Ti, Tl, U, V, W and Zn) was performed by inductively coupled plasma mass spectrometry (ICP-MS) after aqua regia digestion (mixture HCl, HNO_3 and water). Sample splits of 0.5g are leached in hot (95°C) Aqua Regia for one hour. At the ACME Analytical Laboratories, quality control was ensured by analyzing duplicate samples and blanks. The measurement accuracy was determined by measuring certified standards in each analytical set: DS7 and OREAS45PA for the first set of samples (2010) DS8 and OREAS45CA for the second set of samples (2011).

Inductively Coupled Plasma Mass Spectrometry (ICP-MS) is a very powerful tool for trace and ultratrace elemental analysis. ICP-MS is rapidly becoming the technique of choice in many analytical laboratories for the accurate and precise measurements needed for today's demanding applications. In ICP-MS, a plasma or gas consisting of ions, electrons, and neutral particles is formed from Argon gas. The plasma is used to atomize and ionize the elements in a sample. The resulting ions are then passed through a series of apertures (cones) into the high vacuum mass analyzer. The isotopes of the elements are identified by their mass-to-charge ratio (m/e) and the intensity of a specific peak in the mass spectrum is proportional to the amount of that isotope (element) in the original sample.

The results of chemical analyzes of 26 selected elements (Ag, Al, As, Ba, Bi, Cd, Co, Cr, Cu, Fe, Ga, Hg, La, Mg, Mn, Mo, Ni, Pb, Sb, Sc, Th, Ti, Tl, V, W and Zn) of all samples are shown in Appendices C and D.

4. DATA PROCESSING

All data processing and calculations, geostatistical data interpretation and visualization (mapping) have been performed by using following softwares: Statistica (Stat Soft Inc., 2012), Autodesk MAP 3D (Autodesk Inc., 2012), ArcINFO (ESRI Inc.,2004) and Surfer (Golden Software Inc., 2012).

4.1. Data acquisition

In the recent years, geographical information systems (GIS) are used for spatial data management and manipulation. For this purpose various spatial data were acquired by digitalization of existing topographic maps: (1) Vareš 4 (475-4) in scale 1:50000; Vareš 4-1 (475-4-1), (2) Vareš 4-2 (475-4-2), Vareš 4-3 (475-4-3), Vareš 4-4 (475-4-4), Sarajevo 2-2 (525-2-2), Sarajevo 2-1 (525-2-1) in scale 1:25000 (provided by the Geodetic survey of Bosnia and Herzegovina); (3) Google Earth maps (Google Inc., 2010), (4) maps Breza-Vareš, scale 1:50000, (5) Breza-Podlugovi, Brgule, Karaule, in scale 1:10000 (provided by BH Mine Action Centre, in Sarajevo), (6) geological maps Vareš (L 34-133) and Sarajevo (K 34-1) in scale 1:100000 (provided by Geological Survey of Slovenia and Geological Survey Federation of Bosnia and Herzegovina); (7) 80m SRTM Digital Elevation Model (CGIAR Consortium for Spatial Information, 2011.); (8) 30m ASTER Digital Elevation Model (U.S. Geological Survey, 2011a) and (9) Landsat multispectral satellite images – 7 bands (U.S. Geological Survey 2011b).

All aforementioned maps were used for obtaining as much as possible geospatial data that were included into the databases. For data processing two databases have been prepared. One database includes following information for 254 samples: Identification number, Sample label, Sampling material, Land use unit (Figure 3), Lithological unit (Figure 7), Defined zones (Figure 8), Latitude, Longitude, Absolute distance from the ironworks chimneys (Figure 13a), Elliptical distance from the ironworks chimneys (Figure 13b), Distance from the river Stavnja (Figure 13c), Altitude (Figure 14a) Altitude above the bottom of Stavnja valley (Figure 14b), Terrain Slope (Figure 14c), Aspect, Plan Curvature (Figure 15a), Profile Curvature (Figure 15b), Tangent Curvature (Figure 15c), and Landsat spectral bands 1-7 (Table 2, Figure 16). Beside the aforementioned geospatial data and multispectral image bands, this data base includes the analytical data (26 selected elements: Ag, Al, As, Ba, Bi, Cd, Co, Cr, Cu, Fe, Ga, Hg, La, Mg, Mn, Mo, Ni, Pb, Sb, Sc, Th, Ti, Tl, V, W and Zn).

For a modelling of spatial distribution of particular elements with Artificial Neural Network and Multiple Polynomial Regression, a recall grid has been used. This means that whole study area is divided to 50 x 50 m grid cell. Total number of recall points is 41471. This database includes only geospatial data and Landsat multispectral image bands mentioned before.

4.1.1. Topographic and geological data

The maps are constructed with the limitation of representing 3D realworld objects into 2D representation, which involves some distortion of the shape, area, distance and direction of spatial objects. Du to fact that the topographic maps (1:25000 and 1:50000) were reambulated in late 70's, to get more realistic spatial data the maps from Google Earth and multispectral satellite images have been combined. Particular land use units are digitalized and isolated directly from the Google Earth in form of KML files. Such maps have been georeferenced, what means that we defined its existence in physical space, establishing its location in terms of map projections or coordinate system. According to Hill, 2006 the term is used both when establishing the relation between raster or vector images and coordinates, and when determining the spatial location of other geographical features. This procedure

is thus imperative to data modelling in the field of GIS and other cartographic methods. When data from different sources need to be combined and then used in a GIS application, it becomes essential to have a common referencing system. Different maps may use different projection systems. Georeferencing tools contain methods to combine and overlay these maps with minimum distortion.

Beside the topographic maps, the basic geological map (1:100000) has been digitalized and vectored too. Isolation of major lithological units is also important step for determination natural and anthropogenic background. The maps (1:25000 and 1:10000) of remain minefields and possible minefields were obtained from the BH Mine Action Centre, in Sarajevo. Data about the minefields were isolated from then and incorporated into previously digitalized topographic maps.

Given data were presented into three different projection systems: topographic, geological and minefield maps in the Gauss Kruger (zone 6) projection with a Hermanns-Kogel datum; the Google Earth and ASTAR in Unprojected Lat/Long projection with a World Geodetic System 1984 (WGS84) datum; and satellite images in the Universal Transverse Mercator (UTM 34N) projection with a WGS84 datum. All aforementioned data have been converted into one projection system Gauss Kruger.

4.1.2. DEM and Terrain modeling (geomorphometry)

Digital Elevation Model (DEM) is a quantitative representation of the Earth's surface providing basic information about the terrain relief (Guth, 2006). DEM is an important tool for a geomorphometry, its derived attributes (such as slope, aspect, drainage area and network, curvature, topographic index, etc.) which are important parameters for information extraction or assessment of any process using terrain analysis (Wolock and Price, 1994). Providing all these geomorphometrical data, DEM is prerequisite in different applications such as water flow modelling (Jain and Singh, 2003), volcanic hazards (Vassilopouloua et al., 2002), terrain visualization and mapping (Spark and Williams, 1996), flood simulation and management (Ramlal and Baban, 2008, Honghai and Altinakar, 2011), climate and meteorological studies (Thornton et al., 1997), etc. The outcomes of the models depend on the accuracy of DEM (Zhang and Montgomery, 1994; Mukherjee et al., 2013).

Figure 13 provides following geospatial information: (A) a cyclic distance from the ironwork Vareš (the main source of contamination); (B) an elliptic distance from the ironworks Vareš; and (C) the distance from the Stavnja. These three shapes of distance are prepared in scale 1:5. The cyclic and elliptic distances have been calculated from the ironworks chimney. For easier understanding each distance is presented by different color in seven equal percentile classes. Several following morphological spatial information: (A) an altitude,(B) an altitude above the bottom of the Stavnja valley, and (C) a slope are provided in Figure 14. Altitude is distance measurement between referent point (the sea level) and object. The altitude above the river has been calculated from a surface that has a river incline.

Terrain Aspect calculates the downhill direction of the steepest slope (i.e. dip direction) at each grid node. It is the direction that is perpendicular to the contour lines on the surface, and is exactly opposite the gradient direction. Terrain Aspect values are reported in azimuth, where 0 degrees points due North, and 90 degrees points due East. Terrain Slope (Figure 14c), calculates the slope at any grid node on the surface. Terrain Slope is reported in degrees from zero (horizontal) to 90 (vertical). For a particular point on the surface, the Terrain Slope is based on the direction of steepest descent or ascent at that point (Terrain Aspect). This means that across the surface, the gradient direction can change. Grid files of the Terrain Slope can produce contour maps that show isolines of constant steepest slope (Moor et al., 1993).

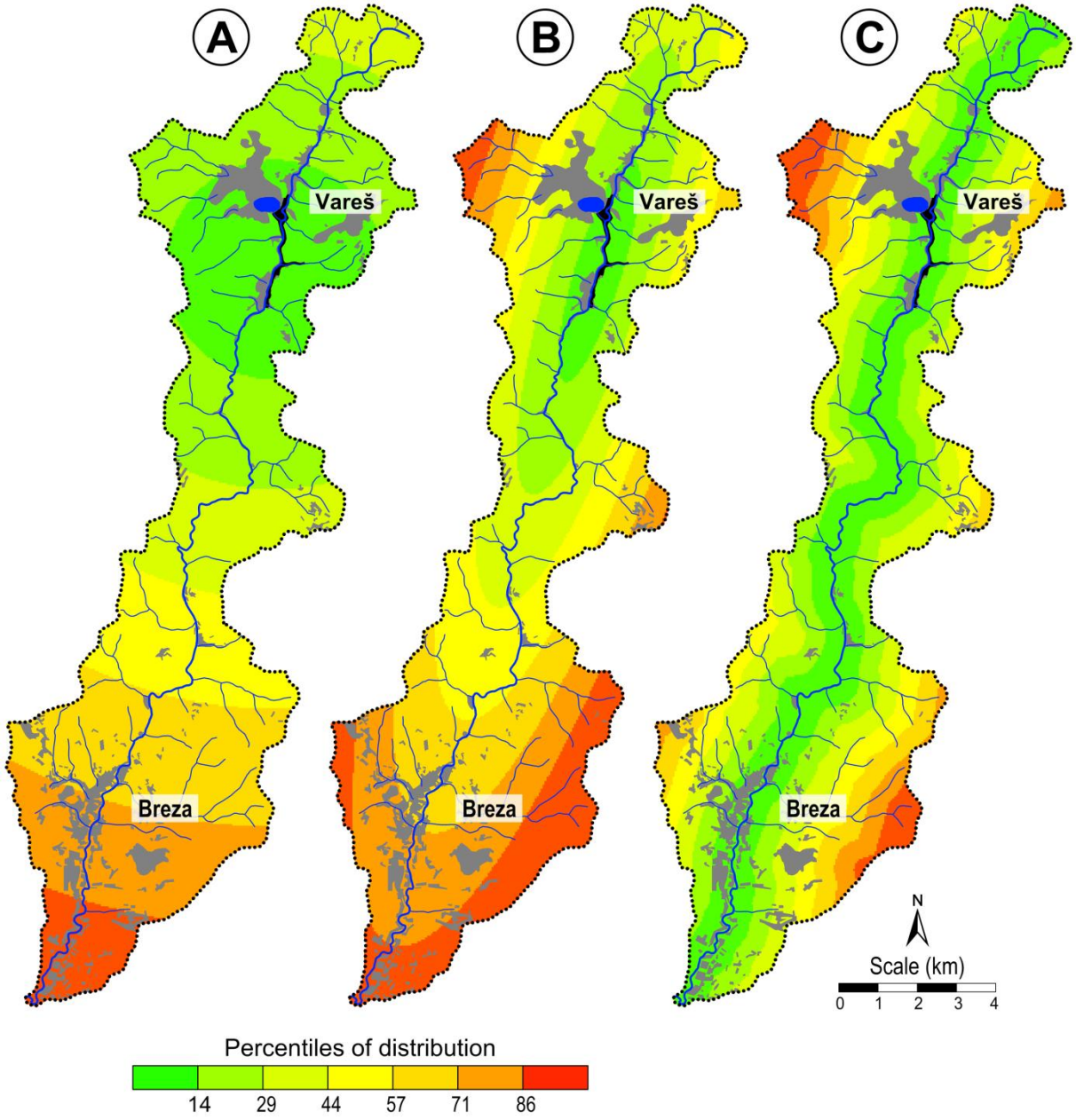

Figure 13: A – Absolute distance from the ironworks chimneys; B –Elliptical distance from the ironworks chimneys (ratio 1/5); C – Distance from the river Stavnja

Plan Curvature (Figure 15a), reflects the rate of change of the Terrain Aspect angle measured in the horizontal plane, and is a measure of the curvature of contours. Negative values indicate divergent water flow over the surface, and positive values indicate convergent flow. Plan Curvature calculates the curvature of the surface in the horizontal plane, or the curvature of the contour. Negative curvature, shown with a gray fill, indicates areas of divergent flow. Profile Curvature (Figure 15b), determines the downhill or uphill rate of change in slope in the gradient direction (opposite of slope aspect direction) at each grid node. Grid files of Profile Curvature produce contour maps that show isolines of constant rate of change of steepest slope across the surface. Negative values are convex upward and indicate accelerated flow of water over the surface. Positive values are concave upward and indicate values are concave upward and indicate slowed flow over the surface. Profile Curvature

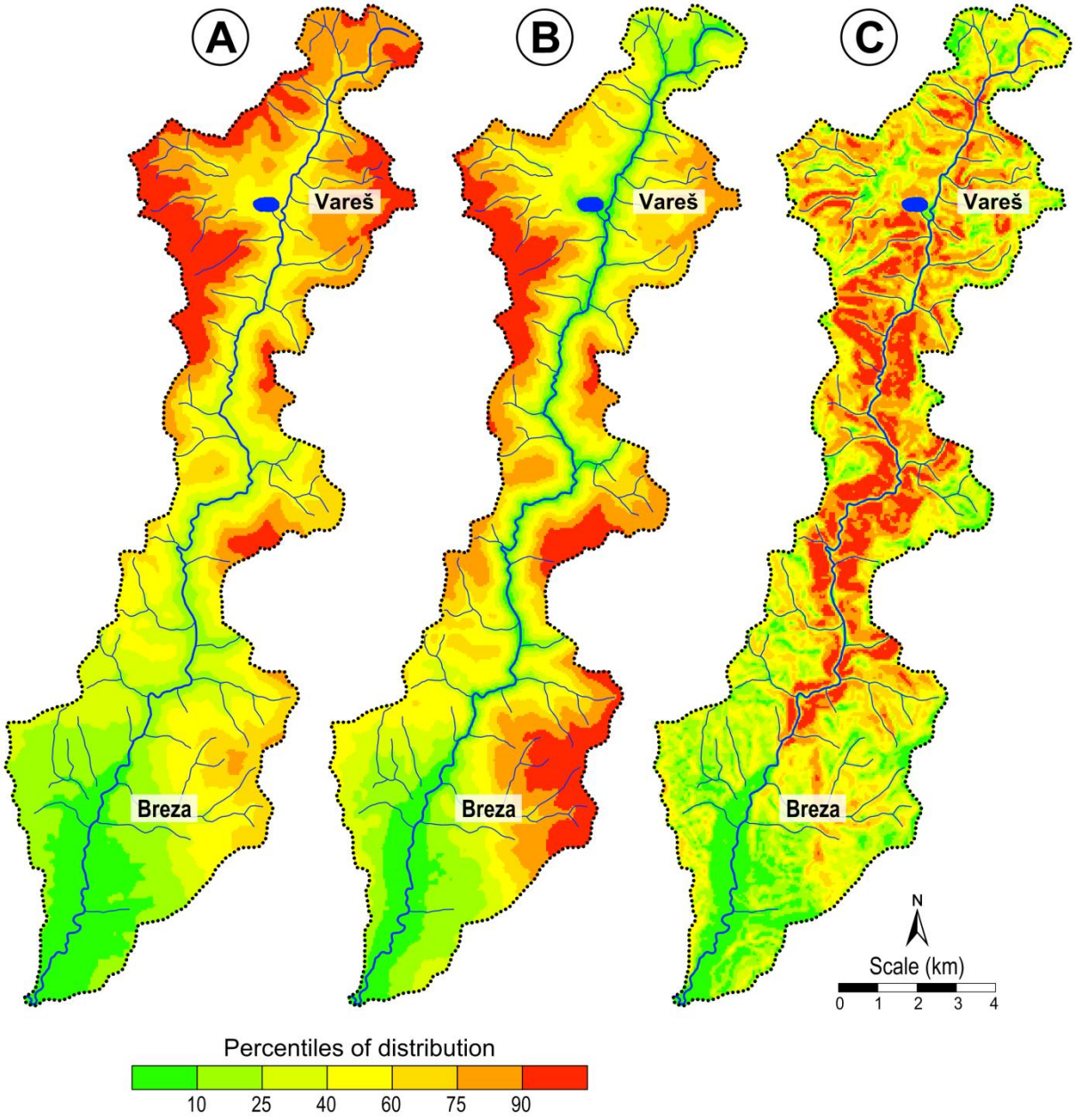

Figure 14: A – Altitude above the sea level (absolute); B – Altitude above the bottom of Stavnja valley (relative); C – Terrain Slope

measures the curvature of the surface in the direction of gradient. Negative curvature, shown with a gray fill, indicates a convex upward surface and accelerated water flow. Tangential Curvature (Figure 15c) measures curvature in relation to a vertical plane perpendicular to the gradient direction, or tangential to the contour. The negative and positive areas are the same as for Plan Curvature, but the curvature values are different. Tangential Curvature measures the curvature of the surface in the vertical plane perpendicular to the gradient direction. Negative curvature, displayed with gray fill, indicates divergent flow conditions.

The mathematical definitions, general review of the methods, and applications of topographic analysis (terrain slope, terrain aspect, plan curvature, profile curvature and tangential curvature) were taken from Mitasova and Hofierka (1993) and Moor et al. (1993).

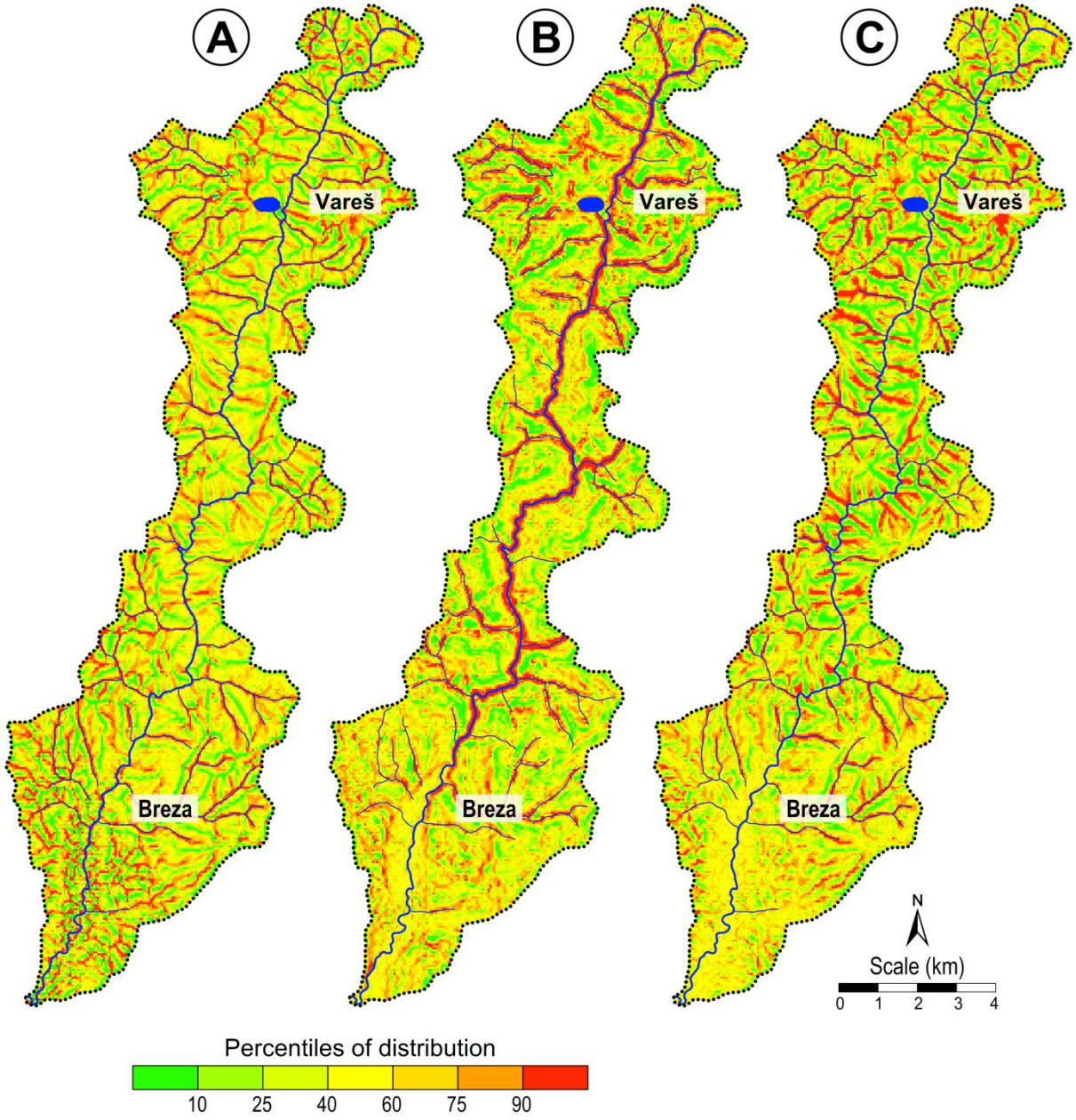

Figure 15: A – Plan terrain curvature, B – Profile terrain curvature, C – Tangent terrain curvature

4.1.3. Satellite images

Since 1972, Landsat satellites have continuously acquired space based images of the Earth's land surface, coastal shallows, and coral reefs. A joint effort of the U.S. Geological Survey (USGS) and the National Aeronautics and Space Administration (NASA), was established to routinely gather land imagery from space. Landsat satellites have since provided worldwide science and resourcemanagement communities with an archive of spacebased land remotely sensed data - a valuable resource for people who work in agriculture, geology, forestry, education, regional planning, mapping, and global change research (U.S. Geological Survey, 2011c).

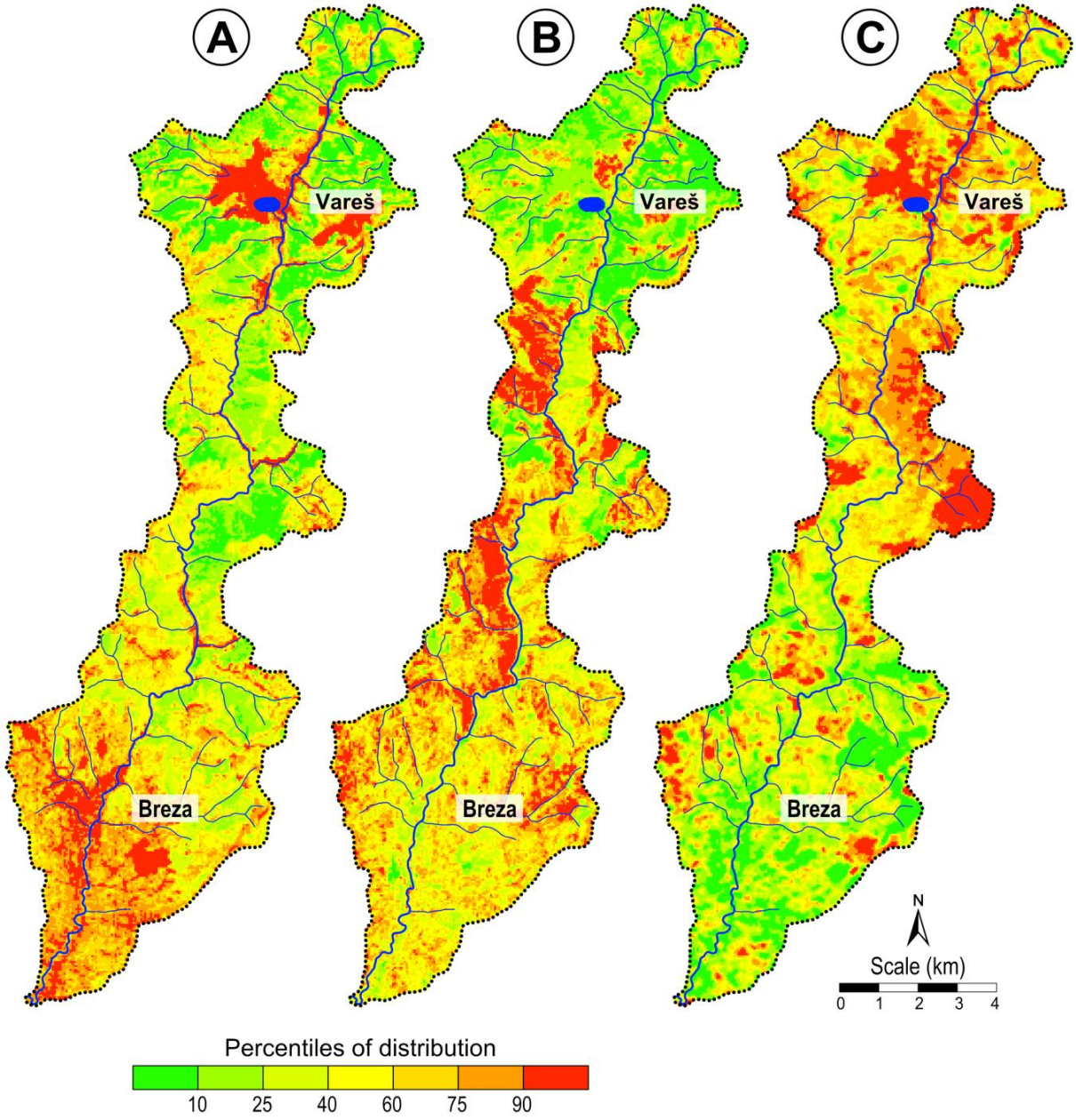

Figure 16: Relative intensity of radiation Landsat spectral bands. A – Visible spectrum, 0.45 – 0.69 µm (Bands 1-3); B – Infrared spectrum, 0.76 – 0.90 µm (Band 4); C– Thermal radiation, 10.4-12.5 µm

Landsats 5 and 7 each complete approximately 14 full orbits of the Earth each day. While each satellite has a 16-day full Earth coverage cycle, their orbits are offset to allow 8-day repeat coverage of any Landsat scene area on the globe. Landsat 7 carries the Enhanced Thematic Mapper Plus (ETM+), with 30-meter visible, near-IR, and shortwave infrared bands, a 60-meter spatial resolution thermal band, and a 15-meter panchromatic band (Table 2).

Moreover, since 2008 the USGS) has freely provided all archived Landsat images, along with newly acquired Landsat 7 (launched in 1999) ETM+ SLC-off and Landsat 5 (launched in 1984) TM images with less than 40% cloud cover , thereby enabling free access to multiple images of the same sectors. Each band of Landsat data in the GeoTIFF format is delivered as a grayscale, uncompressed, 8-bit

string of unsigned integers.GeoTIFF is a format that enables referencing a raster image to a known geodetic model or map projection. A metadata (MTL) file is included with data processed through the Level-1 Product Generation System (LPGS). A file containing the ground control points (GCP) used during image processing is also included. A processing history (WO) file is included with data processed through the National Landsat Archive Production System (NLAPS) (U.S. Geological Survey 2011c).

Table 2: Landsat spectral bands

Spectral bands	Wavelength (μm)	Resolution (ms)	Use
Band 1 (blue)	0.45–0.52	30	Bathymetric mapping; distinguishes soil from vegetation; deciduous from coniferous vegetation.
Band 2 (green)	0.52–0.61	30	Emphasizes peak vegetation, which is useful for assessing plant vigor.
Band 3 (red)	0.63–0.69	30	Emphasizes vegetation slopes.
Band 4 (IR)	0.76–0.90	30	Emphasizes biomass content and shorelines.
Band 5 (IR)	1.55–1.75	30	Discriminates moisture content of soil and vegetation; penetrates thin clouds.
Band 6 (thermal)	10.4–12.5	120/60	Useful for thermal mapping and estimated soil moisture.
Band 7 (IR)	2.08–2.35	30	Useful for mapping hydrothermally altered rocks associated with mineral deposits.

In order to evaluate the capability of mapping contaminated areas from both Landsat TM and ETM data, we processed and analysed two available images for the study area (187 path and 29 row): one acquired by the TM sensor on 1990 and one acquired by ETM on 2005. The selected scenes provided cloud-free pixels. Extracting information from satellite imagery often involves image interpretation techniques as well as GIS integration of other spatial data. Multispectral satellite imagery offers several advantages, such as: a large number of data records, the availability of repeated images of a single place at different times, and the fact that virtually the entire planet is covered. We used images from 1990, in period of intensive mining and smelting and from 2005 after the civil war, period when the production was stopped (Figures 2 and 16).

4.2. Statistic methods

All statistical analyzes were performed in the software Statistica 11 (Stat Soft Inc., 2012) in the next modules: Basic Statistic/Tables (basic statistic), ANOVA (analysis of variance), SANN (automated neural networks) and GRM (general regression models).

4.2.1. Basic statistic

Much of statistics therefore, deals with the organization, presentation, and summary of data. One of the most common and useful presentation of data sets is the frequency table and its corresponding graph, the histogram. The important features of most histograms can be dividing into three categories: measures of location (mean, geometric mean, median, etc.), measures of spread (standard deviation) and measure of shape (skewness, kurtosis and the coefficient of variation).

The mean (X), is the arithmetic average of the data values. The geometric mean (X_G) is the product of all scores to the power of 1/n (one over the valid number of cases). The geometric mean is useful in instances when we know that the measurement scale is not linear. Note that if a variable contains negative values or a zero (0), then the geometric mean cannot be calculated. The median (Md) value is the value that "splits the sample in half," given the respective variable. Fifty percent of the cases will fall below the median, and fifty percent will fall above the median. If the median value is very different from the mean, then the distribution of data is skewed (Isaaks and Srivastava, 1989). The standard deviation (S) is simply the square root of the variance. It is often used instead of the variance since its units are the same as the unit of variable being describe. The standard error of the mean (S_X) gives an indication of how close a sample mean might be to the population mean. The standard error of the sample mean is given by the square root of the sample size. This means that the larger the sample size, the smaller the standard error of the mean. More specifically, the size of the standard error of the mean is inversely proportional to the square root of the sample size (Harris, et al., 2005).

The most commonly used statistic for summarizing the symmetry is a quantity called the coefficient of skewness (A). The coefficient of skewness suffers even more than the mean and variance from sensitivity to erratic high values. A single large value can heavily influence the coefficient of skewness since the difference between each data value and the mean is cubed. In geochemical data sets, positive skewness is typical when the variable being described is the concentration of a minor element. The coefficient of kurtosis (E) is a measure of how "wide" or "skinny" ("flat" or "peaked") the distribution is for the respective variable, relative to the standard normal distribution (for which the kurtosis is equal to 0). It is also sometimes referred to as the fourth moment of the distribution. Higher kurtosis means more of the variance is the result of infrequent extreme deviations, as opposed to frequent modestly sized deviations. The coefficient of variation (CV) is a statistic that is often used as an alternative to skewness to describe the shape of the distribution. It is used primarily for distribution whose values are positive and whose skewness is also positive; though it can be calculated for other type of distribution, its usefulness as an index of shape becomes questionable. It is defined as the ratio of the standard deviation to the mean. A coefficient greater than one, indicates the presence of some erratic high sample values that may have a significant impact on the final estimation.

The Kolmogorov – Smirnov test (KS) is nonparametric test of equality of onedimensional probability distributions used to compare a sample with a reference probability distribution (one-tiled KS test), or to compare two samples (two-tiled KS test). Simply, KS test tries to determine if two datasets differ significantly. The advantage of this test lies in the fact that in a comparison with a continuous theoretical distribution it is not necessary to construct discrete classes first since here one measures the maximum difference between the cumulative distribution function. The Kolmogorov–Smirnov test can be modified to serve as a goodness of fit test. The Chi-Square test (χ^2) is a statistical test commonly used to compare observed data with data we would expect to obtain according to a specific hypothesis. This test checks the null hypothesis that a set of measurements can be taken as a sample of a random variable with a given distribution(Honerkamp, 2002;Stat Soft Inc., 2012).

4.2.2. Data transformation

Transforming data means performing the same mathematical operation on each piece of original data. If the original data is simply multiplied or divided by a specific coefficient or a constant is subtracted or added we talk about linear transformations. But these linear transformations do not change the shape of the data distribution and, therefore, do not help to make data look more normal.

It is often observed that environmental variables are Log-normal (Krige, 1951, 1960; Rose at al., 1979) or positively skewed (Zhang et al., 1995; Zhang and Selinus, 1998), and data transformation is

necessary to normalise such data sets. Logarithmic transformation is widely applied in order to normalise positively skewed data sets. However, it is observed that data sets in environmental sciences do not always follow the Log-normal distribution (Zhang C.S and Zhang S., 1996; Zhang and Selinus, 1998). In such cases, a power transformation is needed, and Box–Cox transformation is one of the most frequently used of these (Box and Cox, 1962; Jobson, 1991; Zhang C.S. and Zhang, C. 1996; Zhang et al., 1998; McGrath, et al., 2004). Each data transformation can dampen the difference between extreme values (Gringarten and Deutsch, 2001).

The Box-Cox transformation is given by:

$$y = \frac{X^{\lambda}-1}{\lambda}; \quad \lambda \neq 0 \qquad (1)$$

$$y = ln(\lambda);\ \lambda = 0 \qquad (2)$$

where y is the transformed value, and x is the value to be transformed. For a data set (x_1, x_2 … x_n), the parameter λ is estimated based on the assumption that the transformed values (y_1, y_2 … y_n) are normally distributed. When λ=0, the transformation becomes the logarithmic transformation.

4.2.3. Analysis of variance (ANOVA)

Analysis of variance is the most widely used tool of modern (post-1950) statistics by researcher workers in the substantive fields of biology, chemistry, sociology, education, agriculture and so forth. The methodology was originally developed by Sir Ronald A. Fisher who gave the name of “analysis of variance”. Nowadays, the analysis of variance models are widely used to analyse the effects of the independent variables under study on the dependent variable or response measure of interest. It is a technique by which variations associated with different factors or defined sources may be isolated and estimated. The purpose of analysis of variance (ANOVA) is to test for significant differences between means by comparing variances. More specifically, by partitioning the total variation into different sources (associated with the different effects in the design), we are able to compare the variance due to the between groups (or treatments) variability with that due to the within groups (treatment) variability. Under the null hypothesis (that there are no mean differences between groups or treatments in the population), the variance estimated from the within groups (treatment) variability should be about the same as the variance estimated from between groups (treatments) variability (Sahai and Ageel, 2000).

F-test is any statistical test in which the test statistic has an F-distribution under the null hypothesis. It is most often used when comparing statistical models that have been fit to a data set, in order to identify the model that best fits the population from which the data were sampled. Exact F-tests mainly arise when the models have been fit to the data using least squares.

4.2.4. Enrichment ratio

The enrichment ratio (ER), defined as the ratio of grade of a metal element in a deposit to the crustal abundance of the metal, is proposed for assessing mineral resources. According to the definition, the enrichment ratio of a polymetallic deposit is given as a sum of enrichment ratios of all metals (Shoji, 2002). This ratio has been calculated by dividing the average concentrations regarding to sampling material, determined zones or soil layer. This simple ratio does not need any normalization, because it is based on previously defined the groups of elements. These calculations the contribution of

anthropogenic influence with trace has been detected, and makes this ratio very useful. Using these ratios it was possible to reveal an increase or decrease between various sampling material such as soil, attic dust, moss, stream sediments or between material that contain background values and increased values. Even it is very simple ratio, but provides a much better measure for comparison and has been used in many studies (Balabanova et al., 2010; Stafilov et al., 2010a,2010b; Bačeva et al., 2011; Balabanova et al., 2011; Šajn et al., 2012).

4.3. The multivariate statistical method

Multivariate analysis involves observation and analysis of more than one statistical variable at a time. The technique is used to perform trade studies across multiple dimensions while taking into account the effects of all variables on the responses of interest.

4.3.1. Bivariate statistical method (correlations)

Statistical relationships between two variables can be measured by correlation. Correlations are useful because they can indicate a predictive relationship that can be exploited in practice. In general statistical usage, correlation can refer to any departure of two or more variables from independence, but most commonly refers to a more specialized type of relationship between mean values. Measure of the correlation between two variables is expressed by correlation coefficient, and the most common is Pearson correlation coefficient (r), which is mainly sensitive to a linear relationship between two variables. Other correlation coefficients have been developed to be more robust than the Pearson correlation, or more sensitive to nonlinear relationships.

The correlation coefficient (r) is actually a measure of how close the observed values come to falling on a straight line. If correlation $r = +1$, then the scatterplot will be a straight line with a positive slope; if $r = -1$, then the scatterplot will be a straight line with a negative slope. For $|r| < 1$ the scatterplot appears as a cloud of points that becomes fatter and more diffuse as $|r|$ decreases from 1 to 0. It is important to note that r provides a measure of the linear relationship between two variables. If the relationship between them is not linear, the correlation coefficient may be a very poor summary statistic.

4.3.2. The cluster analysis

Cluster analysis is a generic name for a variety of mathematical methods, numbering in the hundreds that can be used to find out which objects in a set are similar. Mathematical methods of cluster analysis accomplish this mathematically. Instead of sorting real objects, these methods sort objects described as data. Objects with similar descriptions are mathematically gathered into the same cluster. For a variety of research goals, researches need to find out which objects in a set are similar and dissimilar. The best known of these research goals is the making of classifications. One reason that cluster analysis is so useful is that researches in all fields need to make and revise classification continually.

Most common applications used certain methods of hierarchical cluster analysis. Methods of hierarchical clustering follow a prescribed set of steps, the main ones being: (1) collect a data matrix whose columns stand for the objects to be cluster analysed and whose rows are the attributes that describe the objects; (2) optionally standardize the data matrix; (3) using the data matrix or the standardized data matrix, compute the values of a resemblance coefficient to measure the similarities

among all pairs of objects; (4) use a clustering method to process the values of the resemblance coefficient, which results in a diagram called a tree, or dendrogram, that shows the hierarchy of similarities among all pairs of objects. From the tree the clusters can be read off. But within these steps there is the freedom to choose among alternative ways of standardizing the data matrix, of choosing a resemblance coefficient, and of choosing a clustering method (Romesburg, 2004).

Cluster analysis is not one method, but type of proceedings, that is used to arrange a set of cases into clusters. The aim is to establish a set of clusters such that cases within a cluster are more similar to each other than they are to cases in other clusters (Templ et al., 2008). Known is more cluster techniques, which are based on agglomeration more elements according to their composition, giving different results. Hierarchical clustering is chosen based on correlation coefficient (r).

4.3.3. The factor analysis

Factor analysis is not a single statistical method but rather represents a complex array of structureanalysing procedures used to identify the interrelationship among a large set of observed variables. Factor analysis can be used for theory and instrument development and assessing construct validity of an established instrument when administered to a specific population. Once the international structure of a construct has been established, factor analysis may also be used to identify external variables that appear to relate to the various dimension of the construct of interest.

There are two basic types of factor analysis: exploratory and confirmatory. Exploratory factor analysis (EFA) is used when the researcher does not know how many factors are necessary to explain the interrelationship among a set of characteristics, indicators, or items. Therefore, the researcher uses the techniques of FA to explore the underlying dimensions of the construct of interest. In Contrast, confirmatory factor analysis (CFA) is used to assess the extent to which the hypothesized organization of a set of identified factors fits data. It is used when the researcher has some knowledge about underlying structure of the construct under investigation. CFA could also be used to test the utility of the underlying dimensions of a construct identified through EFA, to compare factor structures across studies, and to test hypotheses concerning the linear structural relationship among a set of factor associated with a specific theory or model (Pett et al., 2003).

Factor analysis (FA) derives from numerous variables a smaller number of new, synthetic variables called factors (Le Maitre, 1982). The factors contain large part information of original variables, and they may have certain meanings. The factor analysis was performed on variables standardized to zero mean and unit of standard deviation (Davis, 1986; Reimann et al., 2002; Filzmoser, 2005). As a measure of similarity between variables, the productmoment correlation coefficient (r) was applied. For orthogonal rotation, the varimax method was used.

4.4. Prediction methods

4.4.1. Kriging (Segment Kriging)

Since the methods were first developed by Krige for use in the mining industry and formalized by Matheron (1971), various forms of kriging have been devised. The Kriging interpolation algorithms are an important group of geostatistical techniques, which have played an important role in many geological fields (Van Beers and Kleijnen, 2004). Over the last 20 years, geostatistical methods like kriging have been used successfully to investigate the spatial variability of continuously varying environmental parameters and to incorporate this information into mapping (Burrough and Mc Donnell,

1998). Geostatistics provides an advanced methodology which facilitates quantification of the spatial features of soil parameters and enables spatial interpolation (Stein et al., 1997; Carlon et al., 2001). In addition, geostatistics has become a useful tool for the study of spatial uncertainty and hazard assessment (Goovaerts, 1999, 2001).

The geostatistics approach consists of two parts: one is the calculation of an experimental variogram from the data and the model fitting, and the second is the estimation or prediction at unsampled locations. The variogram model mathematically specifies the spatial variability of the data set and the resulting grid file. The interpolation weights, which are applied to data points during the grid node calculations, are direct functions of the variogram model.

A variogram (or semi-variogram) is used to measure the spatial variability of a regionalized variable, and provides the input parameters for the spatial interpolation of variogram kriging (Webster and Oliver, 2001). It can be expressed as:

$$\gamma(x) = \frac{1}{2N(h)} \sum_{i=1}^{N(h)} [(Zx_i) - Z(x_i + h)\,] \qquad (3)$$

where γ(h) is the semivariance at a given distance h; $Z(x_i)$ is the value of the variable Z at the xi location, and N(h) is the number of pairs of sample points separated by the lag distance h. If the variogram rises and stabilises around some value, then it has reached a sill (C); i.e. theoretically the sample variance. It could be the case that the variogram does not reach a sill, indicating that it corresponds to phenomena with an unlimited capacity for dispersion. The distance at which the variogram reaches the sill is called the range (a); beyond it, data are independent. Discontinuities at the variogram origin could be present; such an unstructured component of variation at h=0 is known as nugget effect (Co) which may be due to sampling errors and short scale variability. The calculation of the variogram is done in several orientations to assess if the spatial variability is the same in all directions. If it is, the distribution is called isotropic, otherwise it is anisotropic. Then, the variogram plot is fitted with a theorical model, such as spherical, exponential, linear or Gaussian models. It is possible to have a combination of two or more models (nested structure), with a total variance result of added variances of each model. The fitted model provides information about the spatial structure as well as the input parameters for kriging interpolation. Among the several estimation methods, kriging is the most popular because it "is a collection of generalised linear regression techniques for minimising and estimating variance defined from a prior model for a covariance" (Olea, 1991).

Kriging is not just used to estimate unsampled areas it is also used to build probabilistic models of uncertainty about the unknown, but estimated predicted values (Deutsch and Journel, 1998). The kriging estimates can be mapped, to reveal the overall trend of data. Maps provide helpful visual displays of the spatial variability in the field and can be used for the summarization and representation of soil properties where natural hazards can be identified (Goodchild et al., 1993). As in conventional statistics, a normal distribution for the variable under study is desirable in linear geostatistics (Clark and Harper, 2000). To increase the accuracy of the geological model, Kriging on a large data set is a necessity but also computationally demanding. Although the storage requirements only scale linearly with the number of observations in the dataset, the computational complexity in terms of memory and speed, scale quadratically and cubically respectively (Ingram and Cornford, 2010).

The kriging method used in the thesis is modified. In case we know a geological composition of the study area, it is possible to use this innovative and modified method of kriging in individual units in case the chemistry of parental material is showing extreme anomaly, comparing to the surrounding population. Good examples are: Pb distribution, which concentrations are in Quaternary alluvium than in automorphic soil or distribution of Cr and Ni on the Jurassic and Cretaceous clastic carbonate series. They exceed for several times or several ten times exceed from other population level

variation. The same can be observed for Ti distribution on the Triassic clastites, spilite and tuff. Using this method we are entering some kind of subjectivity, but we avoid so called “Bull’s effect”, which is typical in such cases. Extremely high differences on small distances cannot be properly solved by any polynomial.

4.4.2. Multiple Polynomial Regressions

Multiple regression is a statistical method for studying the relationship between a single dependent variable and one or more independent variables. There are two major uses of multiple regression: prediction and causal analysis. In a causal analysis, the independent variables are regarded as causes of the dependent variable (Allison, 1999).

Multiple polynomial regression (MPR) is a form of linear regression in which relationship between the independent variable *x* and the dependent variable *y* is modelled as an *n*th order polynomial. Multiple polynomial regression fits a linear relationship between the value of *x* and the corresponding conditional mean of *y*, and has been used to describe linear phenomena. Although polynomial regression fits a nonlinear model to the data, as a statistical estimation problem it is linear, in the sense that the regression function E(*y*|*x*) is linear in the unknown parameters that are estimated from the data. For this reason, polynomial regression is considered to be a special case of multiple linear regression. The goal of regression analysis is to model the expected value of a dependent variable *y* in terms of the value of an independent variable (or vector of independent variables) *x*. In simple linear regression, the model:

$$\gamma = a_0 + a_1 x + \varepsilon \qquad (4)$$

is used, where ε is an unobserved random error with mean zero conditioned on a scalar variable *x*. In this model, for each unit increase in the value of *x*, the conditional expectation of *y* increases by a_1 units.

In general, we can model the expected value of *y* as an *n*th order polynomial, yielding the general polynomial regression model:

$$\gamma = a_0 + a_1 x + a_2 x^2 + a_3 x^3 + \cdots + a_m x^m + \varepsilon \qquad (5)$$

Conveniently, these models are all linear from the point of view of estimation, since the regression function is linear in terms of the unknown parameters a_0, a_1 ... a^m. Therefore, for least squares analysis, the computational and inferential problems of polynomial regression can be completely addressed using the techniques of multiple regression. This is done by treating *x*, x^2 ... x^m as being distinct independent variables in a multiple regression model.

Although polynomial regression is technically a special case of multiple linear regressions, the interpretation of a fitted polynomial regression model requires a somewhat different perspective. It is often difficult to interpret the individual coefficients in a polynomial regression fit, since the underlying monomials can be highly correlated. The correlation can be reduced by using orthogonal polynomials.

Polynomial regression is one example of regression analysis using basis function to model a functional relationship between two quantities. A drawback of polynomial bases is that the basic functions are "non-local", meaning that the fitted value of *y* at a given value $x = x_0$ depends strongly on data values with *x* far from x_0 (Magee, 1998).

The goal of polynomial regression is to model a nonlinear relationship between the independent and dependent variables (technically, between the independent variable and the conditional mean of the dependent variable). This is similar to the goal of nonparametric regression, which aims to capture nonlinear regression relationships. Therefore, nonparametric regression approaches such as smoothing can be useful alternatives to polynomial regression. Some of these methods make use of a localized form of classical polynomial regression (Isaac et al., 2012).

The MPR model provides information regarding the influence of the combined interactions of the estimator variables on the response, the major conceptual limitation of the regression techniques is that one can only ascertain relationships, but never be sure about the underlying casual mechanism (Sahu et al., 2009 and Singh et al., 2010).

Polynomial regression models are usually fit using the method of least square, because it is a standard approach to the approximate solutions of systems with more equations than unknown variables. But this method has not given good results as a cubic polynomial regression. During the method development, and after many different regressions approaches, the cubic polynomial regression gave the best results for the set of data used in the thesis.Even this method is very demanding and time consuming due to fact that several data transformation and conversion had to be done prior its application. The polynomial multiple regressions fitted the most of predicted results.

4.4.3. Artificial neural networks (Multilayer perceptron)

A neural network is a system of programs and data structures that approximate the operation of the human brain. The main challenge, in addition to acquiring sufficient field and analytical data to model the relationships between each, is to actually produce a modelling system that can handle a large number of input and output parameters. There are many statistical and expert system approaches capable of handling complex mathematical transformations of this nature, but one approach that is relatively easy to implement, reliable and popular for this type of work is artificial neural networks (ANNs) (Aitkenhead et al., 2012). These have been used extensively in environmental modelling where parameter modelling using large, noisy datasets has been a requirement. Their use in modelling soil characteristics is well demonstrated (Aitkenhead et al., 2007; Elshorbagy and Parasuraman, 2008; Anagu et al., 2009; Aitkenhead et al., 2012).

The success of the method can be laid down to the following reasons: (A) They can model extremely complex systems and due to their nature can be used to model nonlinear natural systems (linearity in the sense of mathematical properties of additivity and homogenuosity); when using linear algebra (ie most of multivariate statistics) to describe nonlinear systems we always have to make an approximations; (B) There is no limitation with the dimensionality of the problem; it can be arbitrary, depending on the CPU speed and memory; (C) Due to well developed learning algorithms they are easy to use (Žibret and Šajn, 2010; Žibret et al., 2012)

A neuron is a processing unit in a neural network. It is a node that processes all fan-in from other nodes and generates an output according to a transfer function called the activation function. The activation function represents a liner or nonlinear mapping from the input to the output and is denoted by $\sigma(\xi)$. A neuron is linked tp other neurons by variable synapses (weights). Simple neuron model have been proposed by McCulloch and Pitts. The McCulloch and Pitts model, however, contains a number of simplifying assumptions that do not reflect the true behaviour of biological neurons (Figure 17).

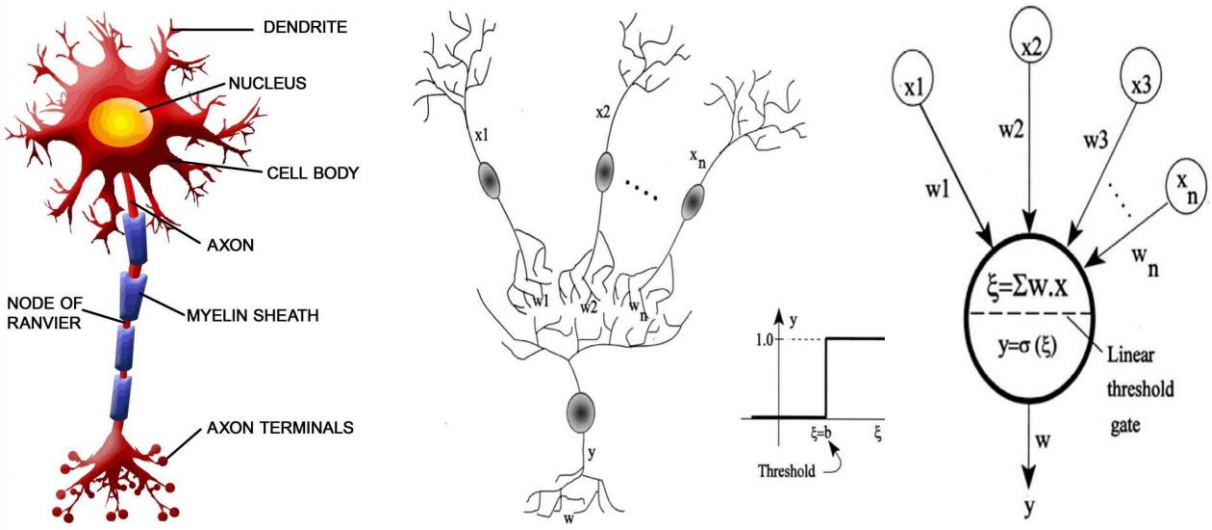

Figure 17: Biological neuron (left) and a mathematical model of McCulloch and Pitts neuron (right)

The output of neuron is given by:

$$\xi = \sum_{i=1}^{n} w_i x_i - b = w^T x - b \qquad (6)$$

$$y = \sigma(\xi) \qquad (7)$$

where x_i is the *i*th input, w_i is the link weight from the *i*th input, $w = (w_i...w_n)^T$, $x = (x_1...x_n)^T$, b is a threshold or bias, and n is the number of inputs. The activation function $\sigma(\xi)$ is usually some continuous or discontinuous function mapping the real numbers into the interval (-1,1) or (0,1) (Du and Swamy, 2006).

Different function can be used as activation function but the most used is sigmoidal activation function. Standard sigmoidal activation function has the following form:

$$\sigma(\xi) = \frac{1}{1 + e^{-\xi}} \qquad (8)$$

There is only 1 output drawn on Figure 18, but the number of outputs can be arbitrary. There are also other types of neurons, such as neurons with radial basis activation function or neurons in topologically ordered computational maps, also called Kohonen maps and many others. In every neural network we can also find input neurons where the data is presented in the network and output units where we can read processed data. The interconnected network of these three basic units can be called neural network (Haykin, 1999; Kohonen, 2001).

Multilayer perceptron (MP) is the earliest and the simplest neural network model. Rosenblatt used a single-layer perceptron for the classification of linearly separable patterns. The multilayer perceptrons can be used for the classification of linearly inseparable patterns, and can also work as universal approximators. MPs are feedforward neural networks (FNNs) with one or more layers of units between the input and output layers (Du and Swamy, 2006).

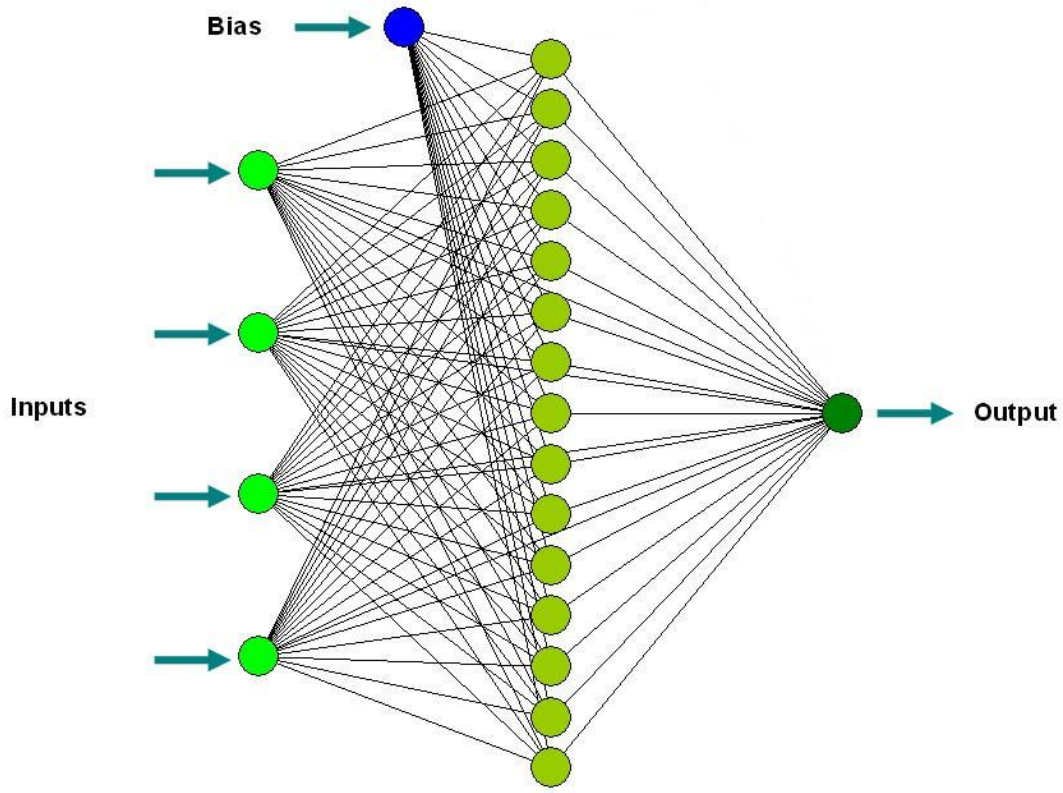

Figure 18: Multilayer perceptron architecture

Based on the connection pattern (architecture), ANNs can be grouped into two categories feedforward networks, in which graphs have no loops, and recurrent (or feedback) networks, in which loops occur because of feedback connections.

In the most common family of FNNs, neurons are organized into layers that have unidirectional connections between them. Different connectivity yield different network behaviors. Generally speaking, feedforward networks are static, that is, they produce only one set of output values rather than a sequence of values from a given input. Feedforward networks are memoryless in the sense that their response to an input is independent of the previous network state. Recurrent, or feedback, networks, on the other hand, are dynamic systems. When a new input pattern is presented, the neuron outputs are computed. Because of the feedback paths, the inputs to each neuron are then modified, which leads the network to enter a new state. Different network architectures require appropriate learning algorithms (Jain et al., 1996).

5. RESULTS AND DISCUSSION

5.1. Reliability of analyses

All samples and replicates were submitted to the laboratory in a random order. This procedure assured an unbiased treatment of samples and a random distribution of possible drift of analytical conditions for all samples.

Sensitivity of the analysis, in the sense of the lower limit of detection for 254 samples, was adequate for 33 out of 36 determined elements, i.e. B (242 samples), S (137 samples) and Se (129 samples) were below the lower detection limit and were removed from the final database used in the statistical analysis, since their contents in the majority of analyzed samples were below the lower detection limit of the analytical method or on detection limit of the analytical method (Table 3). Exceptions are Ag and W because it has less than one third under DL, and is used in further statistical analyses, because of their high content grouped and clearly show certain geochemical trends.

Geological standard materials DS7 (n=7), DS8 (n=5), OREAS45CA (n=7) and OREAS45PA (n=5) were used for estimating trueness (ACME Labs, 2010, 2011). Trueness of the analytical method for 36 elements was estimated by calculation of relative systematic error between determined (X_A) and recommended values (X_P) of geological standards using following equation:

$$T=\frac{|X_A - X_P|}{X_P}\ 100\ [\%] \qquad (9)$$

Most of the elements show very low deviations from the recommended range of values, i.e. the mean of all determined elements in the standards generally differs by less than 15% of the recommended values. Large absolute deviations were observed only for B, Mo, Sb and Na (Figure 19). Recommendation and analyzed values of the standard materials are listed in the Appendix E.

Precision is a measure of repeatability of determining a parameter in the same sample regardless of deviation from the true value (Rose at al., 1979). Precision (P) was tested by relative differences between pairs of analytical determinations (x_1, x_2) of the same sample using equation:

$$P=\frac{2|X_1 - X_2|}{(X_1+X_2)}\ 100\ [\%] \qquad (10)$$

Fifteen(2010, 2011) randomly selected samples were replicated for estimation of precision. Precision was considered good, since of the 36 elements only Na,V, Se and S showed large deviations greater than 15%. A very large deviation (> 50%) shows only the analysis of Au (Figure 20).

Estimation of trueness and precision of two analysed set of data had been performed by t-test (Harvey, 2000) (Table 4). According to the provided results of precission, it is clear that there is no significant differences between particular elements in both analysed sets of data (2010, 2011) but results of trueness showing several significances: Au, Hg, Sb, and Sr (DS7); Cr, Mn, Mo, and Sb (OREAS45PA); and Co, Na, and V (OREAS45CA). The results of analysis of duplicate samples for precision estimation are listed in the Appendix F.

The reliability of analytical procedures was considered adequate for majority of analyzed elements for using the determined elemental contents in further statistical analyses. Four following elements Au, B, S and Se are removed from the further statistical analyses.

Table 3: Number of measurements under DL and above UL (n=254)

	Unit	DL	UL	Min	Max	N (DL)	N (UL)
Ag	mg/kg	0.1	100	<0.10	11	75	-
Al	%	0.01	10	0.62	3.8	-	-
As	mg/kg	0.5	10000	3.7	590	-	-
Au	µg/kg	0.5	100	<0.50	44	31	-
B	mg/kg	20	2000	<20	92	242	-
Ba	mg/kg	1	10000	14	1700	-	-
Bi	mg/kg	0.1	2000	0.10	13	-	-
Ca	%	0.01	40	0.070	16	-	-
Cd	mg/kg	0.1	2000	0.10	14	-	-
Co	mg/kg	0.1	2000	1.9	64	-	-
Cr	mg/kg	1	10000	10	460	-	-
Cu	mg/kg	0.1	10000	5.3	450	-	-
Fe	%	0.01	40	0.98	19	-	-
Ga	mg/kg	1	1000	2.0	10	-	-
Hg	mg/kg	0.01	50	0.040	3.7	-	-
K	%	0.01	10	0.060	0.50	-	-
La	mg/kg	1	10000	2.0	40	-	-
Mg	%	0.01	30	0.070	4.1	-	-
Mn	mg/kg	1	10000	200	>10000	-	1
Mo	mg/kg	0.1	2000	0.10	17	-	-
Na	%	0.001	5	0.001	1.0	-	-
Ni	mg/kg	0.1	10000	4.0	500	-	-
P	%	0.001	5	0.015	0.27	-	-
Pb	mg/kg	0.1	10000	25	2800	-	-
S	%	0.05	10	<0.050	4.4	137	-
Sb	mg/kg	0.1	2000	<0.10	88	5	-
Sc	mg/kg	0.1	100	0.70	11	-	-
Se	mg/kg	0.5	100	<0.50	8.8	129	-
Sr	mg/kg	1	10000	4.0	320	-	-
Th	mg/kg	0.1	2000	0.20	6.6	-	-
Ti	%	0.001	5	<0.001	0.23	12	-
Tl	mg/kg	0.1	1000	0.10	2.5	-	-
U	mg/kg	0.1	2000	0.20	3.7	-	-
V	mg/kg	2	10000	<2.0	130	1	-
W	mg/kg	0.1	100	<0.10	16	98	-
Zn	mg/kg	1	10000	43	7100	-	-

DL – Detection limit; UL – Upper limit; Min – minimum (all samples), Max – Maximum (all samples); N (DL) – number of measurement under DL; N (UL) – number of measurement above DL

In order to reduce a dimensionality of tables and images, beside the aforementioned four elements (Au, B, S and Se), following six elements Ca, K, Na, P, Sr, and U were eliminated from the further analysis, in case they are not showing a logical connection with other chemical elements or their tendency to form independent cluster or factors in the application of multivariate statistical analysis. So following 26 elements: Ag, Al, As, Ba, Bi, Cd, Co, Cr, Cu, Fe, Ga, Hg, La, Mg, Mn, Mo, Ni, Pb, Sb, Sc, Th, Ti, Tl, V, W and Zn have been used in further statistical treatments.

Table 4:Estimation of trueness and precision on the basis of t-test regarding to analysed set of samples

	Precision (2010)	Precision (2011)	DS7 (2010)	DS8 (2011)	OREAS45PA (2010)	OREAS45CA (2011)
Ag	0.04$^{N.S.}$	-0.02$^{N.S.}$	-1.59$^{N.S.}$	-0.64$^{N.S.}$	-1.37$^{N.S.}$	-0.25$^{N.S.}$
Al	0.07$^{N.S.}$	-0.03$^{N.S.}$	1.04$^{N.S.}$	-0.41$^{N.S.}$	-0.93$^{N.S.}$	0.48$^{N.S.}$
As	0.15$^{N.S.}$	0.01$^{N.S.}$	1.69$^{N.S.}$	1.72$^{N.S.}$	0.49$^{N.S.}$	-0.07$^{N.S.}$
Au	-0.10$^{N.S.}$	-0.81$^{N.S.}$	-2.68*	-0.10$^{N.S.}$	-1.78$^{N.S.}$	-0.76$^{N.S.}$
B	–	–	-1.00$^{N.S.}$	–	–	–
Ba	0.02$^{N.S.}$	-0.11$^{N.S.}$	2.11$^{N.S.}$	-1.83$^{N.S.}$	0.19$^{N.S.}$	-0.90$^{N.S.}$
Bi	-0.01$^{N.S.}$	0.21$^{N.S.}$	0.61$^{N.S.}$	0.61$^{N.S.}$	–	–
Ca	-0.01$^{N.S.}$	-0.05$^{N.S.}$	0.29$^{N.S.}$	-0.69$^{N.S.}$	-1.30$^{N.S.}$	-1.02$^{N.S.}$
Cd	0.00$^{N.S.}$	0.00$^{N.S.}$	-0.69$^{N.S.}$	-0.15$^{N.S.}$	-0.40$^{N.S.}$	–
Co	0.14$^{N.S.}$	0.23$^{N.S.}$	-0.33$^{N.S.}$	-0.95$^{N.S.}$	0.41$^{N.S.}$	-3.34*
Cr	0.04$^{N.S.}$	0.09$^{N.S.}$	0.90$^{N.S.}$	-1.21$^{N.S.}$	-5.07*	-0.51$^{N.S.}$
Cu	0.02$^{N.S.}$	0.13$^{N.S.}$	-0.12$^{N.S.}$	-0.57$^{N.S.}$	-0.99$^{N.S.}$	-0.15$^{N.S.}$
Fe	0.01$^{N.S.}$	-0.05$^{N.S.}$	-0.23$^{N.S.}$	-0.46$^{N.S.}$	-0.96$^{N.S.}$	1.30$^{N.S.}$
Ga	0.42$^{N.S.}$	0.40$^{N.S.}$	-0.35$^{N.S.}$	-0.20$^{N.S.}$	-1.30$^{N.S.}$	-0.22$^{N.S.}$
Hg	-0.01$^{N.S.}$	0.08$^{N.S.}$	-2.52*	0.00$^{N.S.}$	-1.00$^{N.S.}$	0.41$^{N.S.}$
K	-0.05$^{N.S.}$	-0.04$^{N.S.}$	-0.38$^{N.S.}$	-1.00$^{N.S.}$	0.57$^{N.S.}$	-0.22$^{N.S.}$
La	-0.03$^{N.S.}$	-0.13$^{N.S.}$	2.12$^{N.S.}$	-0.37$^{N.S.}$	-1.75$^{N.S.}$	0.61$^{N.S.}$
Mg	0.02$^{N.S.}$	0.01$^{N.S.}$	-1.25$^{N.S.}$	-1.23$^{N.S.}$	0.57$^{N.S.}$	0.15$^{N.S.}$
Mn	0.06$^{N.S.}$	-0.03$^{N.S.}$	-0.52$^{N.S.}$	-0.29$^{N.S.}$	-4.24*	-1.74$^{N.S.}$
Mo	0.05$^{N.S.}$	0.00$^{N.S.}$	0.36$^{N.S.}$	-1.08$^{N.S.}$	4.21*	-1.63$^{N.S.}$
Na	0.08$^{N.S.}$	-0.03$^{N.S.}$	2.20$^{N.S.}$	-0.67$^{N.S.}$	-0.23$^{N.S.}$	4.69*
Ni	0.02$^{N.S.}$	0.05$^{N.S.}$	0.17$^{N.S.}$	0.23$^{N.S.}$	0.18$^{N.S.}$	-0.32$^{N.S.}$
P	0.05$^{N.S.}$	-0.14$^{N.S.}$	-0.96$^{N.S.}$	-0.65$^{N.S.}$	-1.08$^{N.S.}$	-1.61$^{N.S.}$
Pb	-0.01$^{N.S.}$	-0.03$^{N.S.}$	-0.27$^{N.S.}$	-0.19$^{N.S.}$	-0.82$^{N.S.}$	0.62$^{N.S.}$
S	0.07$^{N.S.}$	-0.09$^{N.S.}$	0.62$^{N.S.}$	-0.50$^{N.S.}$	–	–
Sb	0.04$^{N.S.}$	-0.04$^{N.S.}$	4.59*	-0.61$^{N.S.}$	5.48*	–
Sc	-0.02$^{N.S.}$	-0.16$^{N.S.}$	-1.10$^{N.S.}$	0.76$^{N.S.}$	-1.35$^{N.S.}$	-2.66$^{N.S.}$
Se	-0.20$^{N.S.}$	0.50$^{N.S.}$	0.21$^{N.S.}$	0.03$^{N.S.}$	-0.52$^{N.S.}$	0.17$^{N.S.}$
Sr	0.04$^{N.S.}$	-0.08$^{N.S.}$	2.71*	-0.21$^{N.S.}$	-0.19$^{N.S.}$	0.87$^{N.S.}$
Th	-0.08$^{N.S.}$	0.13$^{N.S.}$	0.49$^{N.S.}$	0.67$^{N.S.}$	0.53$^{N.S.}$	-0.84$^{N.S.}$
Ti	0.04$^{N.S.}$	-0.12$^{N.S.}$	0.31$^{N.S.}$	-0.34$^{N.S.}$	1.13$^{N.S.}$	-0.30$^{N.S.}$
Tl	0.05$^{N.S.}$	0.27$^{N.S.}$	-0.06$^{N.S.}$	-0.36$^{N.S.}$	–	–
U	0.02$^{N.S.}$	–	0.35$^{N.S.}$	–	-1.16$^{N.S.}$	–
V	0.04$^{N.S.}$	-0.19$^{N.S.}$	-0.47$^{N.S.}$	-1.84$^{N.S.}$	-1.80$^{N.S.}$	-5.66*
W	0.00$^{N.S.}$	-0.49$^{N.S.}$	0.91$^{N.S.}$	1.21$^{N.S.}$	–	–
Zn	0.08$^{N.S.}$	0.03$^{N.S.}$	-1.07$^{N.S.}$	-0.75$^{N.S.}$	-0.64$^{N.S.}$	0.49$^{N.S.}$

NS – no significance; * – significance at $p<0.05$

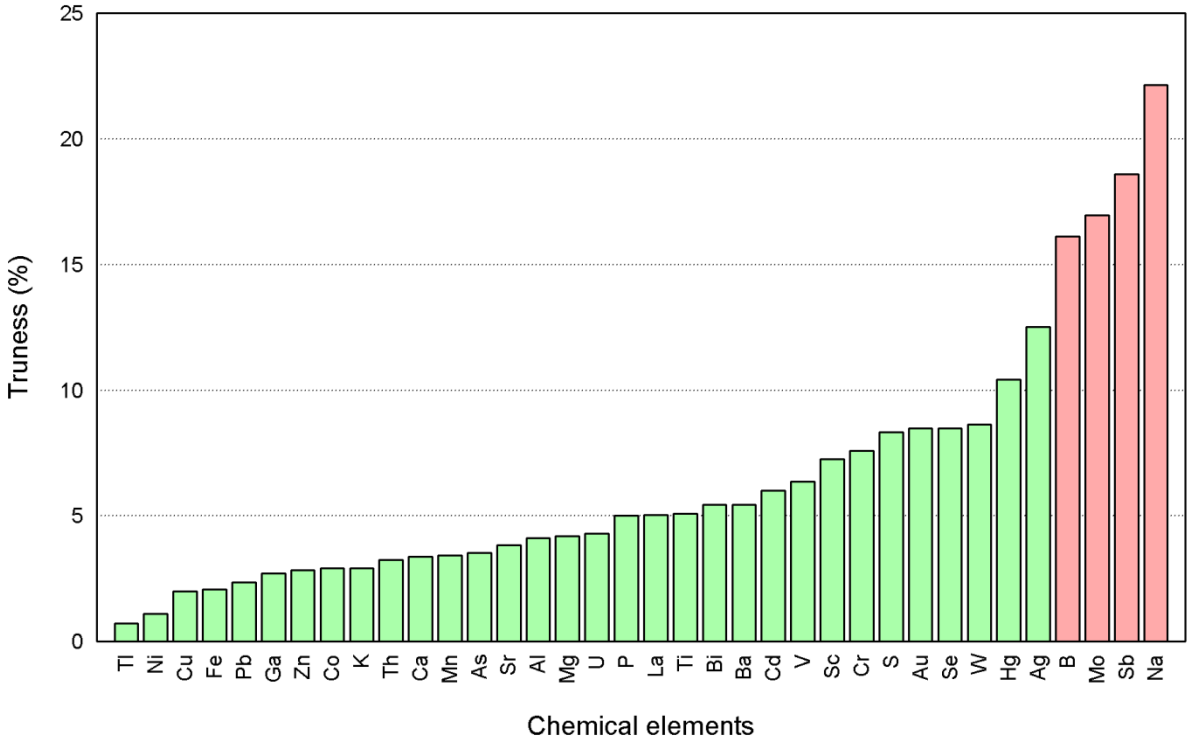

Figure 19: Average absolute trueness of analysed chemical elements

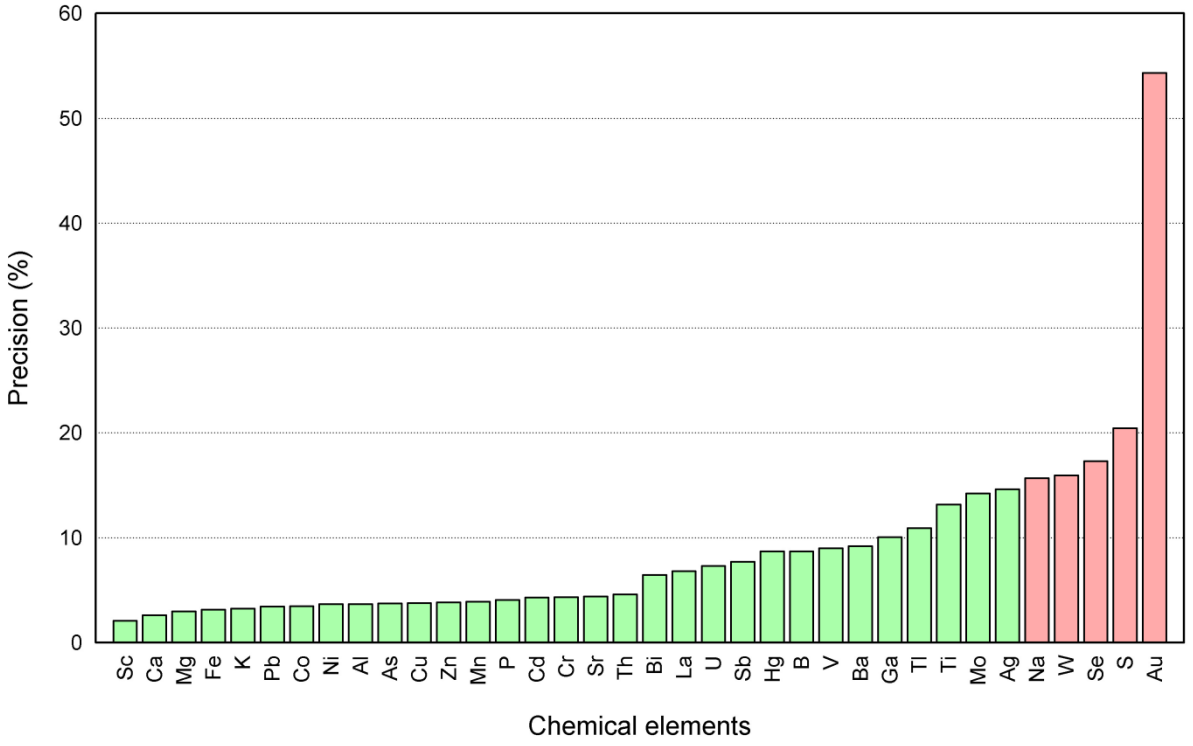

Figure 20: Precision of analysed chemical elements (n=15)

5.2. Basic chemical properties of sampling materials

The methods of parametric and nonparametric statistics were used and normality of data distributions were tested (Snedecor and Cochrane, 1967). Test of normal and Log-normal distribution in soil samples is showed in table 5. According to the results of normality tests and visual inspection of histograms for 26 elements in 222 soil samples, only 3 elements (Sc, Th, and V) have natural distribution. Normality for the other elements (Ag, Al, As, Ba, Bi, Cd, Co, Cr, Cu, Fe, Ga, Hg, La, Mg, Mn, Mo, Ni, Pb, Sb, Ti, Tl, W and Zn) was considered using logarithms values.

The distribution of data was tested for normality by skewness, kurtosis, Kolmogorov–Smirnov (KS) test, and Chi Square test (χ^2). The shape of physical and chemical properties distribution was described by skewness. The skewness and kurtosis are positive for elements that have the normal distribution. Similar pattern is observed for the Log-normal distribution, only several elements have a negative skewness or kurtosis. The positive kurtosis indicates a relatively peaked distribution whereas the negative one indicates a flat distribution compared to the normal distribution. The significance level tested at $p<0.01$ and $p<0.05$.

Table 5: Tests of Normal and Log-normal distribution – soil samples (n=222)

		Normal				Log-normal			
	Dis	**A**	**E**	**KS**	**χ^2**	**A**	**E**	**KS**	**χ^2**
Ag	Log	3.61	16.05	0.37**	193.9**	1.09	-0.03	0.25**	28.0**
Al	Log	0.77	0.78	0.08$^{N.S.}$	20.5*	-0.17	-0.24	0.05$^{N.S.}$	3.8$^{N.S.}$
As	Log	5.20	30.62	0.30**	215.9**	0.44	0.60	0.07$^{N.S.}$	8.2*
Ba	Log	1.95	2.89	0.31**	379.1**	0.89	-0.19	0.16**	48.1**
Bi	Log	3.47	13.87	0.35**	444.4**	1.41	1.84	0.24**	47.5**
Cd	Log	2.73	8.73	0.29**	312.4**	0.62	0.21	0.15**	26.7**
Co	Log	1.47	3.60	0.10*	39.7**	-1.09	6.10	0.06$^{N.S.}$	11.5**
Cr	Log	2.61	7.94	0.23**	104.8**	0.28	0.43	0.08$^{N.S.}$	12.3**
Cu	Log	3.45	14.14	0.23**	135.5**	0.51	1.77	0.08$^{N.S.}$	11.3**
Fe	Log	2.26	8.13	0.17**	52.8**	0.16	3.29	0.10*	15.3**
Ga	Log	0.66	0.50	0.15**	26.2**	-0.22	-0.24	0.15**	16.3**
Hg	Log	3.04	9.07	0.33**	104.0**	1.34	1.01	0.18**	39.0**
La	Log	1.50	3.64	0.16**	38.9**	-0.12	0.58	0.09$^{N.S.}$	6.4$^{N.S.}$
Mg	Log	2.51	7.82	0.20**	148.9**	0.08	-0.62	0.07$^{N.S.}$	0.8$^{N.S.}$
Mn	Log	2.42	6.24	0.21**	168.6**	0.44	1.22	0.10*	26.6**
Mo	Log	4.70	26.20	0.30**	71.9**	1.30	2.55	0.14**	22.2**
Ni	Log	1.99	4.46	0.19**	87.5**	-0.49	1.14	0.07$^{N.S.}$	4.4$^{N.S.}$
Pb	Log	2.69	8.24	0.31**	303.8**	1.00	-0.21	0.18**	22.9**
Sb	Log	4.36	24.66	0.34**	264.8**	0.36	-0.17	0.11*	15.8**
Sc	N	0.73	1.79	0.08$^{N.S.}$	13.2*	-1.22	2.97	0.12**	33.6**
Th	N	0.42	0.61	0.08$^{N.S.}$	4.0$^{N.S.}$	-1.31	2.54	0.13**	31.6**
Ti	Log	5.12	29.17	0.34**	231.0**	0.77	0.96	0.16**	2.2$^{N.S.}$
Tl	Log	2.79	10.50	0.26**	26.9**	0.52	0.07	0.20**	7.6*
V	N	1.58	4.82	0.11*	18.3*	-2.17	16.36	0.09*	17.2**
W	Log	5.18	29.58	0.38**	82.0**	1.83	2.85	0.30**	8.4*
Zn	Log	3.32	13.03	0.31**	58.3**	1.22	0.59	0.20**	14.3**

Dis. – distribution (N – Normal, Log – Log-normal); A – skewness; E – kurtosis; KS – Kolmogorov-Smirnov test; χ^2 – Chi-Square test; NS – no significance; * – significance at $p<0.05$; ** – significance at $p<0.01$

Table 6: Descriptive statistics of measurements (I) – soil (n=222), stream sediments (n=17) and attic dust (n=15) samples

	Material	X	X_G	Md	Min	Max	P_{25}	P_{75}	S	S_X	CV
Ag	Soil	0.69	0.18	0.10	<0.10	11	<0.10	0.30	1.5	0.099	213
Ag	S. Sediment	1.4	0.81	1.3	<0.10	3.6	0.30	2.6	1.2	0.28	83
Ag	A. Dust	2.4	1.64	1.4	0.50	7.4	0.70	3.5	2.3	0.60	96
Al	Soil	1.7	1.58	1.6	0.65	3.8	1.3	2.0	0.58	0.039	35
Al	S. Sediment	1.1	1.12	1.1	0.83	1.8	0.99	1.2	0.25	0.060	22
Al	A. Dust	1.0	1.01	1.0	0.62	1.3	0.95	1.1	0.15	0.039	15
As	Soil	45	27	32	3.7	590	12	45	74	5.0	164
As	S. Sediment	18	16	18	5.9	33	9.6	23	8.1	2.0	45
As	A. Dust	51	44	51	16	97	23	81	27	7.1	54
Ba	Soil	300	200	150	41	1700	110	270	340	23	113
Ba	S. Sediment	570	450	580	130	1300	210	820	350	85	62
Ba	A. Dust	40	34	30	14	87	19	54	24	6.1	60
Bi	Soil	0.68	0.48	0.40	0.10	6.1	0.30	0.50	0.84	0.057	124
Bi	S. Sediment	0.39	0.36	0.40	0.20	0.80	0.20	0.50	0.18	0.044	46
Bi	A. Dust	3.2	1.72	1.2	0.40	13	0.70	5.0	4.0	1.0	125
Cd	Soil	0.96	0.63	0.50	0.10	7.2	0.40	0.90	1.1	0.076	118
Cd	S. Sediment	0.74	0.70	0.70	0.40	1.6	0.60	0.80	0.29	0.070	39
Cd	A. Dust	3.9	3.1	2.7	1.4	14	2.1	3.8	3.4	0.87	86
Co	Soil	23	21	21	7.2	64	16	27	9.5	0.63	42
Co	S. Sediment	14	14	13	11	18	13	14	1.8	0.45	13
Co	A. Dust	13	11	10	6.2	33	8.2	11	8.4	2.2	64
Cr	Soil	83	64	66	10	460	39	89	72	4.8	87
Cr	S. Sediment	66	62	69	38	120	48	76	22	5.4	34
Cr	A. Dust	63	58	56	31	120	43	70	28	7.1	44
Cu	Soil	55	44	42	5.3	360	30	61	51	3.4	92
Cu	S. Sediment	68	61	64	27	120	38	89	30	7.3	45
Cu	A. Dust	150	120	100	46	450	79	170	120	30	76
Fe	Soil	3.5	3.3	3.3	0.98	10	2.9	3.8	1.2	0.081	35
Fe	S. Sediment	3.2	3.1	3.2	2.1	4.5	2.8	3.6	0.66	0.16	21
Fe	A. Dust	5.7	4.2	3.4	2.0	19	2.4	4.7	5.6	1.4	97
Ga	Soil	4.8	4.6	5.0	2.0	10	4.0	6.0	1.6	0.11	33
Ga	S. Sediment	3.2	3.2	3.0	3.0	5.0	3.0	3.0	0.66	0.16	21
Ga	A. Dust	3.3	3.3	3.0	2.0	5.0	3.0	4.0	0.72	0.19	22
Hg	Soil	0.30	0.15	0.11	0.040	2.7	0.08	0.23	0.49	0.033	166
Hg	S. Sediment	0.52	0.34	0.42	0.060	1.5	0.14	0.73	0.44	0.11	86
Hg	A. Dust	1.7	1.23	1.7	0.24	3.7	0.63	2.7	1.2	0.31	71
La	Soil	12	11	11	2.5	40	9.0	15	5.7	0.38	46
La	S. Sediment	6.8	6.6	6.0	6.0	12	6.0	7.0	1.7	0.41	25
La	A. Dust	6.6	6.3	6.0	3.0	10	5.0	8.0	2.0	0.52	31

X –mean; X_G – geometrical mean; Md – median; Min – minimum; Max – maximum; P_{25} – lower quartile; P_{75} – upper quartile; S – standard deviation; S_X – standard error of mean; CV – coefficient of variation (%); *Values of Al, Fe, Mg and Ti are in %, remaining elements in mg/kg*

Table 7: Descriptive statistics of measurements (II) – soil (n=222), stream sediments (n=17) and attic dust (n=15) samples

	Material	X	X_G	Md	Min	Max	P_{25}	P_{75}	S	S_X	CV
Mg	Soil	0.63	0.41	0.42	0.070	4.1	0.19	0.78	0.67	0.045	106
Mg	S. Sediment	1.0	0.97	1.1	0.69	1.5	0.81	1.2	0.22	0.054	22
Mg	A. Dust	0.63	0.61	0.61	0.42	0.99	0.52	0.75	0.15	0.040	25
Mn	Soil	2200	1800	1600	200	10000	1200	2400	1700	120	80
Mn	S. Sediment	1900	1800	1800	1000	3500	1300	2300	760	190	40
Mn	A. Dust	2100	1600	1500	590	6200	910	2100	1900	480	87
Mo	Soil	0.77	0.56	0.50	0.10	7.9	0.40	0.70	1.0	0.068	131
Mo	S. Sediment	0.84	0.73	0.90	0.20	1.6	0.50	1.1	0.41	0.10	49
Mo	A. Dust	4.8	3.4	2.8	1.3	17	1.6	4.0	4.8	1.3	101
Ni	Soil	120	89	90	10	500	59	140	94	6.3	80
Ni	S. Sediment	78	75	78	49	130	60	88	23	5.5	29
Ni	A. Dust	79	71	66	36	140	43	120	37	9.5	47
Pb	Soil	190	93	62	25	1700	43	160	280	19	150
Pb	S. Sediment	240	190	220	46	570	120	340	150	37	64
Pb	A. Dust	820	490	380	140	2800	230	1100	920	240	112
Sb	Soil	5.3	1.48	1.1	<0.10	88	0.60	3.3	11	0.75	210
Sb	S. Sediment	14	8.7	14	1.0	39	2.6	21	11	2.8	80
Sb	A. Dust	27	20	19	4.3	80	9.7	36	23	5.9	85
Sc	Soil	4.3	4.0	4.2	0.70	11	3.4	5.2	1.7	0.11	38
Sc	S. Sediment	3.2	3.1	3.1	2.4	4.0	2.8	3.5	0.47	0.11	15
Sc	A. Dust	2.1	1.99	2.2	0.90	3.1	1.6	2.7	0.68	0.18	32
Th	Soil	2.7	2.4	2.5	0.40	6.6	2.0	3.4	1.1	0.072	40
Th	S. Sediment	1.9	1.83	1.9	1.1	2.2	1.8	2.0	0.25	0.061	14
Th	A. Dust	0.89	0.70	1.00	0.20	1.8	0.40	1.2	0.53	0.14	60
Ti	Soil	0.013	0.005	0.004	<0.001	0.23	0.002	0.008	0.031	0.002	239
Ti	S. Sediment	0.039	0.034	0.033	0.012	0.087	0.026	0.058	0.022	0.005	55
Ti	A. Dust	0.018	0.016	0.017	0.006	0.036	0.013	0.023	0.009	0.002	49
Tl	Soil	0.37	0.29	0.30	0.10	2.3	0.20	0.50	0.32	0.021	85
Tl	S. Sediment	0.19	0.17	0.20	0.050	0.30	0.10	0.30	0.087	0.021	46
Tl	A. Dust	0.70	0.50	0.40	0.10	2.5	0.30	0.90	0.66	0.17	94
V	Soil	43	40	40	<2.0	130	32	51	18	1.2	43
V	S. Sediment	37	36	37	26	49	30	40	7.1	1.7	19
V	A. Dust	39	38	41	20	61	29	47	11	2.8	28
W	Soil	0.26	0.10	0.10	<0.10	5.2	<0.10	0.10	0.69	0.046	262
W	S. Sediment	0.29	0.22	0.30	0.10	0.70	0.10	0.40	0.20	0.048	69
W	A. Dust	3.5	1.96	1.5	0.60	16	0.90	2.9	4.5	1.2	129
Zn	Soil	310	180	130	43	3100	98	260	460	31	146
Zn	S. Sediment	260	240	260	120	470	170	290	100	25	40
Zn	A. Dust	1800	1100	800	270	7100	540	1400	2200	560	122

X –mean; X_G – geometrical mean; Md – median; Min – minimum; Max – maximum; P_{25} – lower quartile; P_{75} – upper quartile; S – standard deviation; S_X – standard error of mean; CV – coefficient of variation (%); *Values of Al, Fe, Mg and Ti are in %, remaining elements in mg/kg*

Descriptive statistical parameters are used to describe all basic information of the data set included in the entire study. This method helps us to simply large amounts of data in a sensible way. Simpler summery data for soil, stream sediments and attic dust are provided in Tables 6 and 7. Values of Al, Fe, Mg, and Ti are expressed in percentages, but other 22 elements in mg/kg. Mean (X), geometric mean (X_G), median (Md), minimum (Min), maximum (Max), lower quartile (P_{25}), upper quartile (P_{75}), standard deviation (S), Standard error of mean (S_X) and coefficient of variation (CV) were determined for all data.

Comparing the summarized data it is possible to see how concentrations of particular element are varying between the sampling media. Some concentrations are high (or even extremely high) in one media but not in two other sampling media, or opposite. This showing us meaning of presence various type of contamination, as well as various transport processes (such as water transport, atmospherically transport, mobility etc.)

Table 8: Results of Analysis of Variance (ANOVA) regarding to sampling materials between determine zones (polluted and unpolluted), lithological units and soil layers

	Soil F (Zone)	**Soil F (Lito)**	**Soil F (Layer)**	**A. Dust F (Zone)**	**S. Sediment F (Zone)**
n	222	222/154*	222	15	17
Ag*	362.5**	2.4*	1.0$^{N.S.}$	0.0$^{N.S.}$	20.0**
Al	5.9**	17.5**	5.1*	5.7*	1.8$^{N.S.}$
As	1.3$^{N.S.}$	13.0**	0.3$^{N.S.}$	0.0$^{N.S.}$	2.9$^{N.S.}$
Ba*	118.4**	9.8**	3.0$^{N.S.}$	1.2$^{N.S.}$	0.1$^{N.S.}$
Bi*	118.6**	3.9**	0.1$^{N.S.}$	0.1$^{N.S.}$	14.6**
Cd*	123.8**	3.7**	3.6$^{N.S.}$	1.0$^{N.S.}$	9.7**
Co	11.3**	42.6**	6.0*	0.0$^{N.S.}$	8.5*
Cr	0.2$^{N.S.}$	76.6**	1.1$^{N.S.}$	1.2$^{N.S.}$	4.3$^{N.S.}$
Cu*	46.6**	16.8**	0.3$^{N.S.}$	1.9$^{N.S.}$	8.4*
Fe*	20.7**	9.4**	8.7**	0.4$^{N.S.}$	12.5**
Ga	37.2**	22.6**	3.3$^{N.S.}$	1.2$^{N.S.}$	3.4$^{N.S.}$
Hg*	180.0**	2.9**	0.3$^{N.S.}$	8.2*	3.1$^{N.S.}$
La	2.3$^{N.S.}$	6.5**	4.8*	0.4$^{N.S.}$	0.2$^{N.S.}$
Mg	33.1**	58.5**	0.0$^{N.S.}$	0.2$^{N.S.}$	1.5$^{N.S.}$
Mn*	161.4**	3.9**	0.9$^{N.S.}$	1.1$^{N.S.}$	24.2**
Mo*	73.8**	6.5**	0.8$^{N.S.}$	4.5$^{N.S.}$	10.3**
Ni	0.0$^{N.S.}$	63.5**	1.1$^{N.S.}$	3.9$^{N.S.}$	2.7$^{N.S.}$
Pb*	484.2**	5.8**	0.1$^{N.S.}$	2.6$^{N.S.}$	19.6**
Sb*	170.7**	4.1**	1.8$^{N.S.}$	0.0$^{N.S.}$	20.3**
Sc	0.4$^{N.S.}$	14.0**	9.2**	1.0$^{N.S.}$	8.4*
Th	2.2$^{N.S.}$	9.1**	26.2**	1.0$^{N.S.}$	10.1**
Ti	28.0**	33.1**	0.2$^{N.S.}$	0.0$^{N.S.}$	12.8**
Tl*	49.2**	2.5*	0.9$^{N.S.}$	4.3$^{N.S.}$	10.7**
V	1.3$^{N.S.}$	37.7**	4.0*	1.4$^{N.S.}$	3.3$^{N.S.}$
W*	129.4**	2.8**	0.5$^{N.S.}$	0.1$^{N.S.}$	12.3**
Zn*	302.9**	3.7**	0.4$^{N.S.}$	0.1$^{N.S.}$	13.4**

n – number of observation; F – ratio (ANOVA); NS – no significant; (* – significance at $p<0.05$; ** – significance at $p<0.01$.). * – In the example of distribution of Ag, As, Ba, Bi, Cd, Cu, Fe, Hg, Mn, Mo, Pb, Sb, Tl, W and Zn (automorphic soil) only samples from the Zone 2 (unpolluted area) were respected.

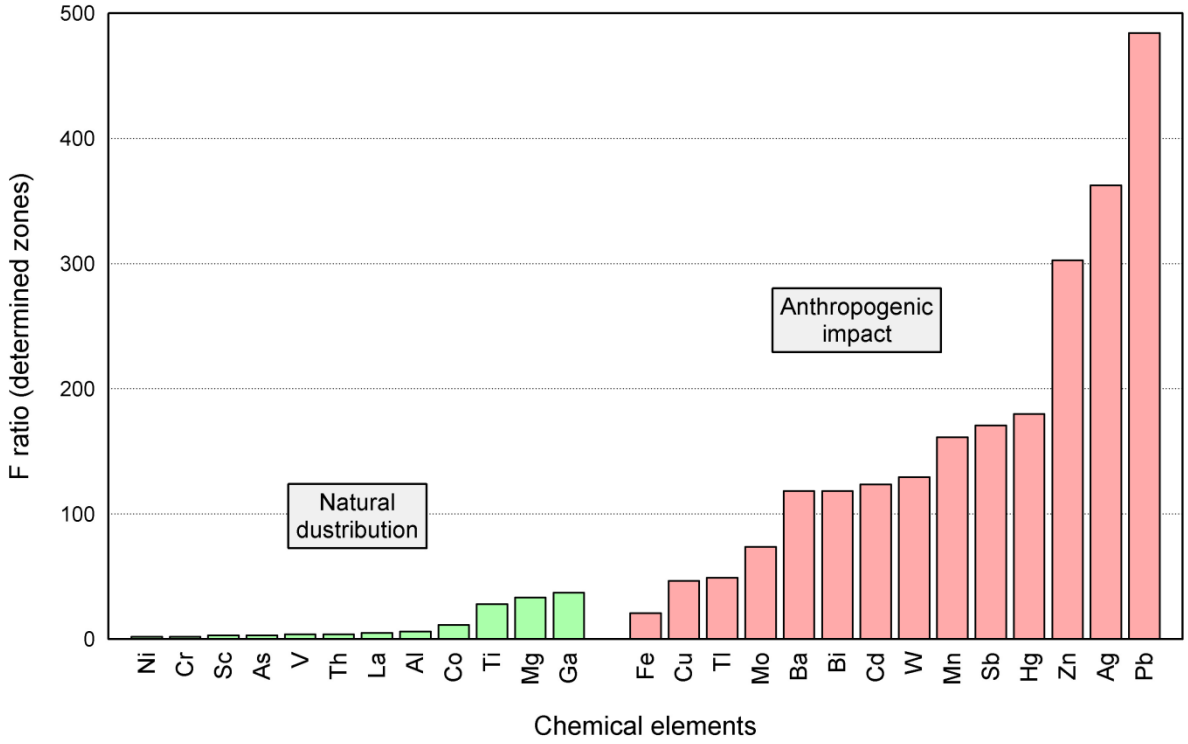

Figure 21: Distribution of F ratios (ANOVA) in soil between the determined zones regarding to group of elements (n=222)

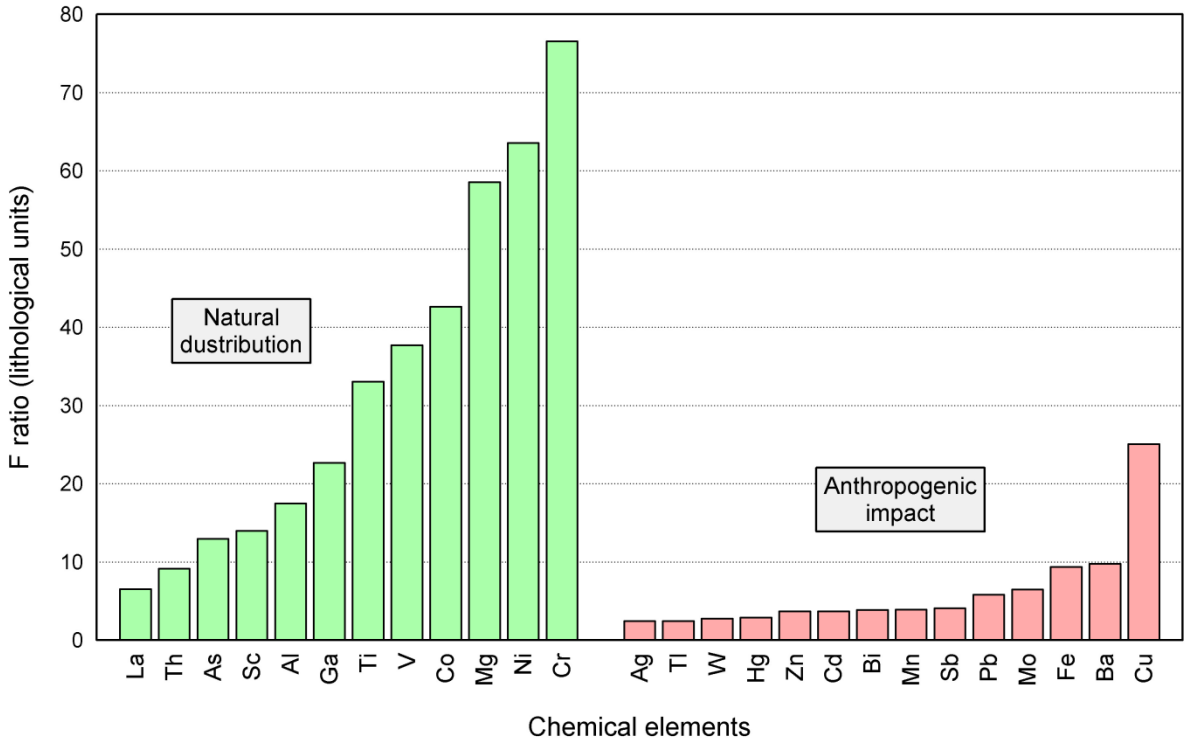

Figure 22: Distribution of F ratios (ANOVA) in soil between the lithological units regarding to group of elements (n=154)

To study the population differences between and within determined zones (Zone 1, 2a, 2b and 3) and defined lithological unit ANOVA method are provided (Table 8, Figures 8, 21 and 22). The development of the theory of ANOVA, the variance between means of determined zones and geological unit vs. the variance within each mean of particular element the F ratio (between/within) is calculated. Average concentration levels of particular elements for the soil depth are used because significant difference is not noticed. However, they are so small compared to ranges through the complete study area.

It can be observed that statistically significant difference for all soil samples is between natural distribution and anthropogenic impact. Particular elements of the natural distribution generally showing a very low F ratio compare to the anthropogenic impact. Among the anthropogenically introduced chemicals, the lowest F ratios have Fe, Cu, Tl, and Mo (between 20 and 70). The highest F ratios have Zn, Ag, and Pb (between 300 and 500), what is several times higher than average ratio for this group of elements (Table 8, Figures 8 and 21). Completely different situation is provided by distribution of F ratio between isolated lithological units and particular chemical elements in the zone 2 (unpolluted zone). Two highest ratios have Ni and Cr because their origin is completely natural and depends solely from the parental material (Table 8, Figures 8, and 22).

Three summary tables that are providing average concentrations through the determined zones (1, 2a, 2b and 3) in soil horizons (Table 9), average concentrations of elements in basic lithological units of topsoil (Table 10), and average concentration of elements in basic lithological units of subsoil (Table 11) are represented.

ER is measure for comparison and has been used for comparison between the determined zones and various sampling material. Figure 23 represents the ER between two zones, polluted Zone 1 and unpolluted Zone 2 in automorphic soil. This ER reveals concentration levels of particular elements between anthropogenic contamination and natural enrichment. Their ratio represents a level of human activities in study area. This comparison shows that the most of anthropogenic elements is strongly enriched in the Zone 1, especially the five following elements Ag, W, Sb, Pb, and Zn. Their ER is between 6 and 14 times higher, whereas natural elements only have between 1 and 2. They do not show significant deviation, and their distribution depends on the terrain geology.

Similar observation is noticed comparing the soil from Zone 3 (alluvial soil) and Zone 2 (Figure 24). Alluvial soil represents an amount of transported material down the river. The results are showing that alluvial plains are depleted by chemical elements in topsoil, what is logical if we consider the fact that the ironworks Vareš do not operate last two decades and have not contributed additional contamination. Strongly enriched are Hg, Pb, Sb, and Ag, from 10 to 40 times. Most of anthropogenic elements have the ER between 5 and 15.

Dividing the concentration of attic dust and topsoil, intensity of air transport of contaminants in the past is detected. The geogenic elements are depleted in the attic dust but in other hand the contaminants transported by atmosphere are more enriched. In the study area Tl, Zn, Cd, Pb, Mo, Ag, Hg, Bi, Sb, and W are showing enrichment in the attic dust between 2 to 4 times (Figure 25).

And the last comparison, ER of alluvial soils (Zone 3) and stream sediments reveals different between former conditions and current river transport, because the stream sediment represent a material deposited on the alluvial plains during the flood periods. There is a particular enrichment of anthropogenic elements such as Ag, Zn, Pb, Mn, Tl, Cd, and Bi, which are enriched from 2 to 3.5 times (Figure 26). From these ratios is possible to conclude that intensity of human impact is much lower than several decades ago. Equivalent to this, amount of transported contaminants is much less than during the intensive mining and smelting.

Table 9: Averageconcentrations of chemical elements according to determined zones (polluted and unpolluted) and soil layers

	Zone 1		Zone 2a		Zone 2b		Zone 3	
	Topsoil	**Subsoil**	**Topsoil**	**Subsoil**	**Topsoil**	**Subsoil**	**Topsoil**	**Subsoil**
Ag	1.3	1.3	0.12	0.072	0.100	0.085	3.4	4.2
Al	1.9	2.0	1.9	2.2	1.3	1.5	1.5	1.6
As	29	31	8.9	9.5	69	79	37	39
Ba	720	600	210	120	140	140	740	530
Bi	1.2	1.4	0.35	0.31	0.37	0.37	1.5	1.9
Cd	1.9	1.7	0.51	0.28	0.52	0.50	2.6	2.9
Co	23	24	22	27	21	24	15	14
Cr	92	92	100	120	63	72	72	69
Cu	90	92	30	33	40	43	100	110
Fe	4.4	4.6	2.8	3.3	3.0	3.5	3.6	3.8
Ga	5.3	5.4	5.2	6.3	4.3	4.7	2.8	2.7
Hg	0.46	0.44	0.11	0.078	0.12	0.13	1.4	1.3
La	13	14	7.8	9.6	13	15	10	11
Mg	0.99	1.0	0.83	1.0	0.24	0.24	0.89	0.89
Mn	2600	2600	1400	1500	1300	1500	6500	7200
Mo	1.6	1.5	0.40	0.34	0.49	0.50	1.4	1.4
Ni	130	130	120	140	100	110	96	89
Pb	400	410	60	50	52	51	680	800
Sb	9.1	9.2	1.0	0.73	1.2	1.0	27	31
Sc	4.1	4.4	3.1	4.1	4.4	5.2	4.0	4.2
Th	2.6	3.0	1.3	2.1	2.8	3.7	2.0	2.4
Ti	0.020	0.021	0.017	0.022	0.003	0.003	0.022	0.024
Tl	0.55	0.57	0.19	0.21	0.30	0.34	0.65	0.72
V	46	49	40	48	39	44	41	43
W	0.81	0.78	0.069	0.059	0.066	0.058	0.56	0.53
Zn	740	740	130	110	110	110	770	870

Zone 1 – polluted area, automorphic soil, the upper part of the Stavnja valley (n=24); Zone 2a – unpolluted area, automorphic soil, the upper part of the Stavnja valley (n=27); Zone 2b – unpolluted area, automorphic soil, the lower part of the Stavnja valley (n=50); Zone 3 – polluted area, alluvial soil, the lower part of the Stavnja valley (n=10) ; *Values of Al, Fe, Mg and Ti are in %, remaining elements in mg/kg*

Table 10: Average concentrations of chemical elements according to basic lithological units – topsoil (0-5 cm)

	Clastites (JK)	Clastites (T)	Carbonates (T)	Series (JK)	Flysch (K)	Clastites (Ol)	Carbonates (M)	Clastites (M)	Terraces (Q)	Alluvium (Q)
Ag*	0.083	0.20	0.10	0.14	0.10	0.083	0.060	0.094	0.13	3.4
Al	2.1	2.9	1.5	2.0	1.3	1.3	1.1	1.4	1.5	1.5
As*	8.7	6.2	6.9	11.1	72.0	98.3	38.7	37.9	48.3	36.7
Ba	170	240	200	290	120	90.5	87.2	140	250	740
Bi	0.37	0.33	0.39	0.31	0.38	0.33	0.30	0.39	0.39	1.5
Cd*	0.57	0.50	0.42	0.50	0.51	0.62	0.50	0.44	0.60	2.6
Co	15.7	23.9	13.5	36.5	20.4	23.2	22.4	19.2	21.2	14.7
Cr	54.5	68.4	31.7	220	50.9	96.5	83.0	43.8	66.6	72.4
Cu*	30.7	19.6	17.4	42.3	43.4	36.9	29.8	34.2	40.8	100
Fe*	2.9	3.5	2.0	3.3	3.0	3.2	2.6	2.9	3.1	3.6
Ga	5.7	7.8	4.7	5.5	4.2	5.0	3.6	4.3	4.6	2.8
Hg*	0.083	0.17	0.091	0.15	0.10	0.11	0.14	0.13	0.12	1.4
La	6.3	7.3	10.8	10.5	13.3	14.3	11.2	11.1	14.6	10.4
Mg	0.49	1.6	0.55	1.5	0.21	0.20	0.19	0.36	0.34	0.89
Mn*	1500	1300	1200	1600	1500	1400	930	1100	1500	6500
Mo*	0.46	0.28	0.33	0.44	0.46	0.52	0.36	0.58	0.57	1.4
Ni	41.5	88.1	39.2	280	80.7	130	130	85.6	110	96.3
Pb*	55.0	74.2	68.4	58.8	47.4	51.8	46.4	47.4	69.3	680
Sb*	0.84	0.97	1.1	1.3	1.1	0.55	0.40	1.0	1.9	27.2
Sc	0.84	6.1	2.5	4.8	4.3	5.0	3.9	3.8	4.6	4.0
Th	1.2	1.1	2.1	2.1	2.7	2.6	2.1	3.0	3.2	2.0
Ti	0.014	0.14	0.005	0.012	0.003	0.005	0.003	0.003	0.004	0.022
Tl*	0.17	0.18	0.20	0.21	0.34	0.33	0.20	0.21	0.24	0.65
V	46.0	88.8	27.1	51.7	41.2	50.8	32.6	24.8	36.1	41.5
W	0.050	0.050	0.075	0.081	0.073	0.058	0.050	0.050	0.072	0.56
Zn*	140	160	140	130	110	100	99.2	100	140	770

Clastites (JK) – Jurassic and Cretaceous breccias and sandstones (n=6); Clastites (T) – Triassic clastites, spilite and tuff (n=4/2*); Carbonates (T) – Triassic limestone; (n=19/8*); Series (JK) – Jurassic and Cretaceous clastic carbonate series (n=16/8*); Flysch (K) – Cretaceous flysch (n=28/25*); Clastite (Ol) – Oligocene clastite complex (6); Carbonates (M) – Miocene carbonate series (n=5); Clastites (M) – Miocene clastic series (n=8); Terraces (Q) – Quaternary river terraces (n=9); Alluvium (Q) – Quaternary alluvium (n=10). * – In assessing the background of Ag, As, Ba, Bi, Cd, Cu, Fe, Hg, Mn, Mo, Pb, Sb, Tl, W and Zn (automorphic soil) only samples from the Zone 2 (unpolluted area) were respected; *Values of Al, Fe, Mg and Ti are in %, remaining elements in mg/kg*

Table 11: Average concentrations of chemical elements according to basic lithological units – subsoil (20-30 cm)

	Clastites (JK)	Clastites (T)	Carbonates (T)	Series (JK)	Flysch (K)	Clastites (Ol)	Carbonates (M)	Clastites (M)	Terraces (Q)	Alluvium (Q)
Ag	0.058	0.050	0.069	0.10	0.076	0.067	0.060	0.069	0.14	4.2
Al	2.4	3.3	1.7	2.3	1.5	1.6	1.1	1.4	1.7	1.6
As	9.0	5.4	7.3	12	82	110	41	41	54	39
Ba	100	110	130	130	110	85	90	140	270	530
Bi	0.27	0.20	0.38	0.28	0.39	0.33	0.28	0.38	0.38	1.9
Cd	0.22	0.35	0.28	0.29	0.41	0.53	0.54	0.44	0.68	2.9
Co	20	30	15	40	24	27	27	21	24	14
Cr	66	80	33	240	59	110	97	45	74	69
Cu	33	21	17	48	48	42	31	33	44	110
Fe	3.5	4.5	2.5	3.9	3.6	3.7	3.0	3.1	3.5	3.8
Ga	6.3	9.3	5.1	6.3	4.8	5.7	3.6	4.0	5.0	2.7
Hg	0.077	0.065	0.060	0.097	0.11	0.12	0.23	0.13	0.12	1.3
La	7.5	9.5	12	12	15	16	13	12	16	11
Mg	0.56	1.8	0.58	1.7	0.21	0.23	0.17	0.37	0.34	0.89
Mn	1600	1300	1200	1700	1600	1500	1100	1200	1700	7200
Mo	0.40	0.20	0.28	0.37	0.46	0.48	0.40	0.54	0.59	1.4
Ni	53	110	42	310	94	160	160	92	120	89
Pb	42	63	67	42	44	51	48	46	71	800
Sb	0.60	0.30	1.0	0.82	1.1	0.31	0.36	0.80	1.8	31
Sc	3.3	7.4	2.9	5.4	5.2	6.3	4.8	4.0	5.3	4.2
Th	1.8	1.7	2.7	2.7	3.5	3.8	3.2	3.7	3.8	2.4
Ti	0.021	0.17	0.005	0.012	0.003	0.004	0.003	0.003	0.004	0.024
Tl	0.17	0.20	0.23	0.24	0.40	0.40	0.18	0.23	0.27	0.72
V	52	110	28	59	47	58	37	26	41	43
W	0.050	0.050	0.063	0.069	0.062	0.050	0.050	0.050	0.061	0.53
Zn	100	150	120	110	100	99	99	94	130	870

Clastites (JK) – Jurassic and Cretaceous breccias and sandstones (n=6); Clastites (T) – Triassic clastites, spilite and tuff (n=4/2*); Carbonates (T) – Triassic limestone; (n=19/8*); Series (JK) – Jurassic and Cretaceous clastic carbonate series (n=16/8*); Flysch (K) – Cretaceous flysch (n=28/25*); Clastite (Ol) – Oligocene clastite complex (6); Carbonates (M) – Miocene carbonate series (n=5); Clastites (M) – Miocene clastic series (n=8); Terraces (Q) – Quaternary river terraces (n=9); Alluvium (Q) – Quaternary alluvium (n=10). * – In assessing the background of Ag, As, Ba, Bi, Cd, Cu, Fe, Hg, Mn, Mo, Pb, Sb, Tl, W and Zn (automorphic soil) only samples from the Zone 2 (unpolluted area) were respected; *Values of Al, Fe, Mg and Ti are in %, remaining elements in mg/kg*

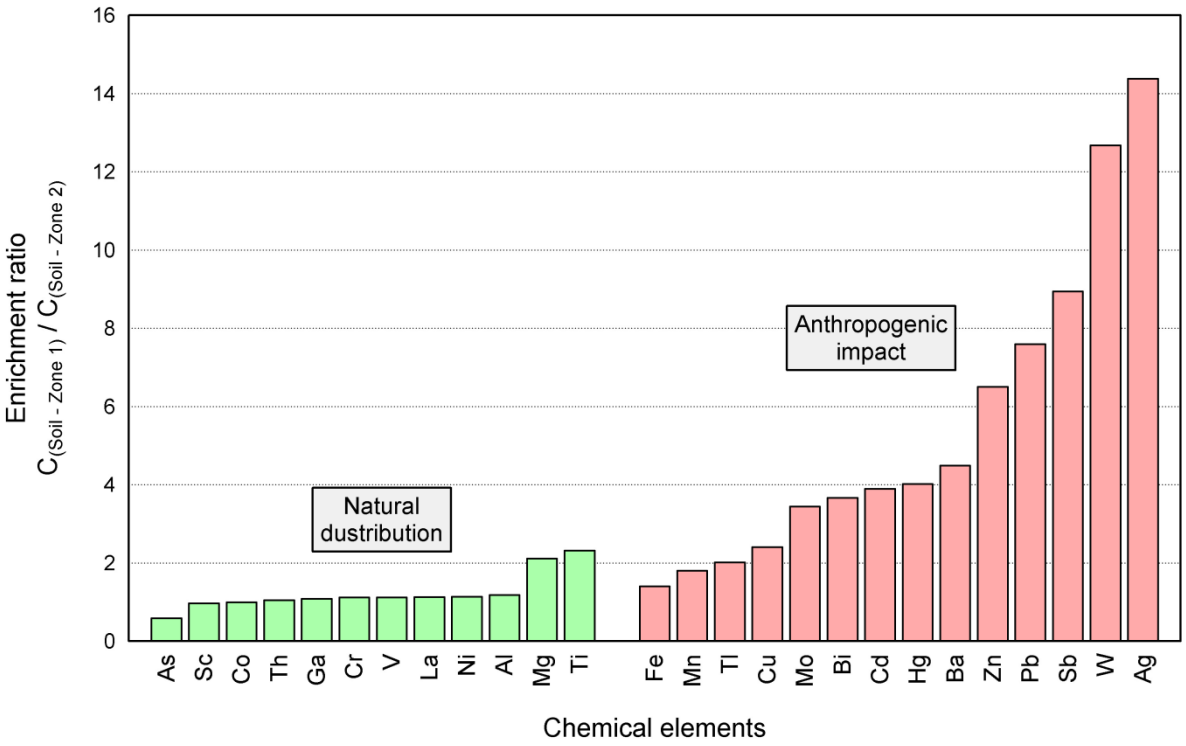

Figure 23: Enrichment ratio of Zone 1 (polluted area – automorphic soil) versus Zone 2 (unpolluted area – automorphic soil)

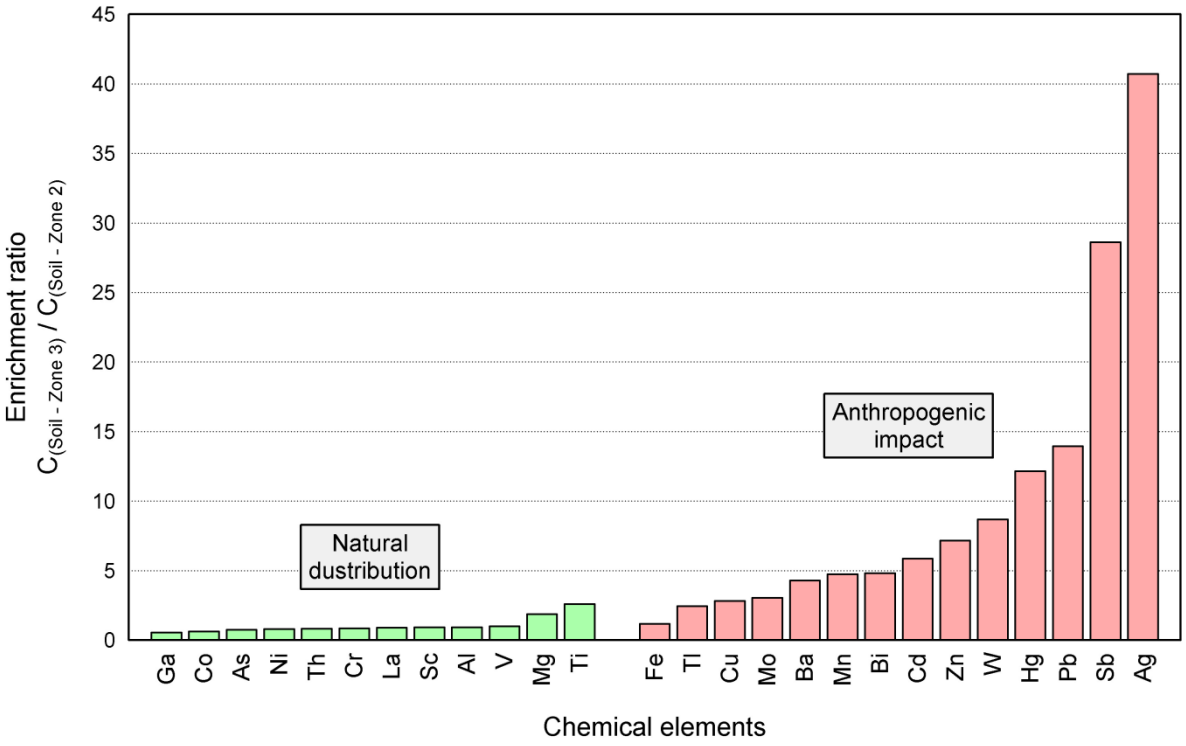

Figure 24: Enrichment ratio of Zone 3 (polluted area – alluvial soil) versus Zone 2 (unpolluted area – automorphic soil)

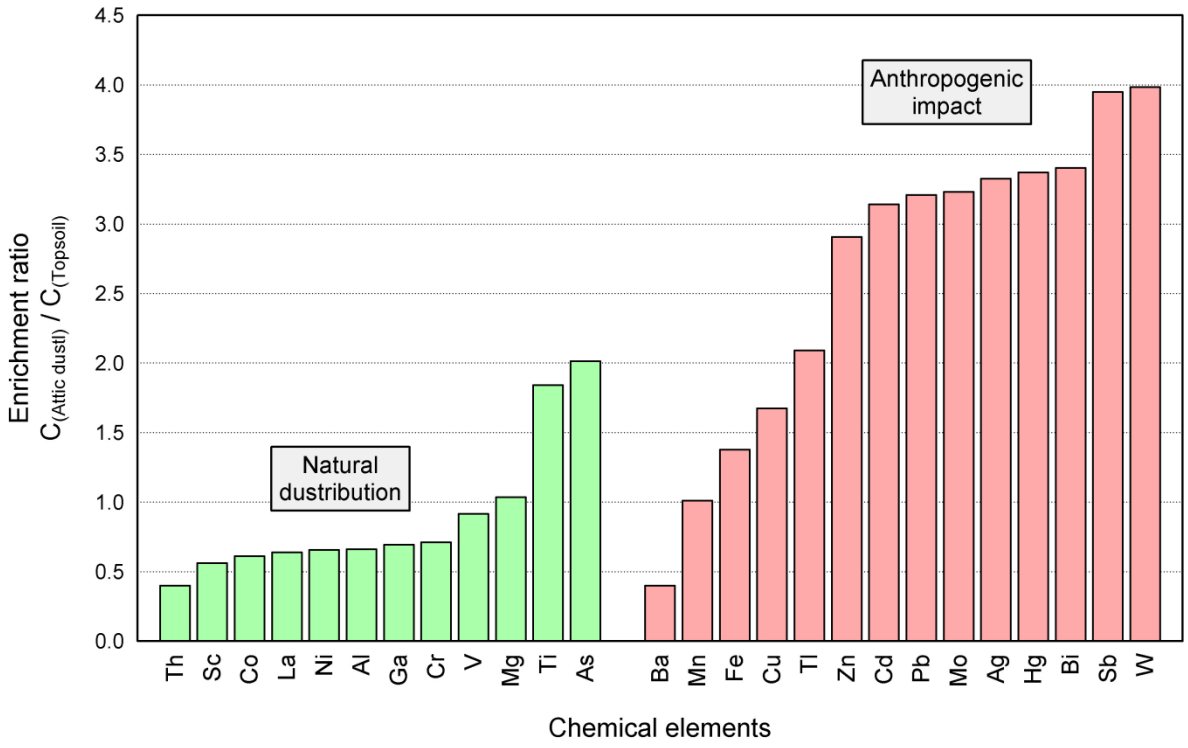

Figure 25: Enrichment ratio of attic dust versus topsoil

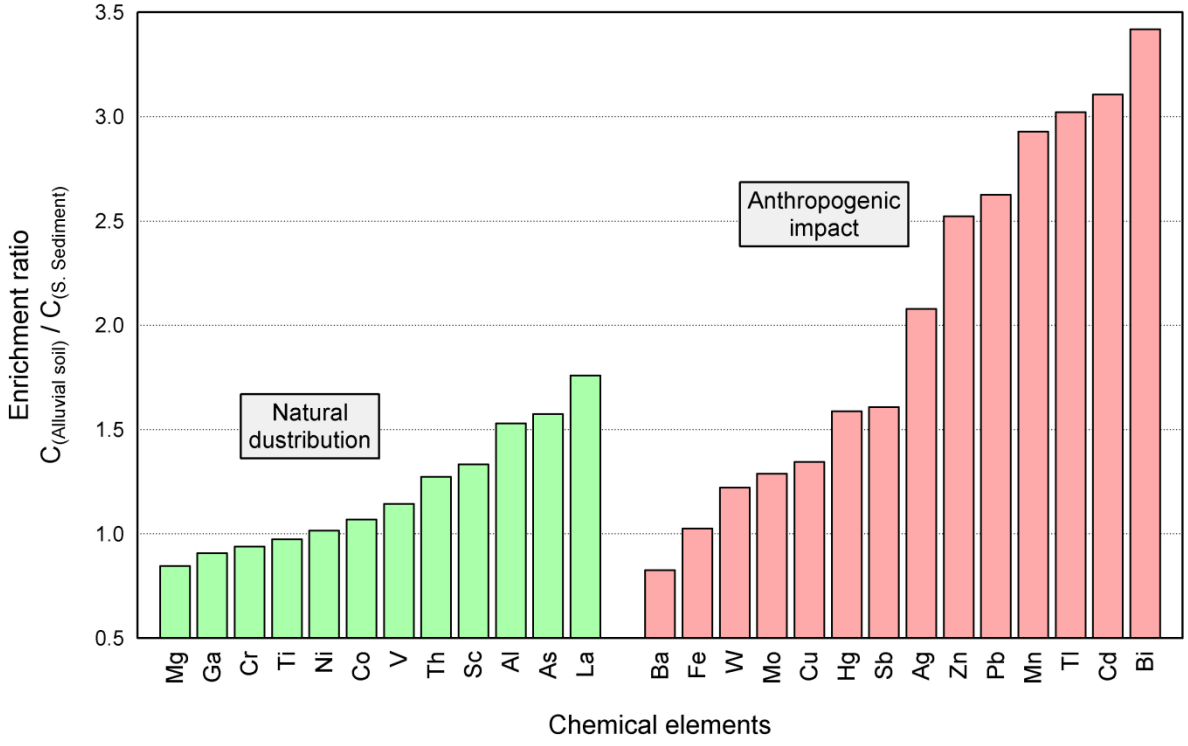

Figure 26: Enrichment ratio of alluvial soil versus stream sediment

5.3. Geochemical associations and their distributions

The degree of chemical elements associationin soil was assessed with the linear coefficient of correlation r (Le Maitre, 1982) between their contents in the samples. It was qualitatively assumed that the absolute values of r between 0.5 and 0.7 indicate good association and those between 0.7 and 1.0 strong association between anthropogenically distributed elements (Table 12). The correlation coefficients between naturally distributed chemical elements represent opposite situation. Only several good or strong correlations are showed in table 13. Based on a several stronger correlation coefficients (0.8 - 0.93) is possible to extract the group that associates Co, Ni and Cr. With this group relatively good correlation has Scandium. Second correlation that merges Ga and Al, has the matrix of correlation coefficient 0.79. Tl is showing both distributions, natural and anthropogenic respectively.

Table 12: Matrix of correlation coefficients (group of 14 selected principally anthropogenically distributed elements, n=222)

Ag	1.00													
Ba	0.83	1.00												
Bi	0.86	0.74	1.00											
Cd	0.80	0.69	0.79	1.00										
Cu	0.70	0.61	0.77	0.67	1.00									
Fe	0.45	0.46	0.53	0.42	0.77	1.00								
Hg	0.84	0.69	0.80	0.74	0.74	0.47	1.00							
Mn	0.74	0.60	0.69	0.70	0.70	0.49	0.70	1.00						
Mo	0.77	0.71	0.80	0.75	0.78	0.65	0.74	0.67	1.00					
Pb	0.94	0.81	0.86	0.86	0.65	0.45	0.82	0.73	0.76	1.00				
Sb	0.87	0.79	0.77	0.78	0.65	0.42	0.75	0.69	0.80	0.88	1.00			
Tl	0.57	0.43	0.65	0.71	0.54	0.44	0.48	0.63	0.61	0.62	0.55	1.00		
W	0.86	0.78	0.87	0.75	0.77	0.58	0.81	0.65	0.84	0.86	0.82	0.54	1.00	
Zn	0.92	0.83	0.89	0.85	0.72	0.57	0.81	0.74	0.80	0.96	0.85	0.65	0.89	1.00
	Ag	Ba	Bi	Cd	Cu	Fe	Hg	Mn	Mo	Pb	Sb	Tl	W	Zn

Table 13: Matrix of correlation coefficients (group of 13 selected principally naturally distributed elements, n=222)

Al	1.00												
As	-0.25	1.00											
Co	0.27	0.10	1.00										
Cr	0.29	0.07	0.80	1.00									
Ga	0.79	-0.17	0.38	0.24	1.00								
La	0.15	0.53	0.21	0.14	0.17	1.00							
Mg	0.69	-0.40	0.14	0.38	0.34	-0.18	1.00						
Ni	0.19	0.22	0.82	0.93	0.16	0.22	0.29	1.00					
Sc	0.28	0.43	0.60	0.57	0.29	0.45	0.03	0.65	1.00				
Th	-0.07	0.55	0.21	0.05	0.02	0.63	-0.29	0.18	0.41	1.00			
Ti	0.46	-0.10	0.05	0.28	0.16	0.08	0.54	0.17	0.18	-0.26	1.00		
Tl	0.22	0.52	-0.02	0.09	0.02	0.39	0.17	0.13	0.25	0.25	0.27	1.00	
V	0.48	0.13	0.49	0.55	0.45	0.30	0.19	0.45	0.57	0.05	0.59	0.24	1.00
	Al	As	Co	Cr	Ga	La	Mg	Ni	Sc	Th	Ti	Tl	V

The hierarchical agglomerate clustering was pronounced for the combination of Pearson r distance with Ward's method (amalgamation rule). Results of cluster analysis are showed in form of hierarchical dendrogram (Figure 27). The dendrogram of cluster analysis givesthe results for 26 remaining chemical elements and their mutual connecting to four groups. Firs group links Al, Ga, ti, Sc, and V, second group links Mg, Co, Cr, and Ni, third group links Fe, Cu, Mo, W, Ba, Ag, Sb, Hg, Mn, Bi, Zn, Cd, and Pb, and the last group links As, Tl, La, and Th. First two groups join on 75%, but third and fourth groups on 80%. These two subgroups join to each other at 100%.

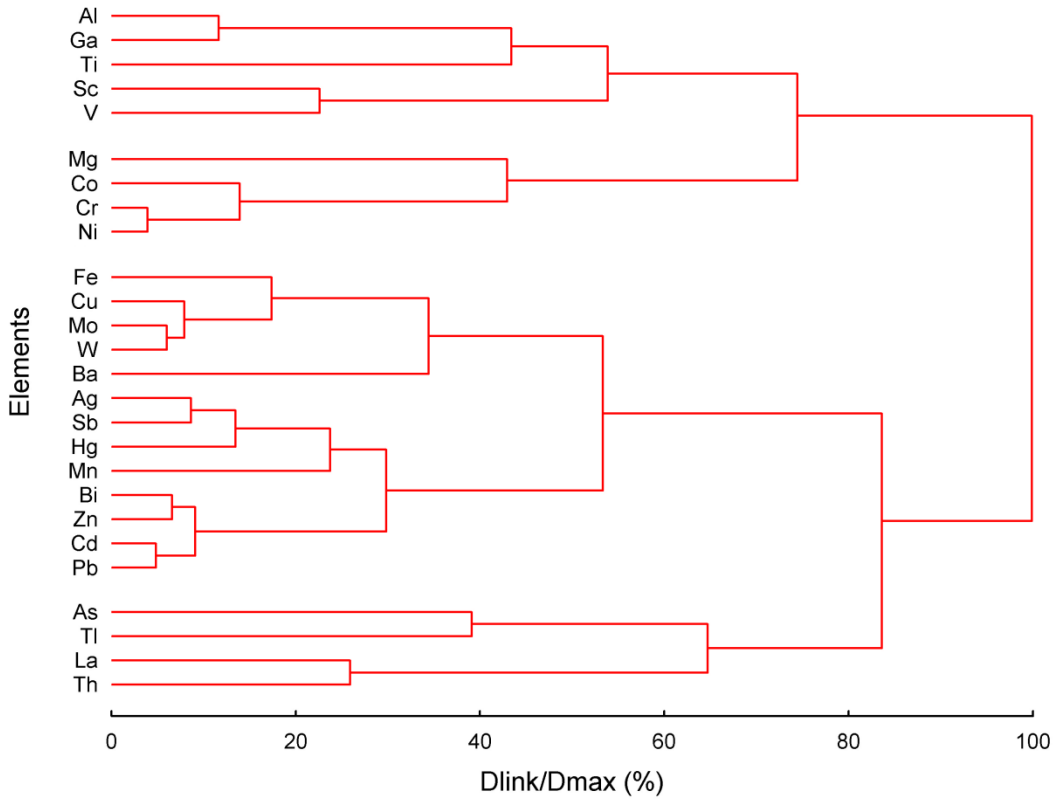

Figure 27: Cluster analysis dendrogram showing element relationship (n=222, 26 selected elements)

In the factor analysis (FA), 222 samples of soil for 26 selected elements were considered. FA isolated five synthetic variables F1-F4, which are connected regarding to geochemical similarities, with principal total variability of 75% (Table 14).

The Factor 1 (F1) is strongest and represents 38% of entire variability of remaining elements. The F1 associate the high concentration of Pb, Zn, Hg, Cd, Cu, Bi, Ag, Sb, Mo, W, Mn, Ba, Fe, and Tl. The group represents chemical elements that are the most probably anthropogenically distributed, associated to the city Vareš (the main industrial and mine zone) and alluvial sediments found downstream of the river Stavnja. Three next factors, F2, F3, and F4 respectively, conduct elements that are most probably naturally distributed. F2 is the second strongest factor including 13.5% of entire variability. This factor associates Ni, Cr, Co, and Mg. F3 associates Th, La, As, and Sc, including 10.4% of entire variability. The last factor is F4. This factor scores last four elements Al, Ti, V, and Ga, including 13% of entire variability (Table 14).

Table 14: Matrix of dominant rotated factor loadings (n=222, 26 selected elements)

	F1	F2	F3	F4	Comm
Pb	**0.95**	-0.08	-0.04	0.09	91.3
Zn	**0.94**	0.08	-0.02	0.05	89.1
Hg	**0.92**	-0.03	-0.07	-0.04	84.7
Cd	**0.91**	-0.07	0.08	0.07	85.0
Cu	**0.91**	0.22	0.11	-0.04	87.9
Bi	**0.89**	0.01	0.04	0.04	79.5
Ag	**0.86**	-0.10	-0.08	0.01	75.9
Sb	**0.85**	-0.06	-0.08	-0.03	72.9
Mo	**0.83**	0.18	0.08	-0.07	73.5
W	**0.81**	0.23	0.00	-0.06	71.6
Mn	**0.75**	-0.16	0.00	0.07	59.2
Ba	**0.73**	0.08	-0.11	-0.05	55.5
Fe	**0.68**	0.39	0.26	0.23	73.6
Tl	**0.57**	-0.08	**0.49**	0.19	60.4
Ni	0.07	**0.95**	0.04	0.12	92.1
Cr	0.08	**0.93**	-0.07	0.18	90.3
Co	-0.11	**0.89**	0.15	0.19	86.0
Mg	0.21	**0.54**	-0.36	**0.52**	73.8
Th	-0.05	0.03	**0.77**	-0.13	61.7
La	0.01	-0.07	**0.75**	0.08	57.8
As	-0.01	0.04	**0.71**	-0.04	51.3
Sc	0.00	0.36	**0.62**	0.46	73.3
Al	0.05	0.16	-0.02	**0.88**	80.7
Ti	0.09	-0.06	-0.21	**0.81**	71.4
V	0.08	0.30	0.25	**0.80**	80.3
Ga	-0.24	0.22	0.14	**0.79**	74.6
Prp.Totl.	38.1	13.5	10.4	13.1	75.1
Expl.Var	9.90	3.50	2.71	3.42	
Eigen.	10.02	4.86	2.61	2.05	

F1 ... F4 – Factor loadings; Com – Communality in %; Prp.Totl – Principal total variance in %; Eigen – Eigenvalues;Expl.Var – Expalanated variance; *Red color represent anthropogenically distributed geochemical association*

The results of principal component analysis (PCA) (Figure 28) are providing a similar information as the results of factor analysis. From the factor loading plot can be concluded even when the factor groups have been compared within each other (F1 vs. F2 and F1 vs.F3), aforementioned geochemical asociations are clearly agglomerated. But same as in the factor analysis several elements show both distributions, natural and anthropogenic, respectively. Talium is one typical example, where several results (Tables 12 and 14, Figure 28) discover its both origin, but in this study an anthropogenic origin is prevailing compare to natural. Similar tendency can be noticed for Fe, Mg, and Sc.

Distribution of F1 scores regarding to the determined zones provides very high concentration of Pb, Zn, Ag, Sb, Hg, Cd, W, Bi, U, Mo, Mn, Ba, Sr, Ca, Cu, Tl, Fe and As which are found around the city Vareš (Zone 1 – mining and industrial zone) (Figures 8 and 29). But the highest concentrations of those elements are determinate in the alluvial sediment (Zone 3). Distribution of F1 scores in all soil

samples according to the basic lithological units and soil layer. This distribution shows that the highest concentrations of those elements are again determinate in the alluvial sediment (Zone 3). If we only consider the samples from Zone 2 (unpolluted area) which represents background of automorphic soil we can see their low concentrations according to different lithological units (right). But again the highest concentrations are associated to the alluvial soil (Quaternary alluvium).

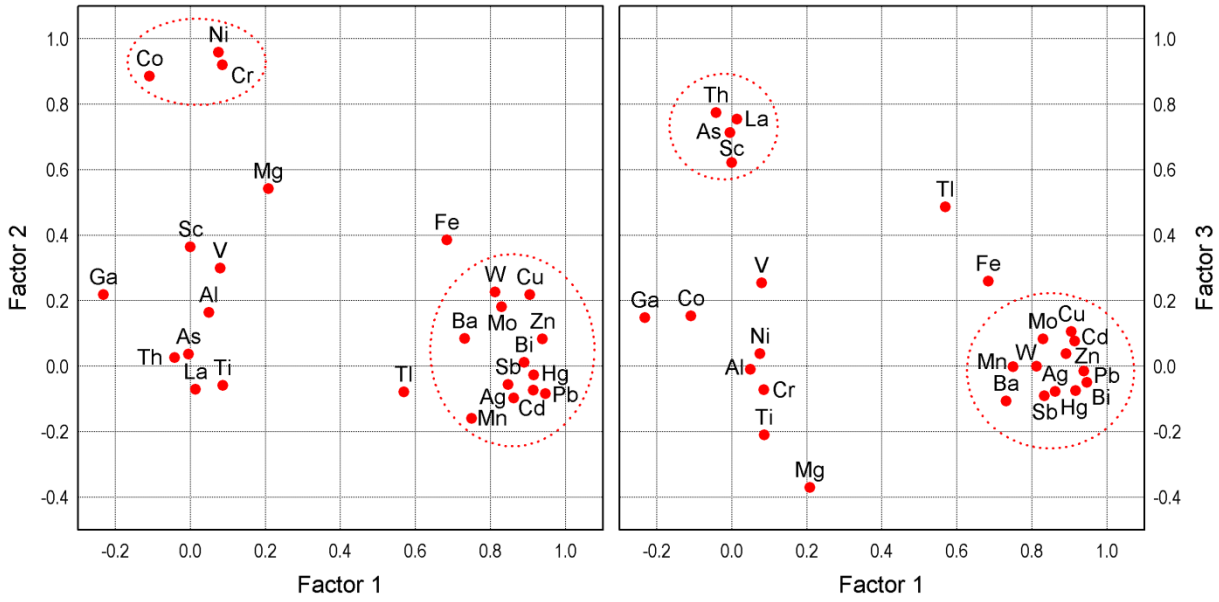

Figure 28: Factor loadings plots: Factor 1 vs. Factor 2 (left) and Factor 1 vs. Factor 3 (right)

According to the depth of sampling, there is no observed significant difference. In the area of the Zone 1, those differences are minimal what can be attributed with strong anthropogenic influence. The higher values of F1 in topsoil are noticed on the sites of Zone 2, which are typically anthropogenically introduced chemical elements. In the Zone 3 (alluvial soil) is reverse situation. Increased values of F1 are found in subsoil (Figure 29).The background valus include the automorphic soil from the Zone 2. Their values are marked with dark red and green colour, and their concentrations are at some lithological units similar or lower but much lower in alluvioum and Jurassic and Cretaceous clastic carbonate series. Distribution of F1 scores in soil according to the river distance showing that the increased concentrations are found almost along the entire river valley (Figure 30). Rapid increase of elements is noticeable around the mines and ironwork, but once again the increased values are found in alluvial sediments.

Distribution of F2 scores according to the depth and determined zones is showing opposite situation than F1 (Figures 8 and 31). Concentration of Cr, Co, Ni, and Mg are almost the same in Zone 1, because they do not depend on the parental rocks in that part of study area. But in Zone 2 their concentrations are increase in subsoil, in depth that is closer to the parental material. They decreased values are found in alluvial sediments, this means that some amount of those elements is transported down to the river.

Distribution of F2 scores according to the isolated lithological unitsclearly shows that the highest concentration of Cr, Ni, Co, and Mg are found in the Jurassic and Cretaceous clastic carbonate series. Those elements are introduced in the environment during natural processes, processes of weathering and erosion. This can be explained with the fact that concentrations are usually higher in deeper soil horizons of each isolated lithological unit, except in Quaternary alluvium.

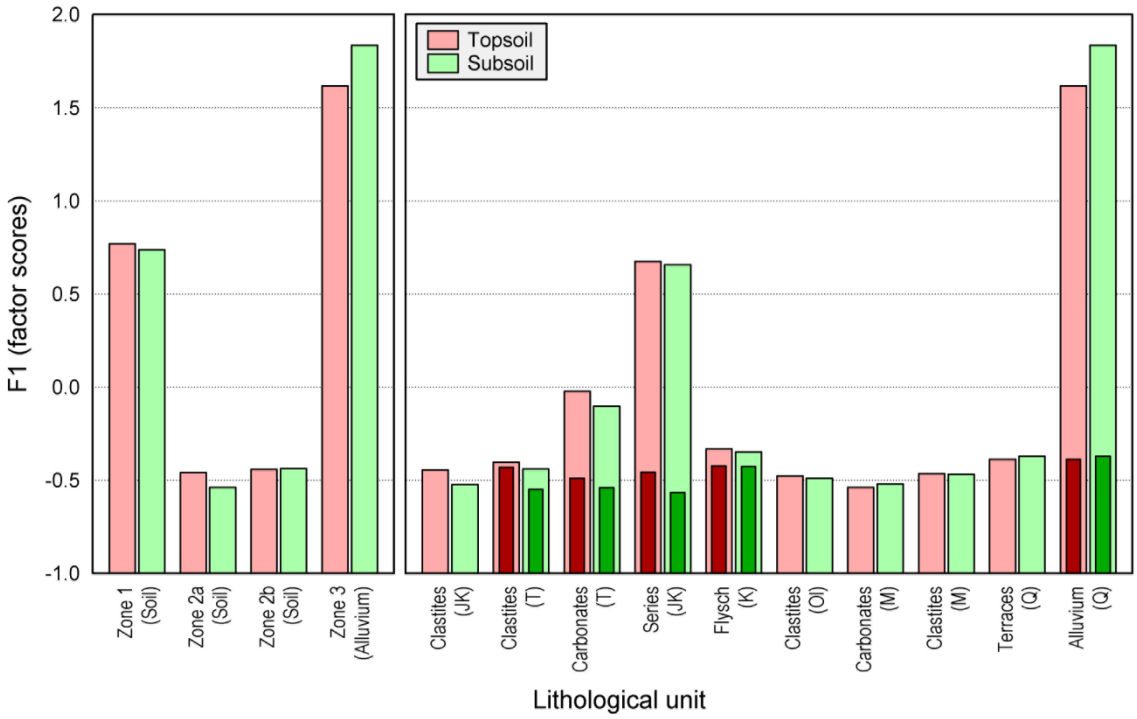

Figure 29: Distribution of Factor 1 scores (Pb, Zn, Hg, Cd, Cu, Bi, Ag, Sb, Mo, W, Mn, Ba, Fe and Tl) through the determined zones (left) and isolated lithological units (right) in soil layers. Darked coloured bares represent an assessment of background values in automorphic soil of Zone 2 (unpolluted area)

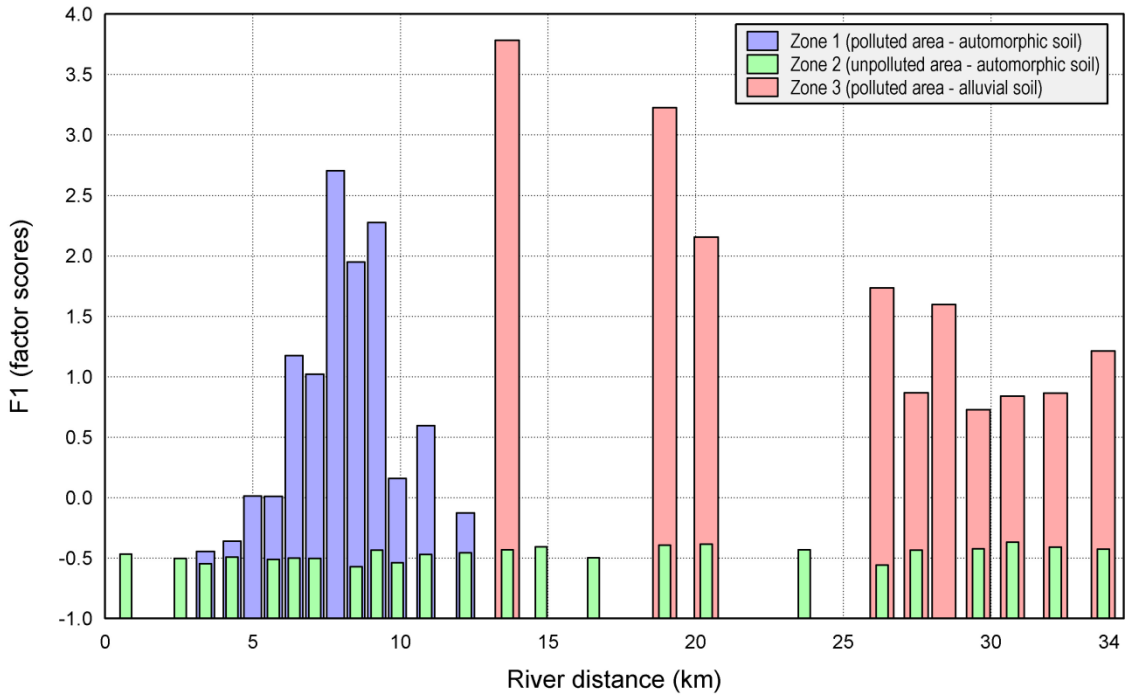

Figure 30: Distribution of Factor 1 scores (Pb, Zn, Hg, Cd, Cu, Bi, Ag, Sb, Mo, W, Mn, Ba, Fe and Tl) in soil according to the river distance

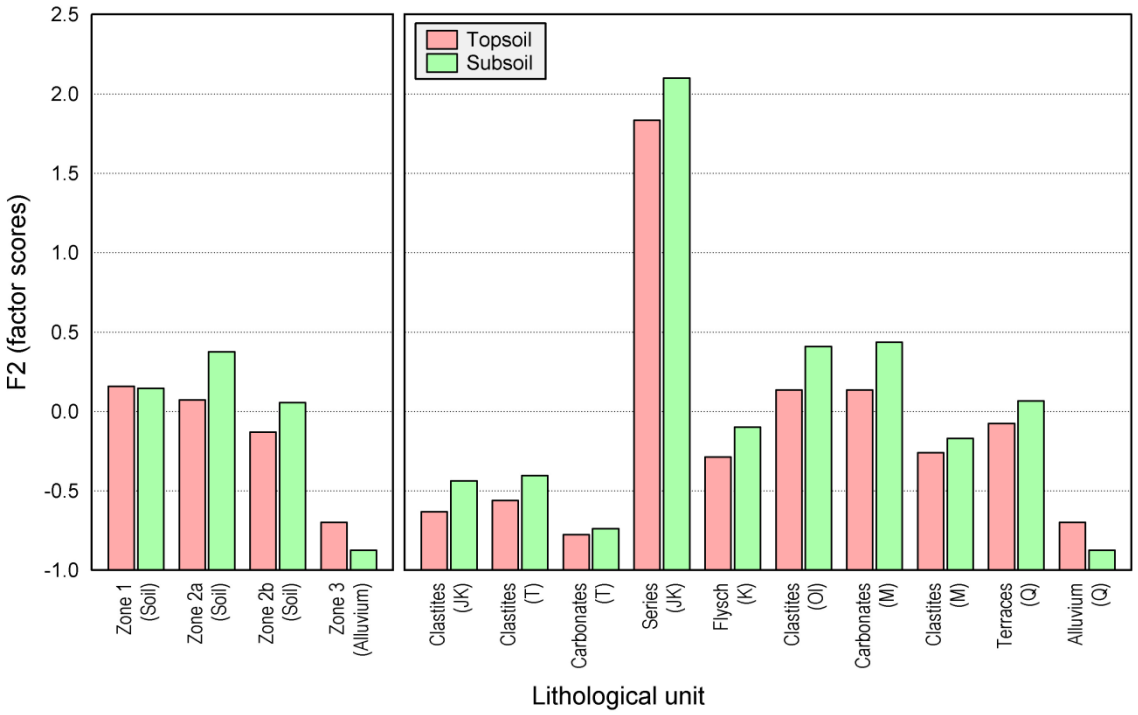

Figure 31: Distribution of Factor 2 scores (Ni, Cr, Co and Mg) *through the determined zones (left) and isolated lithological units (right) in soil layers*

Values of F3 scores (Th, La, As, and Sc) according to the zones are showing similar observation as the previous Factor score. In all three zones their concentrations are increased in subsoil. The highest concentrations are found in Zone 2b (Figures 8 and 32). Their distributions are increasing to the downstream, and highest values are found in Oligocene clastite complex, than in Cretaceous flysch and the Quaternary river terraces. Even for the distribution of F2 is characterized that increased values are found in subsoil of all isolated lithological units. Very interesting increase in background values is noticed through the Zone 1 and especially in Zone 2. In the main industrial zone background concentrations are lower comparing to concentration of automorphic soil, but concentration of Th, La, As, and Sc in all alluvial soil are decreased compering to the automorphic soil of Zone 2.

Distribution of F4 scores (Al, Ti, V, and Ga) according to the depth, the determined zones and the main lithological units are provided in Figure 33. It is very interesting that their concentrations are not varying a lot between the soil horizons. Significant difference is observed only in the Triassic clastites, spilite and tuff. Their distribution is strongly affected by weathering processes, same as in the two previous factors.

Beside the four main patterns of geochemical associations also exist two secondary associations with very weak correlations, Ca and Sr (high concentrations related to the Miocene Carbonates and Quaternary alluvium), and P and K, enriched in topsoil, but without clear spatial distribution pattern. According to the rule that for association is needed minimal 3 elements, these two sub-associations are not concerned as particular geochemical groups.

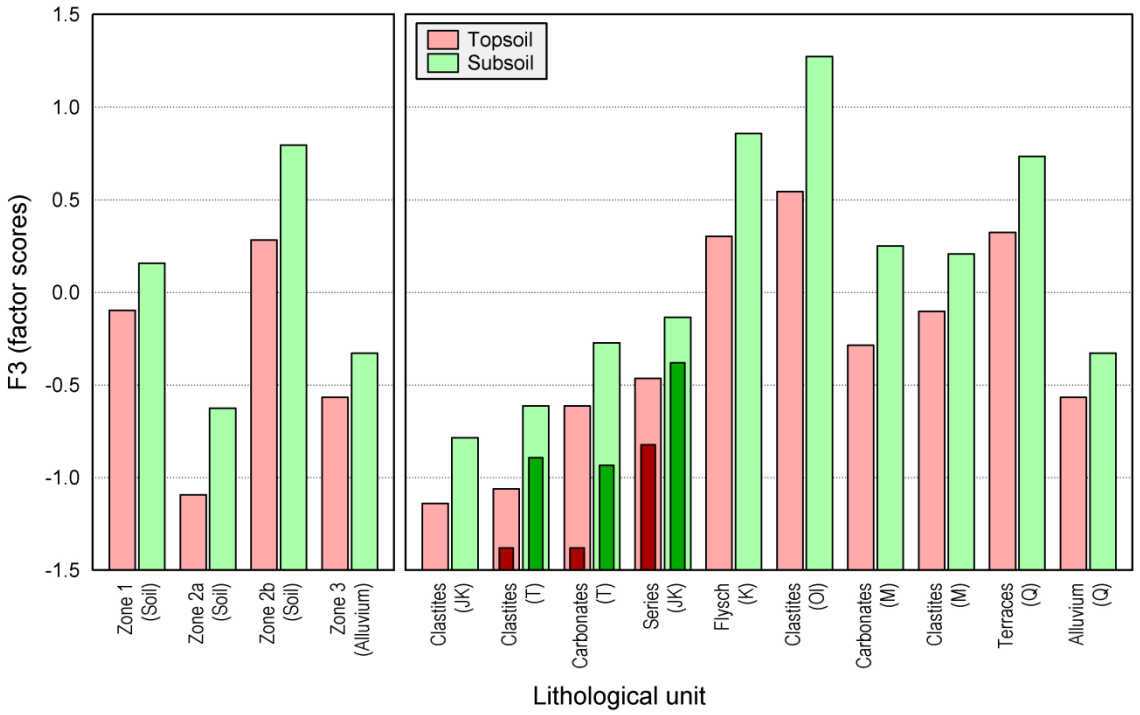

Figure 32: Distribution of Factor 3 scores (Th, La, As, Sc and Tl) through the determined zones (left) and isolated lithological units (right) in soil layers. Darked coloured bares represent an assessment of background values in automorphic soil of Zone 2 (unpolluted area)

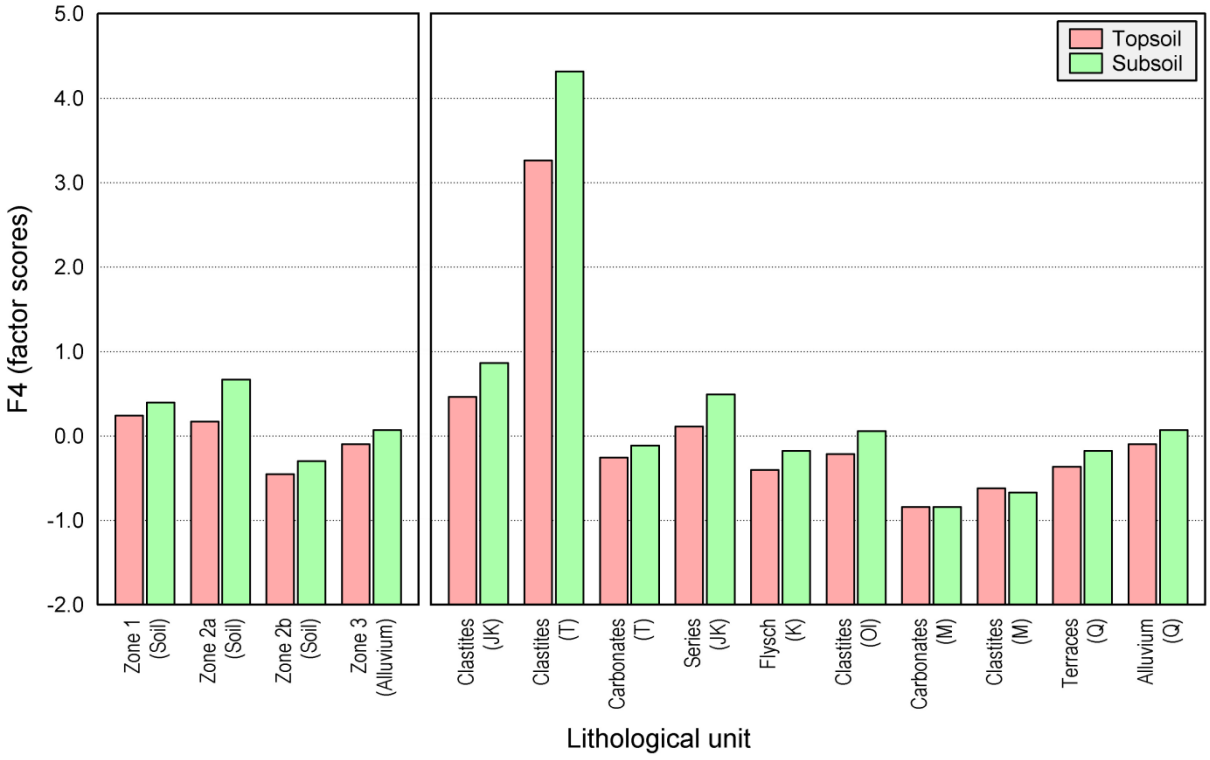

Figure 33: Distribution of Factor 4 scores (Al, Ti, V, Ga and Mg) through the determined zones (left) and isolated lithological units (right) in soil layers

5.4. Linear mathematical methods vs. artificial neural networks (ANN-MP)

5.4.1. (Geo) Spatial data

Collecting of geospatial data have already begun with data acquisition. From the land use map and Digital Elevation Model (DEM) many geospatial data had been sourced and later used in modelling. The main purpose of use such parameters (data), is helpful in preparation of spatial distribution of particular elements as a final product. Geochemical maps, as finial products are necessary in understanding both, natural and anthropogenic processes.

Due to high cost and time-consuming nature of soil sampling, research in developing methods for the creation of soil maps from sparse soil data is becoming increasingly important. In recent years, the development of prediction methods (linear and nonlinear) that use secondary attributes sourced from the DEM, land use, and remote sensing in combination with sparse and expensive soil measurements has been sharpening focus of research. Consequently, the potential for using such information to soil mapping at the withinfields extent is greater than ever before. Appling various modelling techniques different prediction methods for soil prediction were compared, but we also choose the best combination of prediction method and secondary information. Various modelling techniques help us in reconstruction simultaneously different processes that influenced the entire study area. They main purpose is not only the isolation of hotspots with highest concentrations, but they are providing a spatial distribution pattern of particular trace elements. Simultaneously they distinguish natural and anthropogenic influences as well as transportation pattern (such as atmospheric or water transport). Studying aforementioned fact, it will help us in better interpretation and understanding processes that happened in some certain period time that they are related to.

All aforementioned data were used for preparing two spatial distribution models using two predicting methods, modelling by Multiple Polynomial Regression (MPR) and Artificial Neural Network - Multilayer Perceptron (ANN-MP), respectively. For both modelling methods a recall grid has been used. The whole study area is divided to 50 x 50 m grid. Total number of recall points is 41.471. Beside the standard position parameters each particular recall point is also described by some new geospatial parameters (Figures 13 - 15). The both methods were treated by same conditions and same software packages, Statistica 11 (Stat Soft Inc., 2012) and Surfer 11 (Golden Software Inc., 2012). The segment Kriging (SK) is linear method and concerns the sparse measured data only.

Modelling by ANN-MP had been done by using a huge number of input data, 240 of hidden units and 25 train networks. Appling for the best model we try to change some input data, number of neurons, as well as the number of training networks. Our experience showed that more neurons and more architecture are giving better results. Models were constructed for each particular element, then for groups of element extracted by factor analysis. Each particular model is trained to 25 networks but only 5 logical networks have been retained, and finally an average model of retained 5 networks has been calculated. Each training model contain summery table with following parameters: Training perfection, Test perfection, Validation perfection, All perfection, Training error, Test error, Validation error, Training algorithm, Hidden activation, and Output activation. Modelling by MPR is much more difficult than ANN-MP. Many data conversion, corrections and transformation had to be done priory we get useful models. The main reason that we used so many different input data lies in the fact that this method is very demanding compare to the ANN-MP.

Developedmethods and procedures, especially ANN-MP, MPR as a control method, and SK as modified, worldwide successfully established methodhave been usedto predict theconcentrationof four leadingelementsPb, Ni, Ti, andAs from already identifiedgeochemicalassociation.Furtherprocessingof the factorscores valuesareavoidedbecause they representthe new syntheticvariables arecalculatedand

presented asthe standardvalue, which means thatthosemethodscan determinerelativeenrichment relations only. In any case,withany certainty, we cannot judgetheprediction of absolutevalues.

The essence ofwholeapproachis thatunder the same conditionsallthreetested methodsshould givesome stabledistribution results ofthe anthropogenicallyenrichedelements, what was theprimarygoal of this research, as well asnaturalenrichment. The expected resultsmust bestablein all cases. Procedures, approach, preparing data andcalculations weredevelopedso longuntil they become stable. The stable procedures are procedures that under the same conditionscorrectlypredict thedistributionof elementsthat represent thegeochemicalcharacteristics of landscape. Estimation of reliability of predictions and model applicability lies in fact that all given models are repeatable. Sodevelopedprocedures are notrandomorspecific toa particular itemoran isolatedarea, but such modelcanbe usedanywhere, even inthe distribution ofsomeotherobservations. Wecriticallyevaluate themethodsaccording to thesignificance of theappliedtransformations, similarity between models, as well as stabilityof predictions. Basically this represents thebiggestcontribution to the developmentof science.

Sincecomputer equipmentallowing us to prepare a very largenumber of solutionsinreal time, we used the principle which has been used for knotting the Enigma coding system (the Germancoding systemin theSecond World War). The principle is very simple. Discardillogicalsolutionsandfocus onthose whoare logical. The basic principle (principle of Ockham cat) has applied: everything thathappensaround usmust belogicaland indeedsimple.

5.4.2. Stability and significance of models

Predictivedistributionsof the four elements, which representthe dominantgeochemicalpattern ofthe study area, have been reported.Briefly, thedistribution ofPbrepresentsthe impact of miningand smelting, distributions of Ni and Ti represent an influenceorlithology ornaturaldistributions. But the most interestingis "vague" naturaldistribution ofAs,which is not expected andrepresents a realscientific challenge.

The most important fact is that all three prediction methods SK, ANN-MP, and MPR predict real values precisely and not just some relative relationships. The first attempts with artificial intelligence were performed on the factor scores, expressed as standardized values. The first testing methods were based on the relative values which correspond to the true distributions. Much later the real concentrations of elements have been predicted. For this crucial step, lots of experience is needed. Particularly difficult was the MPR method. This linear method is very demanding method, and for its development is needed more time than for artificial inteligence. Table 15 provides basic statistical parameters of raw vales and predicted values of all three methods (SK, MPR, and ANN-MP). The results confirm the previous assumptions. Work with raw values in linear methods does not bring the desired results, because the minimal values are obtained by linear polynomial methods, SK and MPR are negative. For Pb and Ti, the negative values are on 25 percentile, which is in our case about 10.000! Comparing the average values between raw data and predictions can be concluded that the averages of raw data are the highest. ANN-MP is giving slightly lower values. But with should be careful, because the high average values are result of concentrated sampling design in area of large human impact. High natural values of Ni and Ti are consequence of weathering processes of parental material, and the sampling grid is concentrated at some places as well. Their detailed description will be discussed later in following chapter.

Table 15: Comparison between the statistical parameters of raw data (n=111) and predicted values (n=41471)

	Method	Transformation	X	Md	Min	Max	P_{10}	P_{90}	P_{25}	P_{75}
As	Raw data	Normal	45	33	3.9	550	7.5	70	12	45
As	SK	Normal	59	38	2.2	490	6.6	130	14	64
As	MPR	Normal	58	50	-150	250	5.0	120	22	88
As	ANN-MP	Normal	55	47	8.8	240	16	100	27	73
As	Raw data	Log-normal	27	33	3.9	550	7.5	70	12	45
As	SK	Log-normal	30	35	4.6	450	7.3	90	13	56
As	MPR	Log-normal	26	34	0.08	310	6.3	72	14	50
As	ANN-MP	Log-normal	27	36	3.0	100	8.3	60	15	49
As	Raw data	Box-Cox	26	33	3.9	550	7.5	70	12	45
As	SK	Box-Cox	28	35	4.6	450	7.3	88	13	55
As	MPR	Box-Cox	25	33	0.18	390	6.4	70	13	49
As	ANN-MP	Box-Cox	26	34	4.3	100	8.5	58	14	47
Ni	Raw data	Normal	120	91	11	490	34	230	61	140
Ni	SK	Normal	110	87	20	440	38	200	61	140
Ni	MPR	Normal	110	93	-160	440	32	230	63	120
Ni	ANN-MP	Normal	100	77	44	390	60	210	66	120
Ni	Raw data	Log-normal	89	91	11	490	34	230	61	140
Ni	SK	Log-normal	86	83	18	430	36	200	58	130
Ni	MPR	Log-normal	79	79	9.0	890	34	200	52	110
Ni	ANN-MP	Log-normal	80	77	20	290	33	180	63	120
Ni	Raw data	Box-Cox	91	91	11	490	34	230	61	140
Ni	SK	Box-Cox	87	83	19	430	36	200	58	130
Ni	MPR	Box-Cox	81	80	7.7	800	34	210	53	110
Ni	ANN-MP	Box-Cox	82	77	26	270	36	190	64	120
Pb	Raw data	Normal	190	62	26	1700	35	470	42	160
Pb	SK	Normal	100	55	6.8	1700	36	230	42	79
Pb	MPR	Normal	93	58	-410	1200	-63	290	-10	150
Pb	ANN-MP	Normal	90	54	-100	1600	10	190	31	87
Pb	Raw data	Log-normal	94	62	26	1700	35	470	42	160
Pb	SK	Log-normal	65	54	27	1600	36	180	42	73
Pb	MPR	Log-normal	59	48	3.7	2100	32	150	38	76
Pb	ANN-MP	Log-normal	52	41	26	1900	31	120	34	64
Pb	Raw data	Box-Cox	72	62	26	1700	35	470	42	160
Pb	SK	Box-Cox	56	52	27	1600	36	150	41	69
Pb	MPR	Box-Cox	53	47	11	2300	35	120	40	70
Pb	ANN-MP	Box-Cox	50	45	27	2300	32	120	37	65
Ti	Raw data	Normal	0.013	0.0035	0.0005	0.22	0.0015	0.027	0.0025	0.0080
Ti	SK	Normal	0.011	0.0034	-0.001	0.19	0.0020	0.018	0.0027	0.0053
Ti	MPR	Normal	0.014	0.0084	-0.12	0.32	-0.0094	0.033	-0.0015	0.019
Ti	ANN-MP	Normal	0.0083	0.0006	0.0005	0.18	0.0005	0.015	0.0006	0.0064
Ti	Raw data	Log-normal	0.0049	0.0035	0.0005	0.22	0.0015	0.027	0.0025	0.0080
Ti	SK	Log-normal	0.0037	0.0032	0.0006	0.18	0.0016	0.0093	0.0025	0.0045
Ti	MPR	Log-normal	0.0030	0.0029	0.0001	0.23	0.0010	0.0089	0.0020	0.0045
Ti	ANN-MP	Log-normal	0.0035	0.0028	0.0010	0.40	0.0016	0.011	0.0019	0.0049
Ti	Raw data	Box-Cox	0.0042	0.0035	0.0005	0.22	0.0015	0.027	0.0025	0.0080
Ti	SK	Box-Cox	0.0034	0.0031	0.0006	1.2	0.0015	0.010	0.0024	0.0044
Ti	MPR	Box-Cox	0.0027	0.0027	0.0001	0.79	0.0012	0.0076	0.0019	0.0041
Ti	ANN-MP	Box-Cox	0.0030	0.0027	0.0010	0.051	0.0017	0.0081	0.0018	0.0048

X –mean; Md – median; Min – minimum; Max – maximum; P_{25} – P_{75} – quartile range; P_{10} – P_{90} – 10-90 percentile range; Values of Ti are in %, remaining elements in mg/kg

The quality of givenpredictions, is examinedwithregression(cubic polynomial) betweenpredictedandobservedvalues. It is clear thatthis applies only tothe method ofANN-MP andMPR that estimate content according to the spatial parameters(Table 16). A feature for segment kriging cannot be verified because this method uses a linear variogram and the method itself does not depend on spatial parameters. These distributions are only affected by changes in concentrationand distancebetween the observations. Sosignificance of themodelisalways 100%, theoreticallyof course.

Table 16: Regression between observed and predicted values (n=111) according to used prediction method and data transformation

	Transformation	Method	R	D (%)	F ratio
As	Normal	ANN-MP	0.48	23	10
As	Log-normal	ANN-MP	0.78	62	57
As	Box-Cox	ANN-MP	0.79	63	59
Ni	Normal	ANN-MP	0.87	76	120
Ni	Log-normal	ANN-MP	0.89	80	140
Ni	Box-Cox	ANN-MP	0.85	73	95
Pb	Normal	ANN-MP	0.99	97	1200
Pb	Log-normal	ANN-MP	0.97	94	570
Pb	Box-Cox	ANN-MP	0.93	87	240
Ti	Normal	ANN-MP	0.98	96	890
Ti	Log-normal	ANN-MP	0.84	70	84
Ti	Box-Cox	ANN-MP	0.73	54	62
As	Normal	MPR	0.59	35	19
As	Log-normal	MPR	0.78	60	55
As	Box-Cox	MPR	0.79	62	59
Ni	Normal	MPR	0.90	80	220
Ni	Log-normal	MPR	0.90	81	160
Ni	Box-Cox	MPR	0.90	81	160
Pb	Normal	MPR	0.97	94	540
Pb	Log-normal	MPR	0.95	90	510
Pb	Box-Cox	MPR	0.94	88	260
Ti	Normal	MPR	0.96	92	410
Ti	Log-normal	MPR	0.84	70	83
Ti	Box-Cox	MPR	0.78	60	54

R – correlation coefficient (cubic polynomial regression), D (%) – determination coefficient (%); F – ratio (ANOVA test)

Comparison of two prediction methods (ANN-MP and MPR) of four selected elements (As, Ni, Pb, and Ti) three data transformations (Normal, Log-normal, and Box-Cox) have been performed. The regression between observed and predicted values has been calculated by polynomial regression coefficient (R), determination coefficient (D) expressed in (%), and F ratio, respectively (Table 16). Even in some cases the R and D are showing very significant correlation coefficient (even greater than 0.85) but they distributions are either scatteredin plots or the scatterplots itself aremuch skewed. According to the statisticalsignificance it seems that the presentedpredictionmodels, whatever on used transformation, their F test demonstrate quite important statistical significance. But those tests should be approached with some attention. Their significance should be proven by different methods, otherwise it can rapidly lead to some wrong interpretation. Due to this fact, it was assumed that the

model is significant only if a regression coefficient R is higher than 0.75 and determination coefficient D > 50%. In case that R is higher than 0.90 and D > 80%, we talk about high significance. The correlation coefficientis calledregression coefficientin the text, since it is nota simplecorrelation coefficient ofthe straight linea+bxbutthe cubicpolynomialcorrelation coefficient($a+bx+cx^2+dx^3$). The best predictions according the transformations (Table 16, Figures 34 and 35) for both methods are related to the lead distribution, element introduced into environment by human activities. It can be explained due to fact that the structure of geospatial data was primarily designed to predict the anthropogenic distributions, but the models are successful solved the natural distributions of Ni and Ti with high significance as well. But Arsenic is showing the lowest significance and prediction of its distribution is very vague (Table 16, Figures 34 and 35).

According to the results from Table 16 can be concluded that the predictions obtained with MPR are better that predictions obtained by ANN-MP. But this information should be treated with reserve, because the method of artificial intelligence has developed first and gave very good results. MPR method has been developed in order to prove the artificial intelligence as well its superiority. But it was terrible wrong. The linear methods are extremely useful too. But what is the difference? ANN-MP obtaines a quite highly significant results with a small number of input data (only several geospatial parameters) but in other hand the MPR is very demanding method and work with this method need much more mathematical knowledge and much more geospatial data. This is a main difference between two aforementioned methods.

Before application of both methods, data transformation is essential, and special attention was paid. This prepreparation part is time consuming but necessary. In many literatures is noted that the data transformations are necessary to adjust a cloud of data to Gaussian (normal) distribution or by portioning the data, especially the use of multivariate statistical methods (Rose et al., 1979; Pawlowski-Glahn and Egozcue, 2006;Rasmussen et al., 2001; Pawlowski-Glahn et al., 2007) or MPR based on parametric statistic. Inpractice, however,the transformationis usedthatcalculated resultsdo not gobelow zero.It isveryhard to imagine thenegative values of any trace element.Mathematically it is possible. Practicallymost of thetopologicalequations fail in case of huge observations variability over a short distance. This means thattheinterpolationsinan environment of lowvalues, onehighvaluecausesextreme deviations, in 2D projection known as a “Bull’s eye effect” (circles with verylowvalues,next toextremely high values). That problem has been successfully solved using the data transformation. This applies particularly for the natural logarithm or decade logarithm because it is clear that antilogarithm values cannot be below zero.

The prediction significance has been checked between following transformation: untransformed data, logarithm base 10 (most common method), and Box-Cox transformation, which is quite complex, but much better than the previous two. What is advantage of the Box-Cox transformation compare to logarithmic data? Rose et al., 1979 is mentioned that the main elements are normally distributed, but the trace elements have lognormal distribution. In general is true.For simplicity in calculations one transformation for all variables has been used, but feature distribution is verified by tests already mentioned in Chapter 4. Raises at the same time the question of the method reliability, since not all distributions at all levels are under the same rules. The Box-Cox transformation actually adjusts data to the Gaussian distribution, is mathematically very complex, specific for each observation such as the distribution of elements, but it gives much better results.

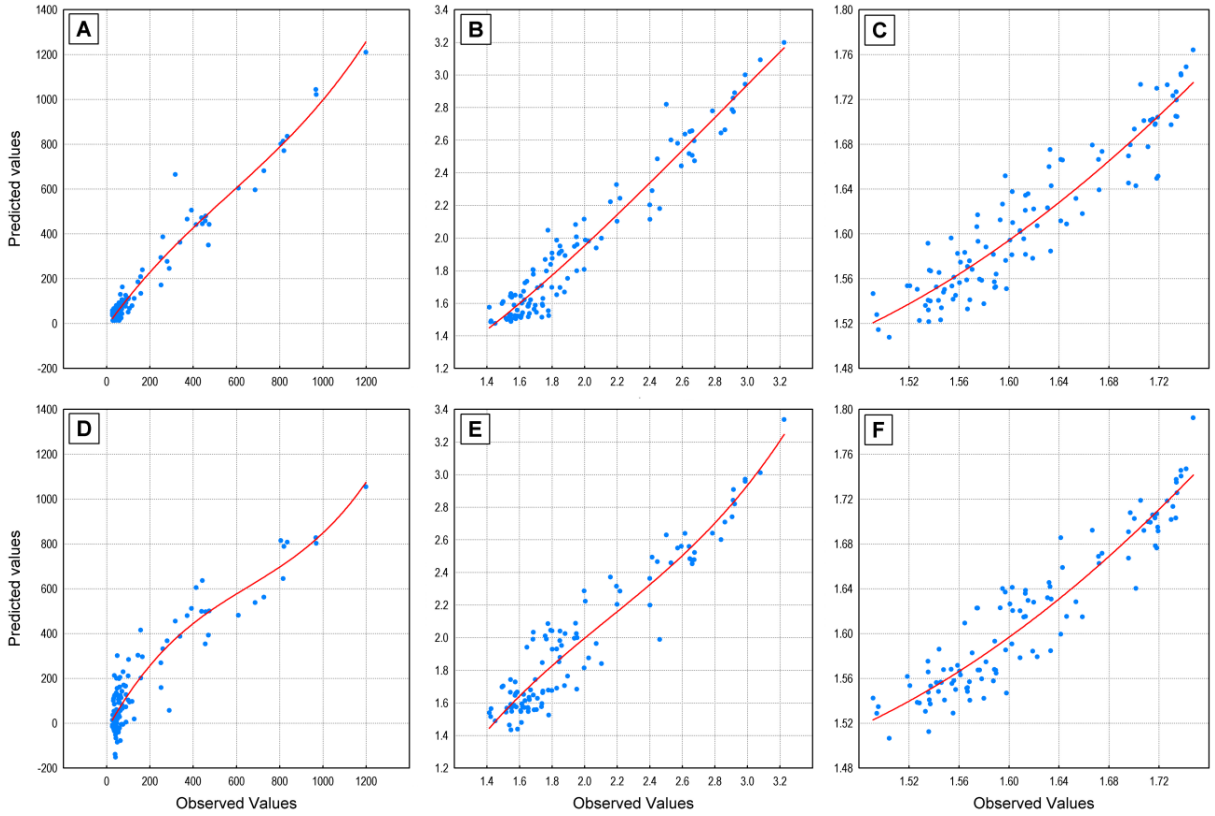

Figure 34: Regression plots of predicted versus observed values of Lead according to predicting methods and transformations; ANN-MP (A – Normal, B – Log-normal, C – Box-Cox) and MPR (D – Normal, E – Log-normal, F – Box-Cox)

Figures 34 and 35 are providing twoextreme eventssuch asPb distribution, the best predicted by both methods, and vague distribution of As, the least predicted distribution by ANN-MP and MPR, respectively. It is clear fromFigure 34 (A and D) that regressionsbetweenobservedandpredictedvalues presented with untransformed data (normal values) is practically useless, because the majority of data is concentrated in area of low values and converging toward the high. The regression line is influenced by several extreme values only. The logarithmic transformation slightly improve the results (Figure 34 **–** B and E), but the most stable regression is obtained by Box-Cox transformed data (Figure 34 **–** C and F).

Similarly is with evaluation of prediction stability for the distribution of As. Correlation diagrams (Figure 35 **–** A and D) are showing that real effective connection between observed and predicted values for normal values do not exist. After using the logarithmic and Box-Cox data transformation the prediction stability models are significantly improved (Figure 35 – B, C, E, and F) for both methods. Actual power connection shown with the determination coefficient D (Table 16) confirms the assumption.

According the all aforementioned facts can be concluded that data transformation is necessary, can be logarithmic in some superficial or fast treatment, but the Box-Cox are much better, and are available in various software. Work with raw data, especially if they are highly asymmetric can lead to some wrong conclusions and wrong data interpretation.

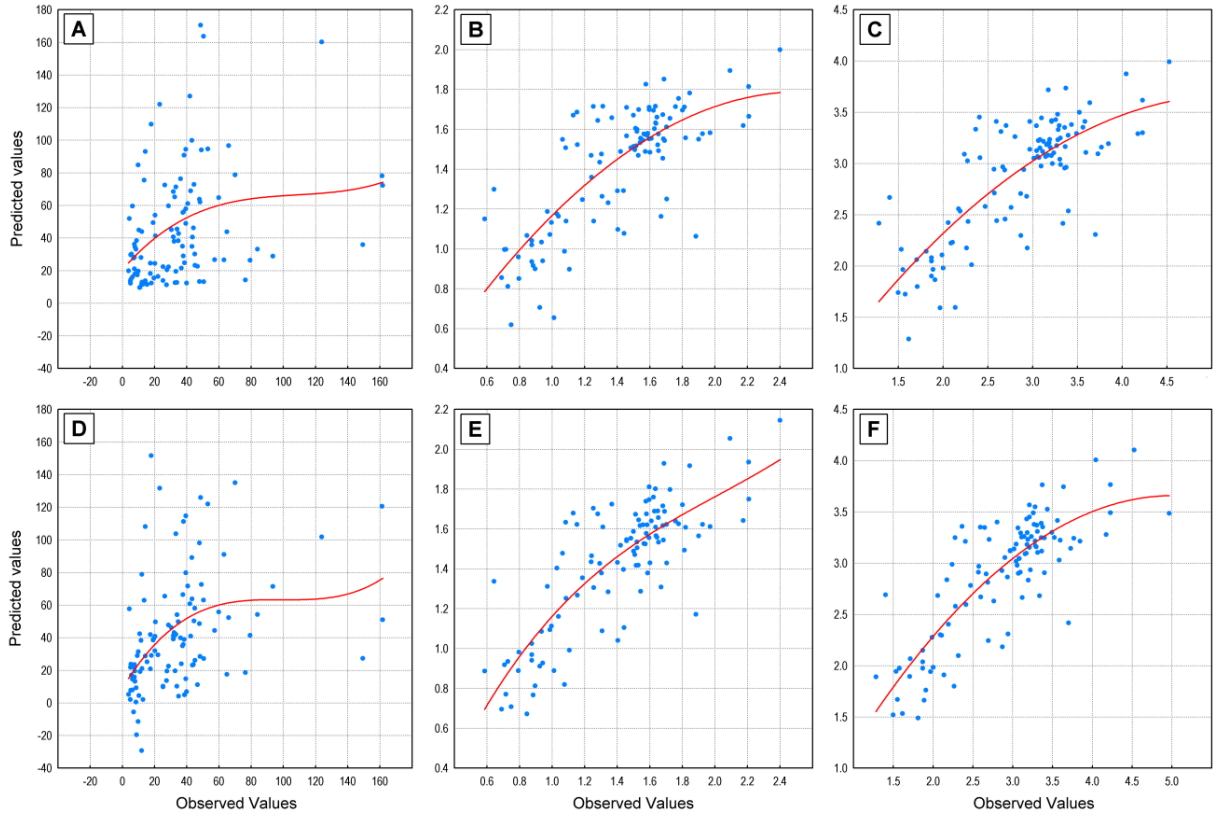

Figure 35: Regression plots of predicted versus observed values of Arsenic according to predicting methods and transformations; ANN-MP (A – Normal, B – Log-normal, C – Box-Cox) and MPR (D – Normal, E – Log-normal, F – Box-Cox)

Table 17: Regression of predicted values between the data transformations within a prediction models in range of 0.1 – 99.9 percentiles (n=41388)

		Normal vs. Log-normal			Normal vs. Box-Cox			Log-normal vs. Box-Cox		
	Method	**R**	**D (%)**	**F ratio**	**R**	**D (%)**	**F ratio**	**R**	**D (%)**	**F ratio**
As	SK	0.97	93	1.9E5	0.96	92	1.6E5	1.00	100	6.0E7
Ni	SK	1.00	99	2.2E6	1.00	99	2.6E6	1.00	100	2.6E8
Pb	SK	0.98	96	4.5E5	0.95	89	1.1E5	0.99	99	1.3E6
Ti	SK	0.79	63	2.3E4	0.98	96	3.0E5	0.93	87	8.9E4
As	MPR	0.83	68	3.0E4	0.81	65	2.6E4	1.00	100	1.5E7
Ni	MPR	0.95	90	1.3E5	0.96	91	1.5E5	1.00	100	2.9E7
Pb	MPR	0.82	67	2.8E4	0.73	53	1.5E4	0.97	94	2.3E5
Ti	MPR	0.79	62	2.2E4	0.71	50	1.4E4	0.97	95	2.5E5
As	ANN-MP	0.77	59	2.0E4	0.76	58	1.9E4	0.99	99	1.2E6
Ni	ANN-MP	0.95	90	1.3E5	0.93	86	8.2E4	0.99	98	6.8E5
Pb	ANN-MP	0.91	82	6.3E4	0.85	73	3.7E4	0.94	89	1.1E5
Ti	ANN-MP	0.80	64	2.5E4	0.67	45	2.5E4	0.93	86	8.6E4

R – correlation coefficient (cubic polynomial regression), D (%) – determination coefficient (%); F – ratio (ANOVA test)

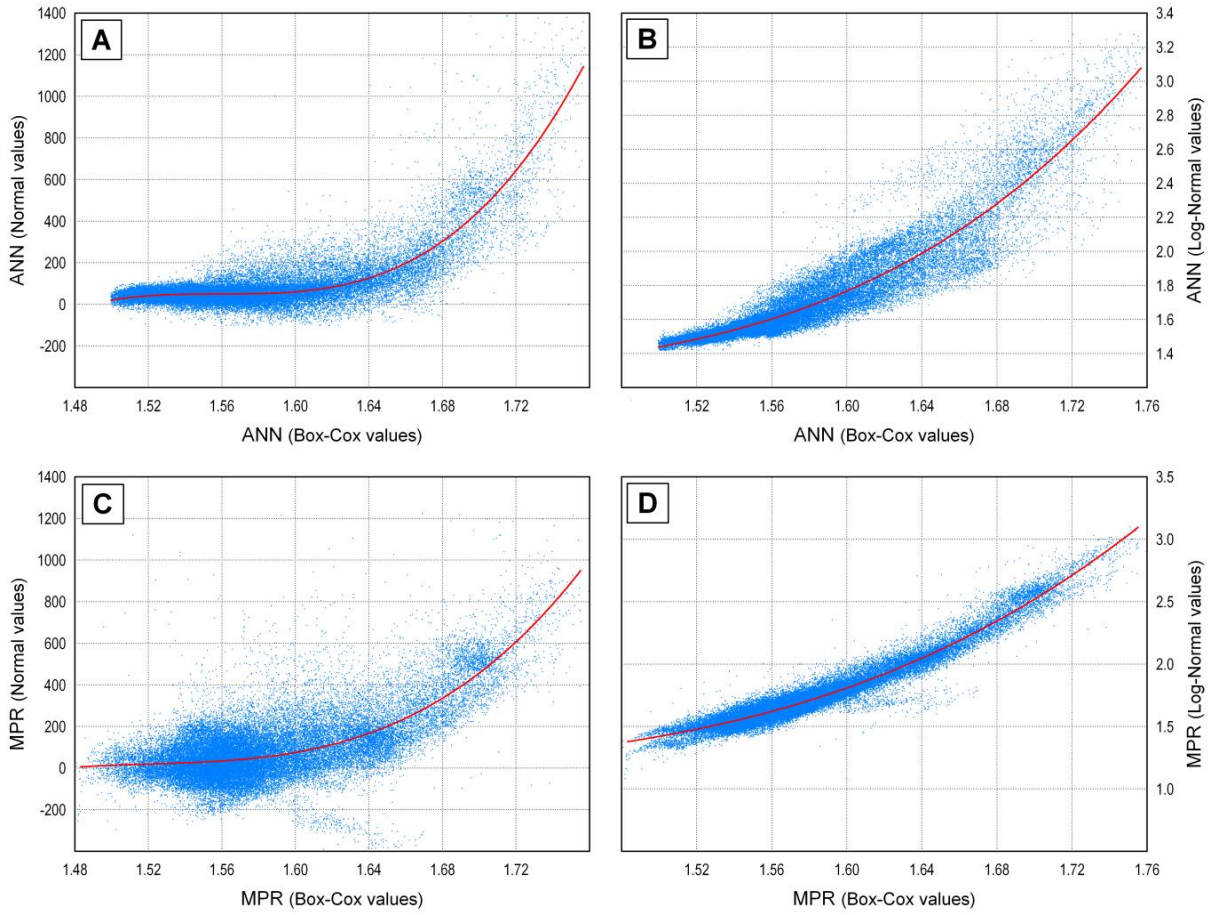

Figure 36: Regression plots of predicted values of Lead after data transformations; ANN-MP (A – Normal vs. Box-Cox, B – Log-normal vs. Box-Cox)and MPR (C–Normal vs. Box-Cox, D – Log-normal vs. Box-Cox)

Significance of the model prediction has been performed by calculating the regression coefficient(Table 17) and with inspection of regression correlograms between the predictedvalues within eachpredictions method,ANN-MPand MPR.The significance has been examined in a range of predicted level from 0.1-99.9 percentiles (or 41388 recall points), which means that the lowest and the highest values in total 83 have been excluded from the further treatment. They deviate significantly from the total number of recall points (41471), calculated values for each variable. In the mentioned rage all calculated values have very realistic values what confirm the model significance and confirmation.

According to the intercorrelations, the predicted results regard to the transformation within the same method not showing significant differences. The lowest determination coefficients are within As and Ti, but partially for Pb, between normal values and transformed data (normal vs. Log-normal and normal vs. Box-Cox). Even this low D values are generally looking quite highly significant. The best intercorrelations are found between Log-normal and Box-Cox transformations. They are in the rank of physical laws. The lowest determination correlation within these data transformation has been found for Ti, 86%. According to the table can be concluded that there is no very significant difference between natural (normal) values and transformed data. But it is a wrong conclusion, because the significance with large number data (in this case 41388) is not same as significance with sparse

number of observations. With large number of data everything becomes statistically significant, which of course in not true.

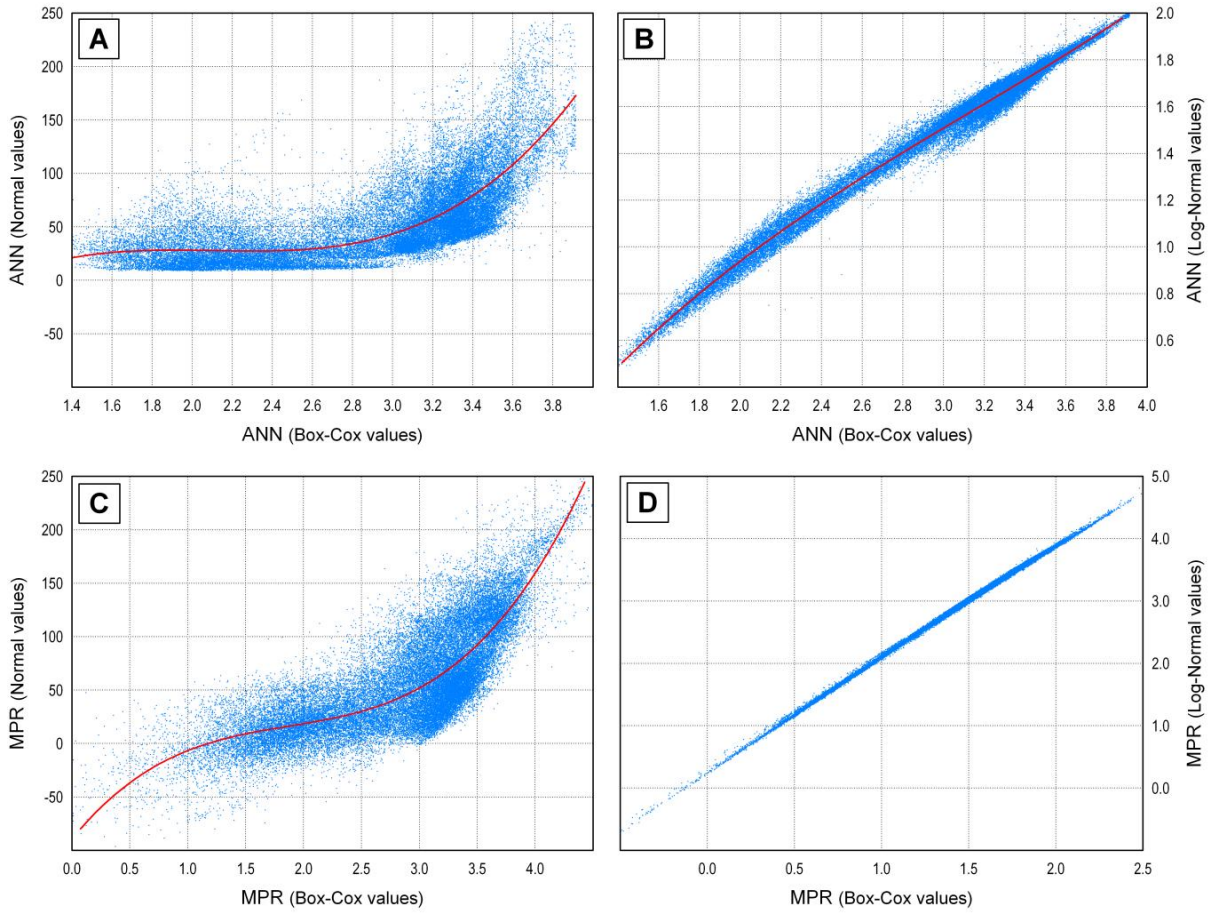

Figure 37: Regression plots of predicted values of Arsenicafter data transformations; ANN-MP (A – Normal vs. Box-Cox, B – Log-normal vs. Box-Cox) and MPR (C – Normal vs. Box-Cox, D – Log-normal vs. Box-Cox)

Regressions between transformations within two predictive methods for Pb and As are provided in scatterplots with fitted regression lines in Figures 36 and 37. There are showing a visible sense of the statistical relationship within each prediction method. It is evident that the Pb distribution is tending to exponential form, but this is affected by several values with very high concentrations. The scatterplots for both methods are showing quite similar tendency what is the result of strong asymmetric distribution. It is typical for anthropogenic elements, where extreme high values deviate from the low values of parental rocks. Differences between transformed data are almost negligible for both methods. But differences between correlations within normal and transformed data for MPR are much higher than correlations within Log-normal and Box-Cox transformations. But is not case for the artificial intelligence. It can be explained with fact that ANN-MP is less influenced by transformations than MPR, because MPR is based on parametric statistic but ANN-MP not, it is nonlinear mathematical method (Figures 36 and 37).

Arsenic is showing the lowest tendency for any geochemical trend, but differences are much higher between normal values and transformed data in both cases (Figure 38 – A and C), respectively. Between transformed data there is almost no difference with no regard to prediction method. This can be visualized for MPR, especially. There is no significant difference between logarithmic and Box-Cox transformation.

The scatterplots (Figures 37 and 38 – A and C) are presenting also very interesting predictions that include the negative natural values as well. For us is quite unthinkable to imagine the negative values of any particular element but obviously for the prediction method is not. Majority of prediction concentration for both, Pb and As is below zero.

The differences between two predictions methods according the same data transformation have been examined as well (Table 18, Figure 38). It can be concluded that both models are providing mutual similarities, because the determination coefficient in all cases is higher than 50%. Major differences and lower determination coefficient is found for asymmetric distributions of As an Pb, in both cases for untransformed data (52% and 57%). Much better correlations are between transformed data, but slight deviations for naturally distributed Ni and Ti is noticed, where asymmetric distribution is not significant.

Table 18: Regression between predicted values (ANN-MP vs. MPR) according to data transformation in range of 0.1 – 99.9 percentiles (n=41388)

	Transformation	R	D (%)	F-ratio
As	Normal	0.72	52	1.5E4
As	Log-normal	0.91	82	6.3E4
As	Box-Cox	0.92	84	7.3E4
Ni	Normal	0.92	85	7.6E4
Ni	Log-normal	0.91	83	6.9E4
Ni	Box-Cox	0.90	80	5.6E4
Pb	Normal	0.75	57	1.8E4
Pb	Log-normal	0.91	84	7.0E4
Pb	Box-Cox	0.89	79	5.3E4
Ti	Normal	0.80	65	2.5E4
Ti	Log-normal	0.88	78	4.8E4
Ti	Box-Cox	0.83	68	3.0E4

R – correlation coefficient (cubic polynomial regression), D (%) – determination coefficient (%); F – ratio (ANOVA test)

Figure 38 is presenting the correlograms between two applied methods. Same as in previous examples, the two different models, the most successful model (Pb) and less successful model have been chosen. Pb and As for predicted values do not showing the real correlation between normal values, despite the typical regression coefficient. The scatterplots in both cases are providing disperse distributions, concentrated in the lower, converging to the area of higher values. The fitted regression line connecting only a small number of calculated values in the area of high values.

Completely opposite situation is with the Box-Cox transformations. The clouds are narrow and represent the real correlations between data obtained by two different prediction methods. These results are basically the confirmation for the previous claim that methods for its validation have to provide similar results. In this case we are talking about distribution of chemical elements, but it can be applied for distribution of any kind of observation.

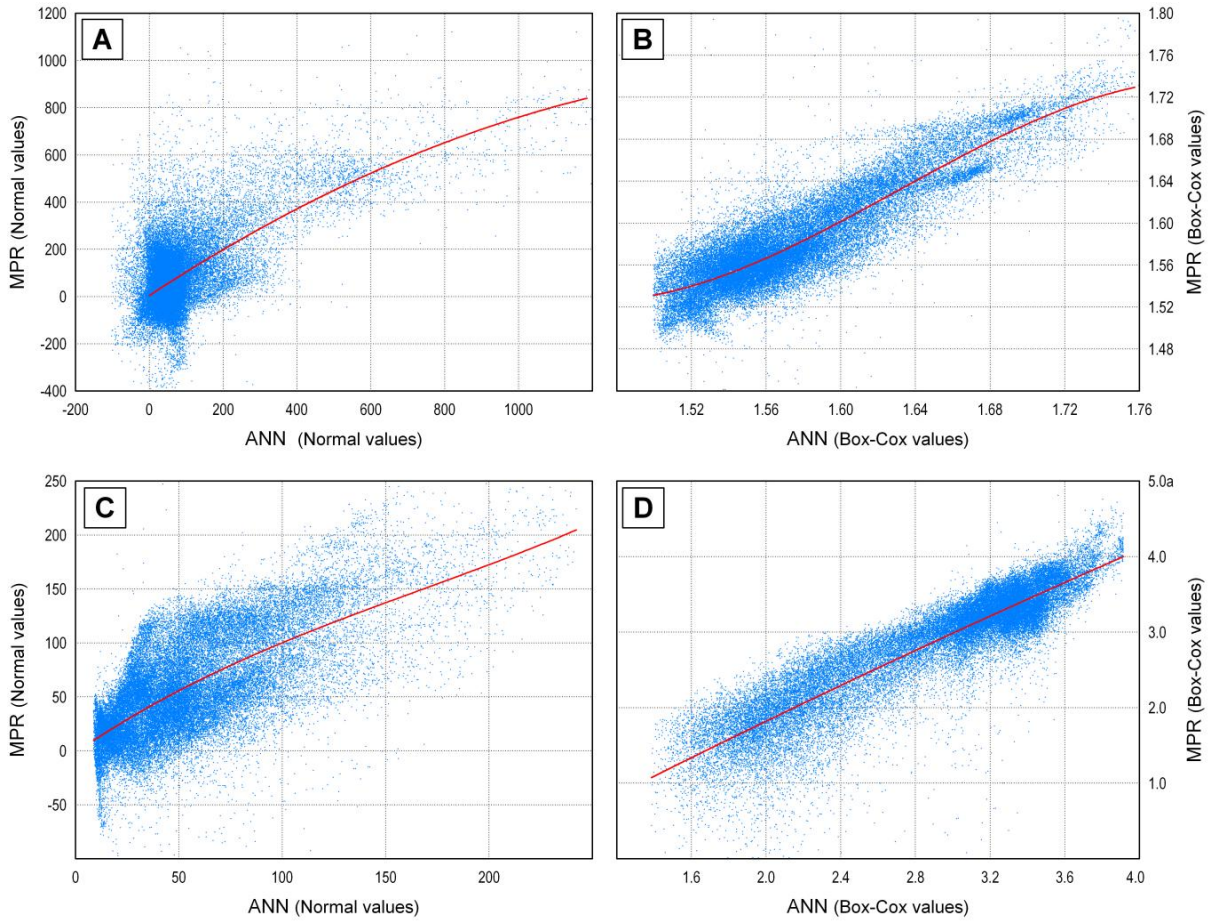

Figure 38: Regression plots of ANN-MP versus MPR predicted values after data transformation; Lead (A – Normal values, B – Box-Cox values; Arsenic (C – Normal values,D –Box-Cox values)

5.4.3. Predicting of Lead anthropogenic distribution

Lead is common anthropogenic chemical element, which concentrations depend on human activities. The mean value in soil 190 mg/kg, in stream sediment 240 mg/kg, and 820 mg/kg in attic dust (Tables 6 and 7). The median values are 62 mg/kg (soil), 220 mg/kg (stream sediments), and 280 mg/kg (attic dust), respectively. Maximum values in these three sampling materials are 1700 mg/kg, 570 mg/kg, and 2800 mg/kg. The F ratio for Pb in ANOVA is deviate significantly from the other anthropogenic elements, and showing its anthropogenic nature (Figure 21). Table 9 is clearly presenting the average concentrations in all three determined zones. In the Zone 1, its concentrations are basically the same in both soil horizons (400 and 410 mg/kg). In the Zone 2 the concentrations are significantly lower, between 50-60 mg/kg, but in the Zone 3, its concentrations are again drastically increased to 680 mg/kg in topsoil and 800 mg/kg in subsoil. High concentrations in alluvial soil are consequences of long lasting mining and smelting in upper part of valley, which is transported by Stavnja and its tributaries. It is very interesting for anthropogenic element that concentrations are higher in subsoil but it can be explained by fact that almost all activities stopped more than 20 years ago.

Enrichment ratio between determined zones and sampled material is clearly showing human impact in study area. ER between the contaminated zones (Zone 1 and Zone 3) and uncontaminated Zone 2, are higher 8 and 15 times (Figures 23 and 24), and it is noticeable that are alluvial soil highly influenced by human impact. Atmospheric transport is proved by the ER between attic dust and topsoil (Figure 25). Lead concentrations are higher 3 times in attic dust than in topsoil. The last ratio is providing significant information about historical and current river transportation (Figure 26). Current sediments contain much lower concentration of trace elements, because the main sources of contamination do not operate.

Distribution of Pb is showing significant anomalies in Zone 1 and Zone 3 (Figure 39). This distribution is consequences of human activities in main industrial zone and river transport downstream. Extreme mobility of Pb causes that concentration varying between sol depths,from 700-800 mg/kg, respectively. Increased values in subsoil are due to fact that intensive mining and ore processing activities were 20 years ago. Comparing to the Standard List, its values are higher 9 times in topsoil and 10 times in subsoil. Background values (dark red and green bares) through the lithological units are less than 80 mg/kg. The lowest values are found in Jurassic and Cretaseous clastic carbonate series, Cretaceous Flysch, Oligocene clastite complex, Miocene carbonates, Miocene clastites, and Quaternary river terraces. To assess a background values for the Zone 2, only soil samples from automorphic soil were considered. The background values are presented with more intensive colours.

Distribution of Pb according to the distance is provided in Figure 40. Here we can see that extreme concentration 1700 mg/kg is noticed in the central part of mining and smelting area. Its concentration is decreasing slowly downstream in form of finest grains. Even in the lower part of the Zone 2 Pb content do not decrease above 400 mg/kg. How big contrast between natural enrichment (green colour) and human impact (blue and light read) is also provided in same figure. Along the entire valley, natural enrichment is about 50 mg/kg. This means that human impact increased its concentration for more than 30 times.

The predictions of spatial distribution of Pb concentrations in soil using three predicting methods are presented in Figure 41**.** All three models, A) Segment Kriging (SK), B) Multiple Polynomial Regression (MPR), and C) Artificial Neural Network – Multilayer perceptron (ANN-MP) identify hotspots with high concentration of Pb. These predicting models are showing arrangement in concentrations across the study area. For a graphical display of spatial distribution, the maps with percentile distribution have been used, where different colours represent different concentration arrangements.

The spatial distribution pattern of Pb is reconstructing its main pathway in study area. These models are providing similar pattern of Pb concentration hotspots, indicating the same source of contamination. In the upper part of study area, all three models are providing the same shape of contamination areola. This part of the study area is surrounded by steep hills, and the contamination areola is caused by the main wind direction which is N-S. River transport of clay fine grain is transported down into alluvial sediments. Eroded material has been transported down the river and embedded in alluvial plain of urban zone Breza, where intensive agriculture is present. Spatial distribution with SK is improved, contamination along the river is continuous (no discontinuous circles so called “Bull’s eye effect”), but still not strict as it is provided in two another models.

The Segment Kriging includes only sparse soil measurements (n=111), connecting the concentrations of Pb in the particular ranges and this change in concentrations cannot be so perfect as with the remaining two predictive methods, which include much more spatial data. Due to this fact, MPR and ANN-MP are showing more realistic arrangement in concentrations than SK. In other hand, their similarities are reconfirmation, refinement and in same time validation of different models. All models are repeatable, what is another success in such modelling.

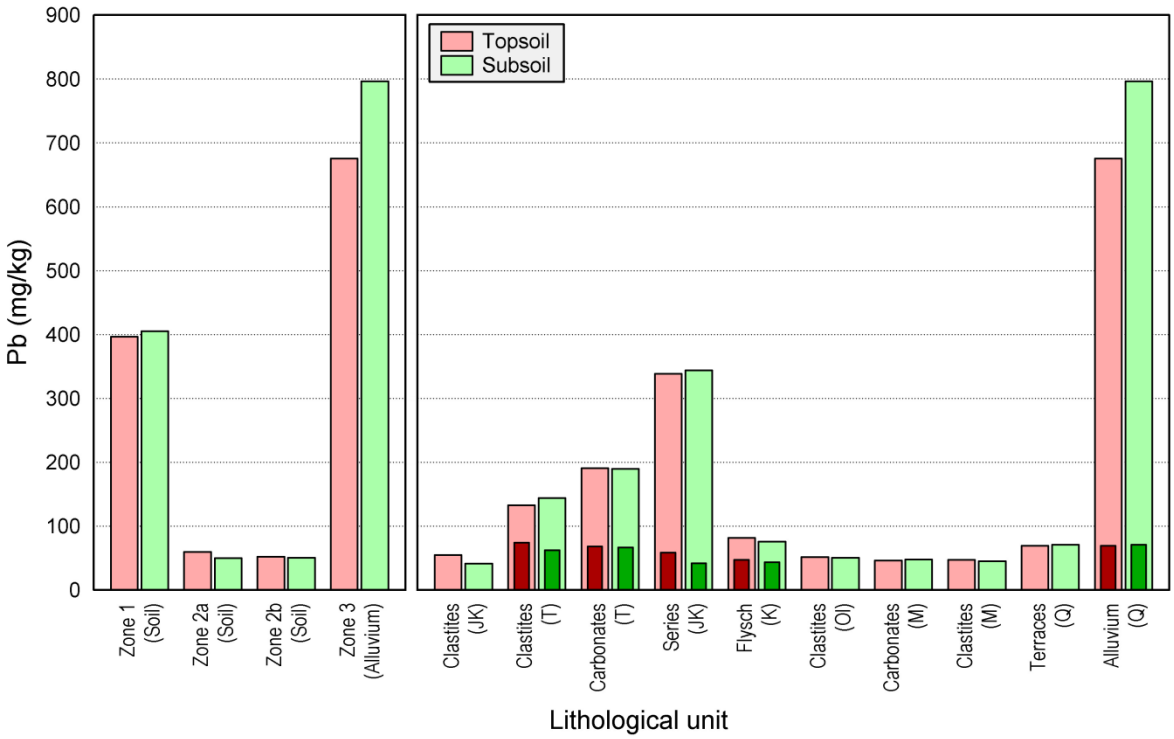

Figure 39: Distribution of Lead concentrationsthrough the determined zones (left) and isolated lithological units (right) in soil layers. Darked coloured bares represnt an assessment of background values in automorphic soil of Zone 2 (unpolluted area)

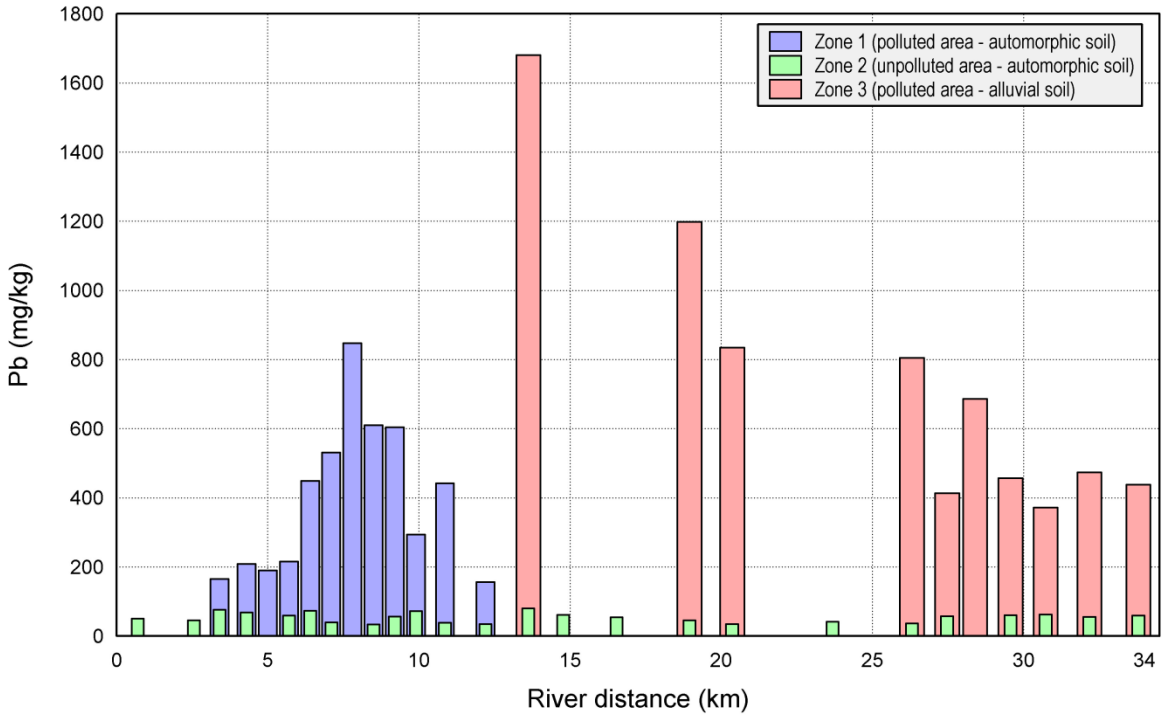

Figure 40: Distribution of Lead in soil according to river distance

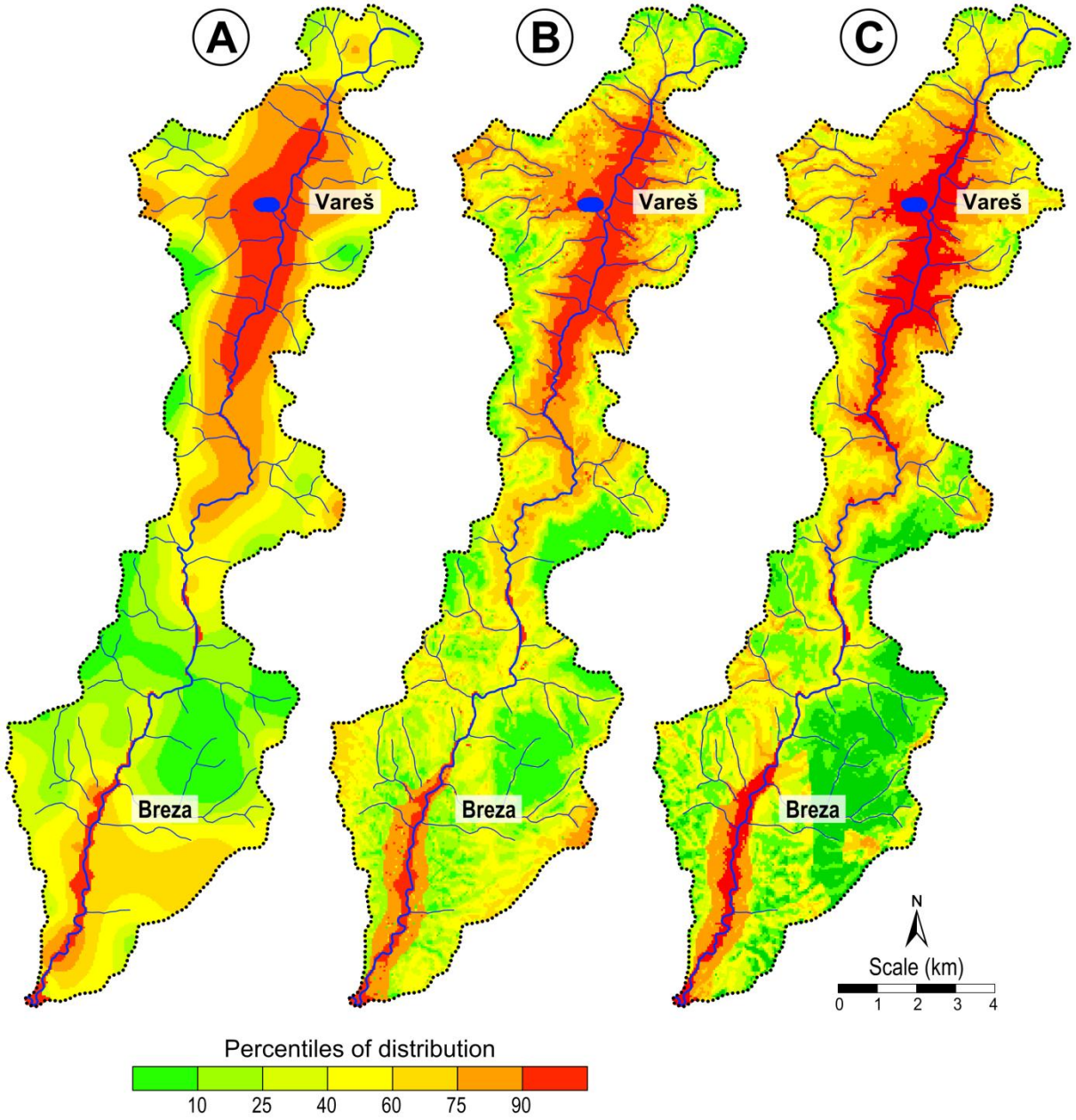

Figure 41: Spatial distribution of Lead using various predicting methods: A – Segment kriging (SK); B – Multiple polynomial regression (MPR); C – Artificial neural network – Multilayer perceptron (ANN-MP)

Distribution of lead within the lithological units according to the raw data and prediction methods is presented in Figure 42. The data transformation used in all three prediction methods is Box-Cox because it gave the best results but also because mutual comparison. There is no significant difference between raw data and transformed data used for each particular prediction method. At some lithological units, the raw data are showing a bit higher values, but it is more subjective. The clear anomaly is on quaternary alluvium, where maximal values rich 610 mg/kg (raw data) and 540 mg/kg (Segment Kriging), respectively.

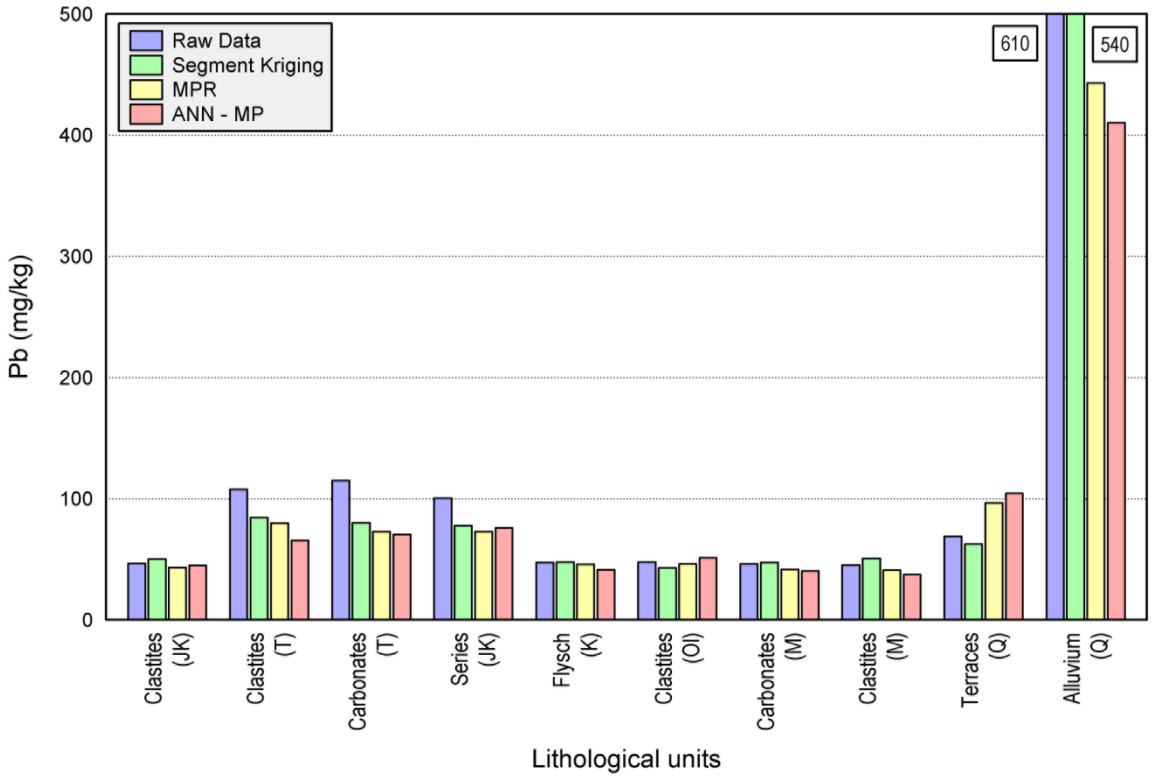

Figure 42: Distribution of Lead values in isolated lithological units according to raw data and prediction methodsafter using the Box-Cox transformation

5.4.4. Predicting of Nickel natural enrichment

The mean values for Ni are 120 mg/kg in soil, 78 mg/kg for stream sediment, and 79 mg/kg in attic dust. The median values are 90 mg/kg, 78 mg/kg, and 66 mg/kg for soil, stream sediments, and attic dust. Maximum values are found in soil, 500 mg/kg what is logical because its concentrations depend on parental rocks (Tables 6 and 7). The value of F ratio is more than 60 times higher comparing to other naturally distributed chemical elements (Figure 22). Only Cr has the F ratio higher. The average concentrations for three determined zones (Table 9) are showing that there are no significant differences between values among them. This can be explained with fact that determined zones contain more isolated lithological units. Natural anomalies are usually connected to the one or two lithological units, and the average values are much lower and not showing the real concentrations.

Tables 10 and 11 are providing average content of Nickel in topsoil and subsoil. Here is possible to see increase and decrease in its average content within the isolated geological units. Difference in concentration through the soil horizons is claiming that this element is naturally introduced into environment. Its concentrations are increasing with depth, but maximum average levels are found in the Jurassic and Cretaceous clastic carbonate series, 280 mg/kg and 310 mg/kg, respectively. Distribution of Nickel in soil samples (Figure 43) according to the determined zones is not showing significant anomalies within the determined zones. Only slight anomalies are noticeable in subsoil of Zone 2a. Distribution according to the lithological units is showing more precisely which parental material is enriched with Ni. Natural enrichment is higher than target (8 - 9 times) and intervention values provided in Table 1. The lowest enrichment found on Jurassic and Cretaceous breccias and sandstones and Triassic carbonates, about 50 mg/kg. Even this low values are higher than the target values.

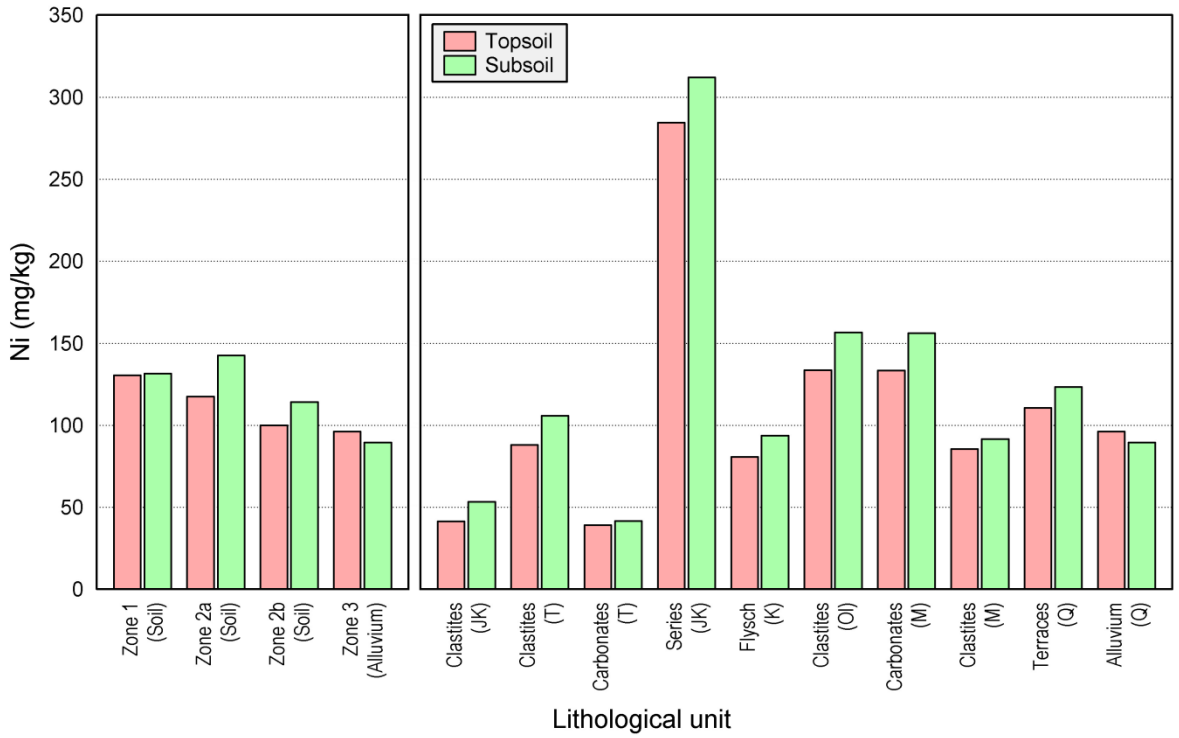

Figure 43: Distribution of Nickel concentrations through the determined zones (left) and isolated litological units (right) in soil layers

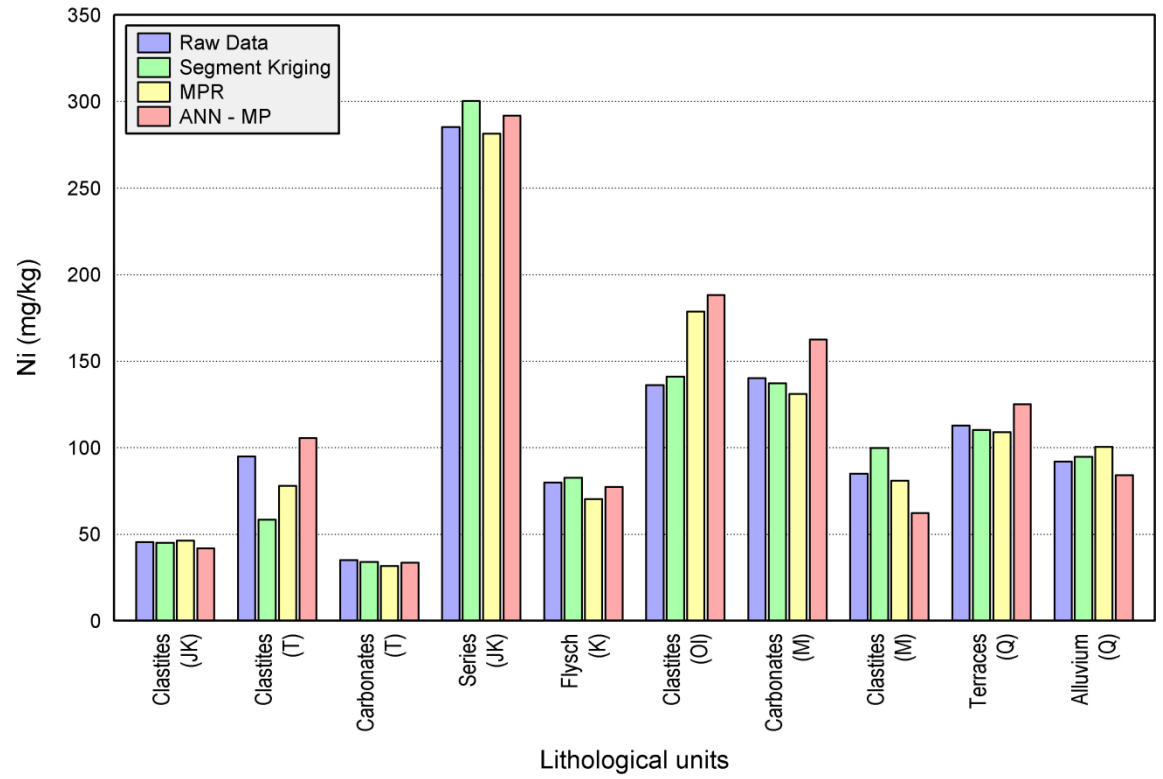

Figure 44: Distribution of Nickel values in isolated lithological units according to raw data and prediction methods afterusing theBox-Cox transformation

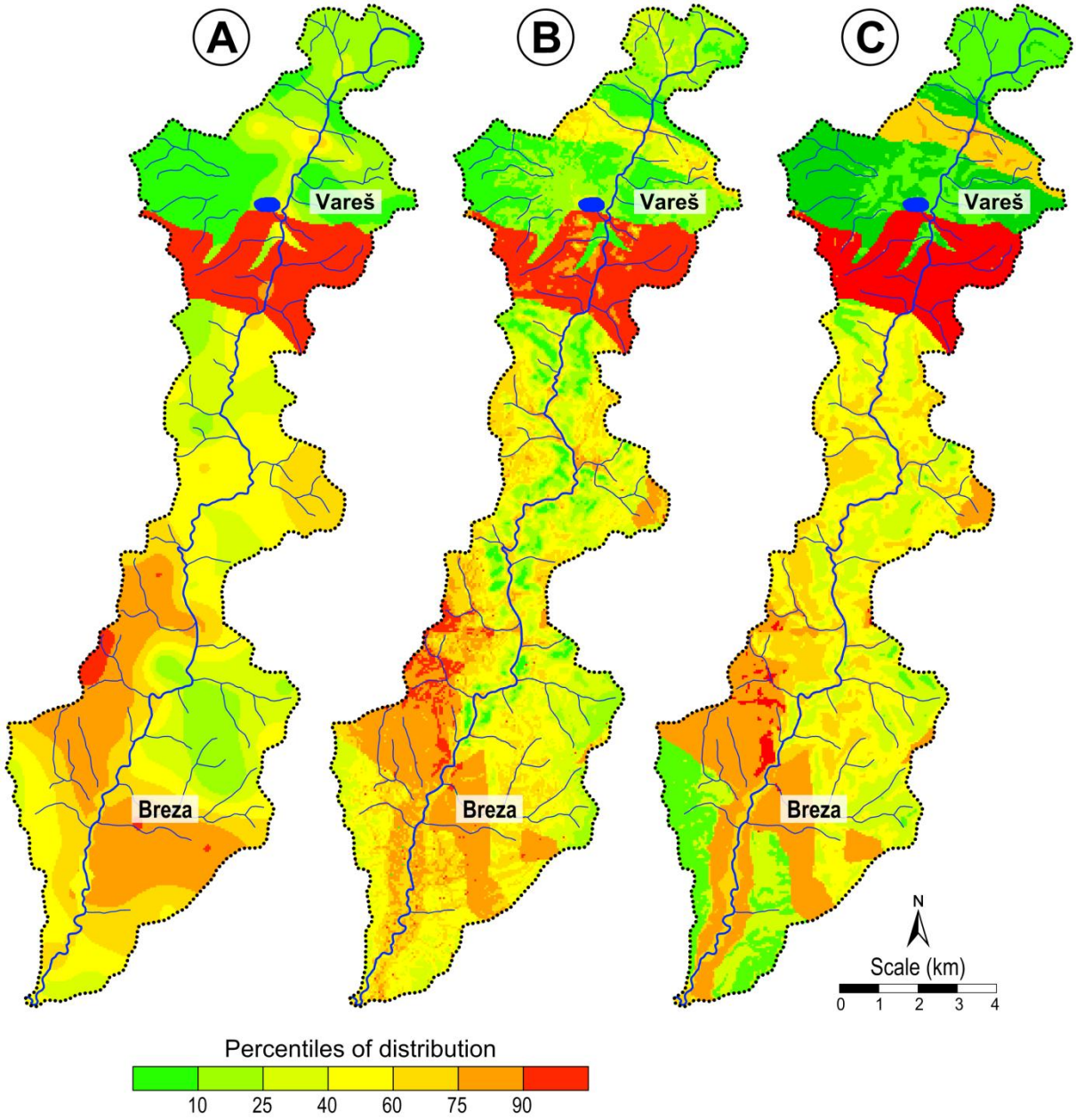

Figure 45: Spatial distribution of Nickel using various predicting methods: A – Segment kriging (SK); B – Multiple polynomial regression (MPR); C – Artificial neural network – Multilayer perceptron (ANN-MP)

Distribution of Nickel within the main lithological units according to the raw data ad prediction methods is presented in Figure 44. It can be seen that the Jurassic and Cretaceous Clastites are again clearly isolated from the other lithological units. The maximum values with transformed and raw data are between 280 and 300 mg/kg. Average values of Box-Cox transformation within the prediction data as well as raw data do not vary so much. At two more units,Oligocene clastite complex and – Miocene carbonate series are showing a slight increase of Ni, which concentration exceeds the target values for 5-6 times.

Spatial distributions of Ni within three predicting methods are provided in Figure 45**.** Arrangement of Ni across the study valley in all three models is pretty well identify. This distribution is clearly conducted to the parental material in upper part of study area. The highest concentrations are found in Jurassic and Cretaceous flysch series composed by marly shale, limestone, sandstone, conglomerate, breccia, and chert. Northern from the city Vareš, enrichment is present only on Triassic clastites what is clearly isolated in ANN-MP model.

All three models are presenting a significant enrichment through all study area southern from the Jurassic and Cretaceous flysch. ANN-MP and MPR isolated two more lithological units (the Miocene carbonates and the Oligocene clastite) with significant enrichment of Ni. ANN-MP prediction very precise distinguish border between alluvial sediments (material that is transported by Stavnja and other tributaries) and Miocene carbonates and Oligocene clastites.

5.4.5. Predicting of Titanium natural enrichment

The mean values for Ti are 0.013% in soil, 0.039% for stream sediment, and 0.018% in attic dust, but the median values are 0.004%, 0.033%, and 0.017% for soil, stream sediments, and attic dust respectively. Maximum values are found in soil, what indicate its natural enrichment (Tables 6 and 7) but the mean and median values are much higher in stream sediments. This high values are describing Ti mobility as well its ability to incorporate into finest clay size particles and transport far from the source of contamination. The lowest (Table 9) values are found in the Zone 2b in both soil horizons. However, the average concentrations of Ti across the major lithological units are showing that there is no difference in concentrations through the depth (Tables 10 and 11). Enrichment ratio between determined zones (Figures 23 and 24) is not showing a significant enrichment because it is conducted to only particular geological units and more samples make the results smoother. Even the ER between the sampling media (Figure 25) does not presenting significant results, but concentrations of Ti are slightly higher in attic dust than in topsoil.

Similar distribution pattern within the isolated lithological units are provided in Figures 46 and 47. There are showing that there is no almost any difference within soil horizons or within raw data and prediction methods. The significant increase in concentration is conducted to the Triassic Clastites in range 0.14 - 0.17%. It is clear that this parental material contains much more Ti than other in study area. Those rocks are the main source of Ti, which is transported by water in alluvial sediments.

Prediction models of Ti spatial distribution are isolating the highest concentrations in Triassic clastites and tuffaceous sandstones, but also along the entire alluvial sediments. ANN-MP and MPR are providing significant information according its transportation downriver. In upper part of the study area, high concentrations of Ti are conducted to almost all tributaries. The spatial distributions show the materials that carry on Ti particles concentrate on the lower parts and in the form of finest grains transport and embed into alluvial sediments. Their enrichment occur in Jurassic and Cretaceous flysch and Jurassic and cretaceous breccia and sandstones. Southern part of study area (Oligocene clastite complex, Miocene clastitc series and Miocene carbonates with coal layers) is enriched too. At several places, SK provides its concentration in form of concentric circles, which is pretty incorrect comparing with other two models.

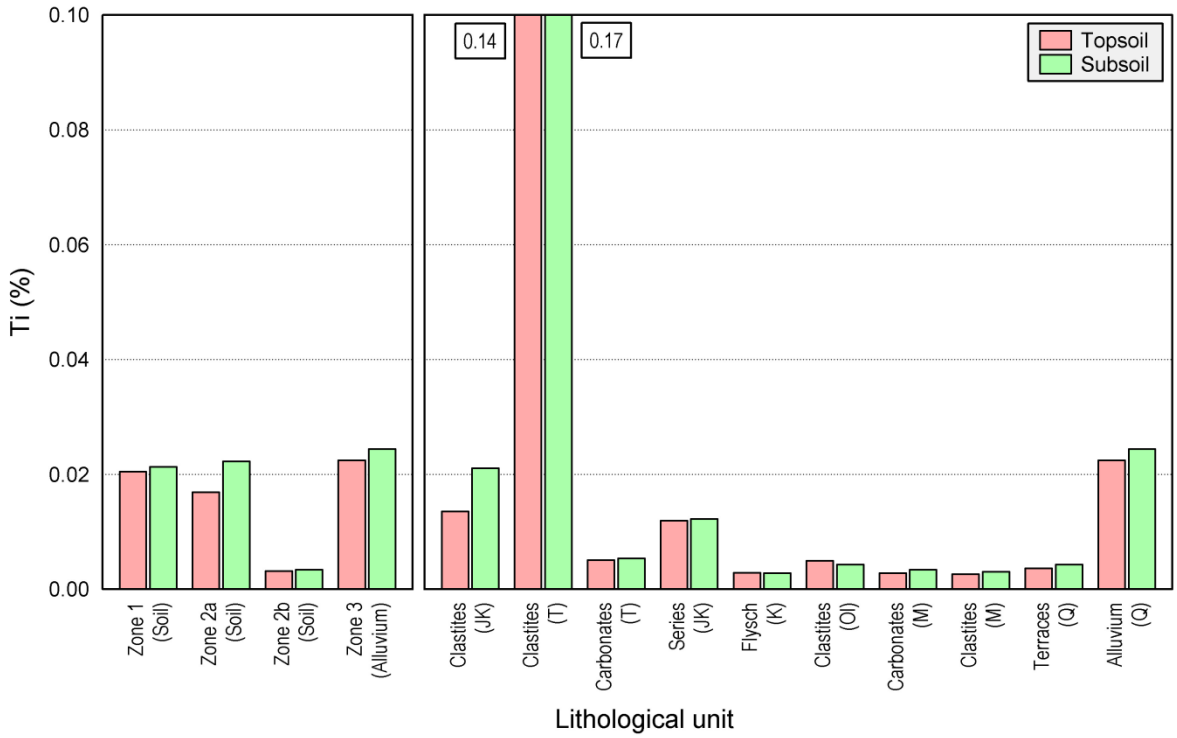

Figure 46: Distribution of Titanium concentrations through the determined zones (left) and isolated lithological units (right) in soil layers

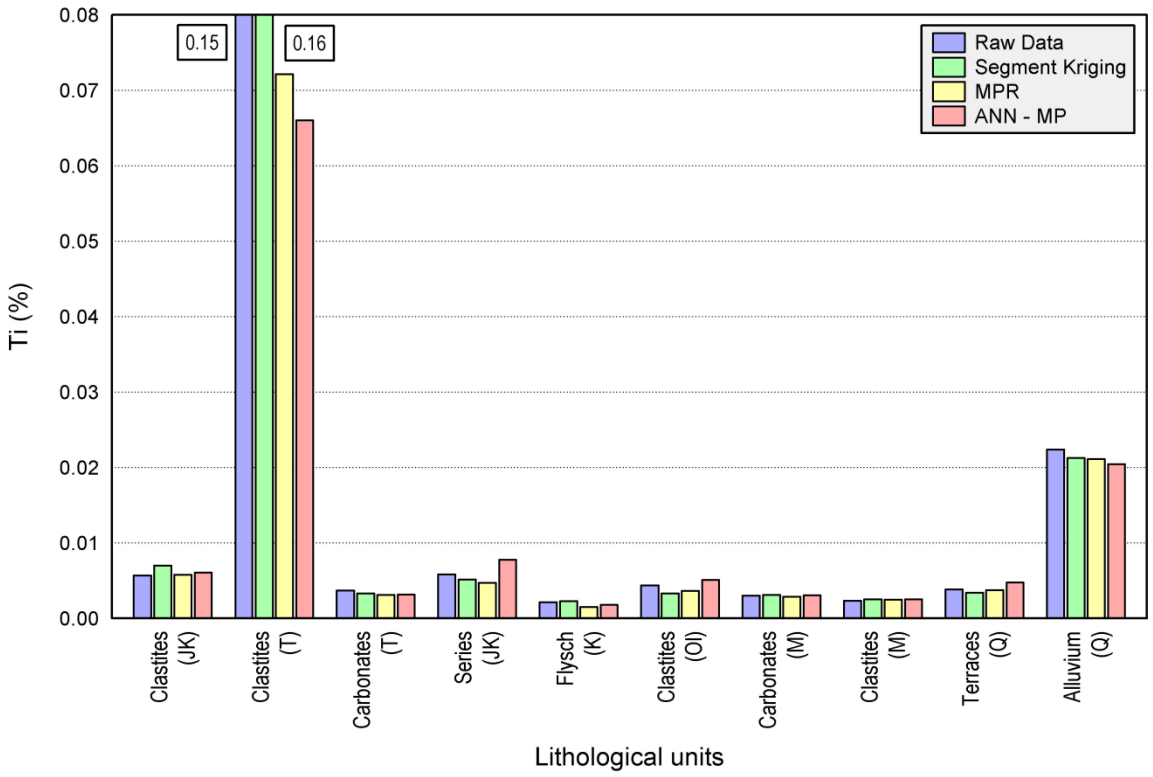

Figure 47: Distribution of Titanium values in isolated lithological units according to raw data and prediction methodsafter using the Box-Cox transformation

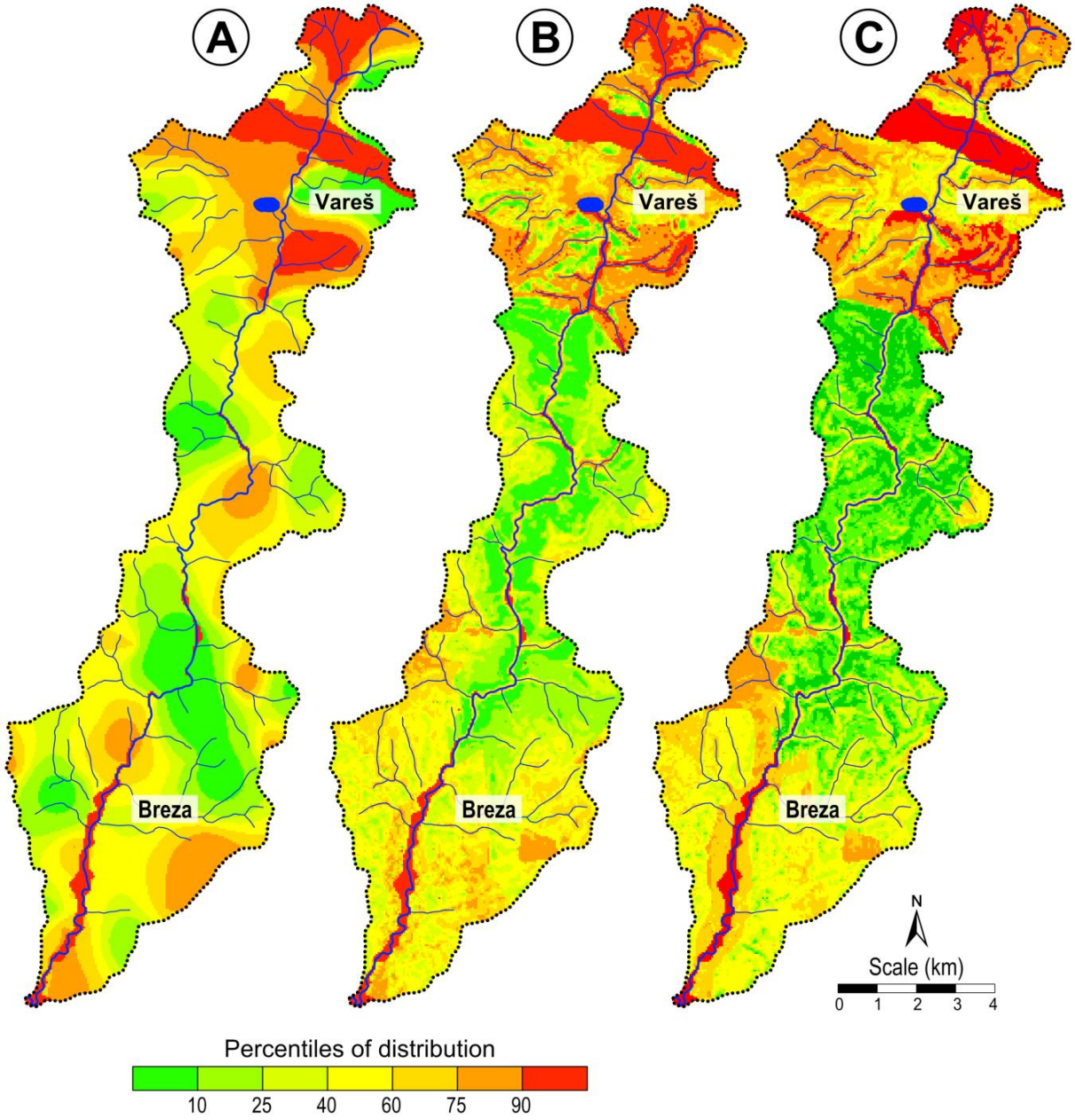

Figure 48: Spatial distribution of Titanium using various predicting methods: A – Segment kriging (SK); B – Multiple polynomial regression (MPR); C – Artificial neural network – Multilayer perceptron (ANN-MP)

5.4.6. Prediction of ambiguous Arsenic distribution

Arsenic is good example of vague distribution, and is influenced by human impact and natural background. The mean value for As in soil is 45 mg/kg, 18 mg/kg in stream sediments and 51 mg/kg in attic dust (Table 6). The median values are a bit lower in soil, 32 mg/kg but same as the mean values for stream sediments and attic dust. The maximum values are found in soil 590 mg/kg (more than 10 times higher than intervention values), then in attic dust 97 mg/kg, and 33 mg/kg in stream sediments. High concentrations of As in attic dust are due to combustion processes during metallurgical processes, but high concentrations in soil are conducted to the outcropping rocks, and claim its natural origin.

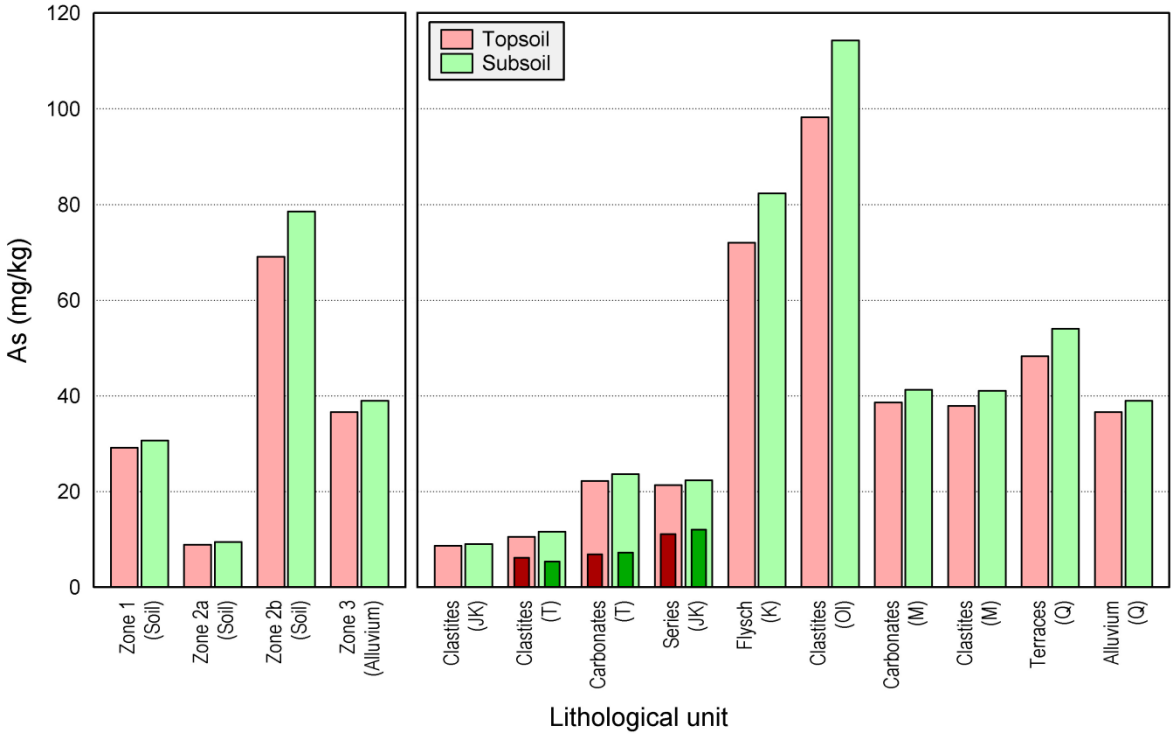

Figure 49: Distribution of Arsenic concentrations through the determined zones (left) and isolated lithological units (right) in soi lyers.Dark coloured bares reprsentan assessmentof background values in automorphic soil of Zone 2 (unpolluted area)

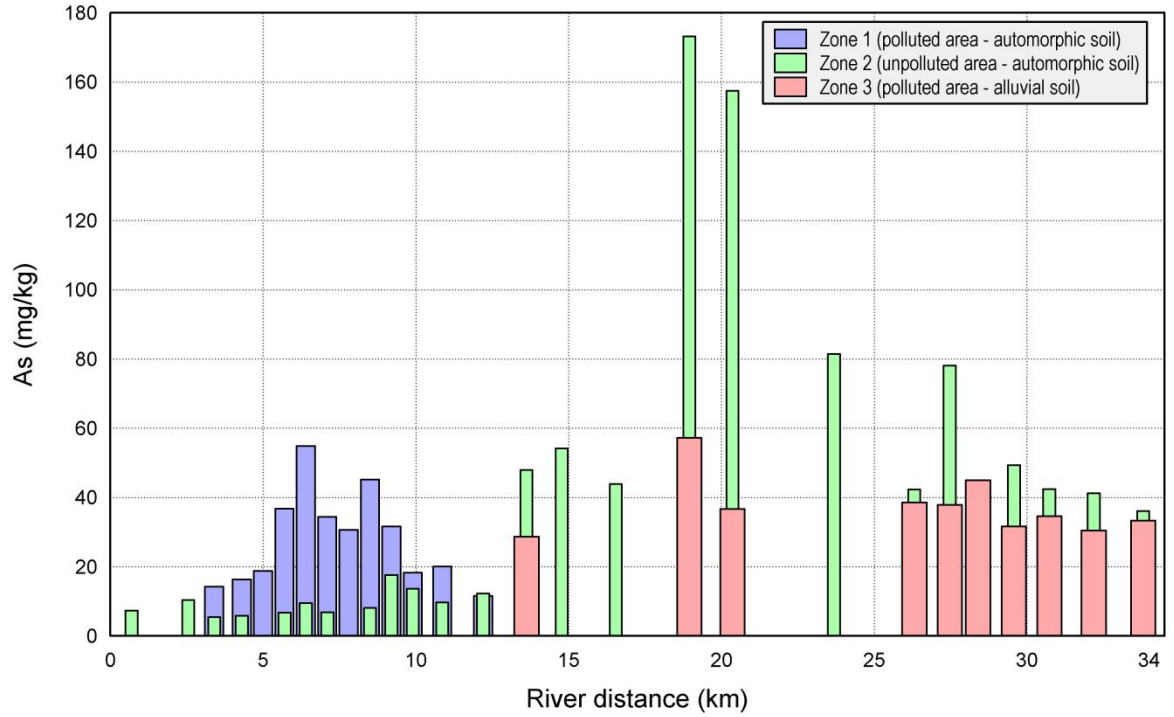

Figure 50: Distribution of Arsenic in soil according to the river distance

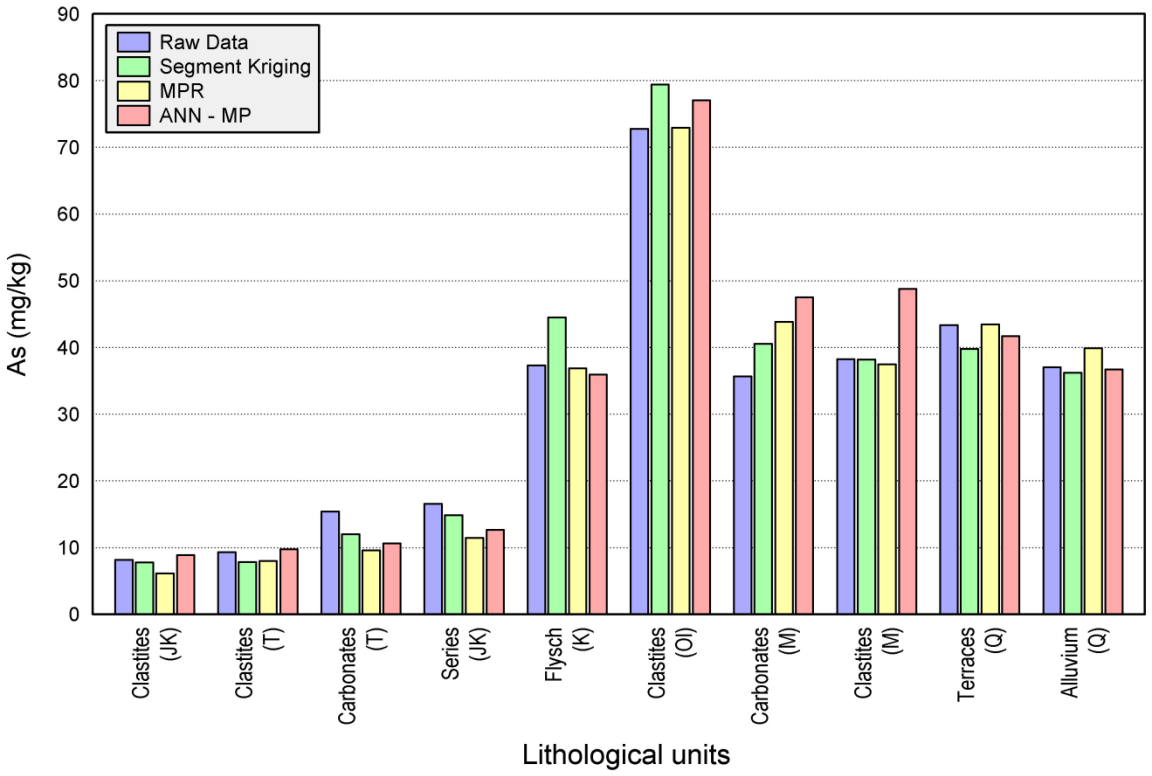

Figure 51: Distribution of Arsenic values in isolated lithological units with accoding to raw data and prediction methodsafter using the Box-Cox transformation

The highest values are found in the unpolluted Zone 2b (Table 9), where average concentration in topsoil is 69 mg/kg and in subsoil 79 mg/kg. The lowest values are found in Zone 2a, 8.9 mg/kg in topsoil and 9.5 mg/kg in subsoil. Tables 10 and 11 are providing average content of Arsenic in topsoil and subsoil for each particular lithological unit. Cretaceous flysch and Oligocene clastite complex have the maximum concentrations.

Distribution of Arsenic in both soil horizons according to determined zones and basic lithological units is showed in Figure 49. Arsenic has a similar distribution as F3 scores. Its increased values are found in lower part of unpolluted area (Zone 2b), on two isolated lithological units K-Flysch (70 mg/kg in topsoil and 80 mg/kg in subsoil) and Ol-Clastites (100 mg/kg in topsoil and 110 mg/kg in subsoil). Average value of As in Zone 2b is between 70-80 mg/kg. The lowest observed concentrations are in Zone 2a or J,K-Clastites and T-Clastites. Distribution of Arsenic along the Stavnja, from source to the mouth is representing significant enrichment in the mining area between 20-55 mg/kg (Figure 50). But extremely high enrichment is found around 20th km from the source where As is released from the outcropping rocks. Maximal average concentration of As is more than 170 mg/kg, or 5.5 times higher than optimum value or more than 3 times higher than intervention value comparing to the Standard List.

Distribution of Arsenic within the lithological units according to the raw data and prediction methods is presented in Figure 51. The data transformation used for all three prediction methods and raw data again not provide significant differences. Similar distribution pattern is showed in Figure 49.Differences between these two patterns is that raw data and transformed data are calculated for one depth, an average value for both soil horizons.

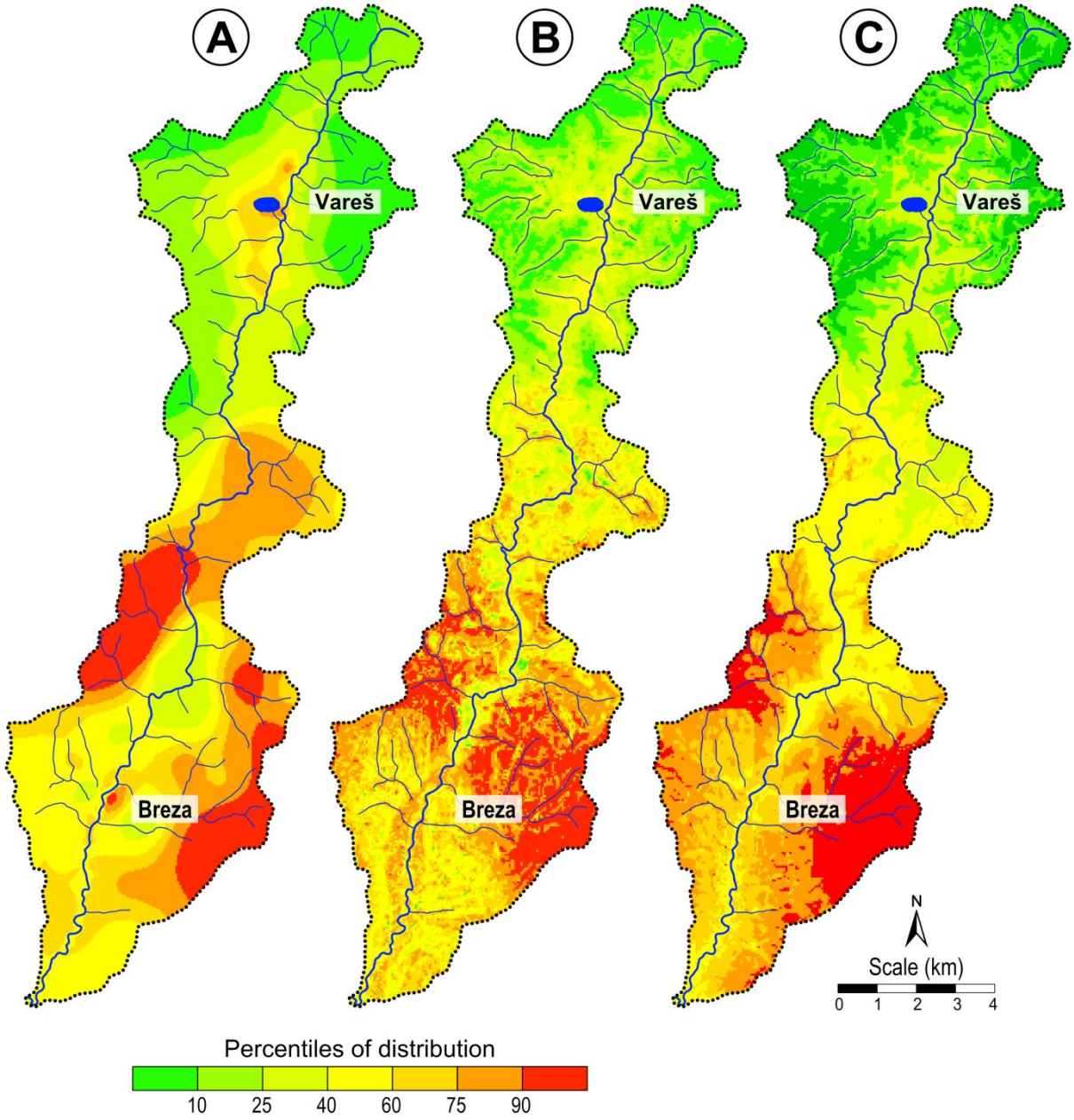

Figure 52: Spatial distribution of Arsenic using various predicting methods: A – Segment kriging (SK); B – Multiple polynomial regression (MPR); C – Artificial neural network – Multilayer perceptron (ANN-MP)

The spatial predictions of As using three prediction methods are represented in Figure 52. These prediction models are providing arrangement in concentrations that is not clearly conducted for any isolated lithological unit, comparing to Ni and Ti, respectively. Applied models show interesting trend in concentration increase from North to South. Slight enrichment with As is visible around the mining area in SK and MPR models. This can be explained with weathering of arsenopyrite (iron arsenic sulphide, FeAsS), which is common mineral in Fe mines. ANN-MP model, that has been superior method before, in this case has not detected enrichment around the mining area, most probably because As is mostly naturally enriched and the presence of some human impact made some confusions inside this modelling. This special type of spatial distribution cannot be applied to any other distribution, either anthropogenic or natural used in study area.

Vague distribution of Arsenic can be probably explained with its enrichment in independent outcropping rocks. The highest concentrations are found in Oligo-Miocene variegated series with coal layers in direction NW-SE. This is direction of the main Central Bosnian coal basin that lays between Sarajevo and Zenica, along the river Bosna.

5.5. Contamination and natural enrichment of chemical elements (application of models)

5.5.1. Anthropogenic impact

The spatial distributions of three common anthropogenic chemical elements Cd, Pb, and Zn according to the Standard List are presented in Figure 53**.**For a graphical display of spatial distribution, the maps with target and intervention values have been used, where different colours represent different concentration arrangements. In the scale used for its distribution we used five ranges: Two green colours represent the ranges under the target values; the light green is one half of target values; the yellow range represents the target values, the orange is one half of the sum of both, target and intervention, and the red range is presenting intervention values.

According to the Standard List, the target value for Cd is 0.8 mg/kg, for Pb 85 mg/kg, and for Zn 140 mg/kg. Intervention value for Cd is 12 mg/kg, for Pb 530 mg/kg, and for Zn 720 mg/kg. High concentrations of these three chemical elements exceed their intervention vales only in Zone 1 and alluvial sediments. Several samples with their high concentration are collected from these two units with maximum concentrations in range 4.0 - 7.2 mg/kg Cd, 880 - 1700 mg/kg Pb and 1500 - 3100 mg/kg Zn.

Maximum concentration of Cd is 7.2 mg/kg, Pb 1700 mg/kg, and Zn 3100 mg/kg. If we compare these values to their target values, they exceed for 9 times for Cd, 20 times for Pb, and 22 times for Zn, respectively. Even the intervention values are exceeded more than 3 times for Pb, and 4 times for Zn.

Almost all entire area is not contaminated with aforementioned group, except the two isolated units.
Fine grained clay size particles are transported far from the source of contamination what have been detected by three applied methods. The concentrations under the target values are detected at 73 km^2 or 70% of entire study area with SK, 70 km^2 or 68% with MPR and 77 km^2 or 74.5% with ANN-MP.The first model extract about 28 km^2 or 27% between target values and intervention (yellow and orange colour), the second model about 31km^2 or 30%, and the third model about 24 km^2 or 23%. The range that represent concentrations higher that intervention values is isolated on about 2.5 km^2 or 2.5% of study area with SK and ANN-MP and 2 km^2 or 2% with MPR (Table 19).

5.5.2. Natural enrichment

The spatial distribution of natural enrichment is presented in summarized map of Co, Ni, and Cr (Figure 54). These predicting models are showing arrangement in natural enrichment across the study area. For a graphical display of spatial distribution, the maps with target and intervention values are presented, where different colours represent change within them. In the scale used for its distribution we used five ranges: Two green colours represent the ranges under the target values; the light green is one half of target values; the yellow range represents the target values, the orange is one half of the sum of both, target and intervention, and the red range is presenting intervention values.

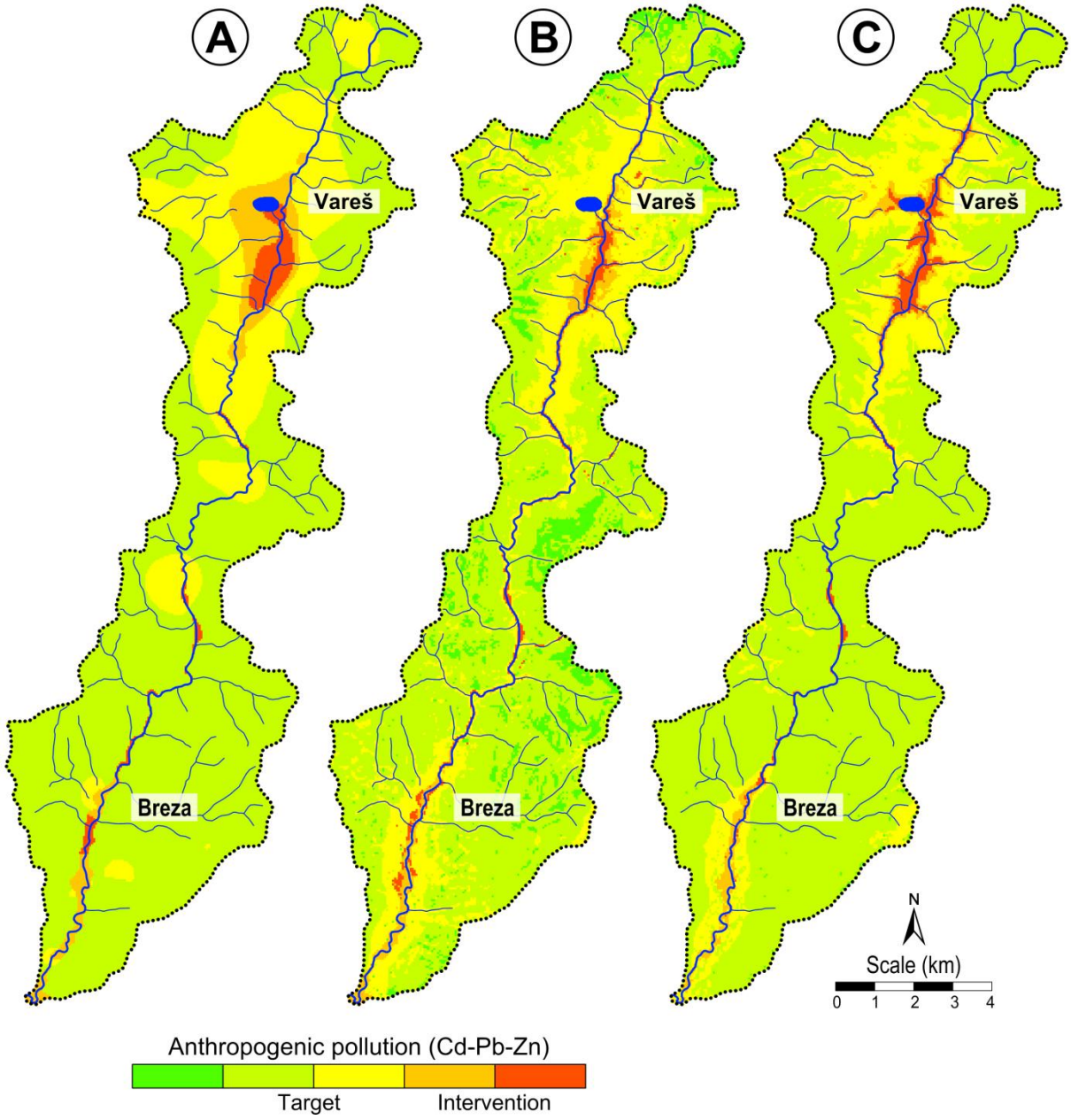

Figure 53: Spatial distribution of Cd–Pb–Zn pollution* according to the Standard list recommendation: *A – Segment kriging (SK); B – Multiple polynomial regression (MPR); C – Artificial neural network – Multilayer perceptron (ANN-MP)

According to the Standard List, the target value for Ni is 35 mg/kg, Co 20 mg/kg, and Cr 100 mg/kg, but intervention value for Ni is 210 mg/kg, Co 240 mg/kg, and Cr 380 mg/kg. The maximum concentration of Ni is 500 mg/kg, Co 64 mg/kg, and Cr 460 mg/kg. Comparing these values to the target values of Standard List, natural enrichment exceed 14 times for Ni, 3 times for Co, and 46 times. Comparing to the intervention values, they exceed for Ni 2.5 times and for Cr more than one time. It seems that the major enrichment is from Ni and Cr.

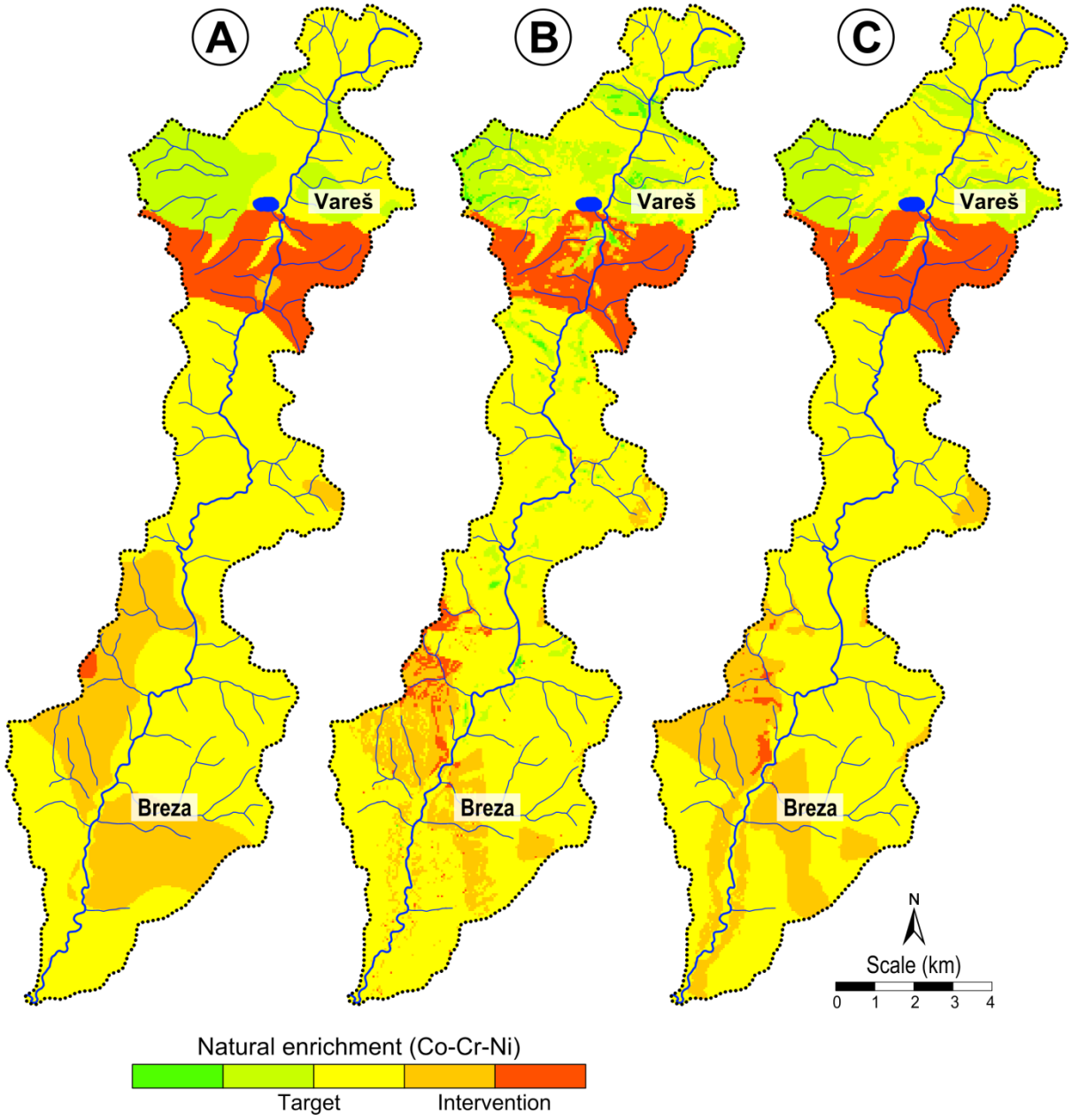

Figure 54: Spatial distribution of natural enrichment Co–Cr–Niaccording* to the Standard list recommendation*: A – Segment kriging (SK); B – Multiple polynomial regression (MPR); C – Artificial neural network – Multilayer perceptron (ANN-MP)

All three models identify one major hotspot with its intervention concentration, the Jurassic and Cretaceous flysch, but also some outcropping rocks on Oligocene clastite complex. The first model isolates about 9 km^2 or 9% of total study area (103.7 km^2), under the range of target values (two green colours), the second model about 11.2 km^2 or 11%, and the last model about 8.6 km^2 or 8%. Almost all entire study area is enriched with these elements (yellow and orange colour), where all three applied models isolated majority of the entire territory: SK and ANN-MP about 85 km^2 or 82% and MPR 82 km^2 or 79% (Table 19). Intervention values are found at 10 km^2 or 10% of entire study area with all applied models.

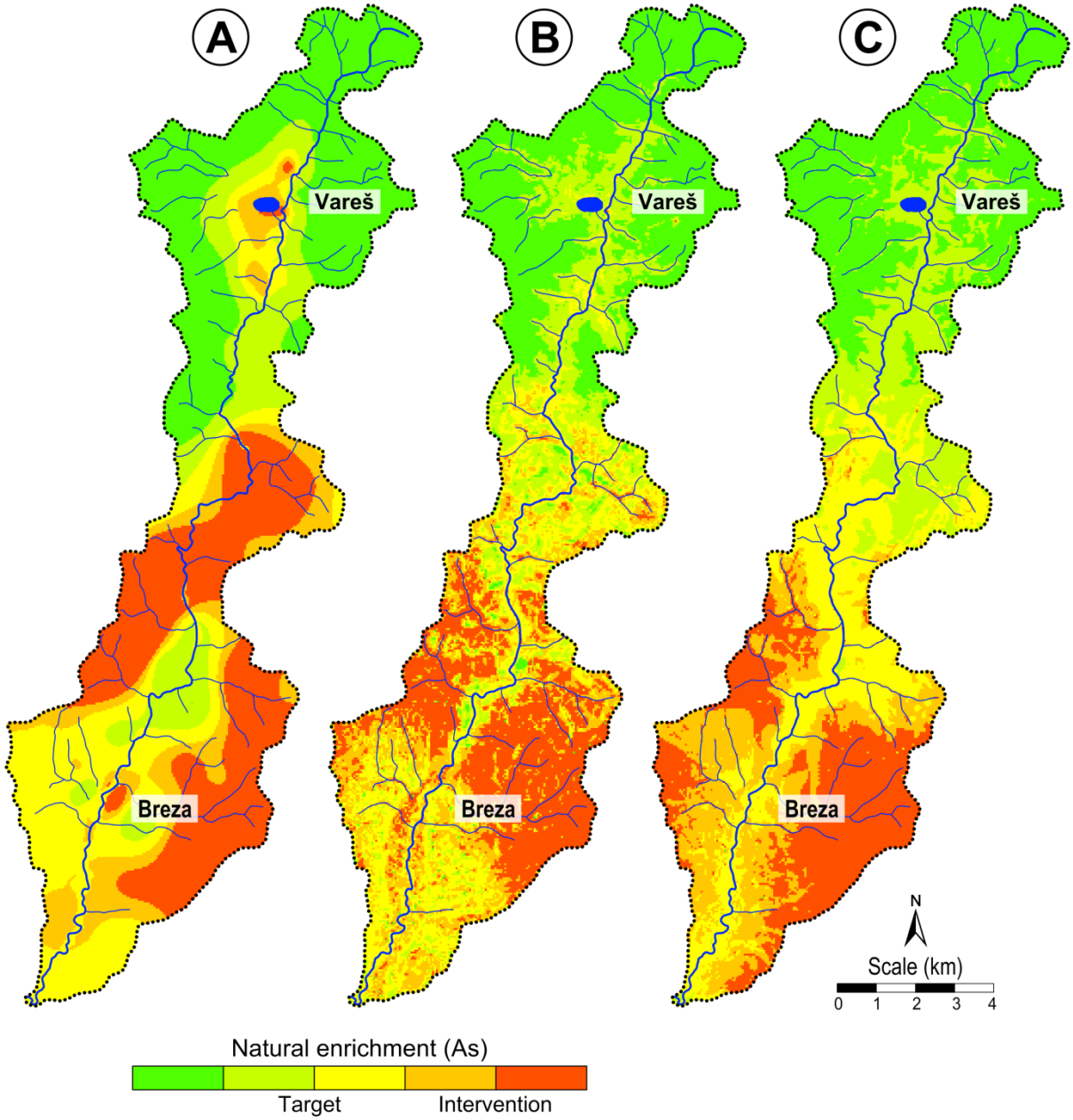

Figure 55: Spatial distribution of Arsenic* according to the Standard list recommendation*: A – Segment kriging (SK); B – Multiple polynomial regression (MPR); C – Artificial neural network – Multilayer perceptron (ANN-MP)

The spatial distribution of Arsenic according to the Standard list within all prediction methods is provided in Figure 55. The target value for As is 29 mg/kg and the intervention value is 55 mg/kg. Comparing the values for As with the Standard list, its concentrations exceed the target values at 35 km^2 with SK, 38 km^2 with MPR and 41 km^2 with ANN-MP (Table 19). In area between 18-26 km^2 its concentrations exceed the intervention value for As. Comparing the surfaces of all selected elements (Pb, Zn, Cr, Ni) that includes major anthropogenic impact and natural enrichment, the natural enrichment with Arsenic is the greatest. This enrichment has been absolutely unexpected, and needs spatial attention in future investigations.

Table 19: Areas of natural enrichment and pollution according to the Standard list recommendation

Anthropogenic origin (Cd-Pb-Zn)	Target level (km^2)	Intervention level (km^2)
SK	28	2.5
MPR	31	2.2
ANN-MP	24	2.6
Natural origin (Co-Cr-Ni)		
SK	85	9.7
MPR	82	10
ANN-MP	85	10
Natural origin (As)		
SK	35	26
MPR	38	20
ANN-MP	41	18
Total (As-Cd-Co-Cr-Ni-Pb-Zn)		
SK	64	37
MPR	67	30
ANN-MP	68	30

Total contamination (As-Cd-Co-Cr-Ni-Pb-Zn**)** that include anthropogenic impact and geogenic enrichment, respectively exceed their target values at two thirds of the entire study area, and one third their values exceed the intervention values. The total contamination is not simple summery of these two types of contamination,but is necessary to mention that some spatial distrubiotions are overlapping and those final values are seems lower that summery of their particular distributions.

5.6. Possibility of using satellite images and their application

Use of satellite images increase in recent years. In order to evaluate the capability of mapping contaminated areas from both LANDSAT TM and ETM data, we processed and analysed two available images for the study area (187 path and 29 row): one acquired by the TM sensor on 27 June 1990 and one acquired by ETM on 14 June 2005. The selected scenes provided cloud-free pixels. Sourcing information from satellite imagery often involves image interpretation techniques as well as GIS integration of other spatial data.

Satellite multispectral images are showing interesting and significant correlation with maps of contamination of entire study area (Figure 16). Some particular bands are showing significant correlation with soil chemism, with both anthropogenic contamination and natural enrichment, respectively. It seems that negative correlations of Arsenic are showing some similarities with hydrothermal changes, but unfortunately these assumptions are not confirmed yet. The main disadvantage of satellite images is shadowing. Due to fact that the study area is in quite hilly, one side of the valley is always shaded, does not metter from wich side is the satellite comming. Big problem are also destroyed surface area around the mines. The satellite multispectral images might be quite useful additional source of information used in data interpretation, but the softwares for their corrections are quite expensive. The given results are pretty useful, but still so many problems should be solved. Hopeffuly this problem will be solved Together with colleagues from the German Aerospace Center.

Table 20: Matrix of correlation coefficient between elements (As, Pb, Ni and Ti) and selected Landsat multispectral bands (set from 1990 and 2005)

	Transformation	B1 1990	B4 1990	B5 1990	B6 1990	B1 2005	B2 2005	B3 2005	B4 2005	B5 2005	B6 2005	B7 2005
As	Normal	0.03	0.09	0.11	0.10	0.11	0.14	0.09	0.14	0.20	0.04	0.10
As	Log-normal	0.18	0.06	0.09	0.30	0.38	0.36	0.24	0.13	0.33	0.15	0.24
As	Box-Cox	0.20	0.06	0.09	0.32	0.39	0.37	0.25	0.12	0.33	0.16	0.24
Ni	Normal	-0.03	-0.12	-0.01	0.07	-0.02	-0.05	-0.01	-0.10	-0.08	0.00	-0.04
Ni	Log-normal	0.09	-0.14	0.01	0.27	0.17	0.10	0.10	-0.08	0.01	0.08	0.05
Ni	Box-Cox	0.08	-0.14	0.01	0.26	0.15	0.09	0.09	-0.08	0.00	0.08	0.05
Pb	Normal	0.21	-0.30	-0.12	0.27	0.30	0.21	0.24	-0.20	0.02	0.30	0.18
Pb	Log-normal	0.24	-0.34	-0.18	0.26	0.32	0.20	0.26	-0.30	-0.05	0.33	0.21
Pb	Box-Cox	0.22	-0.33	-0.22	0.21	0.28	0.17	0.23	-0.33	-0.10	0.31	0.21
Ti	Normal	-0.14	-0.27	-0.34	-0.16	-0.06	-0.16	-0.06	-0.32	-0.33	-0.06	-0.14
Ti	Log-normal	0.07	-0.32	-0.23	0.08	0.16	0.07	0.13	-0.27	-0.20	0.11	0.03
Ti	Box-Cox	0.11	-0.31	-0.18	0.13	0.20	0.13	0.17	-0.22	-0.14	0.16	0.08

Some matrix correlation between selected elements and selected Landsat multispectral bands (from 1990 and 2005) are provided in Table 20. According to the previous experiences, the data transformations have been used again for 111 soil measurements. From the table could be seen that Log-normal and Box-Cox, generally. Statisticaly significant correlations are those positive: B1 1990, B6 1990, B1 2005, B2 2005, B3 2005, B6 2005, B7 2005. Log-normal and Box-Cox data transformations for As have more significant correlations than normal valus. Significant positive correlations for Ni, is found only in B6 1990. But Pb as most of trace elemnts has significant correlation within all transformations. This might be a result of thevalley shape, which is followed by the satellite. Normal values of Titanium show the negative correlations for eacha band.

5.7. Validation and ANN-MP model applicability in various case studies

From the very beginning, we want to achieve two main goals; one is a construction of a very stable ANN-MP model with possibility of repeatability, and second one is the model application within various geochemically and morphologically study areas. This means that once when model is prepared should be applicable under similar conditions (such as input data, number of hidden units, number of training networks), solving a problem of spatial distribution of particular trace elements or their geochemical groups (chapters 4.4. and 5.4). In order to show a validation and ANN-MP model applicability in three other study cases: Zenica, Bosnia and Herzegovina; Kosovska Mitrovica, Kosovo; and Kavadarci, Macedonia. Number of input data had been increased compare to the PhD thesis due to fact that ANN-MP can calculate the distribution with less parameter, and more uncertainties.

5.7.1. The case study Zenica (B&H)

Zenica area (52 km^2) is located in the valley of the river Bosna, about 70 km north from Sarajevo. Construction of the iron and steel works in Zenica began in 1892. Through the years new facilities were built and the production was dramatically expanded and become the biggest ironwork in former Yugoslavia. The rapid growth in coal, iron, and steel production over a long period of time left significant trace metal contamination throughout the area. The entire area had been covered by sampling grid with a density of one sample per square kilometre, but in urban and industrial zones the density was increased.

At 60 sampling sites, topsoil and subsoil were collected. Determination of 41 elements was performed area (Alijagić, 2008; Alijagić and Šajn, 2010).

One anthropogenic geochemical association (Ag, Cd, Pb, Sb and Zn) is result of historical activities of the ironworks Zenica, but also coal mining and other anthropogenic influences in the past. The high concentrations of these elements exceed the New Dutch List target values covering most of the study area. Two geogenic geochemical associations: F1 (Ce, La, Nb, Ta and Th) and F2 (Co, Cr and Ni) are influenced mainly by lithology. The high concentration of particular elements of F1 are found in carbonate rock and Quaternary river terraces, but the second group is related to the Vranduk series— Jurassic–Cretaceous flysch rocks. Two elements, Ni and Cr are showing the highest natural enrichment in the entire area (Alijagić, 2008; Alijagić and Šajn, 2010). Comparing to the Stavnja Valley, this study area is wider but surrounded with high hills. The geology units have direction NW-SE, same as the coal belt.

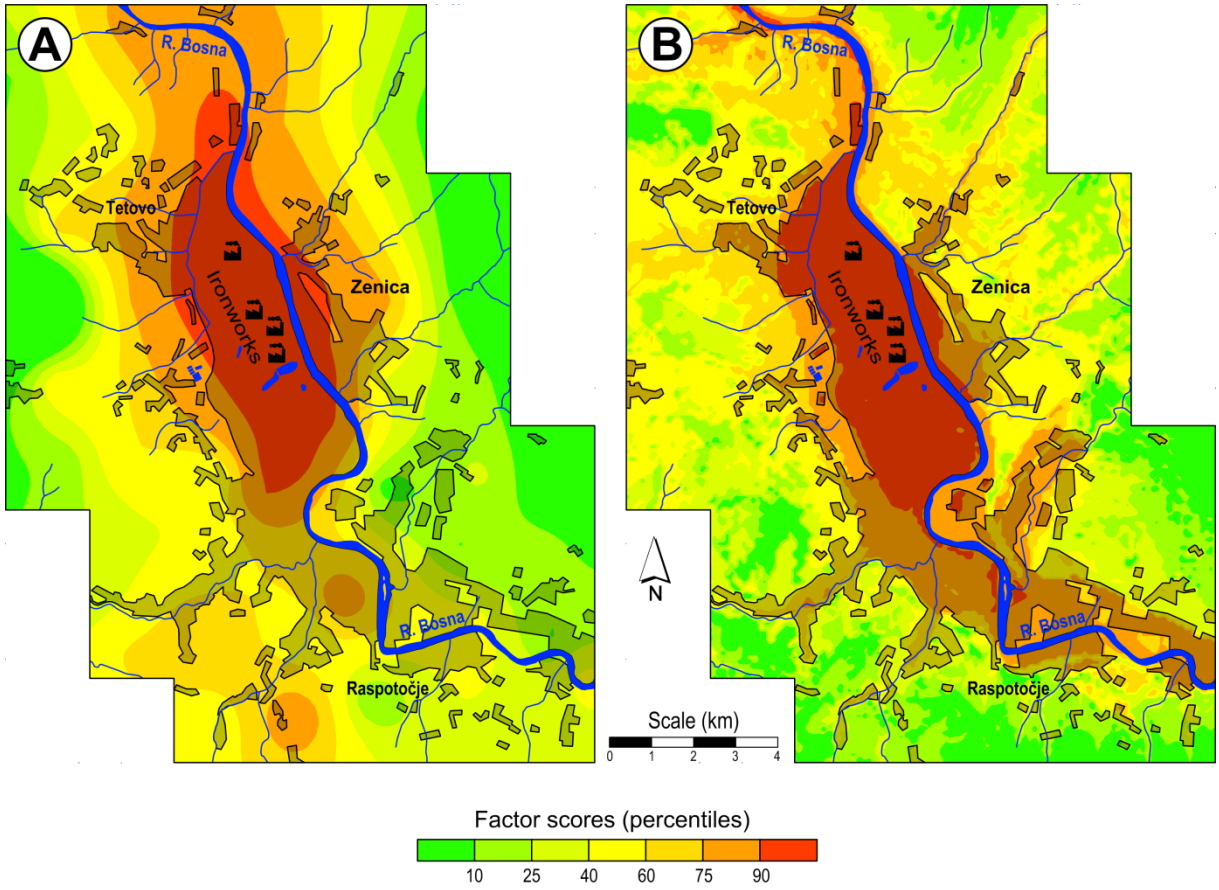

Figure 56: Distribution of factor scores (Ag-Cd-Pb-Sb-Zn) in Zenica area (B&H): A – Universal kriging; B – Artificial neural network – Multilayer perceptron (ANN-MP)

The spatial distribution of Factor 1 score (Ag, Cd, Pb, Sb and Zn) is provided in Figure 56. The figure 56A is obtained by common method, the universal kriging, but the Figure 56B by ANN-MP. It is obvious that the prediction map of spatial distribution obtained by ANN-MP is more realistic and provides the some information that are not visible in A such as elongated contamination halo along the entire river valley and concentration of contamination along the tributaries. This method has been successful in identification the natural enrichment as well. The spatial distributions of particular elements are clearly connected to the particular geological units.

5.7.2. The case study K. Mitrovica (Kosovo)

Mining and metallurgic activities in Kosovo have a long history. The Trepča Mine Limited in K. Mitrovica was built in 1927 and produced lead, arsenic and cadmium from the 1930 until 2000. The smelter close to Zvečan commenced work in 1939. Because of the smelter and three huge tailing dams, environmental pollution in K. Mitrovica increased dramatically. The smelter has been working sporadically since the 1999 conflict between Kosovo's Albanian and Serb population in Kosovo. There was also a unit for production of fertilisers and batteries. The study area is also known with polymetallic deposits (Pb, Zn, Mn and Cr) Stari Trg, with important deposits of lead and zinc.

The entire study area (c 300 km^2) was covered by 156 sampling sites, composite topsoil samples. According to the results obtained by factor analysis and the trends on geochemical maps, one anthropogenic (Ag, Pb, Sb, Bi, Zn, Cd, As, Cu, Hg, Au, Tl, and Mo) and four natural geochemical associations F2 (Co, Ni, Cr, Sc, Mg, and Fe), F3 (Ba, La, Mo, Th, Tl, and U), F4 (Ga, Al, K, and V), F5 (Ca and Sr) have been established.

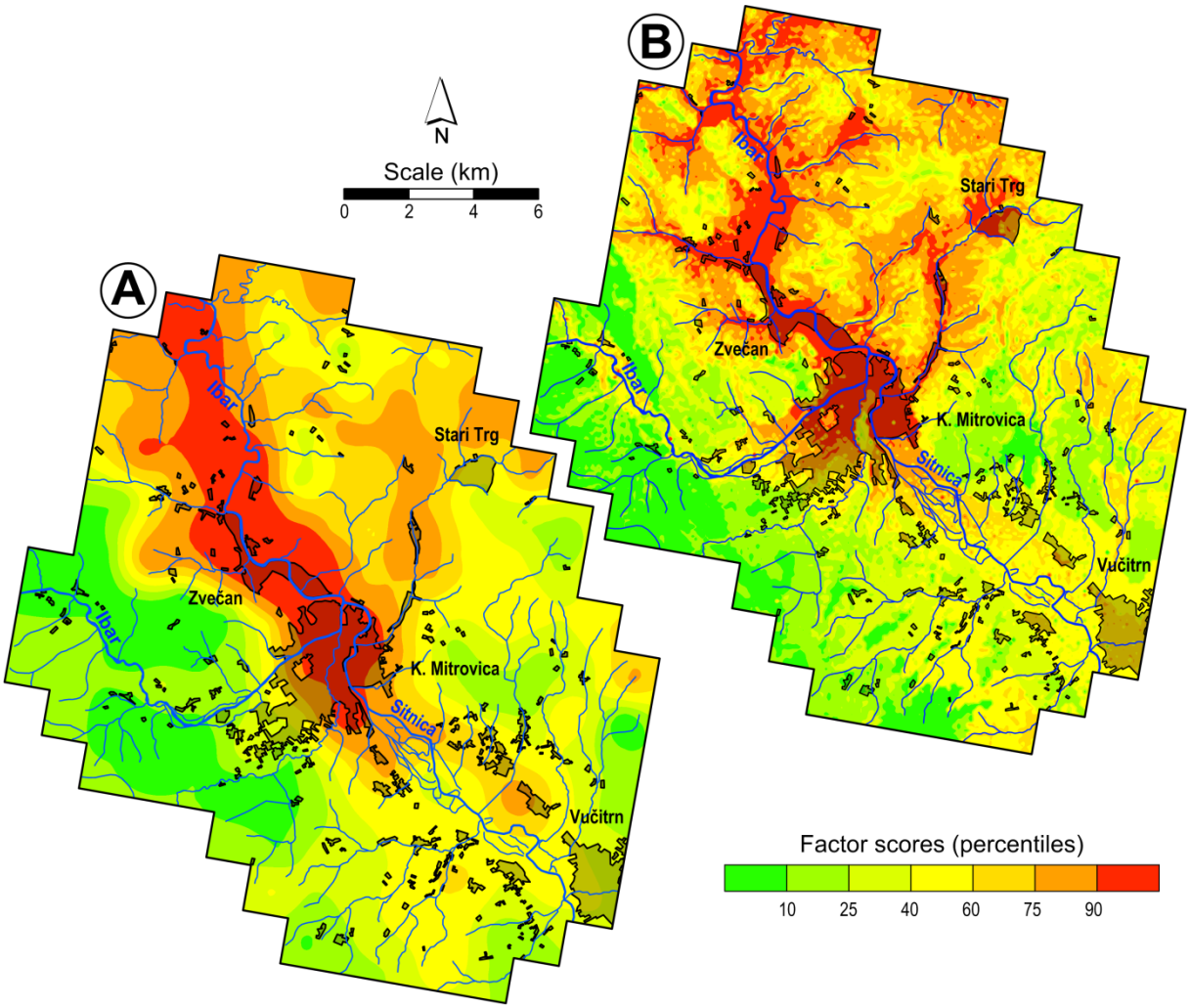

Figure 57: Distribution of factor scores (Ag-As-Au-Bi-Cd-Cu-Hg-Pb-Sb-Zn) in K. Mitrovica area (Kosovo): A – Universal kriging; B – Artificial neural network – Multilayer perceptron (ANN-MP)

The association includes high concentrations of anthropogenic elements are mainly influenced by mining and processing activities. In the vicinity of Zvečan and K. Mitrovica, their concentrations exceed the intervention values of the New Dutch list at 152 km^2. Comparing the results with the European median values their concentrations are much higher: Pb by 20-fold, Cd 11-fold, Hg 5.5-fold, As 4.6-fold, Zn 4.2 and Cu 3.2-fold (Aliu et al., 2009, Aliu, 2010; Stafilov et al., 2010a; Šajn and Alijagić, 2012; Šajn et al., 2013).

The spatial distributions of Factor score (Ag-As-Au-Bi-Cd-Cu-Hg-Pb-Sb-Zn) obtained by universal kriging and ANN-MP are provided in Figure 57. Both distributions very clearly isolate the contamination halo, but the distribution obtained by artificial intelligence giving more information about the contamination transport. This study area is geologically and morphologically different than the Stavnja and Bosna valleys, because the lowland is changed to hilly. Eroded material had been transported down from the mine Stari Trg to the river Ibar, and from there is transported so far from the main sources, mines and smelter. Also, some materials are transported by local wind, and expand the areola of contamination. With this method four geogenic associations have been isolated and concentration of particular elements has been very clearly associated to entire geological unit.

5.7.3. The case study Kavadarci (Macedonia)

The study area is located in the south-central part of Macedonia, in Tikveš valley, about 100 km south from the capital Skopje. The city is well known by Ferro-Nickel smelter FENI, but also famous by its vineyards and it is main vine production region in Macedonia. The complete investigated region (360 km^2) was covered by 172 sampling sites.

Several geogenic and anthropogenic geochemical association were established according to the statistical analyses. The most interesting association is geochemical association of As–Sb–Tl. Their concentrations in soil are similar to the European averages or above them but in other side in the Holocene alluvial sediments of the rivers Crna Reka (32 mg/kg As, 4.8 mg/kg Sb and 1.4 mg/kg Tl) and Vardar their concentrations are very high. Their average enrichment ratios exceed the average of the total investigated area by 4 to 4.5 times. Higher content of As and Sb have been found on Paleozoic-Mesozoic rocks (SW part of investigated area) and Tl on the Pleistocene tuff (SE part of investigated area) what suggest their geogenic influences. This enrichment is consequence of natural erosion from the mine deposits Alšar (As-Sb) on Kožuf Mountain, but also from the mine activities.

Construction of geochemical maps using universal kriging methods (Figure 58 A) is quite useful in determination of distribution patterns, but in such a maps are present mistakes called Bull's eye effect because in the isotropic space appears elongated division. This can only be solved by denser sampling grid. Applying the ANN-MP the above mistakes have been avoided and constructed geochemical maps of contamination are much better, especially from the geological point of view (B). Distribution of As-Tl-Sb is clear limited to the specific geological units, the Holocene alluvium. It was sucesful in identification some other geogenic geochemical association such as Al–Fe–Ga–Sc–V is related to the Paleozoic and Mesozoic rocks; Co–Cr–Mg–Ni ti the Eocene upper flysch zone; Ba–La–Th–U to the Pleistocene tuff.

This method successfully solved several geomorphology and geology of different study areas. According to the presented results of those case studies we can confirm the model stability as well as its applicability representing the milestone in geochemical map construction(Stafilov et al., 2008a, 2010b; Žibret et al., 2012; Stafilov et al., 2013; Šajn and Alijagić, 2012).

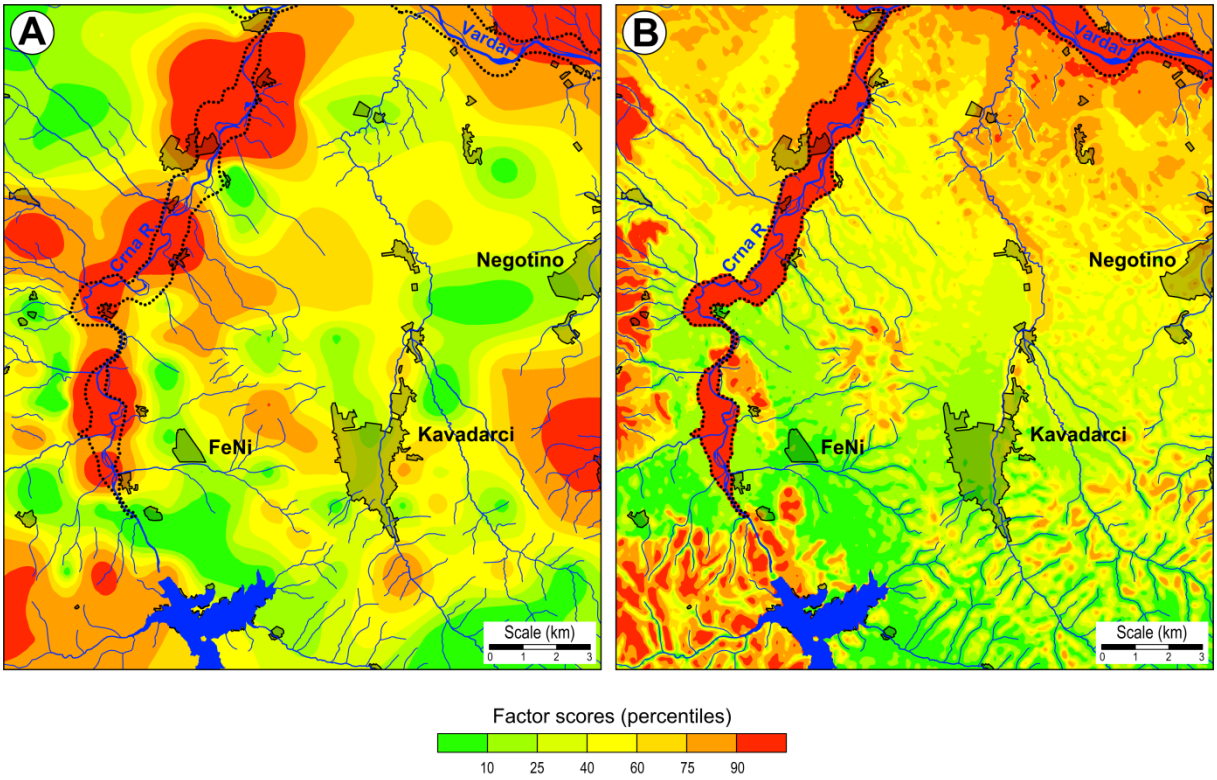

Figure 58: Distribution of factor scores (As-Sb-Tl) in Kavadarci area (Macedonia): A – Universal kriging; B – Artificial neural network – Multilayer perceptron (ANN-MP)

5.8. Geochemical investigations in areas of former military operations

Geochemical investigations in areas of former military operations are very complex and difficult; especially challenge is preparing a sampling design and sampling itself. From our experience, we could not set out any regular sampling grid, but many sampling sites were moved according to suggestions of local residence.

For the sampling in the remained minefields there is no one rule or several rules for safe sampling, only several advices. Basically, we can say that only rule is that there is no rule. The study site for my PhD has been the place of military operation during the last war (1992-95). In the valley, three ethnic groups (Orthodox, Catholics and Bosniaks) were lived close to each other, what resulted to massive conflict, destruction, killing and burning.

The maps of minefields are useful but there are not 100% confident, only about 70-80%. If your entire life depends on such maps, you realise that their confidence is not as high as it should be. Due to this fact is necessary to talk with local people who spend their time during and after the war there. Otherwise they can provide you some incorrect information. At one sampling point happened to us that two different persons told us two different stories. Later on we realised that one of them is basically lives in other country. Other good example is that some people used a garden near their house for cultivation for several years before a tractor activated an unexploded projectile.

Figure 59: High risk sampling locations

At places of intensive military operations so many minefields are still remained, especially parts of the strategic importance such as roads, industrial objects, bridges, etc. Before such sampling it is important: to learn as much as possible about the sampling site (political situation, ethnic groups); to have a map with remained minefields and possible minefield; talk to the local people, and be aware of any object that looks like a mine, such as the wire or small tins, etc. Also good advice about sampling itself is not recommended to go alone, rather in group of two or three people maximum, if possible with one local. Distance between the persons who are doing sampling should be about 40 m, in case that one activate remained mine that another can help to injure person or call for help.

Figure 60: Appropriate sampling locations

Sampling around burned houses or similar object is not recommended too, because of possibility that some unexploded projectiles are present. Also never do sampling around the bridges, because they are usually the objects that divide two military sides/ conflict groups and quite often around them are the remained minefields. On a way to the sampling point and on a way back is good to use the same route, avoiding any bushes, high grass or forest. If possible use existing routes, or hard surface. For soil sampling is more safe if choose the meadows and pastures, the places used for grazing livestock

(cows, sheeps, goats, etc.). During the digging of soil profiles, everyone should be aware that unexploded mine can be activated. Sampling in such areas is very risky, because during the sampling a spade is stabbed into depth of 30 cm. Total number of sampling sites is 111, but each sampling site is composed by minimum five subsamples. Then can be easily calculated the risk during the sampling.Same is for the river sediments sampling. Here is problem that some unexploded projectiles can be transported far from the minefields, and can be embedded in deeper layers of some thicker sediment. Also everyone should be aware of any wires or mine look like objects.

Generally for whole territory of Bosnia and Herzegovina is big problem of unexploded projectile that are castaway everywhere in nature, especially in rivers and forests, even The Stabilization Force (SFOR) several years after the war organized anonymous action for collecting any kinds of weapons.

Aforementioned applied models allow us to be very flexibile with sampling, this means that the sampling points can be moved and arranged to the field conditions without a fear that the final results will be incomplete.

6. CONCLUSION

Along the Stavnja Valley, intensive mining and smelting activities have been occurred for more than 100 years. Diverse mineral occurrence, especially Iron deposits and Lead-Zinc deposits make this study area interesting for geochemical research. Also, the study area has been place of intensive military operation during the last war, 1992-1995, what resulted with numerous remained minefields, and made this research more complex.

The present study has been carried out to establish baseline data regarding the trace metal levels in the Stavnja valley. For this purpose different sampling materials were sampled: soil (automorphic and alluvial), river sediments, and attic dust. At 143 sampling sites, 111 soil samples from topsoil (0-5 cm) and subsoil (20-30 cm), 17 river sediments, and 15 samples of attic dust have been collected. Analysis of 36 chemical elements (Ag, Al, As, Au, B, Ba, Bi, Ca, Cd, Co, Cr, Cu, Fe, Ga, Hg, K, La, Mg, Mn, Mo, Na, Ni, P, Pb, S, Sb, Sc, Se, Sr, Th, Ti, Tl, U, V, W and Zn) was performed at the ACME, Ltd. laboratory in Vancouver, Canada. With various sampling material two important processes such as river transport and atmospheric transport have been determined, as well as natural enrichment and anthropogenic impact.

All data were treated with various statistical methods in order to extract as much as possible information about natural and anthropogenic processes. One anthropogenic and three geogenic geochemical associations were establish on the basis of visually indicated similarity of geographic distribution of elemental patterns in the topsoil and subsoil; comparisons of basic statistic parameters, comparisons of enrichment ratios, correlation coefficient matrices, results of cluster and factor analyses. The Factor 1 associates the high concentration of Pb, Zn, Hg, Cd, Cu, Bi, Ag, Sb, Mo, W, Mn, Ba, Fe, and Tl. The group represents chemical elements that are the most probably anthropogenically distributed, associated to the main industrial and mine zone, and alluvial sediments found downstream of the river Stavnja. Three next factors, F2 (Ni, Cr, Co, and Mg), F3 (Th, La, As, and Sc), and F4 (Al, Ti, V, and Ga) are associating elements that are most probably naturally distributed and influenced by lithology.

Spatial distributions of particular trace elements are helping in reconstruction its main pathway in study area, but simultaneously isolate their hotspots. Problem of contamination along the river represents an anisotropic appearance between the isotropic lithological units, and cannot be solved completely by standard interpolation kriging methods, based only on sparse soil measurements. Two new powerful linear and nonlinear modelling techniques are applied for solving it. They arrangement in concentration across the Valley are more realistic and picturesquely, because they include more geospatial and geomorphological data such as geological background, land use, aspect, slope, altitude, etc. Including all aforementioned facts, it will help us in better interpretation and understanding processes that happened in some certain period time that they are related to.Various modelling techniques help us in reconstruction different processes that influenced the entire area. They main purpose is not only the isolation of hotspots with highest concentrations, simultaneously they distinguish natural and anthropogenic influences as well as transportation pattern (such as atmospheric or water transport).

Four following elements Pb, Ni, Ti, and As have been chosen for further detailed inspection. Lead is typical anthropogenic element, introduced solely by mining and smelting activities. Two isolated hotspots are the mine industrial zone and alluvial sediments, respectively. Its maximum detected value is 1700 mg/kg, comparing to the target value of Standard List, Pb exceed for 20 times, and even 3 times comparing to the intervention value. The spatial distribution of this trace element is good example of river transport, where the fine grained materials are transported far from the source of contamination and embedded in alluvial sediments. Nickel and Titanium are typical natural elements, whose enrichment depends mainly of the parental material degradation. All three applied isolated clearly the lithological units

with their highest concentrations. Comparing these values to the target and intervention values of Standard List, natural enrichment exceed 14 times and 2.5 times for Ni, respectively. Contrary to these two cases, distribution of Arsenic is pretty ambiguous because does not belong to specific isolated lithological unit or group of units, but independent outcropping rocks rich with this trace element. According to the Standard List, its concentrations exceed 3 times target value, and 2 times intervention value.

Summarised maps that comprise solely three anthropogenic trace elements (Pb-Zn-Cd) and three natural trace elements (Ni-Co-Cr) according to the Standard List provide information about overall anthropogenic impact and natural enrichment of study area. The results are very impressive; all provided models show that natural enrichment is much higher than anthropogenic impact. About 71% or 73 km^2 is under target values, in range between target and intervention values about 26.5% or 26 km^2, and over than intervention values only about 2-2.5% or 2-2.5 km^2 of entire study area for Pb-Zn-Cd. Natural enrichment (Ni-Co-Cr) is showing opposite situation, only about 9% or 10 km^2 is under target values, about 84 km^2 or 80% between intervention and target values, and over intervention values 10% or 10 km^2 of study area.

Three applied models are repeatable, what means that very similar spatial distribution can be obtained under the same conditions unrestricted times. Also very important characteristic of each particular modelling is that one model isolates all hotspots simultaneously. In other hand, their similarities are reconfirmation, refinement and in same time validation of different models. All models are repeatable, what is another success in such modelling.

Modelling with ANN-MP and MPR is representing a milestone in geochemical investigations and maping. Main advantages of those methods are first of all that we can construct very eventful and complete maps with spatial distribution of particular elements or geochemical association, sampling at high risky sites can be avoided (such as the Stavnja valley), also number of sampling sites can be reduced but the maps can still remain very qualitative. Reduce number of samples means in same time less timecomsuming operations such as is sampling itself and analytical measurements.

Using all various statistical and modelling techniques, the five goals of doctoral dissertation have been successfully achieved.

7. SUMMARY

The Stavnja river valley is known with intensive mining and metallurgical activities for more than 100 years. In the upper valley, three abandoned iron mines Smreka, Brezik, and Droškovec (two open pits, and one underground), abandoned Lead-Zinc-Barite Veovača mine, and abandoned ironwork Vareš are situated. In the Southern part, in vicinity of town Breza a brown coal open pit is located. In the steep and hilly study area living approximately 30.000 inhabitants, mostly settled in the two small cities Vareš and Breza. The study area has been place of intensive military operation during the last war, 1992-1995, what resulted with numerous remained minefields. The mentioned area is an exceptional polygon for applying linear and nonlinear mathematical methods such as Segment Kriging, Polynomial Multiple Regression and Artificial Neural Network - Multilayer Perceptron, because very narrow and elongated anthropogenic anomaly with increased concentrations of trace elements, almost perpendicularly intersects the isolated lithological units.

The main purpose of the thesis has been an identification of optimal methodology for geochemical research in the area of former military operations (with remains minefields or high risk areas), according to various sampling medium, sampling design, data processing and data interpretation. Content and spatial distributions of trace elements have been determined, a geogenic background according to the main isolated lithological units and anthropogenic impact on their distribution in various secondary sampling material (such as soil, river, and attic dust) have been identified. The main geochemical associations and their spatial distribution have been identified by using multivariate statistics. The optimal methodology for spatial distribution predictions of concentrations using these linear and non-linear mathematical methods have been established and tested.

The sampling design has been initiated to provide high quality environmental geochemical baseline data for the Stavnja Valley. The data are based on sampling of soil, stream sediment and attic dust collected from all over study area. High quality and consistency of the obtained data are ensured by using standardised sampling methods and by treating and analysing all samples in the same way. Preparation of sampling design has been the most challenging part, because of the remained minefields from the last war (1992-1995). At 143 sampling sites, 111 soil samples from each soil horizon (topsoil and subsoil), 17 river sediments, and 15 samples of attic dust have been collected. Analysis of 36 chemical elements (Ag, Al, As, Au, B, Ba, Bi, Ca, Cd, Co, Cr, Cu, Fe, Ga, Hg, K, La, Mg, Mn, Mo, Na, Ni, P, Pb, S, Sb, Sc, Se, Sr, Th, Ti, Tl, U, V, W and Zn) was performed at the ACME, Ltd. laboratory in Vancouver, Canada. Beside the chemical analyses, various geospatial data Web available freely (Digital Elevation Model DEM, satellite images, Google Earth topography) or in archives in public institutions in Slovenia or Bosnia and Herzegovina (topographical and geological maps) have been obtained.

Chemical analysis and obtained spatial data have been processed by the univariate, bivariate, and multivariate statistical methods. The concentration ratios according to the lithological units and determined zones are identified but also the statistical tests for statistical significance and assumptions have been performed. Based on multivariate statistical methods (clusters and factor analysis), four dominant geochemical associations were extracted. The Factor 1 associates the high concentration of Pb, Zn, Hg, Cd, Cu, Bi, Ag, Sb, Mo, W, Mn, Ba, Fe, and Tl. The group represents chemical elements that are the most probably anthropogenically distributed, associated to the main industrial and mine zone, and alluvial sediments found downstream of the river Stavnja. Three next factors, F2 (Ni, Cr, Co, and Mg), F3 (Th, La, As, and Sc), and F4 (Al, Ti, V, and Ga) are associating elements that are most probably naturally distributed and influenced by lithology.

The main problem of linear interpolation methods (including kriging), based only on mutual distances are elongated, highly isotropic halo contaminants which lie mostly in isotropic distributions conducted

to the particular lithological unit. While it should be consider a fact that the study area is highly risky, and the sampling design had to be adjusted. For this purpose, the segment kriging method has been developed and successfully applies. This method concerns an interpolation within the area where individual concentrations extremely deviate. Because this method is highly subjective, one linear method of Multiple Polynomial Regression and nonlinear method of artificial intelligence have been developed additionally. These two methods are based on fact that spatial distribution of particular chemical element or groups of elements depends on lithological background and geospatial data, but less their mutual distances. All three prediction methods are evaluated according to their stability and significance under the condition that all methods are carried out under the same conditions. Each particular prediction method had to solve successfully distributions, anthropogenic and natural, respectively. Detailed data processing has been performed at four leading elements: As, Pb, Ni, and Ti. Each of them is leading element of geochemical association isolated by statistical approaches. For those elements absolute prediction accuracy was evaluated, not only relative relations.

All three methods have been proven as very successful for predicting a spatial distribution of elements which represent a main geochemical pathway. The most significant models are that show anthropogenic Lead distribution, and less significant for vague Arsenic distribution. Segment kriging is a very useful, but requires a quite good knowledge of geology or mutual spatial relationships. In other hand, the method is also highly subjective. Ordinary multiple regression was found to be useless. Unexpectedly good results were obtained by multiple polynomial regressions (MPR), which is based on a cubic polynomial. But a big disadvantage of this method is that a large number of derivative spatial variables must be used, which is a mathematically complex as well as time consuming. At the same time it also raises the question of subjectivity. The best method is found a nonlinear method Artificial Neural network - Multi-layer perceptron (ANN-MP). The method is comparable to the previous one and it obtains a reliable model with less spatial variables, and the subjective influence is avoided.

Based on the above methods an environmental pollution assessment with trace elements has been performed. Anthropogenically distributed chemical elements Pb, Zn, and Cd exceed the intervention values (the Standard List) only at 2.5 km2, despite all expectances. Natural enrichment with Ni and Cr exceeds the intervention values at 10 km2. The biggest surprise is natural enrichment with As. Its values exceed the intervention values at 30 km2, nearly a third of study area.

It can be concluded that even in inaccessible terrain (such as mined areas or risky areas) the geochemical research is possible, even if there are based on sparse measurements. Using data processing methods such as multivariate statistical methods (cluster and factor analysis) and advanced nonlinear Artificial intelligence, the major geochemical trends as well as the reliable spatial distribution models can be determined. It is also the fact that the most reliable spatial data is Web available freely.

7. POVZETEK

Raziskano ozemlje (dolina reke Stavnje) je znano po svoji več kot 100-letni rudarski in metalurški dejavnosti.V zgornjem delu doline sta locirana dva opuščena površinska kopa železove rude Smreka in Brezik, rudnik železove rude Droškovec, zapuščen površinski kop Pb-Zn-Ba rude Veovača, ter zapuščeni obrati nekdanje železarne Vareš.V spodnjem (južnem) delu doline, v bližini Breze, se nahajajo opuščeni ter še aktivni površinski kopi, in rudnik rjavega premoga Breza. Raziskano ozemlje zajema predvsem hribovit svet in strmo dolino, območje na katerem živi okrog 30000 prebivalcev, predvsem v dveh večjih mestih Breza in Vareš. Raziskano ozemlje je bilo prizorišče intenzivnih vojaških operacij v zadnji vojni (1992-1995) posledica česa so danes številna ugotovljena (in tudi neugotovljena) minska polja ali območja visokega tveganja. Navedeno območje predstavlja izjemen poligon za preverjanje uporabnosti in stabilnosti linearnih in nelinearnih matematičnih metod kot so segmentno krigiranje (SK), multipla polinomska regresija (MPR) in umetna inteligenca - večslojni perceptron (ANN-MP), kjer ozka in zelo izdolžena anomalija antopogenega povišanja vsebnosti kemičnih prvin skoraj pravokotno seka pravilno zaporedje litoloških enot.

Glavni namen raziskovalnega dela je bila identifikacija optimalne metodologije geokemijskih raziskav na področju nekdanjih vojaških operacijah (ostanki minskih polj ali območja visokega tveganja) glede na vzorčno sredstvo, gostoto vzorčenja, način obdelave podatkov in interpretacijo samih rezultatov. Ugotovljene so bile vsebnosti in prostorska porazdelitev kemijskih elementov, opredeljena naravna ozadja glede na litološke enote, ter delež vpliva nekdanjega rudarjenja in metalurške dejavnosti na porazdelitev kemičnih elementov v drugih materialih (tla, rečni sedimenti in podstrešni prah). Z uporabo metod multivariatne statistike so bile ugotovljene glavne geokemijske povezave in njihova prostorsko porazdelitev.Ugotovljena in preverjena je bila tudi optimalna metodologija napovedi prostorske porazdelitve koncentracij kemijskih elementov z uporabo navedenih linearnih in nelinearnih matematičnih metod.

Vzorčni načrt je bil izdelan z namenom zagotavljanja enakomerne pokritosti raziskanega ozemlja s posebnim poudarkom na izogibanju območjem visokega tveganja. Osredotočili smo se na vzorčenje zgornje in spodnje ležeče talne plasti, rečnih sedimentov in podstrešnega prahu. Sama priprava in izvedba vzorčnega načrta je bilo zelo zahtevna predvsem zaradi obstoječih minskih polj ali neeksplodiranih eksplozivnih sredstev. Na 143 lokacijah vzorčenja je bilo zbranih 111 vzorcev zgornje (0-5 cm) in spodnje ležeče talne plasti (20-30 cm), 17 vzorcev rečnih sedimentov, ter 15 vzorcev podstrešnega prahu. Analiza 36 kemijskih elementov (Ag, Al, As, Au, B, Ba, Bi, Ca, Cd, Co, Cr, Cu, Fe, Ga, Hg, K, La, Mg, Mn, Mo, Na, Ni, P, Pb, S, Sb, Sc, Se, Sr, Th, Ti, TI, U, V, W in Zn) je bila opravljena v laboratoriju ACME, Vancouver (Kanada) po razklopu vzorcev z zlatotopko. Razen kemičnih analiz zbranega vzorčnega materiala, smo glede na zastavljene naloge, v raziskavo vključili številne prostorske podatke, ki so večinoma prosto dostopni na svetovnem spletu (digitalni model reliefa, satelitski posnetki, Google Earth topografija) in v arhivih javnih institucij v Sloveniji in Bosni in Hercegovini (topografske in geološke karte).

Kemijske analize in prostorski podatki so bili obdelani z metodo univariatne, bivariatne in multivariatne statistike. Ugotovljena so bila tudi koncentracijska razmerja glede na litološke enote in definirana območja, ter opravljeni številni statistični testi s katerimi smo preverjali statistično značilnost naših domnev. Na osnovi multivariatnih statističnih metod (klasterska in faktorska analiza) smo določili štiri prevladujoče geokemijske povezave. Povezava Ag-Ba-Bi-Cd-Cu-Fe-Hg-Mn-Mo-Pb-Sb-Tl-W-Zn združuje tipične »težke kovine« in obenem predstavlja najmočnejši vzorec porazdelitve kemičnih elementov. Ugotovaljena povezava je vezana predvsem na okolico nekdanjih izkopov rude železa in opuščene železarne Vareš, ter na aluvialne sedimente reke Stavnje. Anomalija je jasno izražena, zelo podolgovata in predstavlja predvsem obogatitev antropogenega izvora, ki je posledica nekdanjega

rudarjenja in topilništva.Ostale ugotovljene geokemične grupe Co-Cr-Mg-Ni, Al-Ga-Ti-V in As-La-Sc-Th, predstavljajo vpliv preperevanja posameznih litoloških enot.

Glavni problem vseh linearnih interpolacijskih metod (vključno s krigiranjem), torej metod napovedovanja ki temeljijo le na medsebojnih razdaljah, predstavljajo podolgovate, izjemno izotropne avreole onesnaženja, ki ležijo na predvsem izotropnih distribucijah, vezanih na posamezne litološke enote. Obenem moramo upoštevati dejstvo, da je raziskano ozemlje visoko tvegano in je bila vzorčna mreža temu dejstvu prirejena.V ta namen smo razvili in uporabili metodo segmentnega krigiranja (SK), ki dejansko predstavlja interpolacijo znotraj posameznega območja, kjer posamezne vrednosti značilno in močno izstopajo.Ker je navedena metoda močno subjektivna smo dodatno uporabili linearno metodo multiple polinomske regresije (MPR) ter kot glavno, nelinearno metodo umetne inteligence - večslojnega perceptrona (ANN-MP). Navedeni metodi temeljita na dejstvu, da na porazdelitev posameznega kemičnega elementa ali povezave elementov vplivajo predvsem litološka podlaga in prostorski parametri, v precej manjši meri njihove medsebojne oddaljenosti. Vse tri metode napovedovanja (SK, MPR in ANN-MP) smo ovrednotili glede na njihovo stabilnost in značilnost pod osnovnim pogojem, da je postopek izpeljan pod enakimi pogoji, kar pomeni, da so te metode morale uspešno rešiti antropogeno, kakor tudi naravno povzročene distribucije. Izračune smo opravili na vodilnih elementih, ugotovljenih na geokemičnih povezavah med Pb, Ni, Ti in As, ker smo ocenjevali tudi absolutno točnost napovedi, ne pa le relativne odnose, kar pri obdelavi faktorskih vrednosti ni mogoče.

Vse tri navedene metode so se pokazale kot zelo uspešne za napovedovanje prostorskih porazdelitev prvin, ki ponazarjajo glavne geokemične trende. Najbolj značilni modeli so izpeljani v primeru antropogene porazdelitve Pb najslabši toda še zmeraj visoko značilni v primeru naravne, toda nejasne distribucije As. Segmentno krigiranje (SK), je sicer zelo uporabno, zahteva pa zelo dobro poznavanje geologije ali pa medsebojnih prostorskih odnosov. Metoda je obenem močno subjektivna.Navadna multipla regresija se je izkazala kot neuporabna. Nepričakovano dobre rezultate pa smo dobili z metodo multiple polinomske regresije (MPR), ki temelji na kubičnem polinomu. Pomanjkljivost metode je v tem, da moramo uporabiti večje število izvedenih prostorskih spremenljivk, kar je matematično zahtevno in zelo zamudno.Obenem se tudi postavlja vprašanje subjektivnosti.Kot najboljša metoda se je pokazala nelinearna metoda umetne inteligence - večslojnega perceptrona (ANN-MP). Metoda je primerljiva s prejšnjo, le da zanesljiv model pridobimo že s precej manjšim številom prostorskih spremenljivk, ter se na ta način izognemo tudi subjektivnemu vplivu.

Na osnovi navedenih metod je bila izpeljana ocena onesnaženosti okolja s »težkimi kovinami«. Navkljub pričakovanju se je pokazalo, da antropogeno povzročene vsebnosti Pb, Zn in Cd presegajo priporočeno kritično vrednost (The Dutch Standards) na le približno 2.5 km^2. Naravno obogatene vsebnosti Cr in Ni presežejo omenjeno vrednost na približno 10 km^2. Največje presenečenje raziskave pa su naravno obogatene vsebnosti As. Priporočeno kritično vrednost presežejo na približno 30 km^2, torej na skoraj tretjini raziskanega ozemlja.

Zaključimo lahko, da je tudi na težko dostopnem terenu (minirana območja, ali območja visokega tveganja) mogoče izpeljati geokemične raziskave, ki temeljijo na nepravilnih, dokaj redkih mrežah vzorčenja. Z uporabo naprednih metod obdelave podatkov, kot so multivariatne statistične metode (klasterska in faktorska analiza) ter z uporabo predvsem nelinearne metode umetne inteligence - večslojnega perceptrona (ANN-MP) mogoče določiti glavne geokemijske trende kakor tudi zanesljive modele prostorske porazdelitve elementov. Pomembno je tudi dejstvo, da je večina zanesljivih prostorskih podatkov dostopna na svetovnemu spletu.

8. REFERENCES

8.1. Cited sources

Adriano D.C. 1986. Trace elements in the terrestrial environment. Springer-Verlag, New York, Berlin, Heidelberg, Tokyo, 533 p.

Adriano D.C. 2001. Trace elements in terrestrial environments: biogeochemistry, bioavailability and risks of metals 2nd edition, Springer-Verlag,New York, Berlin, Heidelberg, Tokyo, 867 p.

Agarval S.K. 2009.Heavy metal pollution. APH Publishing Corporation, New Delhi, 267 p.

Aitkenhead M.J., Aitkenhead-Peterson J.A., McDowell W.H., Smart R.P., Cresser M.S. 2007.Modelling DOC export from watersheds in Scotland using neural networks. Computers and Geosciences 33, 3, 423–436

Aitkenhead M.J., Coull M.C., Towers W., Hudson G., Black H.I.J. 2012. Predicting soil chemical composition and other soil parameters from field observations using a neural network. Computers and Electronics in Agriculture 82, 108–116

Alijagić J. 2008. Distribution of chemical elements in an old metallurgic area, Zenica (Central Bosnia).Master thesis, Masaryk University Brno, Brno, 100 p.

Alijagić J., Šajn R. 2006. Influence of ironworks on distribution of chemical elements in Bosnia and Herzegovina and Slovenia. Geologija, 49, 1, 123–132

Alijagić J., Šajn R. 2010. Distribution of chemical elements in an old metallurgical area, Zenica (Bosnia and Herzegovina). Geoderma, 162, 1–2, 71–85

Aliu M. 2010. Distribucija na teški metali vo počvite od Kosovska Mitrovica i nejzinata okolina.Ph.D. thesis, Sts. Cyril and Methodius University, Skopje, 182 p.

Aliu M., Šajn R., Stafilov T. 2009. Distribution of cadmium in surface soils in K. Mitrovica region, Kosovo. Geologica Macedonica, 23, 27-34.

Allison P.D. 1999. Multiple Regression: A Primer. Pine Forge Press, Thousand Oaks, 202 p.

Anagu I., Ingwersen J., Utermann J., Streck T. 2009. Estimation of heavy metal sorption in German soils using artificial neural networks. Geoderma, 15, 1-2, 104–112

Ashton P.J., Love D., Mahachi H., Dirks, P.H. G.M. 2001. An Overview of the Impact of Mining and Mineral Processing Operations on Water Resources and Water Quality in the Zambezi, Limpopo and Olifants Catchments in Southern Africa. Contract Report to the Mining, Minerals and Sustainable Development (Southern Africa).Project, by CSIR Environmentek, Pretoria, South Africa and Geology Department University of Zimbabwe, Harare, Zimbabwe. Report No. ENV-P-C 2001-042, 336 p.

Avila A., Rodrigo A., 2004. Trace metal fluxes in bulk deposition, through fall and stemflow at two evergreen oak stands in NE Spain subject to different exposure to the industrial environment. Atmospheric Environment, 38, 2, 171–180

Balabanova B., Stafilov T., Bačeva K., Šajn R. 2010. Biomonitoring of atmospheric pollution with heavy metals in the copper mine vicinity located near Radoviš, Republic of Macedonia. Journal of Environmental Science and Health, Part A - Toxic / Hazardous Substances and Environmental Engineering, 45, 12, 1504–1518

Balabanova B., Stafilov T., Šajn R., Bačeva K. 2011. Distribution of chemical elements in attic dust as reflection of their geogenic and anthropogenic sources in the vicinity of the copper mine and flotation plant. Archives of Environmental Contamination and Toxicology, 61, 2, 173–184

Banerjee A., 2003. Heavy metal levels and solid phase speciation in street dusts of Delhi, India. Environmental Pollution, 123, 1, 95–105

Baudo R., 1987. Heavy Metal Pollution and Ecosystem Recovery, Ecological Assessment of Evironmental Degradation, Pollution and Recovery. Elsevier Sciences Publishers, Amsterdam, 370 p.

Bačeva K., Stafilov T., Šajn R., Tanaselina C., Ilić Popov S. 2011. Distribution of chemical elements in attic dust in the vicinity of a ferronickel smelter plant. Fresenius environmental bulletin, 20, 9, 2306–2314

Borůvka L., Vacek O., Jehlička J. 2005. Principal component analysis as a tool to indicate the origin of potentially toxic elements in soils. Geoderma, 128, 3-4, 289–300

Boutron C., Vahdal G., Fitzgerald W., Ferrari C. 1998. A forty year record of mercury in central Greenland snow. Geophysical Research Letters, 25, 3315–3318

Box G.E.P., Cox D.R., 1962. An analysis of transformations. Journal of the Royal Statistical Society, Series B, 26, 2, 211–252

Bretzel F., Calderisi M. 2006. Metal contamination in urban soils of coastal Tuscany (Italy). Environmental Monitoring and Assessment, 118, 1-3, 319–335

Brininstool M. 2009: The Mineral Industry of Bosnia and Herzegovina. In: Minerals Yearbook, Area Reports, International, Europe and Central Eurasia. U.S. government printing office, Washington, 344p.

Budkovič T., Šajn R., Gosar M. 2003. Environmental impact of active and abandoned mines and metal smelters in Slovenia. Geologija, 46, 1, 135–140

Burrough P.A., Mc Donnell R.A. 1998. Principles of geographical information systems. Oxford University Press, Oxford, 333 p.

Candelone J., Hong S., Pellone C., Boutron C. 1995. Post-industrial revolution changes in largescale atmospheric pollution of the northern hemisphere by heavy metals as documented in central Greenland snow and ice. Journal of Geophysical Research, 100, D8, 16605–16616

Cappuyns V., Swennen R., Vandamme A., Niclaes M. 2006. Environmental impact of the former Pb–Zn mining and smelting in East Belgium, Journal of Geochemical Exploration, 88, 6–9

Carlon C., Critto A., Marcomini A., Nathanail P. 2001. Risk based chatacterisation of contaminated industrial site using multivariate and geostatistical tools. Environmental Pollution, 11, 3, 417–427

Chen T.B., Zheng Y.M., Lei M., Huang Z.C., Wu H.T., Chen H., Fan K.K., Yu K., Wu X., Tian Q.Z. 2005. Assessment of heavy metal pollution in surface soils of urban parks in Beijing, China. Chemosphere, 60, 4, 542–551

Chopin E.I.B., Alloway B.J. 2007. Distribution and mobility of trace elements in soils and vegetation around the mining and smelting areas of Tharsis, Ríotinto and Huelva, Iberian Pyrite Belt, SW Spain. Water, Air, and Soil Pollution, 182, 1-4, 245–261

Cizdziel J.V., Hodge. V.F. 2000. Attics as archives for house infiltrating pollutants: trace elements and pesticides in attic dust and soil from southern Nevada and Utah. Microchemical Journal, 64, 85-92

Cizdziel J.V., Hodge V.F., Faller S. 1998. Plutonium anomalies in attic dust and soils at locations surrounding the Nevada Test Site. Chemosphere, 37, 6, 1157-1168

Cizdziel J.V., Hodge V.F., Faller S. 1999. Resolving Nevada Test Site and global fallout plutonium in attic dust and soils using 137Cs/239+240Pu activity ratios. Health Physics, 77, 1, 67-75

Clark I., Harper W.V. 2000.Practical geostatistics.Ecosse North America Llc, Columbus, Ohio, 382 p.

Culbard E., Thornton I., Brooks K., Watt J., Thomson M., Moorcroft S. 1983. Metal contamination of dusts and soils in urban and rural households in the United Kingdom: National reconnaissance survey of the United Kingdom to determine metal concentration. In: Trace substances in environmental health XVII. Hemphill D.D. (Ed.). University of Missouri, Colurnbia, 236-241 p.

Davies D.J., Thornton I., Watt J.M., Culbard E.B., Harvey P.G., Delves H.T., Sherlock J.C., Smart G.A., Thomas J.F., Quinn M.J. 1990. Lead intake and blood lead in two-year-old UK urban children. Science of the Total Environment, 90, 13-29

Davis J.C. 1986.Statistic and data analysis in geology. Willey, New York, 646 p.

Deutsch C.V., Journel A.G. 1998. GSLIB: geostatistical software library and user's guide, 2nd Edition. Oxford University Press, Oksford,369 p.

Drever J.I., Hurcomb D.R. 1986. Neutralization of atmospheric acidity by chemical weathering in an alpine drainage basin in the North Cascade Mountains. Geology, 14, 3, 221–224

Du K.L., Swamy M.N.S. 2006. Neural Networks in an Softcomputing Framework. Springer – Verlag, London, 566 p.

Dudka S., Adriano D. C. 1997. Environmental impacts of Metal Ore Mining and processing: A Review. Journal of Environmental Quality, 26, 3, 590–602

Elshorbagy A., Parasuraman K. 2008. On the relevance of using artificial neural networks for estimating soil moisture content. Journal of Hydrology, 362, 1–2, 1–18

Fergusson J.E. 1992. Dust in the environment, elemental composition and sources. In: The science of global change, the impact of human activities on the environment. Dunnette D.A., O'Brien R.J. (Eds.). Portland State University, American Chemical Society, Washington D.C., 116-133 p.

Fergusson J.E., Kim N.D. 1991. Trace elements in street and house dusts: Sources and speciation. The science of the total environment, 100, 125-150.

Filzmoser P., Garrett R.G., Reimann C. 2005. Multivariate outlier detection in exploration geochemistry. Computers and Geosciences, 31, 579–587

Finlayson-Pitts B., Pitts J.N. 2000. Chemistry of the Upper and Lower Atmosphere. Academic Press, San Diego, 969 p.

García-Lorenzo M.L., Pérez-Sirventa C., Martínez-Sánchez M.J., Molina-Ruiz J. 2012.Trace elements contamination in an abandoned mining site in a semiarid zone. Journal of Geochemical Exploration, 113, 23–35

Gerrard J., 2000. Fundamentals of soils. Routledge, London, New York, Cornwall , 230 p.

Gomes M.E.P., Favas P.J.C. 2006. Mineralogical controls on mine drainage of the abandoned Ervedosa tin mine in north-eastern Portugal. Applied Geochemistry, 21, 8, 1322–1334

Goodchild M.F., Parks B.O., Steyaret L.T. 1993. Environmental modelling with GIS, Oxford University Press, New York, 488 p.

Goovaerts P. 1999. Geostatistics in soil science: state of the art and perspectives. Geoderma, 89, 1, 1–45

Goovaerts P. 2001.Geostatistical modelling of uncertainty in soil science. Geoderma, 103, 1-2, 3–26

Gorlach U., Boutron C. 1992. Variations in heavy metals concentrations in Antarctic snows from 1940 to 1980. Journal of Atmospheric Chemistry, 14, 1-4, 205-222

Gosar M., Šajn R., Biester H. 2002. Mercury speciation in soils and attic dust in the Idrija area. Geologija, 45, 2, 373-378

Gosar M., Šajn R., Biester H. 2006. Binding of mercury in soils and attic dust in the Idrija mercury mine area (Slovenia). The Science of the Total Environment, 369, 1-3, 150-162

Gringarten E., Deutsch C.V. 2001. Teacher's aide: variogram interpretation and modeling. Mathematical Geology 33, 4, 507–534

Gspan P., Hrašovec B. 1993. Dust in production. Zavod Republike Slovenije za varnost pri delu, Ljubljana, 160 p.

Guicharnaud R., Paton G.I. 2006. An evaluation of acid deposition on cation leaching and weathering rates of an Andosol and Cambisol. Journal of Geochemical Exploration, 88, 1–3, 279–283

Guth P.L. 2006.Geomorphometry from SRTM – comparison to NED. Photogrammetric Engineering and Remote Sensing, 72, 3, 269–277

Harris M., Taylor G., Taylor J. 2005. Catch Up Maths and Stats: For the Life and Medical Sciences. Scion Publishing, Oxfordshire, 187 p.

Harvey D. 2000. Modern analytical chemistry.McGraw-Hill Higher Education, New York, 798 p.

Haykin S. 1999. Neural Networks: A comprehensive foundation, 2nd edition. Pearson, Singapore, 842 p.

Hill L.L. 2006. Georeferencing: The Geographic Associations of Information. The MIT Press, Cambridge, Massachusetts, 260 p.

Honerkamp J. 2002. Statistical physics: An Advanced Approach with Applications. Springer-Verlag, Berlin, Heidelrberg, 515 p.

Hong S., Candelone J., Patterson C., Boutron C. 1996. History of ancient copper smelting pollution during Roman and medieval times recorded in Greenland ice. Science, 272, 5259, 246-249

Honghai Qi., Altinakar M.S. 2011. A GIS-based decision support system for integrated flood management under uncertainty with two dimensional numerical simulations. Environmental Modelling and Software, 26, 6, 817–821

Hoskin W., Bird G., Stanley T. 2000. Mining - facts, figures and environment. Industry and environment, 23, 4-8

Hou H., Takamatsu T., Koskiwa M.K., Hosomi M. 2005.Trace metal sin bulk precipitation and through fall in a suburban area of Japan. Atmospheric Environment, 39, 20, 3583-3595

Hršak J., Škrbec A., Balagovič I., Šega K. 2003. Thallium content in Zagreb air. Bulletin of Environmental Contamination and Toxicology, 71, 1, 131-134

Huang L.M., Zhang G.L., Yang J.L. 2013. Weathering and soil formation rates based on geochemical mass balances in a small forested watershed under acid precipitation in subtropical China. Catena, 105, 11–20

Hudson-Edwards K. A. 2003. Sources, mineralogy, chemistry and fate of heavy metal-bearing particles in mining-affected river systems. Mineral Mag, 67, 2, 205–217

Hur S., Cunde X., Hong S., Barbante C., Gabrielli P., Lee K., Boutron C., Ming Y. 2007. Seasonal patterns of heavy metal deposition to the snow on Lambert Glacier basin, East Antarctica. Atmospheric Environment, 41, 38, 8567-8578

Imperato M., Adamo P., Naimo D., Arienzo M., Stanzione D., Violante P. 2003. Spatial distribution of heavy metals in urban soils of Naples city (Italy). Environmental Pollution, 124, 2, 247-256

Ingram B., Cornford D. 2010. Parallel geostatistics for sparse and dense datasets.geoENV. Geostatistics for Environmental Applications, 16, 371–381

Isaaks E.H., Srivastava R.M. 1989. An Introduction to Applied Geostatistics.Oxford university press, New York, 561 p.

Jain A.K., Mao J., Mohiuddin K.M. 1996. Artificial Neural Networks: A Tutorial.IEEE Computer, 29, 3, 31-44.

Jain S.K., Singh V.P. 2003. Water Resources Systems Planning and Management, 51, 858

Jemec M., Šajn R. 2007. Geochemical research of soil and attic dust in Litija area, Slovenia. Geologija, 50, 2, 497-505

Jobson J.D. 1991.Applied Multivariate Data Analysis.Vol. I: Regression and Experimental Design. Springer-Verlag, New York, 662 p.

Johnson N., Driscoll C., Eaton J., Liken G., McDowell W. 1981. “Acid rain”, dissolved aluminum and chemical weathering at the Hubbard Brook Experimental Forest, New Hampshire. Geochimica et Cosmochimica Acta, 45, 9, 1421–1437

Jordan G. 2009. Sustainable mineral resources management: from regional mineral resources exploration to spatial contamination risk assessment of mining. Environmental Geology, 58,153–169

Jovanović R., Mojićević M., Tokić S., Rokić Lj. 1977. Basic geological map of SFRJ, sheet Sarajevo 1:100.000 (map and interpreter). Federal Geological Survey, Beograd, 52p.

Kabata-Pendias A., Pendias H. 2001 Trace elements in soil and plants, Third Edition. CRC Press, Boca Raton, 413 p.

Krige D.G. 1951. A statistical approach to some basic mine valuation problems on the Witwatersrand. Journal of the Chemical, Metallurgical and Mining Society of South Africa, 52, 6, 119–139

Krige D.G. 1960. On the departure of ore value distributions from lognormal models in South African gold mines.Journal of the South African Institute of Mining and Metallurgy., 61, 231–244

Kohenen T. 2001. Self-Organizing Map, 3rd Edition. Springer-Verlag, Berlin, Heidelberg, New York, 501 p.

Kunwar P.S., Mohan D., Singh V.K., Malik A. 2005. Studies on distribution and fractionation of heavy metals in Gomti river sediments - a tributary of the Ganges, India. Journal of Hydrology, 312, 1-4, 14–27

Le Maitre R.W. 1982.Numerical Petrology, Statistical interpretation of geochemical data. Elsevier, Amsterdam, 281p.

Lee C.H. 2003. Assessment of contamination load on water, soil and sediment affected by the Kongjujiel mine drainage, Republic of Korea. Environmental Geology, 44, 501–515

Lioy P.J. 1990. Assessing total human exposure to contaminants. Environmental Science and Technology, 24, 7, 938-945

Matheron G. 1971. The theory of regionalised variables and its applications.Les Cahiers du Centre de Morphologie Mathematique de Fontainblue, Ecole Nationale Superiore de Paris, Paris, 212 p.

Mattigod S.V., Page A.L. 1983. Assessment of metal pollution in soil. In: Applied environmental geochemistry. Thornton I. (ed.). Academic Press, London, 355–393 p.

McBride M.B. 2003. Toxic metals in sewage sludge-amended soils: has promotion of beneficial use discounted the risks? Advances in Environtal Researches, 8, 1, 5–19

McGrath D., Zhang C., Carton O.T. 2004. Geostatistical analyses and hazard assessment on soil lead in Silvermines area, Ireland. Environmental Pollution, 127, 2, 239–248

McLaughlin M.J., Parker D.R., Clarke J.M. 1999. Metals and micronutrients-food safety issues. Field Crops Research, 60, 1, 143–163

Mielke H.W., Adams J.L., Reagan P.L., Mielke Jr. P.W. 1989. Soil-dust lead and childhood lead exposure as a function of city size and community traffic flow: The case for lead abatement in Minnesota. In: Lead in soil: issues and guidelines. Davies B.E. Wixson B.G. (eds.). Environmental Geochemistry and Health Supplement, 243–271 p.

Mitasova H., Hofierka J. 1993. Interpolation by Regularized Spline with Tension: II. Application to Terrain Modeling and Surface Geometry Analysis. Mathematical Geology, 25, 6, 657-669

Molhave L., Schneider T., Kjvrgaard S.K., Larsen L., Norn S., Jorgensen O. 2000. House dust in seven Danish offices. Atmospheric Environment, 34, 4767-4779

Moller A., Muller H.W., Abdullah A., Abdelgawad G., Utermann J. 2005. Urban soil pollution in Damascus, Syria: concentrations and patterns of heavy metals in the soils of the Damascus Ghouta. Geoderma, 124, 1, 63–71

Moor I.D., Lewis A., Gallant J.C. 1993. Terrain properties: Estimation Methods and Scale Effects. In: Modeling Change in Environmental Systems. Jakeman A.J. (ed.), John Wiley and Sons, New York, 189-214 p.

Mukherjee S, Joshi P.K., Mukherjeea S., Ghosh A., Garg R.D., Mukhopadhyay A. 2013. Evaluation of vertical accuracy of open source Digital Elevation Model (DEM). International Journal of Applied Earth Observation and Geoinformation, 21, 205–217

Navarro A., Collado D., Carbonell M., Sánchez J.A. 2004. Impact of mining activities on soils in a semi-arid environment: Sierra Almagrera district, SE Spain. Environmental Geochemistry and Health, 26, 383–393

Navarro M.C., Pérez-Sirvent C., Martínez-Sánchez M.J., Vidal J., Tovar P.J., Bech J. 2008. Abandoned mine sites as a source of contamination by heavy metals: a case study in a semi-arid zone. Journal of Geochemical Exploration, 96, 4, 183–193

Olea R. 1991.Geostatistical glossary and multilingual dictionary. Oxford University Press, New York, 177 p.

Olujić J., Pamić O., Pamić J., Milojević R., Veljković D., Kapeler I. 1978. Basic geological map of SFRJ, sheet Vareš 1:100.000 (map). Federal Geological Survey, Beograd.

Ozaki H., Watanabe I., Kuno K. 2004.As, Sb and Hg distribution and pollution sources in the roadside soil and dust around Kamikochi, Chubu Sangaku National Park, Japan. Geochemical Journal, 38, 5, 473-484

Pacyna E.G., Pacyna J.M., Fudala J., Strzelecka-Jastrzab E., Hlawiczka S., Panasiuk D., Nitter S., Pregger T., Pfeiffer H., Friedrich R. 2007. Current and future emissions of selected heavy metals to the atmosphere from anthropogenic sources in Europe. Atmospheric Environment, 41, 38, 8557-8566

Palinkaš L.A., Šoštarić S.B., Palinkaš S.S. 2008. Metallogeny of the Northwestern and Central Dinarides and Southern Tisia. Ore Geology Reviews, 34, 501–520

Pamić J., Pamić O., Olujić J., Milojević R., Veljković D., Kapeler I. 1978: Basic geological map of SFRJ, sheet Vareš 1:100.000 (interpreter). Federal Geological Survey, Beograd, 68 p.

Pawlowsky-Glahn V., Egozcue J.J. 2006. Compositional data and their analysis: an introduction. In: Compositional Data Analysis in the Geosciences: From Theory to Practice. Buccianti A., Mateu-Figueras G., Pawlowski-Glahn V. (eds.). Geological Society, London, 1-10 p.

Pett M.A., Lackey N.R., Sullivan J.J. 2003. Making Sense Of Factor Analysis: The Use Of Factor Analysis For Instrument Development in Health Care Research. Sage Publication, Thosandoaks, London, New Delhi, 348 p.

Pruvot C., Douay F., Herve F., Waterlot C. 2006.Heavy metals in soil, crops and grass as a source of human exposure in the former mining areas. Journal of Soils Sediments, 6, 215–220

Ramlal B., Baban S. 2008. Developing a GIS based integrated approach to flood management in Trinidad, West Indies. Journal of Environmental Management, 88, 4, 1131–1140

Rasmussen P.E., Subramanian K.S., Jessiman B.J. 2001. A multi-element profile of housedust in relation to exterior dust and soils in the city of Ottawa, Canada. Science of the Total Environment, 267, 1-3, 125-140

Reimann C., Filzmoser P., Garrett R.G. 2002. Factor analysis applied to regional geochemical data: problems and possibilities. Applied Geochemistry, 17, 3, 185-206

Romesburg H.C. 2004. Cluster Analysis for Researchers. Lulu Press, North Carolina, 341 p.

Rose A.W., Hawkes H.E., Webb J.S. 1979. Geochemistry in mineral exploration, 2nd edition. Academic Press, London, 657 p.

Sahu J.N., Acharyab J., Meikapa, B.C. 2009. Response surface modeling and optimization of chromium (VI) removal from aqueous solution using Tamarind wood activated carbon in batch process. Journal of Hazardous Materials, 172, 2-3, 818–825

Sahai H., Ageel M.I. 2000. The analysis of variance: fixed, random, and mixed models. Birkhäuser, Boston, 742 p.

Salminen R., Batista M.J., Bidovec M., Demetriades A., De Vivo B., De Vos W., Duris M., Gilucis A., Gregorauskiene V., Halamić J., Heitzmann P., Jordan G., Klaver G., Klein P., Lis J., Locutura J., Marsina K., Mazreku A., O'Connor P.J., Olsson S.A., Ottesen R.T., Petersell V., Plant J.A., Reeder S., Salpeteur I., Sandström H., Siewers U., Steenfelt A., Tarvainen T. 2005. Geochemical Atlas of Europe, Part 1, Background Information, Methodology and Maps.Geological Survey of Finland, Espoo, 526 p.

Shoji T. 2002. Enrichment Ratio-Tonnage Diagrams for Resource Assessment. Natural Resources Research,11, 273-287

Siegel F.R. 2002. Environmental Geochemistry of Potentially Toxic Metals, Springer Verlag, Heidelberg, 218 p.

Singh A.N. Zeng D.H., Chen F.S. 2005. Heavy metal concentrations in redeveloping soil of mine spoil under plantations of certain native woody species in dry tropical environment, India. Journal of Environmental Science, 17, 1, 168–174

Singha K.P., Basantb N., Malika A., Jaina G. 2010. Modeling the performance of "up-flow anaerobic sludge blanket" reactor based wastewater treatment plant using linear and nonlinear approaches—A case study. Analytica Chimica Acta, 658, 1, 1-11

Snedecor G.W., Cochran W.G. 1967. Statistical methods.The Iowa State University Press, Ames, Iowa, 593 p.

Stafilov T., Aliu, M., Šajn, R 2010a.Arsenic in surface soils affected by mining and metallurgical processing in K. Mitrovica Region, Kosovo. International Journal of Environmental Research and Public Health, 7, 11, 4050-4061

Stafilov T., Šajn R., Alijagić J. 2013. Distribution of Arsenic, Antimony and Thallium in Soil in Kavadarci and the Environs, Republic of Macedonia. Soil sediment contamination, 22, 1, 105-118

Stafilov, T., Šajn, R., Boev, B., Cvetković, J., Mukaetov, D., Andreevski, M., 2008a. Geochemical atlas of Kavadarci and the environment, Sts. Cyril and Methodius University , Faculty of Natural Science, Skopje, 109 p.

Stafilov T., Šajn R., Boev B., Cvetković J., Mukaetov D., Andreevski M., Lepitkova S. 2010b. Distribution of some elements in surface soil over the Kavadarci region, Republic of Macedonia. Environmental earth sciences, 61, 7, 1515-1530

Stafilov T., Šajn R., Pančevski Z., Boev B., Frotasyeva M.V., Strelkova L.P., 2008b. Geochemical atlas of Veles and the environs.Sts. Cyril and Methodius University, Faculty of natural sciences and matematics, Skopje, 123 p.

Stafilov T., Šajn R., Pančevski Z., Boev B., Frontasyeva M.V., Strelkova L.P. 2010c. Heavy metal contamination of topsoils around a lead and zinc smelter in the Republic of Macedonia. Journal of Hazardous Material, 175, 1-3, 896-914

Stein A., Brouwer J., Bouma J. 1997. Methods for comparing spatial variability patterns of millet yield and soil data. Soil Science Society of America Journal, 61, 3, 861–870

Stumm W., Morgan J.J. 1996. Aquatic chemistry: chemical equilibria and rates in natural waters. A Waley Interscience Publication, New York, 1022 p.

Šajn R. 1998. Influence of lithology and antropogenic activity on distribution of chemical elements in dwelling dust, Slovenia. Geologija, 43, 1, 85-101

Šajn R. 1999.Geochemical properties of urban sediments on the territory of Slovenia.Geological survey of Slovenia, Ljubljana, 136 p.

Šajn R. 2003.Distribution of chemical elements in attic dust and soil as reflection of lithology and anthropogenic influence in Slovenia. Journal de Physique, 107, 1, 1173-1176

Šajn R. 2005.Using attic dust and soil for the separation of anthropogenic and geogenic elemental distributions in an old metallurgic area (Celje, Slovenia). Geochemistry, Exploration Environment Analysis, 5, 1, 59-67

Šajn R. 2006.Factor analysis of soil and attic-dust to separate mining and metallurgy influence, Meža Valley, Slovenia. Mathematical geology, 38, 6, 735-747

Šajn R., Alijagić J. 2012.Cooperation of GeoZS in geochemical investigation in former Yugoslavia.RMZ Materials and Geoenvironment, 59, 2/3, 159-180.

Šajn R., Gosar M. 2007.Soil pollution in surroundings of Litija as a reflection of mining, metallurgy and natural conditions. Geologija, 50, 1, 131-145

Šajn R., Gosar M., Bidovec M. 2000. Geochemical properties of soil, overbank sediment, household and attic dust in Mežica area (Slovenia). Geologija, 43, 2, 235-245

Šajn R., Halamić J., Peh Z., Galović L., Alijagić J. 2011.Assessment of the natural and anthropogenic sources of chemical elements in alluvial soils from the Drava River using multivariate statistical methods. Journal of geochemical exploration, 110, 3, 278-289

Šajn R., Aliu M., Stafilov T., Alijagić J. 2013. Heavy metal contamination of topsoil around a lead and zinc smelter in Kosovska Mitrovica/Mitrovicë, Kosovo/Kosovë. Journal of geochemical exploration (in press).

Šajn R., Žibret G., Alijagić J. 2012: Chemical Composition of Urban Dusts in Slovenia In: Dust: sources, environmental concerns, and control (Environmental health - physical, chemical and biological factors). Wouters L.B., Pauwels M. (eds.). Nova Science Publishers, New York, 1-56 p.

Tasdemir Y., Kural C. 2005. Atmospheric dry deposition fluxes of trace elements measured in Bursa, Turkey. Environmental Pollution, 138, 3, 462-472

Taylor L.L., Banwart S.A., Valdes P.J., Leake J.R., Beering D.J. 2012. Evaluating the effects of terrestrial ecosystems, climate and carbon dioxide on weathering over geological time: a global-scale process-based approach. Philosophical Transactions of the Royal Society, 367, 565–582

Tembo B.D., Sichilongo K., Cernak J. 2006. Distribution of copper, lead, cadmium and zinc concentrations in soils around Kabwe town in Zambia, Chemosphere, 63, 3, 497–501

Templ M., Filzmoser P., Reimann C. 2008. Cluster analysis applied to regional geochemical data: Problems and possibilities. Applied Geochemistry, 23, 8, 2198–2213

Thornton P.E., Running S.W., White M.A. 1997. Generating surface of daily meteorological variable over large regions of complex terrain. Journal of Hydrology, 190, 3, 214–250

Van Beers W.C.M., Kleijnen, J.P.C. 2004. Application-driven sequential designs for simulation experiments: Kriging metamodelling. Journal of the Operational Research Society, 55, 9, 876-883

Van de Velde K., Vallelonga P., Candelone J., Rosman K., Gaspari V., Cozzi G., Barbante C., Udisti R., Cescon P., Boutron C. 2005. Pb isotope record over one century in snow from Victoria Land, Antarctica. Earth and Planetary Science Letters, 232, 1-2, 95-108

Vassilopouloua S., Hurnia L., Dietrichb V., Baltsaviasc E., Paterakic M., Lagiosd E., Parcharidis L. 2002. Orthophoto generation using IKONOS imagery and high resolution DEM: a case study on volcanic hazard monitoring of Nisyros Island (Greece). ISPRS Journal of Photogrammetry and Remote Sensing, 57, 24–38

Von Blanckenburg F. 2005. The control mechanisms of erosion and weathering at basin scale from cosmogenic nuclides in river sediment. Earth and Planetary Science Letters, 237, 3–4, 462–479

Wang X.S., Qin Y., Sang S.X. 2005. Accumulation and sources of heavy metals in urban topsoils: Case study from the city of Xuzhou, China. Environmental Geology, 48, 1, 101–107

Webster R., and Oliver M.A. 2001. Geostatistics for environmental scientists. John Wiley and Sons Ltd, Chichester, 271 p.

White A.F., Blum, A.E. 1995. Effects of climate on chemical weathering in watersheds. Geochimica et Cosmochimica Acta, 59, 9, 1729–1747

Wilson B., Pyatt F. 2007. Heavy Metal Bioaccumulation by the Important Food Plant, Olea europaea L., in an Ancient Metalliferous Polluted Area of Cyprus. Bulletin of Environmental Contamination and Toxicology 78, 5, 390-394

Wolock D.M., Price C.V. 1994. Effects of digital elevation model map scale and data resolution on a topography-based watershed model. Water Resources Research, 30, 11, 3041–3052

Yaron B., Calvet R., Prost R. 1996. Soil pollution. Springer Verlag, Berlin, Heidelberg, 313 p.

Zhang C.S., Selinus O. 1998. Statistics and GIS in environmental geochemistry—some problems and solutions. Journal of Geochemical Exploration, 64, 1-3, 339–354

Zhang C.S., Selinus O., Schedin J. 1998. Statistical analyses on heavy metal contents in till and root samples in an area of southeastern Sweden. The Science of the Total Environment, 212, 2-3, 217– 232

Zhang C.S., Zhang S. 1996. A robust-symmetric mean: A new way of mean calculation for environmental data. Geo Journal, 40, 1-2, 209–212

Zhang C.S., Zhang S., Zhang L.C., Wang L.J. 1995. Background contents of heavy metals in sediments of the Changjiang River system and their calculation methods. Journal of Environmental Sciences, 7, 4, 422–429

Zhang W., Montgomery D.R. 1994.Digital elevation model grid size, landscape representation, and hydrologic simulation. Water Resources Research, 30, 4, 1019–1028

Žibret G. 2008. Determination of historical emission of heavy metals into the atmosphere: Celje case study. Environ. geol., 56, 189-196.

Žibret G., Šajn R. 2008a. Impacts of the mining and smelting activities to the environment - Slovenian case studies. In: Causes and effects of heavy metal pollution. Sánchez, M.L. (eds.).Nova Science Publishers, New York, 1-80p.

Žibret G., Šajn R. 2008b.Modelling of atmospheric dispersion of heavy metals in the Celje area, Slovenia. Journal ofGeochemicalExploration, 97, 1, 29-41

Žibret G., Šajn R. 2010.Hunting for geochemical associations of elements: factor analysis and self-organising maps. MathematicalGeology,42, 6,681-703

Žibret G., Šajn R., Alijagić J., Stafilov T. 2012.Use of neural networks in the geochemical data interpretation.Zeitschrift für Geologische Wissenschaften, 40, 4-5, 253-266

8.2. Other sources

ACME Labs 2010. Sample preparation & Analysis (Catalogue of services), 36 p. (http://acmelab.com/pdfs/Acme_Price_Brochure.pdf)

ACME Labs 2010. Sample preparation & Analysis (Catalogue of services), 40 p. (http://acmelab.com/pdfs/Acme_Price_Brochure.pdf)

Autodesk, Inc. 2012.Autodesk MAP 3D, Version 2012 - Software. Autodesk, Inc. (http://www.autodesk.com)

ESRI, Inc. 2004.ArcINFO ver 9, Software. Environmental research institute (http://www.esri.com/)

FAO 2006.World reference base for soil resources 2006, a framework for international classification, correlation and communication. Rome. Food and Agriculture Organisation of the Unitaded Nations, 128 p.

Golden Software, Inc. 2012.Surfer (surface mapping system), ver 11 – Software.Golden Software, Inc. (http://www.goldensoftware.com/)

Google Inc. 2010. Google Earth. Area Breza - Vareš (http://earth.google.com)

Layla Resources Ltd. 2011. The new Dutchlist (http://www.contaminatedland.co.uk/std-guid/dutch-l.htm)

Pawlowsky-Glahn V., Egozcue J.J., Tolosana-Delgado R. 2007. Lecture notes on compositional data analysis. (http://www.wepapers.com/Papers/61766/)

Stat Soft, Inc. 2012.STATISTICA (data analysis software system), version 11 – Software. Stat Soft, Inc.(www.statsoft.com)

The CGIAR Consortium for Spatial Information, 2011.SRTM 90m Digital Elevation Data. Database: SRTM_40_04 (http://srtm.csi.cgiar.org)

U.S. Geological Survey 2011a.ASTER Global Digital Elevation Data (30 m). Database: 20130113055119_468788446 (http://gdex.cr.usgs.gov/gdex/)

U.S. Geological Survey 2011b.Global Land Survey multispectral landsat satelite images P187-R29. Databases: P188R029_5x19920914 and LE71880292007259ASN00 (http://earthexplorer.usgs.gov/)

U.S. Geological Survey 2011c. Landsat project description and Land Remote Sensing (http://landsat.usgs.gov/)

ACKNOWLEDGEMENTS

I would like to express my gratitude to all those who gave me the possibility to complete this dissertation. This thesis was funded by the Slovenian research agency, through the Young researchers programme, and I would like to give my special thanks to the Slovenian research agency because without them it would not be possible to complete my dissertation.

My first debt of gratitude must go to my supervisor, Dr. Robert Šajn, who helped and supported me in all the time of research for and writing of this thesis. I sincerely thank you for taking time off to picking up important points I missed when putting together my PhD thesis and for all your kind advices, discussions, and patience.

I would like to express my deepest gratitude to my family, especially to Matej and my lovely daughter Emma.

I would also like to thank the members of my thesis committee, Prof. Dr. Marjana Novič, Prof. Kurt Kalcher, and Dr. Gregor Muri for giving me a new ideas, constructive comments and corrections.

I want to thank the Geological Survey of Slovenia and Federal Geological Survey of Bosnia and Herzegovina that stimulating my work and helped in the data acquisition necessary for my dissertation, and Dr. Christian Fischer from the German Aerospace Centre who provided me in use of satellite images.

.

Appendix A: Locations and basic properties of sampled materials (I)

Sample	Material	Lon (WGS84)	Lat (WGS84)	Altitude (M)	Location	Year	Area
T-01/1 (0-5)	Topsoil	18.33095	44.19802	1113	Sjenokos	2011	Rural
T-01/2 (0-5)	Topsoil	18.34598	44.19091	1071	Strijica	2009	Rural
T-01/3 (0-5)	Topsoil	18.36298	44.19426	1089	Zarađe	2009	Rural
T-02/1 (0-5)	Topsoil	18.33179	44.18713	1164	Sjenokos	2009	Rural
T-02/2 (0-5)	Topsoil	18.34180	44.18490	966	Stavnja (Zg. tok)	2009	Rural
T-02/3 (0-5)	Topsoil	18.34947	44.18246	1066	Javornik	2009	Rural
T-03/1 (0-5)	Topsoil	18.32086	44.17997	1159	Pobrin Han	2009	Rural
T-03/2 (0-5)	Topsoil	18.33692	44.17857	922	Vareš (Stijenje)	2009	Rural
T-03/3 (0-5)	Topsoil	18.34059	44.17388	1024	Zabrezje	2009	Rural
T-04/1 (0-5)	Topsoil	18.31483	44.17303	1094	Vijenac	2011	Natural
T-04/2 (0-5)	Topsoil	18.32878	44.17165	999	Vijenac (Veleski p.)	2009	Rural
T-04/3 (0-5)	Topsoil	18.33492	44.16992	887	Lijepovići	2009	Rural, Urban
T-04/4 (0-5)	Topsoil	18.34399	44.16522	1162	Kapetanovići	2011	Rural
T-05/1 (0-5)	Topsoil	18.32991	44.16509	842	Vareš - Benići	2009	Urban
T-05/2 (0-5)	Topsoil	18.33116	44.16303	911	Vareš (Terzijino B.)	2009	Rural
T-06/1 (0-5)	Topsoil	18.28727	44.17289	1173	Semizova Ponikva	2011	Rural
T-06/2 (0-5)	Topsoil	18.30338	44.16807	1120	Stijene	2011	Rural
T-06/3 (0-5)	Topsoil	18.31928	44.16528	1066	Vareš (W)	2009	Rural
T-06/4 (0-5)	Topsoil	18.32474	44.16431	947	Vareš	2009	Rural
T-06/5 (0-5)	Topsoil	18.32598	44.16129	829	Vareš (Put mira 29)	2009	Urban
T-06/6 (0-5)	Topsoil	18.32784	44.15806	902	Vareš	2009	Rural
T-06/7 (0-5)	Topsoil	18.33854	44.15448	1122	Diknići	2009	Rural
T-06/8 (0-5)	Topsoil	18.35758	44.15484	1186	Borak	2011	Rural
T-07/1 (0-5)	Topsoil	18.27961	44.15481	1366	G. Rajčevac	2011	Rural
T-07/2 (0-5)	Topsoil	18.29245	44.16082	1161	Kicelj	2011	Rural
T-07/3 (0-5)	Topsoil	18.30939	44.15604	922	Papale	2011	Rural
T-07/4 (0-5)	Topsoil	18.32313	44.15421	804	Vareš (C.R.)	2009	Industrial, Urban
T-08/1 (0-5)	Topsoil	18.31699	44.14698	903	G. Rajčevac	2009	Rural
T-08/2 (0-5)	Topsoil	18.32065	44.14754	827	D. Rajčevac	2009	Rural, Urban
T-08/3 (0-5)	Topsoil	18.32258	44.14704	788	Vareš - Majdan (N)	2009	Industrial, Urban
T-08/4 (0-5)	Topsoil	18.33168	44.14604	1024	Mlakve	2009	Rural
T-08/5 (0-5)	Topsoil	18.34286	44.14466	1109	Brezik	2009	Rural
T-09/1 (0-5)	Topsoil	18.31999	44.14249	818	Vareš (Metalska ul. 20)	2009	Rural, Urban
T-09/2 (0-5)	Topsoil	18.32135	44.14179	775	Vareš (Metalska ul. 20)	2009	Industrial, Urban
T-10 (0-5)	Topsoil	18.31888	44.13898	773	Vareš - Majdan (N)	2009	Industrial, Urban
T-11/1 (0-5)	Topsoil	18.28798	44.14440	1371	Mijakovačke p.	2011	Rural
T-11/2 (0-5)	Topsoil	18.30092	44.14040	1279	Perun	2009	Natural
T-11/3 (0-5)	Topsoil	18.31177	44.13955	897	Vareš - Majdan (W)	2009	Rural
T-11/4 (0-5)	Topsoil	18.31724	44.13457	764	Vareš - Majdan	2009	Urban
T-11/5 (0-5)	Topsoil	18.31942	44.13356	828	Vareš - Majdan	2009	Rural, Urban
T-11/6 (0-5)	Topsoil	18.32717	44.13570	1054	Gar	2009	Rural
T-11/7 (0-5)	Topsoil	18.34157	44.13719	1093	Tisovci	2011	Rural
T-12/1 (0-5)	Topsoil	18.30517	44.13248	1022	Bor	2009	Rural
T-12/2 (0-5)	Topsoil	18.31143	44.13039	762	Prnjavor	2009	Rural
T-12/3 (0-5)	Topsoil	18.32115	44.12805	915	Stupni Do (W)	2009	Rural
T-12/4 (0-5)	Topsoil	18.32880	44.12411	988	Stupni Do (E)	2009	Rural
T-13/1 (0-5)	Topsoil	18.29201	44.12645	1397	Karasanovina	2011	Rural
T-13/2 (0-5)	Topsoil	18.30779	44.12130	745	Podjavor	2009	Rural, Natural
T-14/1 (0-5)	Topsoil	18.28798	44.11356	1076	Planinica	2011	Rural
T-14/2 (0-5)	Topsoil	18.30451	44.11160	685	Pajtov Han (N)	2009	Rural
T-14/3 (0-5)	Topsoil	18.32087	44.11352	1133	Mir	2011	Rural
T-15/1 (0-5)	Topsoil	18.29677	44.10476	881	Samari	2009	Rural
T-15/2 (0-5)	Topsoil	18.30786	44.10106	670	Pajtov Han (S)	2009	Rural
T-16/1 (0-5)	Topsoil	18.29735	44.09565	1008	Striježevo	2009	Rural
T-16/2 (0-5)	Topsoil	18.31305	44.09192	643	Pajtov Han (S)	2009	Rural
T-16/3 (0-5)	Topsoil	18.32926	44.09122	953	Budoželje	2009	Rural
T-16/4 (0-5)	Topsoil	18.34011	44.08596	1027	Budoželje	2011	Rural
T-17/1 (0-5)	Topsoil	18.28258	44.08318	971	Brda (N)	2011	Rural
T-17/2 (0-5)	Topsoil	18.29619	44.08648	616	Strana (Stavnja)	2011	Natural
T-17/3 (0-5)	Topsoil	18.31411	44.07640	1237	Budoželjska pl.	2011	Rural
T-18/1 (0-5)	Topsoil	18.27547	44.07554	961	Brda	2011	Rural
T-18/2 (0-5)	Topsoil	18.28299	44.07091	951	Brdo	2009	Rural
T-18/4 (0-5)	Topsoil	18.29233	44.06811	606	Dabravine (Hodžići)	2009	Rural

Sample	Material	Lon (WGS84)	Lat (WGS84)	Altitude (M)	Location	Year	Area
T-18/5 (0-5)	Topsoil	18.30074	44.06185	835	Pomenići	2009	Rural
T-19/1 (0-5)	Topsoil	18.27473	44.05472	826	Vardište	2011	Rural
T-19/2 (0-5)	Topsoil	18.28384	44.05032	784	Vardište	2009	Rural
T-19/3 (0-5)	Topsoil	18.29407	44.05836	561	Dabravine (S)	2009	Rural
T-19/5 (0-5)	Topsoil	18.30984	44.04647	778	Neprivaj (W)	2011	Rural
T-19/6 (0-5)	Topsoil	18.32335	44.04423	1013	Neprivaj	2011	Rural
T-20/1 (0-5)	Topsoil	18.26042	44.04782	751	Koščane	2011	Rural
T-20/2 (0-5)	Topsoil	18.28132	44.04256	532	Nedići	2011	Natural
T-20/3 (0-5)	Topsoil	18.29357	44.04096	819	Trtorići	2009	Rural
T-20/4 (0-5)	Topsoil	18.31823	44.03175	1042	Slivno	2011	Rural
T-21/1 (0-5)	Topsoil	18.24629	44.03797	683	G. Breza	2011	Rural
T-21/2 (0-5)	Topsoil	18.26147	44.03843	706	Smrekovica	2011	Rural
T-21/3 (0-5)	Topsoil	18.26994	44.03438	615	Sutješčica	2011	Rural
T-21/5 (0-5)	Topsoil	18.27682	44.03284	547	Vrankamen	2009	Rural
T-21/6 (0-5)	Topsoil	18.27626	44.02665	560	Vrankamen	2011	Rural
T-21/7 (0-5)	Topsoil	18.29038	44.02768	905	Orpeč (Vrh)	2011	Rural
T-21/8 (0-5)	Topsoil	18.30220	44.02374	1015	Seoce - Crni vrh	2011	Rural
T-22/1 (0-5)	Topsoil	18.23617	44.02686	638	Breza (Blaca)	2011	Rural
T-22/2 (0-5)	Topsoil	18.25130	44.02111	531	Breza (Založje)	2011	Rural
T-22/3 (0-5)	Topsoil	18.25689	44.02663	550	Smrekovica	2011	Rural
T-22/4 (0-5)	Topsoil	18.26201	44.02109	498	Breza (Centre)	2009	Urban
T-22/6 (0-5)	Topsoil	18.26666	44.01967	506	Breza (N)	2009	Rural, Urban
T-22/7 (0-5)	Topsoil	18.27551	44.01486	570	Borak	2011	Rural
T-22/8 (0-5)	Topsoil	18.29823	44.00829	886	Vlahinje	2011	Rural
T-24/1 (0-5)	Topsoil	18.24690	44.00634	681	Mahala	2011	Rural
T-24/2 (0-5)	Topsoil	18.25536	44.00853	479	Breza (S)	2009	Rural, Urban
T-24/4 (0-5)	Topsoil	18.26347	44.00303	475	Potkraj	2009	Rural
T-24/5 (0-5)	Topsoil	18.27389	44.00046	499	Izbod	2011	Rural
T-24/6 (0-5)	Topsoil	18.28502	43.99454	545	Erići	2011	Rural
T-25/1 (0-5)	Topsoil	18.25426	43.99714	465	Potkraj - Breza	2011	Rural
T-26/1 (0-5)	Topsoil	18.24848	43.99411	506	Potkraj	2011	Rural
T-26/2 (0-5)	Topsoil	18.25208	43.98983	458	Župča - Vrbovik	2009	Rural
T-26/4 (0-5)	Topsoil	18.25864	43.98814	456	Podžupča	2009	Rural
T-26/5 (0-5)	Topsoil	18.27329	43.98649	523	Župča	2011	Rural
T-27/1 (0-5)	Topsoil	18.24419	43.97834	454	Ilijaš (Lješevo)	2011	Rural
T-27/2 (0-5)	Topsoil	18.24719	43.98194	442	Vrbovik	2011	Rural
T-27/4 (0-5)	Topsoil	18.25092	43.97617	447	Podlugovi	2011	Rural
T-27/5 (0-5)	Topsoil	18.25938	43.97715	502	Sovrle	2011	Rural
A-15/3 (0-5)	Topsoil	18.30897	44.10086	651	Pajtov Han (S)	2009	Rural
A-18/3 (0-5)	Topsoil	18.29099	44.07187	583	Dabravine (Hodžići)	2009	Rural
A-19/4 (0-5)	Topsoil	18.29542	44.05754	561	Dabravine	2009	Rural
A-21/4 (0-5)	Topsoil	18.27481	44.03284	519	Vrankamen	2009	Rural
A-22/5 (0-5)	Topsoil	18.26500	44.01756	483	Breza (N)	2009	Rural, Urban
A-23 (0-5)	Topsoil	18.25985	44.01109	478	Breza	2009	Urban
A-24/3 (0-5)	Topsoil	18.25940	44.00333	472	Potkraj	2009	Rural, Urban
A-25/2 (0-5)	Topsoil	18.25858	43.99419	460	Podžupča	2009	Rural
A-26/3 (0-5)	Topsoil	18.25400	43.98813	454	Župča	2009	Rural, Urban
A-27/3 (0-5)	Topsoil	18.24524	43.97780	442	Podlugovi	2011	Rural
T-01/1 (20-30)	Subsoil	18.33095	44.19802	1113	Sjenokos	2011	Rural
T-01/2 (20-30)	Subsoil	18.34598	44.19091	1071	Strijica	2009	Rural
T-01/3 (20-30)	Subsoil	18.36298	44.19426	1089	Zarađe	2009	Rural
T-02/1 (20-30)	Subsoil	18.33179	44.18713	1164	Sjenokos	2009	Rural
T-02/2 (20-30)	Subsoil	18.34180	44.18490	966	Stavnja (Zg. tok)	2009	Rural
T-02/3 (20-30)	Subsoil	18.34947	44.18246	1066	Javornik	2009	Rural
T-03/1 (20-30)	Subsoil	18.32086	44.17997	1159	Pobrin Han	2009	Rural
T-03/2 (20-30)	Subsoil	18.33692	44.17857	922	Vareš (Stijenje)	2009	Rural
T-03/3 (20-30)	Subsoil	18.34059	44.17388	1024	Zabrezje	2009	Rural
T-04/1 (20-30)	Subsoil	18.31483	44.17303	1094	Vijenac	2011	Natural
T-04/2 (20-30)	Subsoil	18.32878	44.17165	999	Vijenac (Veleski p.)	2009	Rural
T-04/3 (20-30)	Subsoil	18.33492	44.16992	887	Lijepovići	2009	Rural, Urban
T-04/4 (20-30)	Subsoil	18.34399	44.16522	1162	Kapetanovići	2011	Rural
T-05/1 (20-30)	Subsoil	18.32991	44.16509	842	Vareš - Benići	2009	Urban
T-05/2 (20-30)	Subsoil	18.33116	44.16303	911	Vareš (Terzijino B.)	2009	Rural
T-06/1 (20-30)	Subsoil	18.28727	44.17289	1173	Semizova Ponikva	2011	Rural
T-06/2 (20-30)	Subsoil	18.30338	44.16807	1120	Stijene	2011	Rural
T-06/3 (20-30)	Subsoil	18.31928	44.16528	1066	Vareš (W)	2009	Rural

Sample	Material	Lon (WGS84)	Lat (WGS84)	Altitude (M)	Location	Year	Area
T-06/4 (20-30)	Subsoil	18.32474	44.16431	947	Vareš	2009	Rural
T-06/5 (20-30)	Subsoil	18.32598	44.16129	829	Vareš (Put mira 29)	2009	Urban
T-06/6 (20-30)	Subsoil	18.32784	44.15806	902	Vareš	2009	Rural
T-06/7 (20-30)	Subsoil	18.33854	44.15448	1122	Diknići	2009	Rural
T-06/8 (20-30)	Subsoil	18.35758	44.15484	1186	Borak	2011	Rural
T-07/1 (20-30)	Subsoil	18.27961	44.15481	1366	Goruške p.	2011	Rural
T-07/2 (20-30)	Subsoil	18.29245	44.16082	1161	Kicelj	2011	Rural
T-07/3 (20-30)	Subsoil	18.30939	44.15604	922	Papale	2011	Rural
T-07/4 (20-30)	Subsoil	18.32313	44.15421	804	Vareš (C.R.)	2009	Industrial, Urban
T-08/1 (20-30)	Subsoil	18.31699	44.14698	903	G. Rajčevac	2009	Rural
T-08/2 (20-30)	Subsoil	18.32065	44.14754	827	D. Rajčevac	2009	Rural, Urban
T-08/3 (20-30)	Subsoil	18.32258	44.14704	788	Vareš - Majdan (N)	2009	Industrial, Urban
T-08/4 (20-30)	Subsoil	18.33168	44.14604	1024	Mlakve	2009	Rural
T-08/5 (20-30)	Subsoil	18.34286	44.14466	1109	Brezik	2009	Rural
T-09/1 (20-30)	Subsoil	18.31999	44.14249	818	Vareš (Metalska ul. 20)	2009	Rural, Urban
T-09/2 (20-30)	Subsoil	18.32135	44.14179	775	Vareš (Metalska ul. 20)	2009	Industrial, Urban
T-10 (20-30)	Subsoil	18.31888	44.13898	773	Vareš - Majdan (N)	2009	Industrial, Urban
T-11/1 (20-30)	Subsoil	18.28798	44.14440	1371	Mijakovačke p.	2011	Rural
T-11/2 (20-30)	Subsoil	18.30092	44.14040	1279	Perun	2009	Natural
T-11/3 (20-30)	Subsoil	18.31177	44.13955	897	Vareš - Majdan (W)	2009	Rural
T-11/4 (20-30)	Subsoil	18.31724	44.13457	764	Vareš - Majdan	2009	Urban
T-11/5 (20-30)	Subsoil	18.31942	44.13356	828	Vareš - Majdan	2009	Rural, Urban
T-11/6 (20-30)	Subsoil	18.32717	44.13570	1054	Gar	2009	Rural
T-11/7 (20-30)	Subsoil	18.34157	44.13719	1093	Tisovci	2011	Rural
T-12/1 (20-30)	Subsoil	18.30517	44.13248	1022	Bor	2009	Rural
T-12/2 (20-30)	Subsoil	18.31143	44.13039	762	Prnjavor	2009	Rural
T-12/3 (20-30)	Subsoil	18.32115	44.12805	915	Stupni Do (W)	2009	Rural
T-12/4 (20-30)	Subsoil	18.32880	44.12411	988	Stupni Do (E)	2009	Rural
T-13/1 (20-30)	Subsoil	18.29201	44.12645	1397	Karasanovina	2011	Rural
T-13/2 (20-30)	Subsoil	18.30779	44.12130	745	Podjavor	2009	Rural, Natural
T-14/1 (20-30)	Subsoil	18.28798	44.11356	1076	Planinica	2011	Rural
T-14/2 (20-30)	Subsoil	18.30451	44.11160	685	Pajtov Han (N)	2009	Rural
T-14/3 (20-30)	Subsoil	18.32087	44.11352	1133	Mir	2011	Rural
T-15/1 (20-30)	Subsoil	18.29677	44.10476	881	Samari	2009	Rural
T-15/2 (20-30)	Subsoil	18.30786	44.10106	670	Pajtov Han (S)	2009	Rural
T-16/1 (20-30)	Subsoil	18.29735	44.09565	1008	Striježevo	2009	Rural
T-16/2 (20-30)	Subsoil	18.31305	44.09192	643	Pajtov Han (S)	2009	Rural
T-16/3 (20-30)	Subsoil	18.32926	44.09122	953	Budoželje	2009	Rural
T-16/4 (20-30)	Subsoil	18.34011	44.08596	1027	Budoželje	2011	Rural
T-17/1 (20-30)	Subsoil	18.28258	44.08318	971	Brda (N)	2011	Rural
T-17/2 (20-30)	Subsoil	18.29619	44.08648	616	Strana (Stavnja)	2011	Natural
T-17/3 (20-30)	Subsoil	18.31411	44.07640	1237	Budoželjska pl.	2011	Rural
T-18/1 (20-30)	Subsoil	18.27547	44.07554	961	Brda	2011	Rural
T-18/2 (20-30)	Subsoil	18.28299	44.07091	951	Brdo	2009	Rural
T-18/4 (20-30)	Subsoil	18.29233	44.06811	606	Dabravine (Hodžići)	2009	Rural
T-18/5 (20-30)	Subsoil	18.30074	44.06185	835	Pomenići	2009	Rural
T-19/1 (20-30)	Subsoil	18.27473	44.05472	826	Vardište	2011	Rural
T-19/2 (20-30)	Subsoil	18.28384	44.05032	784	Vardište	2009	Rural
T-19/3 (20-30)	Subsoil	18.29407	44.05836	561	Dabravine (S)	2009	Rural
T-19/5 (20-30)	Subsoil	18.30984	44.04647	778	Neprivaj (W)	2011	Rural
T-19/6 (20-30)	Subsoil	18.32335	44.04423	1013	Neprivaj	2011	Rural
T-20/1 (20-30)	Subsoil	18.26042	44.04782	751	Koščane	2011	Rural
T-20/2 (20-30)	Subsoil	18.28132	44.04256	532	Nedići	2011	Natural
T-20/3 (20-30)	Subsoil	18.29357	44.04096	819	Trtorići	2009	Rural
T-20/4 (20-30)	Subsoil	18.31823	44.03175	1042	Slivno	2011	Rural
T-21/1 (20-30)	Subsoil	18.24629	44.03797	683	G. Breza	2011	Rural
T-21/2 (20-30)	Subsoil	18.26147	44.03843	706	Smrekovica	2011	Rural
T-21/3 (20-30)	Subsoil	18.26994	44.03438	615	Sutješčica	2011	Rural
T-21/5 (20-30)	Subsoil	18.27682	44.03284	547	Vrankamen	2009	Rural
T-21/6 (20-30)	Subsoil	18.27626	44.02665	560	Vrankamen	2011	Rural
T-21/7 (20-30)	Subsoil	18.29038	44.02768	905	Orpeč (Vrh)	2011	Rural
T-21/8 (20-30)	Subsoil	18.30220	44.02374	1015	Seoce - Crni vrh	2011	Rural
T-22/1 (20-30)	Subsoil	18.23617	44.02686	638	Breza (Blaca)	2011	Rural
T-22/2 (20-30)	Subsoil	18.25130	44.02111	531	Breza (Založje)	2011	Rural
T-22/3 (20-30)	Subsoil	18.25689	44.02663	550	Smrekovica	2011	Rural
T-22/4 (20-30)	Subsoil	18.26201	44.02109	498	Breza (Centre)	2009	Urban

Sample	Material	Lon (WGS84)	Lat (WGS84)	Altitude (M)	Location	Year	Area
T-22/6 (20-30)	Subsoil	18.26666	44.01967	506	Breza (N)	2009	Rural, Urban
T-22/7 (20-30)	Subsoil	18.27551	44.01486	570	Borak	2011	Rural
T-22/8 (20-30)	Subsoil	18.29823	44.00829	886	Vlahinje	2011	Rural
T-24/1 (20-30)	Subsoil	18.24690	44.00634	681	Mahala	2011	Rural
T-24/2 (20-30)	Subsoil	18.25536	44.00853	479	Breza (S)	2009	Rural, Urban
T-24/4 (20-30)	Subsoil	18.26347	44.00303	475	Potkraj	2009	Rural
T-24/5 (20-30)	Subsoil	18.27389	44.00046	499	Izbod	2011	Rural
T-24/6 (20-30)	Subsoil	18.28502	43.99454	545	Erići	2011	Rural
T-25/1 (20-30)	Subsoil	18.25426	43.99714	465	Potkraj - Breza	2011	Rural
T-26/1 (20-30)	Subsoil	18.24848	43.99411	506	Potkraj	2011	Rural
T-26/2 (20-30)	Subsoil	18.25208	43.98983	458	Župča - Vrbovik	2009	Rural
T-26/4 (20-30)	Subsoil	18.25864	43.98814	456	Podžupča	2009	Rural
T-26/5 (20-30)	Subsoil	18.27329	43.98649	523	Župča	2011	Rural
T-27/1 (20-30)	Subsoil	18.24419	43.97834	454	Ilijaš (Lješevo)	2011	Rural
T-27/2 (20-30)	Subsoil	18.24719	43.98194	442	Vrbovik	2011	Rural
T-27/4 (20-30)	Subsoil	18.25092	43.97617	447	Podlugovi	2011	Rural
T-27/5 (20-30)	Subsoil	18.25938	43.97715	502	Sovrle	2011	Rural
A-15/3 (20-30)	Subsoil	18.30897	44.10086	651	Pajtov Han (S)	2009	Rural
A-18/3 (20-30)	Subsoil	18.29099	44.07187	583	Dabravine (Hodžići)	2009	Rural
A-19/4 (20-30)	Subsoil	18.29542	44.05754	561	Dabravine	2009	Rural
A-21/4 (20-30)	Subsoil	18.27481	44.03284	519	Vrankamen	2009	Rural
A-22/5 (20-30)	Subsoil	18.26500	44.01756	483	Breza (N)	2009	Rural, Urban
A-23 (20-30)	Subsoil	18.25985	44.01109	478	Breza	2009	Urban
A-24/3 (20-30)	Subsoil	18.25940	44.00333	472	Potkraj	2009	Rural, Urban
A-25/2 (20-30)	Subsoil	18.25858	43.99419	460	Podžupča	2009	Rural
A-26/3 (20-30)	Subsoil	18.25400	43.98813	454	Župča	2009	Rural, Urban
A-27/3 (20-30)	Subsoil	18.24524	43.97780	442	Podlugovi	2011	Rural
S-01	S. Sediment	18.36298	44.19426	1089	Zarude	2009	Rural
S-02	S. Sediment	18.34180	44.18490	966	Stavnje (Zg. tok)	2009	Rural
S-03	S. Sediment	18.33692	44.17857	922	Vareš (Stijenje)	2009	Rural
S-04	S. Sediment	18.33492	44.16992	887	Lijepovići	2009	Rural, Urban
S-06	S. Sediment	18.32598	44.16129	829	Vareš (Put mira 29)	2009	Urban
S-07	S. Sediment	18.32313	44.15421	804	Vareš (C.R.)	2009	Industrial, Urban
S-09	S. Sediment	18.32162	44.14407	785	Vareš - Majdan (N)	2009	Industrial, Urban
S-11	S. Sediment	18.31724	44.13457	764	Vareš - Majdan	2009	Urban
S-13	S. Sediment	18.30779	44.12130	745	Podjavor	2009	Rural
S-15	S. Sediment	18.30897	44.10086	651	Pajtov Han (S)	2009	Rural
S-17	S. Sediment	18.29564	44.08585	616	Stavnja - Strana	2009	Natural
S-18	S. Sediment	18.29099	44.07187	583	Dabravine (Hodžići)	2009	Rural
S-20	S. Sediment	18.28103	44.04347	537	Nedići	2009	Natural, Rural
S-22	S. Sediment	18.26761	44.02140	495	Breza	2009	Rural, Urban
S-23	S. Sediment	18.25985	44.01109	478	Breza	2009	Urban
S-26	S. Sediment	18.25400	43.98813	454	Župča	2009	Rural, Urban
S-27	S. Sediment	18.24524	43.97780	442	Podlugovi	2011	Rural
P-01/2	Attic dust	18.34598	44.19091	1071	Strijica	2009	Rural
P-02/1	Attic dust	18.33179	44.18713	1164	Sjenokos	2009	Rural
P-02/3	Attic dust	18.34947	44.18246	1066	Javornik	2009	Rural
P-05/1	Attic dust	18.32991	44.16509	842	Vareš - Benići	2009	Urban
P-06/5	Attic dust	18.32598	44.16129	829	Vareš (Put mira 29)	2009	Urban
P-08/4	Attic dust	18.33168	44.14604	1024	Mlakve	2009	Rural
P-09/2	Attic dust	18.32135	44.14179	775	Vareš (Metalska ul. 20)	2009	Industrial, Urban
P-10	Attic dust	18.31888	44.13898	773	Vareš - Majdan (N)	2009	Industrial, Urban
P-11/4	Attic dust	18.31724	44.13457	764	Vareš - Majdan	2009	Urban
P-15/2	Attic dust	18.30786	44.10106	670	Pajtov Han (S)	2009	Rural
P-16/1	Attic dust	18.28943	44.09500	952	Striježevo	2009	Rural
P-19/2	Attic dust	18.28407	44.05292	832	Vardište	2009	Rural
P-19/3	Attic dust	18.29407	44.05836	561	Dabravine (S)	2009	Rural
P-20/3	Attic dust	18.29357	44.04096	819	Trtorići	2009	Rural
P-22/4	Attic dust	18.26201	44.02109	498	Breza (Centre)	2009	Urban

Appendix B: Locations and basic properties of sampled materials (II)

Sample	Land use	Lithology	Pollution	Texture	Structure	Skeleton	Org.
T-01/1 (0-5)	Meadow	Series (JK)	Not visible	Clay loam	Granular	Non	Humic
T-01/2 (0-5)	Meadow	Clastites (JK)	Not visible	Sity clay loam	Granular	Non	Humic
T-01/3 (0-5)	Meadow	Clastites (JK)	Not visible	Sity clay loam	Granular	Non	Humic
T-02/1 (0-5)	Meadow	Clastites (JK)	Not visible	Sity clay loam	Granular	Roughly	Humic
T-02/2 (0-5)	Meadow	Clastites (JK)	Not visible	Sity clay loam	Granular	Non	Humic
T-02/3 (0-5)	Meadow	Clastites (JK)	Not visible	Clay loam	Granular	Non	Humic
T-03/1 (0-5)	Meadow	Carbonates (T)	Not visible	Sity clay loam	Granular	Non	Humic
T-03/2 (0-5)	Meadow	Carbonates (T)	Not visible	Sity clay loam	Granular	Non	Humic
T-03/3 (0-5)	Meadow	Carbonates (T)	Not visible	Sity clay loam	Granular	Non	Humic
T-04/1 (0-5)	Forest	Clastites (T)	Industry	Silty clay	Granular	Non	Organic
T-04/2 (0-5)	Meadow	Clastites (T)	Not visible	Sity clay loam	Granular	Non	Humic
T-04/3 (0-5)	Meadow	Clastites (T)	Households	Sity clay loam	Granular	Non	Humic
T-04/4 (0-5)	Meadow	Clastites (T)	Industry	Silty loam	Granular	Non	Humic
T-05/1 (0-5)	Garden	Carbonates (T)	Households	Loam	Granular	Mixed	Humic
T-05/2 (0-5)	Meadow	Carbonates (T)	Industry	Sandy clay loam	Granular	Non	Humic
T-06/1 (0-5)	Meadow	Carbonates (T)	Industry	Clay loam	Granular	Non	Humic
T-06/2 (0-5)	Meadow	Carbonates (T)	Not visible	Sity clay loam	Granular	Non	Humic
T-06/3 (0-5)	Meadow	Carbonates (T)	Not visible	Sity clay loam	Granular	Non	Humic
T-06/4 (0-5)	Meadow	Carbonates (T)	Not visible	Sandy clay loam	Granular	Non	Humic
T-06/5 (0-5)	Garden	Carbonates (T)	Industry	Sandy clay	Crumb	Mixed	Humic
T-06/6 (0-5)	Meadow	Carbonates (T)	Industry	Sity clay loam	Granular	Non	Humic
T-06/7 (0-5)	Meadow	Carbonates (T)	Not visible	Sity clay loam	Granular	Non	Humic
T-06/8 (0-5)	Meadow	Carbonates (T)	Not visible	Silty loam	Granular	Non	Humic
T-07/1 (0-5)	Meadow	Carbonates (T)	Not visible	Loam	Granular	Non	Humic
T-07/2 (0-5)	Meadow	Carbonates (T)	Not visible	Sity clay loam	Granular	Non	Humic
T-07/3 (0-5)	Meadow	Carbonates (T)	Industry	Silty loam	Granular	Non	Humic
T-07/4 (0-5)	Abandoned land	Series (JK)	Industry	Sandy clay loam	Granular	Mixed	Humic
T-08/1 (0-5)	Meadow	Carbonates (T)	Not visible	Silty clay	Crumb	Non	Humic
T-08/2 (0-5)	Meadow	Carbonates (T)	Industry	Silty clay	Crumb	Non	Humic
T-08/3 (0-5)	Abandoned land	Series (JK)	Industry	Clay loam	Granular	Mixed	Humic
T-08/4 (0-5)	Meadow	Series (JK)	Not visible	Sity clay loam	Granular	Non	Humic
T-08/5 (0-5)	Meadow	Series (JK)	Not visible	Sity clay loam	Granular	Non	Humic
T-09/1 (0-5)	Meadow	Series (JK)	Industry	Clay loam	Granular	Non	Humic
T-09/2 (0-5)	Garden	Series (JK)	Industry	Clay loam	Granular	Mixed	Humic
T-10 (0-5)	Garden	Series (JK)	Industry	Loam	Crumb	Mixed	Humic
T-11/1 (0-5)	Meadow	Clastites (JK)	Not visible	Loam	Granular	Non	Humic
T-11/2 (0-5)	Meadow	Series (JK)	Not visible	Clay loam	Granular	Non	Humic
T-11/3 (0-5)	Meadow	Series (JK)	Not visible	Clay loam	Granular	Non	Humic
T-11/4 (0-5)	Abandoned land	Series (JK)	Industry	Sandy clay	Granular	Mixed	Humic
T-11/5 (0-5)	Meadow	Series (JK)	Industry	Clay loam	Granular	Non	Humic
T-11/6 (0-5)	Meadow	Series (JK)	Not visible	Clay loam	Granular	Non	Humic
T-11/7 (0-5)	Meadow	Clastites (JK)	Industry	Silty loam	Granular	Non	Humic
T-12/1 (0-5)	Meadow	Series (JK)	Not visible	Clay loam	Granular	Non	Humic
T-12/2 (0-5)	Meadow	Flysch (K)	Not visible	Clay loam	Granular	Non	Humic
T-12/3 (0-5)	Meadow	Series (JK)	Not visible	Clay loam	Granular	Non	Humic
T-12/4 (0-5)	Meadow	Series (JK)	Not visible	Clay loam	Granular	Non	Humic
T-13/1 (0-5)	Meadow	Flysch (K)	Not visible	Clay loam	Granular	Non	Humic
T-13/2 (0-5)	Meadow	Flysch (K)	Not visible	Sity clay loam	Granular	Non	Humic
T-14/1 (0-5)	Meadow	Flysch (K)	Not visible	Loam	Granular	Non	Humic
T-14/2 (0-5)	Meadow	Flysch (K)	Not visible	Silty loam	Granular	Non	Humic
T-14/3 (0-5)	Meadow	Flysch (K)	Not visible	Clay loam	Granular	Non	Humic
T-15/1 (0-5)	Meadow	Flysch (K)	Not visible	Silty loam	Granular	Non	Humic
T-15/2 (0-5)	Meadow	Flysch (K)	Not visible	Silty loam	Granular	Non	Humic
T-16/1 (0-5)	Meadow	Flysch (K)	Not visible	Silty clay	Crumb	Non	Humic
T-16/2 (0-5)	Meadow	Flysch (K)	Not visible	Silty loam	Granular	Non	Humic
T-16/3 (0-5)	Meadow	Flysch (K)	Not visible	Silty loam	Granular	Non	Humic
T-16/4 (0-5)	Meadow	Clastite (Ol)	Not visible	Clay loam	Granular	Non	Humic
T-17/1 (0-5)	Meadow	Flysch (K)	Not visible	Sity clay loam	Granular	Non	Humic
T-17/2 (0-5)	Forest	Flysch (K)	Traffic	Silty clay	Granular	Non	Organic
T-17/3 (0-5)	Meadow	Flysch (K)	Not visible	Silty loam	Granular	Roughly	Humic
T-18/1 (0-5)	Meadow	Flysch (K)	Not visible	Clay loam	Granular	Non	Humic
T-18/2 (0-5)	Meadow	Flysch (K)	Not visible	Clay loam	Granular	Non	Humic
T-18/4 (0-5)	Meadow	Flysch (K)	Not visible	Sity clay loam	Granular	Non	Humic

Sample	Land use	Lithology	Pollution	Texture	Structure	Skeleton	Org.
T-18/5 (0-5)	Meadow	Flysch (K)	Not visible	Clay loam	Granular	Non	Humic
T-19/1 (0-5)	Meadow	Flysch (K)	Not visible	Sity clay loam	Granular	Non	Humic
T-19/2 (0-5)	Meadow	Flysch (K)	Not visible	Sity clay loam	Granular	Non	Humic
T-19/3 (0-5)	Meadow	Flysch (K)	Not visible	Sity clay loam	Granular	Non	Humic
T-19/5 (0-5)	Meadow	Flysch (K)	Not visible	Clay loam	Granular	Non	Humic
T-19/6 (0-5)	Meadow	Flysch (K)	Not visible	Sity clay loam	Granular	Non	Humic
T-20/1 (0-5)	Meadow	Clastite (Ol)	Not visible	Sity clay loam	Granular	Non	Humic
T-20/2 (0-5)	Forest	Flysch (K)	Not visible	Silty clay	Granular	Non	Organic
T-20/3 (0-5)	Meadow	Flysch (K)	Not visible	Clay loam	Granular	Non	Humic
T-20/4 (0-5)	Meadow	Clastite (Ol)	Not visible	Clay loam	Granular	Non	Humic
T-21/1 (0-5)	Meadow	Karbonates (M)	Not visible	Sity clay loam	Granular	Non	Humic
T-21/2 (0-5)	Meadow	Karbonates (M)	Not visible	Clay loam	Granular	Non	Humic
T-21/3 (0-5)	Meadow	Clastite (Ol)	Industry	Clay loam	Granular	Non	Humic
T-21/5 (0-5)	Meadow	Flysch (K)	Not visible	Clay loam	Granular	Non	Humic
T-21/6 (0-5)	Meadow	Clastite (Ol)	Industry	Clay loam	Granular	Non	Humic
T-21/7 (0-5)	Meadow	Flysch (K)	Not visible	Clay loam	Granular	Non	Humic
T-21/8 (0-5)	Meadow	Flysch (K)	Not visible	Clay loam	Granular	Non	Humic
T-22/1 (0-5)	Meadow	Clastites (M)	Industry	Sity clay loam	Granular	Non	Humic
T-22/2 (0-5)	Meadow	Clastites (M)	Industry	Sity clay loam	Granular	Non	Humic
T-22/3 (0-5)	Meadow	Karbonates (M)	Traffic	Sity clay loam	Granular	Non	Humic
T-22/4 (0-5)	Garden	Terraces (Q)	Traffic	Sity clay loam	Granular	Mixed	Humic
T-22/6 (0-5)	Meadow	Terraces (Q)	Traffic	Silty clay	Crumb	Non	Humic
T-22/7 (0-5)	Meadow	Clastites (M)	Not visible	Loam	Granular	Non	Humic
T-22/8 (0-5)	Meadow	Karbonates (M)	Not visible	Silty clay	Granular	Non	Humic
T-24/1 (0-5)	Meadow	Clastites (M)	Industry	Clay loam	Granular	Non	Humic
T-24/2 (0-5)	Meadow	Terraces (Q)	Agriculture	Clay loam	Granular	Non	Humic
T-24/4 (0-5)	Meadow	Terraces (Q)	Agriculture	Silty clay	Granular	Non	Humic
T-24/5 (0-5)	Meadow	Clastites (M)	Industry	Silty clay	Granular	Non	Humic
T-24/6 (0-5)	Meadow	Karbonates (M)	Agriculture	Silty loam	Granular	Non	Humic
T-25/1 (0-5)	Meadow	Terraces (Q)	Industry	Silty clay	Granular	Non	Humic
T-26/1 (0-5)	Meadow	Clastites (M)	Not visible	Loam	Granular	Non	Humic
T-26/2 (0-5)	Meadow	Terraces (Q)	Agriculture	Clay loam	Granular	Non	Humic
T-26/4 (0-5)	Meadow	Terraces (Q)	Agriculture	Clay loam	Granular	Non	Humic
T-26/5 (0-5)	Meadow	Clastites (M)	Not visible	Sity clay loam	Granular	Non	Humic
T-27/1 (0-5)	Meadow	Clastites (M)	Not visible	Sandy clay loam	Granular	Non	Humic
T-27/2 (0-5)	Meadow	Terraces (Q)	Not visible	Clay loam	Granular	Roughly	Humic
T-27/4 (0-5)	Meadow	Terraces (Q)	Not visible	Silty loam	Granular	Non	Humic
T-27/5 (0-5)	Meadow	Clastites (M)	Not visible	Clay loam	Granular	Non	Humic
A-15/3 (0-5)	Meadow	Alluvium (Q)	Not visible	Sandy loam	Structureless	Non	Humic
A-18/3 (0-5)	Meadow	Alluvium (Q)	Not visible	Sandy loam	Structureless	Non	Humic
A-19/4 (0-5)	Meadow	Alluvium (Q)	Not visible	Sandy loam	Structureless	Non	Humic
A-21/4 (0-5)	Meadow	Alluvium (Q)	Not visible	Sandy loam	Structureless	Non	Humic
A-22/5 (0-5)	Meadow	Alluvium (Q)	Agriculture	Sandy loam	Structureless	Non	Humic
A-23 (0-5)	Meadow	Alluvium (Q)	Households	Sandy loam	Structureless	Non	Humic
A-24/3 (0-5)	Meadow	Alluvium (Q)	Agriculture	Sandy loam	Granular	Non	Humic
A-25/2 (0-5)	Meadow	Alluvium (Q)	Agriculture	Sandy loam	Granular	Non	Humic
A-26/3 (0-5)	Meadow	Alluvium (Q)	Agriculture	Sandy loam	Granular	Non	Humic
A-27/3 (0-5)	Meadow	Alluvium (Q)	Industry	Sandy loam	Structureless	Non	Mineral
T-01/1 (20-30)	Meadow	Series (JK)	Not visible	Clay loam	Subangular	Non	Mineral
T-01/2 (20-30)	Meadow	Clastites (JK)	Not visible	Silty clay	Crumb	Non	Mineral
T-01/3 (20-30)	Meadow	Clastites (JK)	Not visible	Silty clay	Crumb	Non	Mineral
T-02/1 (20-30)	Meadow	Clastites (JK)	Not visible	Sity clay loam	Subangular	Roughly	Mineral
T-02/2 (20-30)	Meadow	Clastites (JK)	Not visible	Sity clay loam	Crumb	Rounded	Mineral
T-02/3 (20-30)	Meadow	Clastites (JK)	Not visible	Clay loam	Crumb	Rounded	Mineral
T-03/1 (20-30)	Meadow	Carbonates (T)	Not visible	Sity clay loam	Crumb	Non	Mineral
T-03/2 (20-30)	Meadow	Carbonates (T)	Not visible	Silty clay	Crumb	Roughly	Mineral
T-03/3 (20-30)	Meadow	Carbonates (T)	Not visible	Sity clay loam	Crumb	Non	Mineral
T-04/1 (20-30)	Forest	Clastites (T)	Industry	Silty clay	Subangular	Roughly	Mineral
T-04/2 (20-30)	Meadow	Clastites (T)	Not visible	Sity clay loam	Crumb	Non	Mineral
T-04/3 (20-30)	Meadow	Clastites (T)	Households	Sity clay loam	Subangular	Roughly	Mineral
T-04/4 (20-30)	Meadow	Clastites (T)	Industry	Silty loam	Subangular	Rounded	Mineral
T-05/1 (20-30)	Garden	Carbonates (T)	Households	Loam	Granular	Mixed	Humic
T-05/2 (20-30)	Meadow	Carbonates (T)	Industry	Sandy clay loam	Crumb	Non	Mineral
T-06/1 (20-30)	Meadow	Carbonates (T)	Industry	Clay loam	Crumb	Non	Mineral
T-06/2 (20-30)	Meadow	Carbonates (T)	Not visible	Sity clay loam	Crumb	Non	Mineral
T-06/3 (20-30)	Meadow	Carbonates (T)	Not visible	Sity clay loam	Crumb	Non	Mineral

Sample	Land use	Lithology	Pollution	Texture	Structure	Skeleton	Org.
T-06/4 (20-30)	Meadow	Carbonates (T)	Not visible	Sandy clay loam	Subangular	Non	Mineral
T-06/5 (20-30)	Garden	Carbonates (T)	Industry	Sandy clay	Crumb	Mixed	Humic
T-06/6 (20-30)	Meadow	Carbonates (T)	Industry	Sity clay loam	Subangular	Non	Mineral
T-06/7 (20-30)	Meadow	Carbonates (T)	Not visible	Sity clay loam	Crumb	Non	Mineral
T-06/8 (20-30)	Meadow	Carbonates (T)	Not visible	Silty loam	Crumb	Roughly	Mineral
T-07/1 (20-30)	Meadow	Carbonates (T)	Not visible	Loam	Crumb	Non	Mineral
T-07/2 (20-30)	Meadow	Carbonates (T)	Not visible	Sity clay loam	Subangular	Roughly	Mineral
T-07/3 (20-30)	Meadow	Carbonates (T)	Industry	Silty loam	Subangular	Non	Mineral
T-07/4 (20-30)	Abandoned land	Series (JK)	Industry	Sandy clay loam	Granular	Mixed	Humic
T-08/1 (20-30)	Meadow	Carbonates (T)	Not visible	Silty clay	Subangular	Roughly	Mineral
T-08/2 (20-30)	Meadow	Carbonates (T)	Industry	Silty clay	Subangular	Roughly	Mineral
T-08/3 (20-30)	Abandoned land	Series (JK)	Industry	Clay loam	Granular	Mixed	Humic
T-08/4 (20-30)	Meadow	Series (JK)	Not visible	Sity clay loam	Crumb	Non	Mineral
T-08/5 (20-30)	Meadow	Series (JK)	Not visible	Silty clay	Subangular	Non	Mineral
T-09/1 (20-30)	Meadow	Series (JK)	Industry	Clay loam	Subangular	Roughly	Mineral
T-09/2 (20-30)	Garden	Series (JK)	Industry	Clay loam	Granular	Mixed	Humic
T-10 (20-30)	Garden	Series (JK)	Industry	Loam	Crumb	Mixed	Humic
T-11/1 (20-30)	Meadow	Clastites (JK)	Not visible	Loam	Crumb	Non	Mineral
T-11/2 (20-30)	Meadow	Series (JK)	Not visible	Clay loam	Subangular	Non	Mineral
T-11/3 (20-30)	Meadow	Series (JK)	Not visible	Clay loam	Subangular	Non	Mineral
T-11/4 (20-30)	Abandoned land	Series (JK)	Industry	Sandy clay	Granular	Mixed	Humic
T-11/5 (20-30)	Meadow	Series (JK)	Industry	Clay loam	Subangular	Roughly	Mineral
T-11/6 (20-30)	Meadow	Series (JK)	Not visible	Clay loam	Crumb	Non	Mineral
T-11/7 (20-30)	Meadow	Clastites (JK)	Industry	Silty loam	Subangular	Roughly	Mineral
T-12/1 (20-30)	Meadow	Series (JK)	Not visible	Clay loam	Subangular	Roughly	Mineral
T-12/2 (20-30)	Meadow	Flysch (K)	Not visible	Clay loam	Subangular	Roughly	Mineral
T-12/3 (20-30)	Meadow	Series (JK)	Not visible	Clay loam	Crumb	Non	Mineral
T-12/4 (20-30)	Meadow	Series (JK)	Not visible	Clay loam	Subangular	Non	Mineral
T-13/1 (20-30)	Meadow	Flysch (K)	Not visible	Clay loam	Subangular	Non	Mineral
T-13/2 (20-30)	Meadow	Flysch (K)	Not visible	Sity clay loam	Subangular	Roughly	Mineral
T-14/1 (20-30)	Meadow	Flysch (K)	Not visible	Loam	Subangular	Non	Mineral
T-14/2 (20-30)	Meadow	Flysch (K)	Not visible	Silty loam	Subangular	Non	Mineral
T-14/3 (20-30)	Meadow	Flysch (K)	Not visible	Clay loam	Subangular	Roughly	Mineral
T-15/1 (20-30)	Meadow	Flysch (K)	Not visible	Silty loam	Subangular	Non	Mineral
T-15/2 (20-30)	Meadow	Flysch (K)	Not visible	Silty loam	Subangular	Non	Mineral
T-16/1 (20-30)	Meadow	Flysch (K)	Not visible	Silty clay	Subangular	Rounded	Mineral
T-16/2 (20-30)	Meadow	Flysch (K)	Not visible	Silty loam	Subangular	Roughly	Mineral
T-16/3 (20-30)	Meadow	Flysch (K)	Not visible	Silty loam	Subangular	Non	Mineral
T-16/4 (20-30)	Meadow	Clastite (Ol)	Not visible	Clay loam	Subangular	Non	Mineral
T-17/1 (20-30)	Meadow	Flysch (K)	Not visible	Sity clay loam	Subangular	Non	Mineral
T-17/2 (20-30)	Forest	Flysch (K)	Traffic	Silty clay	Crumb	Roughly	Mineral
T-17/3 (20-30)	Meadow	Flysch (K)	Not visible	Silty loam	Subangular	Roughly	Mineral
T-18/1 (20-30)	Meadow	Flysch (K)	Not visible	Clay loam	Subangular	Non	Mineral
T-18/2 (20-30)	Meadow	Flysch (K)	Not visible	Clay loam	Subangular	Non	Mineral
T-18/4 (20-30)	Meadow	Flysch (K)	Not visible	Sity clay loam	Subangular	Roughly	Mineral
T-18/5 (20-30)	Meadow	Flysch (K)	Not visible	Clay loam	Crumb	Roughly	Mineral
T-19/1 (20-30)	Meadow	Flysch (K)	Not visible	Sity clay loam	Crumb	Non	Mineral
T-19/2 (20-30)	Meadow	Flysch (K)	Not visible	Sity clay loam	Crumb	Non	Mineral
T-19/3 (20-30)	Meadow	Flysch (K)	Not visible	Sity clay loam	Subangular	Roughly	Mineral
T-19/5 (20-30)	Meadow	Flysch (K)	Not visible	Clay loam	Subangular	Non	Mineral
T-19/6 (20-30)	Meadow	Flysch (K)	Not visible	Sity clay loam	Subangular	Non	Mineral
T-20/1 (20-30)	Meadow	Clastite (Ol)	Not visible	Sity clay loam	Crumb	Non	Mineral
T-20/2 (20-30)	Forest	Flysch (K)	Not visible	Silty clay	Subangular	Roughly	Mineral
T-20/3 (20-30)	Meadow	Flysch (K)	Not visible	Clay loam	Subangular	Non	Mineral
T-20/4 (20-30)	Meadow	Clastite (Ol)	Not visible	Clay loam	Subangular	Non	Mineral
T-21/1 (20-30)	Meadow	Karbonates (M)	Not visible	Sity clay loam	Subangular	Non	Mineral
T-21/2 (20-30)	Meadow	Karbonates (M)	Not visible	Clay loam	Subangular	Non	Mineral
T-21/3 (20-30)	Meadow	Clastite (Ol)	Industry	Clay loam	Subangular	Non	Mineral
T-21/5 (20-30)	Meadow	Flysch (K)	Not visible	Clay loam	Crumb	Roughly	Mineral
T-21/6 (20-30)	Meadow	Clastite (Ol)	Industry	Clay loam	Subangular	Non	Mineral
T-21/7 (20-30)	Meadow	Flysch (K)	Not visible	Clay loam	Crumb	Non	Mineral
T-21/8 (20-30)	Meadow	Flysch (K)	Not visible	Clay loam	Subangular	Non	Mineral
T-22/1 (20-30)	Meadow	Clastites (M)	Industry	Sity clay loam	Crumb	Non	Mineral
T-22/2 (20-30)	Meadow	Clastites (M)	Industry	Sity clay loam	Crumb	Non	Mineral
T-22/3 (20-30)	Meadow	Karbonates (M)	Traffic	Sity clay loam	Crumb	Non	Mineral
T-22/4 (20-30)	Garden	Terraces (Q)	Traffic	Sity clay loam	Crumb	Mixed	Humic

Sample	Land use	Lithology	Pollution	Texture	Structure	Skeleton	Org.
T-22/6 (20-30)	Meadow	Terraces (Q)	Traffic	Silty clay	Subangular	Non	Mineral
T-22/7 (20-30)	Meadow	Clastites (M)	Not visible	Loam	Crumb	Non	Mineral
T-22/8 (20-30)	Meadow	Karbonates (M)	Not visible	Silty clay	Subangular	Non	Mineral
T-24/1 (20-30)	Meadow	Clastites (M)	Industry	Clay loam	Crumb	Non	Mineral
T-24/2 (20-30)	Meadow	Terraces (Q)	Agriculture	Clay loam	Subangular	Non	Mineral
T-24/4 (20-30)	Meadow	Terraces (Q)	Agriculture	Silty clay	Crumb	Non	Mineral
T-24/5 (20-30)	Meadow	Clastites (M)	Industry	Clay loam	Subangular	Non	Mineral
T-24/6 (20-30)	Meadow	Karbonates (M)	Agriculture	Silty loam	Subangular	Non	Mineral
T-25/1 (20-30)	Meadow	Terraces (Q)	Industry	Silty clay	Subangular	Non	Mineral
T-26/1 (20-30)	Meadow	Clastites (M)	Not visible	Loam	Subangular	Roughly	Mineral
T-26/2 (20-30)	Meadow	Terraces (Q)	Agriculture	Clay loam	Crumb	Non	Mineral
T-26/4 (20-30)	Meadow	Terraces (Q)	Agriculture	Clay loam	Crumb	Non	Mineral
T-26/5 (20-30)	Meadow	Clastites (M)	Not visible	Sity clay loam	Subangular	Non	Mineral
T-27/1 (20-30)	Meadow	Clastites (M)	Not visible	Sandy clay loam	Crumb	Non	Mineral
T-27/2 (20-30)	Meadow	Terraces (Q)	Not visible	Clay loam	Subangular	Roughly	Mineral
T-27/4 (20-30)	Meadow	Terraces (Q)	Not visible	Silty loam	Subangular	Non	Mineral
T-27/5 (20-30)	Meadow	Clastites (M)	Not visible	Clay loam	Subangular	Non	Mineral
A-15/3 (20-30)	Meadow	Alluvium (Q)	Not visible	Sandy loam	Structureless	Non	Mineral
A-18/3 (20-30)	Meadow	Alluvium (Q)	Not visible	Sandy loam	Structureless	Non	Mineral
A-19/4 (20-30)	Meadow	Alluvium (Q)	Not visible	Sandy loam	Structureless	Non	Mineral
A-21/4 (20-30)	Meadow	Alluvium (Q)	Not visible	Sandy loam	Structureless	Non	Mineral
A-22/5 (20-30)	Meadow	Alluvium (Q)	Agriculture	Sandy loam	Structureless	Non	Mineral
A-23 (20-30)	Meadow	Alluvium (Q)	Households	Sandy loam	Structureless	Non	Mineral
A-24/3 (20-30)	Meadow	Alluvium (Q)	Agriculture	Sandy loam	Crumb	Non	Mineral
A-25/2 (20-30)	Meadow	Alluvium (Q)	Agriculture	Sandy loam	Crumb	Non	Mineral
A-26/3 (20-30)	Meadow	Alluvium (Q)	Agriculture	Sandy loam	Crumb	Non	Mineral
A-27/3 (20-30)	Meadow	Alluvium (Q)	Industry	Sandy loam	Structureless	Non	Mineral
S-01	Meadow	Alluvium (Q)	Not visible	-	-	-	-
S-02	Meadow	Alluvium (Q)	Not visible	-	-	-	-
S-03	Meadow	Alluvium (Q)	Not visible	-	-	-	-
S-04	Meadow	Alluvium (Q)	Households	-	-	-	-
S-06	Garden	Alluvium (Q)	Industry	-	-	-	-
S-07	Abandoned land	Alluvium (Q)	Industry	-	-	-	-
S-09	Garden	Alluvium (Q)	Industry	-	-	-	-
S-11	Abandoned land	Alluvium (Q)	Industry	-	-	-	-
S-13	Meadow	Alluvium (Q)	Not visible	-	-	-	-
S-15	Meadow	Alluvium (Q)	Not visible	-	-	-	-
S-17	Forest	Alluvium (Q)	Not visible	-	-	-	-
S-18	Meadow	Alluvium (Q)	Not visible	-	-	-	-
S-20	Forest	Alluvium (Q)	Not visible	-	-	-	-
S-22	Meadow	Alluvium (Q)	Households	-	-	-	-
S-23	Meadow	Alluvium (Q)	Households	-	-	-	-
S-26	Meadow	Alluvium (Q)	Households	-	-	-	-
S-27	Meadow	Alluvium (Q)	Industry	-	-	-	-
P-01/2	-	Clastites (JK)	Not visible	-	-	-	-
P-02/1	-	Clastites (JK)	Not visible	-	-	-	-
P-02/3	-	Clastites (JK)	Not visible	-	-	-	-
P-05/1	-	Carbonates (T)	Households	-	-	-	-
P-06/5	-	Carbonates (T)	Industry	-	-	-	-
P-08/4	-	Series (JK)	Not visible	-	-	-	-
P-09/2	-	Series (JK)	Industry	-	-	-	-
P-10	-	Series (JK)	Industry	-	-	-	-
P-11/4	-	Series (JK)	Industry	-	-	-	-
P-15/2	-	Flysch (K)	Not visible	-	-	-	-
P-16/1	-	Flysch (K)	Not visible	-	-	-	-
P-19/2	-	Flysch (K)	Not visible	-	-	-	-
P-19/3	-	Flysch (K)	Not visible	-	-	-	-
P-20/3	-	Flysch (K)	Not visible	-	-	-	-
P-22/4	-	Alluvium (Q)	Traffic	-	-	-	-

Appendix C: Chemical analyses of collected sampling materials (I); Values of Al, Fe, Mg and Ti are in %, remaining elements in mg/kg

Sample	Material	Ag	Al	As	Ba	Bi	Cd	Co	Cr	Cu	Fe	Ga	Hg	La
T-01/1 (0-5)	Topsoil	0.1	2.31	4.4	158	0.3	0.6	15.1	69	33.2	2.70	6.0	0.08	7
T-01/2 (0-5)	Topsoil	0.1	2.15	5.4	236	0.6	0.9	14.6	68	31.7	2.65	6.0	0.09	6
T-01/3 (0-5)	Topsoil	0.1	1.86	11.1	156	0.3	0.5	16.5	36	25.0	2.86	5.0	0.09	6
T-02/1 (0-5)	Topsoil	<0.1	1.93	7.8	148	0.3	0.5	13.2	39	27.6	2.61	6.0	0.08	7
T-02/2 (0-5)	Topsoil	0.1	2.65	11.4	144	0.3	0.5	22.1	86	43.9	4.19	6.0	0.07	9
T-02/3 (0-5)	Topsoil	<0.1	1.64	11.7	157	0.4	0.4	12.2	28	21.5	2.54	5.0	0.08	2
T-03/1 (0-5)	Topsoil	0.2	1.08	7.3	139	0.3	0.5	9.9	26	13.2	1.55	4.0	0.08	5
T-03/2 (0-5)	Topsoil	0.3	1.40	13.8	138	0.3	0.5	20.6	32	14.3	1.99	4.0	0.08	11
T-03/3 (0-5)	Topsoil	<0.1	0.72	3.7	77	0.2	0.3	12.0	21	5.9	0.99	2.0	0.04	4
T-04/1 (0-5)	Topsoil	0.3	2.43	7.4	266	0.4	0.4	20.5	60	20.0	3.35	7.0	0.26	5
T-04/2 (0-5)	Topsoil	0.2	2.85	20.6	173	0.3	0.9	23.0	75	24.1	3.52	8.0	0.11	7
T-04/3 (0-5)	Topsoil	0.2	3.77	9.1	147	0.2	0.5	30.8	86	33.7	4.74	10.0	0.08	8
T-04/4 (0-5)	Topsoil	0.1	2.30	5.0	207	0.3	0.6	21.8	52	19.5	3.67	6.0	0.09	9
T-05/1 (0-5)	Topsoil	0.7	1.44	20.2	1315	0.5	0.8	12.7	38	54.8	3.44	4.0	0.19	10
T-05/2 (0-5)	Topsoil	0.4	1.02	19.0	526	0.4	0.4	8.4	13	21.4	2.45	3.0	0.10	9
T-06/1 (0-5)	Topsoil	<0.1	1.44	5.6	158	0.3	0.6	8.0	23	11.3	1.67	5.0	0.06	7
T-06/2 (0-5)	Topsoil	0.1	1.72	7.3	370	0.4	0.5	12.1	26	17.8	2.38	6.0	0.07	6
T-06/3 (0-5)	Topsoil	0.2	1.44	21.4	231	0.5	1.8	11.2	23	20.4	3.09	5.0	0.12	11
T-06/4 (0-5)	Topsoil	0.3	1.64	64.2	248	0.6	4.0	12.5	30	42.2	3.07	5.0	0.25	13
T-06/5 (0-5)	Topsoil	1.5	1.32	33.0	1088	0.5	0.9	15.7	66	87.7	4.95	5.0	0.34	12
T-06/6 (0-5)	Topsoil	0.4	2.09	12.1	300	0.7	0.3	12.2	27	25.8	2.85	6.0	0.17	24
T-06/7 (0-5)	Topsoil	<0.1	1.66	6.9	203	0.5	0.5	12.7	18	21.4	2.57	5.0	0.07	5
T-06/8 (0-5)	Topsoil	0.1	2.09	5.3	398	0.4	0.3	12.8	27	22.8	2.94	6.0	0.28	4
T-07/1 (0-5)	Topsoil	0.2	1.77	10.0	186	0.5	0.3	14.0	24	22.4	2.19	6.0	0.05	5
T-07/2 (0-5)	Topsoil	0.1	1.99	9.0	219	0.5	0.4	16.1	29	24.3	1.87	6.0	0.08	5
T-07/3 (0-5)	Topsoil	1.1	1.53	46.6	1197	0.6	2.1	15.0	26	34.1	3.45	5.0	0.17	10
T-07/4 (0-5)	Topsoil	7.1	1.57	64.1	1151	1.5	2.8	18.9	81	141.7	6.96	4.0	0.65	10
T-08/1 (0-5)	Topsoil	1.1	1.58	47.2	579	1.2	3.0	12.5	22	68.8	2.84	4.0	0.32	40
T-08/2 (0-5)	Topsoil	0.8	1.84	26.1	667	1.0	1.3	19.4	51	66.9	3.30	5.0	0.25	15
T-08/3 (0-5)	Topsoil	2.4	2.29	31.8	1280	2.6	2.7	20.1	156	153.5	6.39	6.0	0.76	11
T-08/4 (0-5)	Topsoil	0.1	2.60	8.7	196	0.3	0.4	43.6	267	51.2	3.77	7.0	0.09	13
T-08/5 (0-5)	Topsoil	<0.1	2.26	5.2	409	0.2	0.3	41.1	344	43.0	3.39	6.0	0.20	10
T-09/1 (0-5)	Topsoil	2.3	1.87	25.7	1084	2.7	2.2	38.4	191	118.1	5.49	5.0	0.41	11
T-09/2 (0-5)	Topsoil	2.5	1.57	33.1	1379	3.4	4.5	33.0	189	247.7	7.90	4.0	1.55	9
T-10 (0-5)	Topsoil	2.7	1.99	38.5	1475	3.0	3.5	28.7	159	210.5	6.14	6.0	1.59	12
T-11/1 (0-5)	Topsoil	0.1	1.64	8.1	96	0.2	0.4	47.3	229	34.5	3.45	4.0	0.08	8
T-11/2 (0-5)	Topsoil	0.1	2.23	8.1	104	0.3	0.8	34.6	169	53.3	3.14	6.0	0.08	12
T-11/3 (0-5)	Topsoil	0.2	2.64	52.0	149	0.5	2.5	35.0	165	60.1	4.22	7.0	0.10	15
T-11/4 (0-5)	Topsoil	2.4	1.65	46.0	1244	2.8	4.0	24.8	121	347.2	9.68	5.0	2.57	12
T-11/5 (0-5)	Topsoil	1.4	2.27	16.3	790	1.7	1.5	35.3	210	80.2	4.60	6.0	0.29	9
T-11/6 (0-5)	Topsoil	0.2	1.69	25.2	202	0.3	0.8	26.8	179	29.0	2.89	5.0	0.07	12
T-11/7 (0-5)	Topsoil	0.2	2.18	7.7	927	0.3	0.4	27.9	145	47.3	3.48	6.0	0.34	7
T-12/1 (0-5)	Topsoil	0.4	1.79	9.7	222	0.7	0.8	55.8	307	55.2	3.01	5.0	0.19	8
T-12/2 (0-5)	Topsoil	1.7	1.83	18.4	903	1.8	1.7	26.4	57	86.9	4.04	5.0	0.25	14
T-12/3 (0-5)	Topsoil	0.3	1.57	16.0	240	0.6	0.6	55.9	264	49.0	2.89	4.0	0.19	10
T-12/4 (0-5)	Topsoil	0.1	2.04	9.8	116	0.3	0.3	35.8	404	31.1	3.73	6.0	0.12	9
T-13/1 (0-5)	Topsoil	0.2	1.10	8.4	115	0.4	0.9	11.5	23	24.4	1.87	3.0	0.12	8
T-13/2 (0-5)	Topsoil	1.3	1.80	20.4	792	1.6	2.2	20.9	46	86.6	3.71	5.0	0.32	18
T-14/1 (0-5)	Topsoil	<0.1	1.19	3.8	67	0.3	0.3	11.8	38	35.4	2.29	3.0	0.08	10
T-14/2 (0-5)	Topsoil	0.4	1.39	11.2	271	0.8	0.6	20.3	33	67.2	3.51	4.0	0.18	13
T-14/3 (0-5)	Topsoil	<0.1	1.69	19.3	124	0.4	0.8	21.4	35	42.4	2.81	4.0	0.08	18
T-15/1 (0-5)	Topsoil	0.2	1.59	12.0	130	0.5	0.3	18.2	31	33.8	3.35	5.0	0.11	5
T-15/2 (0-5)	Topsoil	0.2	1.59	77.3	158	0.4	0.6	24.1	41	33.9	3.17	5.0	0.14	14
T-16/1 (0-5)	Topsoil	0.1	1.71	30.1	139	0.5	0.9	20.8	59	67.6	3.10	6.0	0.11	20
T-16/2 (0-5)	Topsoil	0.2	2.48	80.3	219	0.5	1.0	17.3	51	35.9	3.04	6.0	0.09	24
T-16/3 (0-5)	Topsoil	<0.1	1.46	61.1	108	0.3	0.5	29.4	78	39.8	3.05	4.0	0.05	15
T-16/4 (0-5)	Topsoil	0.2	1.62	36.8	89	0.3	0.9	25.3	69	33.3	2.10	5.0	0.13	6
T-17/1 (0-5)	Topsoil	0.1	1.62	37.9	100	0.4	0.4	25.3	69	42.7	3.19	5.0	0.06	21
T-17/2 (0-5)	Topsoil	0.3	1.52	46.2	153	0.5	0.6	18.9	43	44.2	2.58	5.0	0.27	17
T-17/3 (0-5)	Topsoil	<0.1	1.60	46.4	104	0.3	0.8	18.7	50	45.4	2.69	5.0	0.09	19
T-18/1 (0-5)	Topsoil	0.1	1.22	49.1	106	0.4	0.3	18.9	71	41.6	2.85	5.0	0.05	17
T-18/2 (0-5)	Topsoil	<0.1	1.27	480.7	102	0.4	0.7	24.1	66	52.7	3.99	5.0	0.05	14
T-18/4 (0-5)	Topsoil	0.1	0.70	83.8	123	0.4	0.4	16.1	37	45.4	2.83	3.0	0.10	8
T-18/5 (0-5)	Topsoil	<0.1	1.43	46.7	103	0.2	0.6	23.2	50	28.5	3.44	4.0	0.06	10

Sample	Material	Ag	Al	As	Ba	Bi	Cd	Co	Cr	Cu	Fe	Ga	Hg	La
T-19/1 (0-5)	Topsoil	0.1	1.43	505.4	146	0.4	0.6	31.8	83	68.4	3.28	5.0	0.08	15
T-19/2 (0-5)	Topsoil	<0.1	0.97	16.5	72	0.3	0.2	11.4	33	34.1	2.99	3.0	0.05	9
T-19/3 (0-5)	Topsoil	0.1	0.81	20.8	154	0.5	0.3	29.3	104	65.6	4.16	3.0	0.23	8
T-19/5 (0-5)	Topsoil	0.1	1.77	140.3	128	0.4	0.5	18.3	43	38.9	3.27	5.0	0.06	21
T-19/6 (0-5)	Topsoil	<0.1	0.88	32.5	65	0.3	0.2	18.5	38	32.9	3.15	3.0	0.09	8
T-20/1 (0-5)	Topsoil	<0.1	0.96	153.3	65	0.3	0.5	31.6	142	33.1	3.21	3.0	0.10	11
T-20/2 (0-5)	Topsoil	0.1	1.01	26.2	160	0.5	0.5	24.0	78	63.2	3.74	3.0	0.26	10
T-20/3 (0-5)	Topsoil	0.1	0.65	13.2	115	0.3	0.2	15.9	33	39.2	2.55	3.0	0.13	8
T-20/4 (0-5)	Topsoil	0.1	2.22	105.6	108	0.4	0.4	15.1	63	48.2	3.36	8.0	0.11	27
T-21/1 (0-5)	Topsoil	<0.1	1.17	44.2	72	0.2	0.4	18.4	79	26.4	2.15	4.0	0.08	7
T-21/2 (0-5)	Topsoil	<0.1	0.72	37.7	52	0.2	0.6	24.5	103	20.0	2.48	2.0	0.07	8
T-21/3 (0-5)	Topsoil	<0.1	0.98	22.4	92	0.3	0.5	20.6	127	28.6	2.62	4.0	0.09	10
T-21/5 (0-5)	Topsoil	0.1	1.21	31.6	165	0.4	0.6	18.7	52	55.5	3.32	4.0	0.13	12
T-21/6 (0-5)	Topsoil	<0.1	0.89	39.4	71	0.3	0.7	19.4	72	25.1	2.64	4.0	0.08	10
T-21/7 (0-5)	Topsoil	<0.1	0.77	52.4	70	0.2	0.3	20.9	51	45.8	2.47	3.0	0.08	9
T-21/8 (0-5)	Topsoil	<0.1	0.95	48.3	87	0.3	0.2	16.4	34	28.1	2.56	3.0	0.06	9
T-22/1 (0-5)	Topsoil	<0.1	1.14	34.3	112	0.4	0.3	22.3	39	28.8	3.13	4.0	0.21	15
T-22/2 (0-5)	Topsoil	<0.1	1.07	30.3	117	0.3	0.5	13.8	43	26.9	1.93	3.0	0.13	7
T-22/3 (0-5)	Topsoil	<0.1	1.04	40.2	126	0.4	0.4	18.5	69	33.3	2.64	4.0	0.11	13
T-22/4 (0-5)	Topsoil	0.2	1.17	18.9	579	0.4	0.6	20.2	92	48.6	2.83	4.0	0.26	12
T-22/6 (0-5)	Topsoil	<0.1	0.95	137.7	111	0.3	0.7	19.6	63	33.8	2.76	4.0	0.08	13
T-22/7 (0-5)	Topsoil	<0.1	1.03	13.8	67	0.3	0.5	24.2	106	33.1	2.54	4.0	0.32	11
T-22/8 (0-5)	Topsoil	<0.1	1.24	232.0	118	0.4	0.7	27.2	106	52.9	4.99	6.0	0.14	22
T-24/1 (0-5)	Topsoil	0.1	1.51	40.8	130	0.5	0.4	20.8	42	34.7	3.21	4.0	0.14	10
T-24/2 (0-5)	Topsoil	0.1	1.42	32.3	154	0.3	0.5	22.1	70	40.8	3.03	4.0	0.07	15
T-24/4 (0-5)	Topsoil	0.1	1.68	45.4	188	0.4	0.7	25.8	77	48.4	3.35	5.0	0.07	15
T-24/5 (0-5)	Topsoil	0.1	1.68	58.9	170	0.4	0.6	24.8	67	46.1	3.64	6.0	0.07	16
T-24/6 (0-5)	Topsoil	0.1	1.29	57.4	119	0.4	0.6	26.5	58	36.4	3.11	4.0	0.11	17
T-25/1 (0-5)	Topsoil	0.1	2.18	39.8	262	0.5	0.6	23.8	64	45.2	3.34	7.0	0.11	14
T-26/1 (0-5)	Topsoil	0.2	1.16	42.9	147	0.4	0.4	16.4	34	34.5	2.72	3.0	0.15	7
T-26/2 (0-5)	Topsoil	<0.1	1.66	45.1	279	0.4	0.5	21.6	53	39.1	3.35	5.0	0.10	18
T-26/4 (0-5)	Topsoil	0.1	1.62	43.9	212	0.4	0.7	20.1	60	39.7	2.92	5.0	0.09	16
T-26/5 (0-5)	Topsoil	0.1	1.30	28.4	166	0.3	0.4	16.4	46	33.7	2.30	4.0	0.08	7
T-27/1 (0-5)	Topsoil	0.1	1.38	35.4	135	0.4	0.4	16.4	37	34.2	2.86	4.0	0.15	9
T-27/2 (0-5)	Topsoil	0.3	1.30	38.6	306	0.4	0.6	20.2	78	40.3	3.17	4.0	0.15	11
T-27/4 (0-5)	Topsoil	0.1	1.57	33.0	211	0.4	0.5	18.0	44	33.5	3.00	4.0	0.13	17
T-27/5 (0-5)	Topsoil	<0.1	1.88	32.2	154	0.4	0.5	22.4	42	35.0	3.18	6.0	0.11	18
A-15/3 (0-5)	Topsoil	4.4	2.10	27.6	158	5.0	6.6	10.7	45	83.2	2.94	3.0	1.67	13
A-18/3 (0-5)	Topsoil	7.9	1.57	55.4	887	1.8	4.1	14.2	79	240.5	4.71	3.0	2.66	11
A-19/4 (0-5)	Topsoil	3.1	1.45	37.9	735	1.6	3.0	14.9	90	98.2	3.34	3.0	2.22	9
A-21/4 (0-5)	Topsoil	4.2	1.52	36.2	1068	1.3	3.1	15.3	83	102.8	3.86	3.0	1.10	11
A-22/5 (0-5)	Topsoil	2.3	1.29	38.3	835	0.8	1.2	16.5	80	89.0	3.67	3.0	0.99	9
A-23 (0-5)	Topsoil	3.4	1.28	41.9	1672	1.1	1.8	17.2	78	115.4	4.09	3.0	1.80	10
A-24/3 (0-5)	Topsoil	1.6	1.54	33.2	320	0.8	1.5	14.1	66	58.9	2.99	2.0	0.78	11
A-25/2 (0-5)	Topsoil	2.0	1.20	33.0	657	0.6	1.1	14.8	67	82.2	3.38	2.0	0.75	9
A-26/3 (0-5)	Topsoil	2.2	1.24	30.2	872	1.2	1.8	15.3	68	62.7	3.07	3.0	0.95	9
A-27/3 (0-5)	Topsoil	2.9	1.52	33.4	168	0.8	1.3	14.1	70	85.9	3.51	3.0	1.15	12
T-01/1 (20-30)	Subsoil	<0.1	3.15	5.4	96	0.2	0.2	22.8	90	37.2	4.02	8.0	0.09	10
T-01/2 (20-30)	Subsoil	<0.1	2.53	4.8	116	0.2	0.3	18.7	78	33.8	3.17	7.0	0.09	8
T-01/3 (20-30)	Subsoil	0.1	2.11	12.5	101	0.3	0.2	21.0	44	28.9	3.56	6.0	0.09	7
T-02/1 (20-30)	Subsoil	<0.1	2.29	7.5	115	0.3	0.2	15.0	46	31.9	2.82	6.0	0.08	7
T-02/2 (20-30)	Subsoil	<0.1	2.44	10.5	78	0.2	0.2	26.6	99	38.6	4.11	5.0	0.05	10
T-02/3 (20-30)	Subsoil	<0.1	2.14	13.3	111	0.4	0.2	14.4	38	25.4	3.19	6.0	0.06	3
T-03/1 (20-30)	Subsoil	<0.1	1.13	6.7	85	0.2	0.4	11.5	25	13.3	1.65	4.0	0.06	7
T-03/2 (20-30)	Subsoil	0.3	1.49	14.8	131	0.3	0.5	20.5	33	14.0	2.08	4.0	0.10	11
T-03/3 (20-30)	Subsoil	<0.1	0.69	4.0	71	0.1	0.3	11.9	21	5.3	0.98	2.0	0.06	4
T-04/1 (20-30)	Subsoil	<0.1	3.48	5.1	64	0.2	0.3	32.0	76	21.6	4.65	9.0	0.06	7
T-04/2 (20-30)	Subsoil	0.2	3.09	23.5	129	0.3	0.6	29.5	85	23.8	4.48	10.0	0.14	9
T-04/3 (20-30)	Subsoil	0.2	3.64	12.3	186	0.3	0.6	30.7	95	33.9	4.74	10.0	0.10	9
T-04/4 (20-30)	Subsoil	<0.1	3.14	5.7	148	0.2	0.4	26.6	65	20.4	4.40	8.0	0.07	13
T-05/1 (20-30)	Subsoil	0.6	1.54	19.0	1189	0.5	0.7	12.1	37	50.7	3.24	4.0	0.17	11
T-05/2 (20-30)	Subsoil	0.3	0.91	17.0	493	0.4	0.3	7.2	10	16.8	2.34	3.0	0.11	9
T-06/1 (20-30)	Subsoil	<0.1	1.78	6.8	99	0.3	0.2	10.8	28	9.4	2.15	6.0	0.05	12
T-06/2 (20-30)	Subsoil	0.1	1.93	7.7	144	0.4	0.3	13.8	29	16.5	2.72	7.0	0.06	9
T-06/3 (20-30)	Subsoil	0.1	2.11	29.2	101	0.4	0.5	15.0	31	24.5	3.29	6.0	0.16	17
T-06/4 (20-30)	Subsoil	0.1	2.21	88.5	168	0.5	1.8	16.8	36	56.3	3.20	5.0	0.34	26
T-06/5 (20-30)	Subsoil	1.5	1.39	33.5	852	0.6	0.9	15.4	65	86.5	5.01	5.0	0.31	13
T-06/6 (20-30)	Subsoil	0.4	2.35	12.5	239	0.6	0.3	13.9	29	25.2	3.05	7.0	0.13	26

Sample	Material	Ag	Al	As	Ba	Bi	Cd	Co	Cr	Cu	Fe	Ga	Hg	La
T-06/7 (20-30)	Subsoil	<0.1	1.83	8.1	136	0.5	0.4	15.1	22	24.9	3.00	6.0	0.06	6
T-06/8 (20-30)	Subsoil	<0.1	2.67	5.9	99	0.5	0.1	16.4	34	24.4	3.66	8.0	0.07	4
T-07/1 (20-30)	Subsoil	0.2	1.86	10.5	183	0.5	0.2	14.0	25	22.4	3.04	6.0	0.06	5
T-07/2 (20-30)	Subsoil	0.1	2.07	8.5	370	0.5	0.3	16.8	29	23.5	2.59	7.0	0.06	6
T-07/3 (20-30)	Subsoil	0.4	1.42	47.2	744	0.5	1.7	19.3	20	24.6	3.77	4.0	0.08	11
T-07/4 (20-30)	Subsoil	6.9	1.62	62.2	926	1.5	2.7	18.0	78	136.3	6.78	4.0	0.58	10
T-08/1 (20-30)	Subsoil	1.0	1.54	43.0	572	1.4	2.5	11.2	20	65.1	2.66	4.0	0.31	36
T-08/2 (20-30)	Subsoil	0.9	1.77	24.3	685	0.9	1.2	21.1	53	72.7	3.28	5.0	0.25	14
T-08/3 (20-30)	Subsoil	2.8	2.51	33.8	924	3.4	3.1	19.6	145	162.9	6.84	6.0	0.68	12
T-08/4 (20-30)	Subsoil	0.1	2.90	8.5	178	0.3	0.4	48.5	309	57.0	4.31	8.0	0.07	14
T-08/5 (20-30)	Subsoil	<0.1	2.55	5.2	140	0.2	0.2	43.8	344	43.9	3.64	8.0	0.23	10
T-09/1 (20-30)	Subsoil	2.5	1.88	29.2	1323	3.0	2.5	38.1	194	119.1	5.71	5.0	0.46	12
T-09/2 (20-30)	Subsoil	2.9	1.71	34.6	1005	4.3	5.2	32.3	182	266.8	8.35	4.0	1.43	10
T-10 (20-30)	Subsoil	3.7	2.12	41.3	1306	4.1	3.9	27.8	159	248.6	7.01	5.0	1.77	11
T-11/1 (20-30)	Subsoil	0.1	2.50	8.7	94	0.2	0.3	61.0	375	38.4	4.39	6.0	0.07	10
T-11/2 (20-30)	Subsoil	<0.1	2.82	7.6	63	0.2	0.2	42.6	198	63.1	3.78	8.0	0.07	16
T-11/3 (20-30)	Subsoil	0.2	2.88	49.1	154	0.5	2.6	37.3	172	62.4	4.47	8.0	0.12	16
T-11/4 (20-30)	Subsoil	2.6	1.79	49.7	797	3.4	4.5	24.5	113	356.7	9.97	5.0	2.36	13
T-11/5 (20-30)	Subsoil	1.1	2.37	14.4	598	1.3	1.0	35.3	220	67.6	4.40	7.0	0.23	10
T-11/6 (20-30)	Subsoil	0.1	2.14	29.8	149	0.3	0.5	33.8	214	33.0	3.54	6.0	0.08	14
T-11/7 (20-30)	Subsoil	0.1	2.68	7.3	179	0.3	0.2	35.2	179	57.5	4.07	7.0	0.11	8
T-12/1 (20-30)	Subsoil	0.2	1.92	9.0	156	0.5	0.5	49.9	285	62.1	3.49	6.0	0.14	9
T-12/2 (20-30)	Subsoil	1.4	1.95	16.3	786	1.8	1.5	26.1	53	78.5	3.69	5.0	0.23	15
T-12/3 (20-30)	Subsoil	0.3	1.84	18.9	186	0.5	0.4	64.2	274	56.0	3.14	5.0	0.10	12
T-12/4 (20-30)	Subsoil	<0.1	2.47	10.0	67	0.2	0.1	42.3	456	31.9	4.13	7.0	0.05	11
T-13/1 (20-30)	Subsoil	<0.1	1.51	11.0	77	0.3	0.1	20.9	35	29.8	3.12	5.0	0.10	14
T-13/2 (20-30)	Subsoil	1.4	1.92	19.8	743	1.4	2.0	21.2	46	78.5	3.51	5.0	0.25	19
T-14/1 (20-30)	Subsoil	<0.1	1.57	5.0	70	0.4	0.2	23.6	54	47.7	3.33	4.0	0.09	12
T-14/2 (20-30)	Subsoil	0.4	1.42	12.0	303	0.6	0.6	23.6	39	79.3	3.94	4.0	0.11	14
T-14/3 (20-30)	Subsoil	<0.1	2.00	21.2	118	0.4	0.6	27.1	43	46.0	3.14	6.0	0.06	19
T-15/1 (20-30)	Subsoil	0.1	1.66	12.2	102	0.4	0.2	20.5	31	33.1	3.51	5.0	0.09	6
T-15/2 (20-30)	Subsoil	0.2	1.57	90.4	156	0.5	0.6	23.7	41	32.0	3.19	5.0	0.11	15
T-16/1 (20-30)	Subsoil	0.1	2.10	36.9	151	0.5	1.0	25.7	73	82.9	3.84	6.0	0.10	24
T-16/2 (20-30)	Subsoil	0.1	2.24	79.2	207	0.5	0.8	16.9	49	35.5	2.84	6.0	0.11	23
T-16/3 (20-30)	Subsoil	<0.1	1.64	70.8	114	0.3	0.5	37.1	90	46.0	3.67	5.0	0.06	18
T-16/4 (20-30)	Subsoil	0.1	2.47	39.9	60	0.3	0.3	34.4	100	44.4	2.98	6.0	0.10	9
T-17/1 (20-30)	Subsoil	<0.1	1.77	40.3	94	0.4	0.3	27.3	83	43.2	3.80	5.0	0.13	23
T-17/2 (20-30)	Subsoil	0.2	2.20	48.4	139	0.5	0.5	21.1	60	48.7	3.18	6.0	0.13	22
T-17/3 (20-30)	Subsoil	<0.1	1.96	52.5	92	0.4	0.4	20.6	59	51.9	3.05	7.0	0.09	21
T-18/1 (20-30)	Subsoil	<0.1	1.38	56.9	103	0.4	0.2	24.6	80	44.2	3.43	6.0	0.09	19
T-18/2 (20-30)	Subsoil	<0.1	1.40	516.2	77	0.4	0.5	27.7	80	54.9	5.69	5.0	0.05	16
T-18/4 (20-30)	Subsoil	0.1	0.89	103.2	131	0.4	0.4	18.3	44	52.7	3.20	3.0	0.10	9
T-18/5 (20-30)	Subsoil	<0.1	1.52	49.0	97	0.2	0.5	26.8	57	29.5	3.59	4.0	0.06	12
T-19/1 (20-30)	Subsoil	<0.1	1.73	585.1	106	0.4	0.6	32.7	102	67.6	3.76	6.0	0.06	16
T-19/2 (20-30)	Subsoil	<0.1	1.12	19.3	76	0.4	0.2	20.8	36	34.8	3.71	4.0	0.07	10
T-19/3 (20-30)	Subsoil	<0.1	0.75	20.2	119	0.4	0.4	29.3	105	63.7	4.27	3.0	0.43	8
T-19/5 (20-30)	Subsoil	<0.1	2.28	183.1	133	0.4	0.6	22.2	53	42.4	4.21	6.0	0.04	25
T-19/6 (20-30)	Subsoil	<0.1	0.94	51.3	58	0.3	0.2	23.6	40	36.3	3.81	3.0	0.10	9
T-20/1 (20-30)	Subsoil	<0.1	0.91	169.4	66	0.3	0.4	32.4	130	34.3	3.24	3.0	0.08	11
T-20/2 (20-30)	Subsoil	0.1	1.07	26.5	136	0.4	0.4	24.0	82	60.6	3.79	4.0	0.18	10
T-20/3 (20-30)	Subsoil	<0.1	0.83	15.2	102	0.4	0.1	21.5	43	45.6	3.18	3.0	0.12	11
T-20/4 (20-30)	Subsoil	0.1	2.70	142.1	119	0.5	0.7	17.2	104	50.8	4.30	9.0	0.13	32
T-21/1 (20-30)	Subsoil	<0.1	1.40	42.1	75	0.2	0.4	25.7	107	25.0	2.56	4.0	0.09	10
T-21/2 (20-30)	Subsoil	<0.1	0.90	41.1	41	0.2	0.4	27.1	128	21.6	2.97	3.0	0.08	9
T-21/3 (20-30)	Subsoil	<0.1	0.92	24.1	96	0.2	0.6	24.3	123	32.4	2.79	4.0	0.08	10
T-21/5 (20-30)	Subsoil	0.1	1.38	32.7	153	0.4	0.5	19.3	58	62.6	3.30	5.0	0.09	12
T-21/6 (20-30)	Subsoil	<0.1	0.92	39.4	58	0.3	0.4	23.3	74	26.3	2.94	4.0	0.11	12
T-21/7 (20-30)	Subsoil	<0.1	1.02	87.6	62	0.3	0.2	32.8	86	71.0	3.36	4.0	0.12	10
T-21/8 (20-30)	Subsoil	<0.1	1.01	49.0	85	0.3	0.1	23.3	37	30.3	3.20	4.0	0.06	10
T-22/1 (20-30)	Subsoil	<0.1	1.32	40.9	121	0.4	0.3	27.7	48	29.9	3.76	4.0	0.24	21
T-22/2 (20-30)	Subsoil	<0.1	1.07	32.9	117	0.3	0.4	16.3	40	30.1	2.36	3.0	0.12	7
T-22/3 (20-30)	Subsoil	<0.1	0.98	48.0	136	0.3	0.5	23.6	75	38.3	3.38	3.0	0.12	14
T-22/4 (20-30)	Subsoil	0.2	1.16	19.3	652	0.3	0.7	23.2	94	44.6	3.05	4.0	0.21	11
T-22/6 (20-30)	Subsoil	0.1	1.03	161.1	126	0.3	0.9	25.2	76	41.4	3.29	4.0	0.08	15
T-22/7 (20-30)	Subsoil	<0.1	0.79	13.2	73	0.3	0.8	27.9	119	29.5	2.78	3.0	0.78	11
T-22/8 (20-30)	Subsoil	0.1	1.57	270.8	113	0.4	0.8	32.9	143	61.3	5.84	8.0	0.19	24
T-24/1 (20-30)	Subsoil	<0.1	1.46	40.5	121	0.4	0.3	21.2	42	31.5	3.25	4.0	0.15	10
T-24/2 (20-30)	Subsoil	0.1	1.47	32.8	155	0.3	0.5	22.3	71	43.3	3.14	5.0	0.07	16

Sample	Material	Ag	Al	As	Ba	Bi	Cd	Co	Cr	Cu	Fe	Ga	Hg	La
T-24/4 (20-30)	Subsoil	0.1	1.93	52.7	227	0.4	0.9	30.2	89	55.2	3.95	6.0	0.06	19
T-24/5 (20-30)	Subsoil	0.1	1.98	70.9	186	0.5	0.8	28.5	83	50.1	4.31	6.0	0.07	18
T-24/6 (20-30)	Subsoil	0.1	1.36	62.2	125	0.4	0.6	30.1	58	41.6	3.41	5.0	0.08	19
T-25/1 (20-30)	Subsoil	0.2	2.38	44.8	313	0.5	0.7	27.0	72	47.3	3.93	6.0	0.13	16
T-26/1 (20-30)	Subsoil	0.1	1.31	44.0	133	0.3	0.4	15.4	38	29.8	2.72	4.0	0.16	8
T-26/2 (20-30)	Subsoil	<0.1	1.92	51.4	185	0.4	0.6	22.4	59	40.4	3.76	5.0	0.12	20
T-26/4 (20-30)	Subsoil	0.1	1.70	45.1	216	0.4	0.7	23.1	67	46.3	3.38	5.0	0.13	19
T-26/5 (20-30)	Subsoil	<0.1	1.24	29.0	140	0.3	0.5	17.4	45	30.1	2.51	3.0	0.07	7
T-27/1 (20-30)	Subsoil	<0.1	1.16	34.5	111	0.4	0.4	15.3	28	29.8	2.72	3.0	0.15	8
T-27/2 (20-30)	Subsoil	0.3	1.41	40.1	307	0.3	0.5	18.9	85	36.2	3.13	4.0	0.17	11
T-27/4 (20-30)	Subsoil	0.1	2.06	39.2	207	0.5	0.6	23.0	56	40.4	3.58	6.0	0.11	21
T-27/5 (20-30)	Subsoil	0.1	1.70	35.8	168	0.4	0.4	25.1	39	32.9	3.33	5.0	0.09	19
A-15/3 (20-30)	Subsoil	5.9	2.12	29.8	214	6.1	7.2	11.9	51	101.8	3.01	3.0	2.19	13
A-18/3 (20-30)	Subsoil	11.0	1.76	59.1	369	2.7	4.5	11.7	68	273.7	5.93	2.0	2.42	10
A-19/4 (20-30)	Subsoil	3.3	1.84	35.4	440	2.5	4.1	14.2	75	100.9	3.44	3.0	1.20	11
A-21/4 (20-30)	Subsoil	4.3	1.65	41.0	507	1.6	3.4	15.5	75	95.8	3.94	3.0	0.89	12
A-22/5 (20-30)	Subsoil	1.7	1.30	37.7	766	0.8	1.3	16.0	74	65.1	3.54	3.0	0.54	9
A-23 (20-30)	Subsoil	5.3	1.39	49.3	1302	1.3	2.5	16.8	81	161.8	4.74	3.0	1.94	13
A-24/3 (20-30)	Subsoil	1.5	1.37	30.2	150	0.7	1.2	11.7	52	46.2	2.79	2.0	0.69	10
A-25/2 (20-30)	Subsoil	2.4	1.37	36.3	212	0.7	1.3	14.9	71	86.7	3.65	3.0	1.05	10
A-26/3 (20-30)	Subsoil	1.7	1.40	30.8	974	1.3	1.9	16.8	79	59.1	3.04	3.0	0.76	10
A-27/3 (20-30)	Subsoil	4.7	1.50	41.3	263	1.5	1.8	14.8	68	129.1	4.30	3.0	1.53	13
S-01	S. Sediment	0.2	1.63	9.6	207	0.3	0.5	15.8	69	68.0	3.22	5.0	0.14	12
S-02	S. Sediment	0.1	1.76	5.9	187	0.2	0.4	18.0	73	38.4	3.12	5.0	0.06	10
S-03	S. Sediment	<0.1	1.35	9.5	134	0.2	0.4	13.5	44	27.3	2.41	3.0	0.10	7
S-04	S. Sediment	0.2	1.21	8.8	165	0.2	0.6	12.1	41	28.5	2.28	3.0	0.07	7
S-06	S. Sediment	0.3	0.98	7.8	192	0.2	0.5	10.5	38	32.6	2.13	3.0	0.14	6
S-07	S. Sediment	0.7	1.02	12.8	438	0.2	0.7	12.1	48	37.1	2.38	3.0	0.22	6
S-09	S. Sediment	1.4	1.18	16.1	647	0.4	0.7	12.7	40	64.0	2.80	3.0	0.23	6
S-11	S. Sediment	3.6	1.20	23.3	823	0.5	1.0	13.2	48	120.1	3.70	3.0	0.42	6
S-13	S. Sediment	2.6	1.21	18.1	746	0.5	0.8	16.5	116	101.3	3.63	3.0	0.52	6
S-15	S. Sediment	0.8	1.12	16.3	583	0.4	0.7	13.1	76	53.4	2.98	3.0	0.34	7
S-17	S. Sediment	1.4	1.07	20.8	626	0.4	0.7	15.5	99	84.2	3.41	3.0	0.71	6
S-18	S. Sediment	1.4	1.05	17.8	827	0.4	0.7	13.8	85	81.6	3.40	3.0	0.75	6
S-20	S. Sediment	3.0	0.93	27.9	1063	0.7	1.0	13.9	83	111.3	4.46	3.0	1.28	6
S-22	S. Sediment	2.8	1.06	29.1	1271	0.8	1.6	14.0	75	101.7	3.84	3.0	1.54	6
S-23	S. Sediment	1.3	0.99	22.3	986	0.4	0.7	13.1	69	61.1	3.18	3.0	0.74	6
S-26	S. Sediment	1.1	0.83	24.6	322	0.3	0.6	12.7	63	52.2	3.42	3.0	0.44	6
S-27	S. Sediment	2.8	0.88	33.1	457	0.6	1.0	12.4	53	89.3	4.16	3.0	1.08	6
P-01/2	Attic Dust	1.0	0.98	17.9	18	1.0	1.8	6.5	43	60.5	2.20	3.0	1.69	6
P-02/1	Attic Dust	0.7	1.20	20.4	48	0.4	2.6	10.0	56	90.3	3.97	4.0	0.38	7
P-02/3	Attic Dust	0.7	1.05	15.9	54	0.6	2.7	8.2	38	174.8	2.26	3.0	0.70	5
P-05/1	Attic Dust	2.0	1.01	31.8	30	1.6	2.2	7.1	35	79.2	3.05	3.0	0.80	3
P-06/5	Attic Dust	2.5	1.11	56.7	19	2.0	3.4	10.2	56	145.8	3.54	3.0	2.71	5
P-08/4	Attic Dust	1.4	1.15	22.5	23	1.2	2.1	10.2	67	135.4	3.38	3.0	1.78	8
P-09/2	Attic Dust	5.2	1.10	81.8	39	8.8	6.5	26.8	102	350.6	14.14	4.0	3.46	9
P-10	Attic Dust	6.9	1.03	76.0	49	12.6	14.4	32.6	108	451.7	19.26	4.0	3.74	10
P-11/4	Attic Dust	7.4	1.29	92.9	69	10.1	7.6	27.8	126	261.2	15.63	5.0	1.50	9
P-15/2	Attic Dust	3.5	0.89	50.8	14	5.0	2.7	11.3	57	163.1	4.70	4.0	3.26	6
P-16/1	Attic Dust	1.6	1.01	32.8	19	1.5	1.4	9.2	55	104.1	3.79	3.0	2.12	7
P-19/2	Attic Dust	1.0	1.12	45.6	86	0.7	1.4	10.7	48	57.7	2.39	3.0	0.31	8
P-19/3	Attic Dust	1.1	0.91	52.5	26	1.1	2.8	9.0	70	88.8	3.24	3.0	1.90	5
P-20/3	Attic Dust	0.5	0.62	96.5	87	0.7	3.8	6.2	31	46.0	2.00	2.0	0.24	5
P-22/4	Attic Dust	0.6	0.95	80.8	24	0.8	3.6	10.9	57	84.1	2.92	3.0	0.63	5

Appendix D: Chemical analyses of collected sampling materials (II); Values of Al, Fe, Mg and Ti are in %, remaining elements in mg/kg

Sample	Material	Mg	Mn	Mo	Ni	Pb	Sb	Sc	Th	Ti	Tl	V	W	Zn
T-01/1 (0-5)	Topsoil	0.59	1284	0.3	41.8	44.7	0.5	2.5	0.4	0.033	0.2	59	<0.1	126
T-01/2 (0-5)	Topsoil	0.47	1626	0.5	52.0	86.4	1.2	2.4	0.6	0.012	0.2	51	0.1	230
T-01/3 (0-5)	Topsoil	0.35	1805	0.6	32.8	43.3	0.9	1.9	1.5	0.006	0.2	47	<0.1	107
T-02/1 (0-5)	Topsoil	0.48	1428	0.4	32.5	48.1	0.7	2.0	1.5	0.003	0.2	41	<0.1	123
T-02/2 (0-5)	Topsoil	0.60	1208	0.4	58.8	57.2	1.0	4.5	1.5	0.027	0.1	50	<0.1	116
T-02/3 (0-5)	Topsoil	0.41	1505	0.5	29.2	48.0	0.8	1.7	1.6	<0.001	0.1	25	<0.1	151
T-03/1 (0-5)	Topsoil	0.23	2731	0.4	33.5	87.9	2.4	0.7	0.5	0.003	0.2	20	<0.1	146
T-03/2 (0-5)	Topsoil	0.39	1029	0.4	30.1	160.9	2.5	1.8	2.4	0.005	0.3	25	0.1	174
T-03/3 (0-5)	Topsoil	0.29	204	0.4	20.7	65.6	1.0	0.7	1.0	0.003	0.1	14	<0.1	51
T-04/1 (0-5)	Topsoil	1.37	1129	0.3	68.9	80.0	1.4	5.5	0.9	0.141	0.2	70	0.1	193
T-04/2 (0-5)	Topsoil	1.33	1020	0.6	80.0	152.9	1.3	5.3	1.3	0.102	0.6	97	0.1	250
T-04/3 (0-5)	Topsoil	2.27	1250	0.4	132.0	230.3	1.4	9.4	1.8	0.227	0.1	126	0.1	344
T-04/4 (0-5)	Topsoil	1.29	1455	0.3	71.7	69.2	0.6	4.1	0.5	0.086	0.2	63	<0.1	131
T-05/1 (0-5)	Topsoil	0.92	3267	0.8	46.9	282.0	6.5	3.3	1.5	0.019	0.2	36	0.3	568
T-05/2 (0-5)	Topsoil	0.18	1651	0.4	12.3	108.7	1.1	1.8	2.1	0.004	0.2	25	0.1	193
T-06/1 (0-5)	Topsoil	0.49	1095	0.2	17.7	38.6	0.2	1.0	0.5	0.007	0.2	22	0.1	109
T-06/2 (0-5)	Topsoil	0.57	1151	0.3	25.5	44.3	0.7	2.4	2.0	0.005	0.2	24	0.1	120
T-06/3 (0-5)	Topsoil	0.35	1972	0.6	20.3	131.4	1.2	0.9	3.4	0.005	0.5	26	0.1	206
T-06/4 (0-5)	Topsoil	0.33	2765	0.6	53.9	234.2	2.8	1.7	3.5	0.004	0.6	31	0.1	339
T-06/5 (0-5)	Topsoil	0.77	2443	1.1	81.6	328.1	8.6	3.7	2.9	0.009	0.3	34	0.4	596
T-06/6 (0-5)	Topsoil	0.59	1119	0.6	25.9	148.9	2.6	2.0	3.7	0.001	0.3	26	0.1	243
T-06/7 (0-5)	Topsoil	0.54	1371	0.3	26.7	101.2	1.0	2.1	2.4	0.002	0.3	18	0.1	184
T-06/8 (0-5)	Topsoil	0.66	843	0.3	31.1	62.3	0.6	2.4	1.2	<0.001	0.2	23	0.1	155
T-07/1 (0-5)	Topsoil	0.61	1094	0.4	29.2	97.1	1.9	3.3	0.5	0.002	0.2	23	0.1	197
T-07/2 (0-5)	Topsoil	0.65	1207	0.3	33.2	50.0	1.1	3.7	0.5	0.003	0.2	26	0.1	131
T-07/3 (0-5)	Topsoil	0.38	3253	1.1	28.6	313.0	3.1	3.6	2.4	0.004	1.0	32	0.1	662
T-07/4 (0-5)	Topsoil	1.53	2741	4.3	114.1	596.8	16.4	4.6	3.0	0.010	0.7	47	0.7	887
T-08/1 (0-5)	Topsoil	0.50	3971	1.1	39.6	458.0	9.9	4.7	3.0	0.008	0.7	28	0.4	680
T-08/2 (0-5)	Topsoil	0.53	2322	0.8	73.6	315.8	8.1	4.0	2.7	0.003	0.5	37	0.3	516
T-08/3 (0-5)	Topsoil	1.33	4152	2.5	226.3	760.4	18.1	5.7	2.4	0.010	0.7	60	1.3	1490
T-08/4 (0-5)	Topsoil	2.08	2239	0.4	345.7	48.9	1.1	5.2	1.4	0.040	0.2	68	0.1	120
T-08/5 (0-5)	Topsoil	2.95	1787	0.3	394.4	31.6	1.3	2.2	1.4	0.050	0.1	54	0.1	99
T-09/1 (0-5)	Topsoil	1.04	2537	2.7	281.9	703.0	16.8	4.0	2.3	0.007	0.7	51	1.6	1208
T-09/2 (0-5)	Topsoil	1.21	4374	5.4	256.4	955.9	19.0	4.0	1.9	0.026	0.9	42	3.8	3075
T-10 (0-5)	Topsoil	1.10	3372	2.7	208.8	901.9	20.5	4.5	2.5	0.007	0.8	57	2.8	1663
T-11/1 (0-5)	Topsoil	0.35	1838	0.3	346.8	31.5	0.3	5.9	1.3	0.004	0.3	48	0.1	93
T-11/2 (0-5)	Topsoil	1.36	1840	0.5	241.5	44.0	0.9	4.6	1.5	0.003	0.2	59	<0.1	120
T-11/3 (0-5)	Topsoil	1.83	3116	0.7	245.4	250.3	4.9	8.3	3.0	0.003	1.3	66	0.1	491
T-11/4 (0-5)	Topsoil	0.63	3401	7.9	158.1	788.2	35.7	4.2	2.6	0.025	0.8	45	5.2	1845
T-11/5 (0-5)	Topsoil	1.47	1805	1.4	264.1	439.6	10.9	5.2	2.3	0.002	0.5	51	0.6	664
T-11/6 (0-5)	Topsoil	1.07	1213	0.4	182.7	63.1	1.4	3.6	2.2	0.002	0.4	41	0.1	141
T-11/7 (0-5)	Topsoil	1.25	1334	0.5	201.4	67.8	1.0	5.2	1.9	0.003	0.1	48	<0.1	128
T-12/1 (0-5)	Topsoil	3.84	2355	0.5	495.2	149.0	2.7	3.9	2.7	0.002	0.3	38	0.1	203
T-12/2 (0-5)	Topsoil	0.57	2602	0.8	109.4	505.4	11.3	4.6	3.4	0.003	0.5	37	0.6	669
T-12/3 (0-5)	Topsoil	0.41	1895	0.7	312.6	124.7	3.1	3.6	2.8	0.004	0.3	36	0.2	198
T-12/4 (0-5)	Topsoil	2.80	843	0.4	388.6	58.5	1.3	6.1	1.9	0.003	0.1	63	<0.1	115
T-13/1 (0-5)	Topsoil	0.17	1740	0.5	33.6	46.9	0.5	1.9	0.9	0.003	0.2	28	<0.1	114
T-13/2 (0-5)	Topsoil	0.44	2704	1.2	80.0	448.0	9.2	4.5	3.0	0.004	0.4	45	0.5	634
T-14/1 (0-5)	Topsoil	0.19	1001	0.3	60.1	25.2	0.2	2.6	1.4	0.002	0.1	22	<0.1	81
T-14/2 (0-5)	Topsoil	0.32	2052	0.5	66.5	159.8	3.6	3.5	3.2	0.002	0.2	33	0.1	258
T-14/3 (0-5)	Topsoil	0.31	2087	0.6	58.0	44.4	0.4	3.0	1.8	0.005	0.2	38	0.1	109
T-15/1 (0-5)	Topsoil	0.44	1026	0.4	46.3	78.2	1.3	3.3	3.2	<0.001	0.1	27	<0.1	130
T-15/2 (0-5)	Topsoil	0.28	1228	0.6	83.4	89.2	3.3	3.8	3.3	0.002	0.4	40	0.1	137
T-16/1 (0-5)	Topsoil	0.17	2246	0.5	89.9	59.3	1.3	5.4	3.6	0.002	0.3	56	0.1	108
T-16/2 (0-5)	Topsoil	0.46	1128	0.7	75.4	76.9	3.3	3.9	3.9	0.010	0.5	44	0.2	160
T-16/3 (0-5)	Topsoil	0.21	2342	0.4	107.4	36.6	0.8	5.0	3.0	0.002	0.2	41	<0.1	88
T-16/4 (0-5)	Topsoil	0.50	2012	0.4	99.8	81.5	0.6	1.9	0.6	0.003	0.3	38	0.1	125
T-17/1 (0-5)	Topsoil	0.17	1474	0.7	95.0	43.6	0.4	4.9	3.2	0.002	0.2	52	0.1	88
T-17/2 (0-5)	Topsoil	0.20	971	0.3	65.2	94.9	0.9	4.6	3.1	0.003	0.3	37	<0.1	123
T-17/3 (0-5)	Topsoil	0.16	1547	0.3	64.7	40.7	0.3	4.8	2.5	0.004	0.2	46	<0.1	81
T-18/1 (0-5)	Topsoil	0.14	982	0.3	94.7	36.1	0.3	4.9	3.0	0.004	0.2	47	<0.1	98
T-18/2 (0-5)	Topsoil	0.10	1490	0.7	177.1	44.8	3.0	6.3	3.4	0.003	0.6	53	0.1	165

Sample	Material	Mg	Mn	Mo	Ni	Pb	Sb	Sc	Th	Ti	Tl	V	W	Zn
T-18/4 (0-5)	Topsoil	0.12	1145	0.4	67.8	54.4	2.8	2.8	2.0	0.002	0.6	26	0.1	182
T-18/5 (0-5)	Topsoil	0.20	2567	0.6	89.9	45.6	0.9	5.0	2.2	0.004	0.4	62	<0.1	85
T-19/1 (0-5)	Topsoil	0.13	1783	0.7	164.2	38.1	1.0	9.9	2.5	0.002	1.7	63	<0.1	97
T-19/2 (0-5)	Topsoil	0.10	625	0.4	36.0	33.0	0.8	3.2	3.3	<0.001	0.1	30	<0.1	82
T-19/3 (0-5)	Topsoil	0.11	1760	0.4	161.9	44.0	1.1	5.4	2.3	0.001	0.2	41	0.1	141
T-19/5 (0-5)	Topsoil	0.24	1556	0.5	56.5	37.7	0.8	4.7	3.2	0.008	0.7	50	0.1	121
T-19/6 (0-5)	Topsoil	0.09	1007	0.3	51.4	27.8	0.2	3.4	2.6	<0.001	0.2	31	<0.1	85
T-20/1 (0-5)	Topsoil	0.17	1170	0.3	226.5	35.0	0.1	6.0	2.0	0.003	0.2	49	<0.1	85
T-20/2 (0-5)	Topsoil	0.14	1677	0.5	116.4	47.9	1.6	5.3	2.4	0.003	0.3	51	0.1	127
T-20/3 (0-5)	Topsoil	0.07	1235	0.4	46.3	35.2	0.7	2.8	2.2	<0.001	0.2	30	<0.1	85
T-20/4 (0-5)	Topsoil	0.17	1871	0.7	82.5	49.1	0.6	6.2	4.8	0.004	0.8	62	<0.1	104
T-21/1 (0-5)	Topsoil	0.42	644	0.2	135.5	33.6	0.3	3.5	1.7	0.002	0.1	17	<0.1	77
T-21/2 (0-5)	Topsoil	0.08	777	0.3	117.1	47.9	0.4	3.3	2.0	0.003	0.2	39	<0.1	87
T-21/3 (0-5)	Topsoil	0.15	560	0.3	138.2	36.7	0.3	5.3	2.2	0.007	0.1	45	<0.1	89
T-21/5 (0-5)	Topsoil	0.17	1594	0.4	70.9	51.8	2.0	5.3	2.5	0.004	0.3	61	0.1	113
T-21/6 (0-5)	Topsoil	0.09	748	0.3	79.5	40.9	0.3	4.4	1.8	0.005	0.2	45	<0.1	86
T-21/7 (0-5)	Topsoil	0.08	1104	0.3	51.8	27.3	0.3	3.2	2.0	0.002	0.1	31	<0.1	77
T-21/8 (0-5)	Topsoil	0.09	1275	0.3	36.3	27.9	0.1	2.8	2.1	0.001	0.1	32	<0.1	73
T-22/1 (0-5)	Topsoil	0.18	1466	0.7	61.6	52.0	1.6	3.2	3.3	0.005	0.2	30	<0.1	100
T-22/2 (0-5)	Topsoil	0.50	714	0.4	93.9	35.6	0.5	3.2	2.2	0.001	0.2	17	<0.1	80
T-22/3 (0-5)	Topsoil	0.19	964	0.4	131.8	43.1	0.6	4.2	2.2	0.003	0.2	35	<0.1	101
T-22/4 (0-5)	Topsoil	0.33	1037	0.4	162.0	94.8	2.3	4.8	2.4	0.003	0.1	44	0.1	248
T-22/6 (0-5)	Topsoil	0.14	964	0.4	97.1	59.5	1.2	5.2	2.8	0.002	0.2	36	<0.1	100
T-22/7 (0-5)	Topsoil	0.12	639	0.4	195.5	48.0	0.4	4.9	2.2	0.002	0.2	32	<0.1	124
T-22/8 (0-5)	Topsoil	0.12	2045	1.1	174.7	67.4	1.4	6.0	4.4	0.008	0.4	66	0.1	136
T-24/1 (0-5)	Topsoil	0.39	1247	0.7	88.5	52.9	1.4	4.1	3.4	0.003	0.2	27	<0.1	111
T-24/2 (0-5)	Topsoil	0.32	1591	0.7	103.3	69.6	2.5	4.4	2.9	0.004	0.3	35	0.1	126
T-24/4 (0-5)	Topsoil	0.31	1462	0.5	146.5	58.5	2.0	5.2	4.0	0.003	0.3	42	0.1	140
T-24/5 (0-5)	Topsoil	0.24	1251	0.4	130.3	57.8	0.6	5.1	3.1	0.002	0.3	40	0.1	139
T-24/6 (0-5)	Topsoil	0.16	1650	0.5	86.6	59.4	0.3	3.7	2.4	0.004	0.3	40	<0.1	107
T-25/1 (0-5)	Topsoil	0.47	1639	0.5	126.3	60.0	1.0	4.4	3.7	0.002	0.3	28	<0.1	143
T-26/1 (0-5)	Topsoil	0.40	1074	0.7	76.8	44.9	1.5	3.1	2.3	0.002	0.2	9	<0.1	102
T-26/2 (0-5)	Topsoil	0.29	2102	0.9	83.7	69.0	3.3	4.4	3.9	0.004	0.3	34	0.1	124
T-26/4 (0-5)	Topsoil	0.29	1756	0.6	91.2	65.0	2.1	4.7	3.5	0.004	0.3	38	0.1	123
T-26/5 (0-5)	Topsoil	0.46	971	0.4	106.5	42.3	0.8	3.1	1.8	0.001	0.2	14	<0.1	104
T-27/1 (0-5)	Topsoil	0.42	942	0.5	66.5	43.1	0.8	3.9	3.1	0.003	0.2	25	<0.1	97
T-27/2 (0-5)	Topsoil	0.58	1655	0.4	127.8	91.1	1.7	4.2	2.3	0.004	0.2	33	0.1	166
T-27/4 (0-5)	Topsoil	0.30	1381	0.7	59.5	54.9	0.9	4.0	3.3	0.006	0.2	32	<0.1	104
T-27/5 (0-5)	Topsoil	0.32	1329	0.8	60.6	50.8	1.0	4.3	4.6	0.004	0.2	36	<0.1	96
A-15/3 (0-5)	Topsoil	0.91	9900	1.0	58.6	1623.8	18.2	4.8	2.2	0.034	1.7	48	0.4	1693
A-18/3 (0-5)	Topsoil	1.05	6862	3.4	88.5	1025.3	81.1	3.6	2.4	0.031	0.8	46	2.0	1195
A-19/4 (0-5)	Topsoil	1.07	5203	1.1	113.5	732.5	25.9	4.0	1.9	0.020	0.8	33	0.4	934
A-21/4 (0-5)	Topsoil	0.94	7415	1.4	102.9	781.7	27.2	4.1	1.9	0.024	0.5	50	0.4	726
A-22/5 (0-5)	Topsoil	0.83	4984	1.1	97.7	440.3	23.0	3.6	1.8	0.014	0.3	41	0.5	491
A-23 (0-5)	Topsoil	0.91	4903	1.6	112.4	565.3	36.9	3.9	1.9	0.016	0.5	36	0.6	701
A-24/3 (0-5)	Topsoil	0.73	8605	1.0	97.2	468.1	13.1	4.4	2.0	0.026	0.5	46	0.3	496
A-25/2 (0-5)	Topsoil	0.81	5574	1.1	93.0	333.0	20.6	3.7	2.1	0.023	0.4	41	0.4	372
A-26/3 (0-5)	Topsoil	0.75	4426	0.8	101.8	446.5	16.8	3.7	1.9	0.013	0.5	32	0.3	558
A-27/3 (0-5)	Topsoil	0.87	7189	1.2	95.1	347.0	8.8	4.2	2.3	0.023	0.5	40	0.3	514
T-01/1 (20-30)	Subsoil	0.76	1496	0.2	56.7	28.9	0.1	4.4	0.8	0.066	0.2	79	<0.1	103
T-01/2 (20-30)	Subsoil	0.53	1808	0.4	60.8	64.0	0.7	3.5	1.4	0.017	0.2	60	0.1	173
T-01/3 (20-30)	Subsoil	0.36	2177	0.6	39.4	39.5	1.0	2.6	2.3	0.007	0.2	55	<0.1	80
T-02/1 (20-30)	Subsoil	0.53	1351	0.4	36.1	37.2	0.6	2.6	2.1	0.003	0.2	42	<0.1	96
T-02/2 (20-30)	Subsoil	0.64	1105	0.3	90.5	39.5	0.7	4.5	2.0	0.033	0.1	42	<0.1	77
T-02/3 (20-30)	Subsoil	0.51	1409	0.5	38.0	42.7	0.6	2.2	2.3	<0.001	0.1	34	<0.1	97
T-03/1 (20-30)	Subsoil	0.21	2587	0.4	35.0	90.7	2.6	1.0	1.1	0.003	0.2	23	<0.1	127
T-03/2 (20-30)	Subsoil	0.37	1151	0.4	39.1	168.6	2.8	1.7	2.4	0.006	0.3	27	0.1	187
T-03/3 (20-30)	Subsoil	0.28	207	0.2	24.0	60.8	0.9	0.8	1.2	0.004	0.1	17	<0.1	43
T-04/1 (20-30)	Subsoil	2.05	880	0.1	109.8	59.0	0.3	8.3	1.6	0.217	0.2	99	0.1	177
T-04/2 (20-30)	Subsoil	1.49	1333	0.5	95.9	163.1	0.8	7.0	2.1	0.127	0.8	122	0.1	261
T-04/3 (20-30)	Subsoil	2.16	1395	0.5	135.0	288.2	2.1	8.5	1.9	0.215	0.2	131	0.1	402
T-04/4 (20-30)	Subsoil	1.64	1642	0.3	82.9	66.3	0.3	5.9	1.0	0.114	0.2	77	<0.1	124
T-05/1 (20-30)	Subsoil	0.92	3107	0.8	43.3	277.4	6.2	3.3	1.8	0.016	0.2	35	0.2	508
T-05/2 (20-30)	Subsoil	0.15	1538	0.3	10.3	89.8	1.1	1.3	1.9	<0.001	0.2	21	0.1	174
T-06/1 (20-30)	Subsoil	0.58	1121	0.2	19.9	36.3	0.1	1.8	2.2	0.011	0.3	26	<0.1	87
T-06/2 (20-30)	Subsoil	0.62	1160	0.3	26.5	41.6	0.6	2.8	3.1	0.007	0.3	26	<0.1	106

Sample	Material	Mg	Mn	Mo	Ni	Pb	Sb	Sc	Th	Ti	Tl	V	W	Zn
T-06/3 (20-30)	Subsoil	0.53	1724	0.4	27.7	122.7	0.4	2.0	3.9	0.010	0.6	32	0.1	185
T-06/4 (20-30)	Subsoil	0.41	2996	0.5	72.2	268.7	1.9	3.4	3.8	0.006	0.7	36	0.1	357
T-06/5 (20-30)	Subsoil	0.78	2607	1.0	79.3	349.9	8.9	3.8	3.3	0.009	0.3	35	0.3	598
T-06/6 (20-30)	Subsoil	0.66	1234	0.5	27.3	137.1	2.5	2.3	4.6	0.001	0.3	30	0.1	235
T-06/7 (20-30)	Subsoil	0.55	1548	0.3	28.7	110.2	1.0	2.7	3.5	0.002	0.3	22	0.1	177
T-06/8 (20-30)	Subsoil	0.80	891	0.2	36.5	46.3	<0.1	4.0	2.3	0.001	0.2	26	<0.1	118
T-07/1 (20-30)	Subsoil	0.63	1107	0.3	30.5	101.5	2.1	3.5	1.4	0.002	0.2	24	0.1	185
T-07/2 (20-30)	Subsoil	0.66	1198	0.3	33.1	46.9	1.0	3.8	1.1	0.002	0.2	26	0.1	125
T-07/3 (20-30)	Subsoil	0.29	3337	0.5	28.1	267.2	2.5	4.2	4.0	0.005	1.1	29	0.1	599
T-07/4 (20-30)	Subsoil	1.52	2751	4.2	106.9	621.3	16.4	4.5	3.4	0.009	0.7	45	0.6	835
T-08/1 (20-30)	Subsoil	0.50	3561	1.0	34.9	454.5	10.0	4.0	2.7	0.004	0.7	21	0.3	695
T-08/2 (20-30)	Subsoil	0.54	2347	0.8	86.9	318.9	8.5	4.4	3.2	0.004	0.5	39	0.3	462
T-08/3 (20-30)	Subsoil	1.33	4791	2.2	204.6	879.3	19.1	5.9	2.8	0.011	0.7	66	1.2	1691
T-08/4 (20-30)	Subsoil	2.56	2427	0.4	407.3	47.2	1.0	5.9	2.1	0.036	0.2	77	0.1	123
T-08/5 (20-30)	Subsoil	3.38	1655	0.3	433.5	30.6	0.8	2.5	1.9	0.046	0.1	56	0.1	84
T-09/1 (20-30)	Subsoil	1.01	2786	2.6	272.3	749.9	18.7	4.0	2.4	0.009	0.7	54	1.8	1332
T-09/2 (20-30)	Subsoil	1.21	4946	5.3	241.3	978.4	20.6	4.1	2.2	0.029	0.9	45	3.6	2987
T-10 (20-30)	Subsoil	1.13	3301	2.2	196.9	1035.3	20.0	4.3	2.8	0.007	0.8	66	3.0	1897
T-11/1 (20-30)	Subsoil	0.51	2285	0.3	465.6	31.6	0.1	8.3	1.8	0.006	0.4	65	0.1	92
T-11/2 (20-30)	Subsoil	1.63	1925	0.4	298.7	26.6	0.5	6.3	2.1	0.003	0.2	67	<0.1	88
T-11/3 (20-30)	Subsoil	1.87	3417	0.6	260.4	251.6	4.8	9.0	3.6	0.003	1.6	72	0.1	497
T-11/4 (20-30)	Subsoil	0.62	3735	7.9	149.8	843.0	38.8	4.2	3.0	0.028	0.8	48	5.2	2034
T-11/5 (20-30)	Subsoil	1.69	1562	0.8	290.3	344.8	9.0	5.1	2.8	0.002	0.3	55	0.5	491
T-11/6 (20-30)	Subsoil	1.37	1354	0.4	240.1	50.8	1.3	4.8	2.9	0.004	0.4	59	<0.1	128
T-11/7 (20-30)	Subsoil	1.52	1477	0.4	257.9	43.0	0.3	7.0	2.6	0.002	0.2	57	<0.1	117
T-12/1 (20-30)	Subsoil	4.06	2511	0.4	487.5	86.3	1.8	4.4	3.4	0.002	0.2	42	0.1	148
T-12/2 (20-30)	Subsoil	0.55	2469	0.8	105.8	435.2	10.0	4.6	3.3	0.002	0.5	32	0.4	579
T-12/3 (20-30)	Subsoil	0.46	1957	0.5	347.0	77.3	1.8	4.7	3.7	0.004	0.3	40	0.1	144
T-12/4 (20-30)	Subsoil	3.47	855	0.3	439.4	29.9	0.8	6.6	2.7	0.004	0.1	78	<0.1	83
T-13/1 (20-30)	Subsoil	0.21	1697	0.4	44.9	30.1	0.2	3.3	2.5	0.002	0.2	41	<0.1	78
T-13/2 (20-30)	Subsoil	0.44	2578	0.8	80.8	436.9	10.0	4.9	3.6	0.003	0.4	48	0.3	469
T-14/1 (20-30)	Subsoil	0.21	1730	0.3	102.1	26.7	<0.1	4.4	2.5	0.002	0.2	35	<0.1	85
T-14/2 (20-30)	Subsoil	0.30	2315	0.6	79.6	153.6	3.3	4.6	3.8	0.003	0.2	37	0.1	220
T-14/3 (20-30)	Subsoil	0.32	2702	0.6	64.3	45.2	0.3	3.8	2.7	0.003	0.3	45	<0.1	108
T-15/1 (20-30)	Subsoil	0.43	1032	0.4	49.4	62.9	1.1	3.3	3.6	0.001	0.1	25	<0.1	106
T-15/2 (20-30)	Subsoil	0.26	1218	0.5	90.9	90.6	4.1	3.6	3.9	0.002	0.5	40	0.1	117
T-16/1 (20-30)	Subsoil	0.17	2520	0.4	111.1	52.2	1.4	7.1	4.8	0.003	0.3	72	0.1	102
T-16/2 (20-30)	Subsoil	0.42	1017	0.6	74.2	74.5	3.0	3.8	4.0	0.008	0.5	40	0.1	153
T-16/3 (20-30)	Subsoil	0.21	2906	0.4	143.3	38.0	0.9	6.5	3.8	0.001	0.2	42	<0.1	82
T-16/4 (20-30)	Subsoil	0.73	2224	0.2	150.4	75.5	<0.1	2.8	0.5	0.003	0.4	49	0.1	107
T-17/1 (20-30)	Subsoil	0.17	1530	0.7	108.1	40.0	0.2	6.1	4.2	0.004	0.2	59	<0.1	89
T-17/2 (20-30)	Subsoil	0.25	922	0.2	78.8	78.3	0.2	6.1	4.4	0.004	0.3	54	<0.1	101
T-17/3 (20-30)	Subsoil	0.18	1484	0.4	75.5	29.7	0.1	6.4	4.1	0.002	0.3	55	<0.1	65
T-18/1 (20-30)	Subsoil	0.13	1134	0.2	106.8	32.9	0.2	6.0	4.7	0.002	0.3	49	<0.1	91
T-18/2 (20-30)	Subsoil	0.09	1352	1.1	234.4	37.0	4.6	7.4	4.0	0.001	0.8	58	0.1	182
T-18/4 (20-30)	Subsoil	0.13	1290	0.4	73.3	71.2	3.2	3.2	2.4	0.003	0.7	31	0.1	185
T-18/5 (20-30)	Subsoil	0.21	2898	0.7	105.3	44.4	0.8	5.8	2.7	0.004	0.4	63	<0.1	76
T-19/1 (20-30)	Subsoil	0.13	1870	0.7	187.2	32.9	0.7	11.1	2.9	0.005	2.3	80	<0.1	92
T-19/2 (20-30)	Subsoil	0.09	1241	0.4	44.9	32.8	0.7	3.8	4.5	<0.001	0.2	36	<0.1	73
T-19/3 (20-30)	Subsoil	0.10	1715	0.5	168.5	40.3	0.9	5.7	2.4	0.001	0.1	41	<0.1	126
T-19/5 (20-30)	Subsoil	0.27	1735	0.5	66.7	37.9	0.6	6.3	4.9	0.008	0.9	61	<0.1	125
T-19/6 (20-30)	Subsoil	0.07	1264	0.3	60.5	25.5	0.3	4.3	4.1	0.002	0.2	33	<0.1	75
T-20/1 (20-30)	Subsoil	0.14	1175	0.3	221.4	35.0	0.3	6.5	3.1	0.003	0.3	45	<0.1	75
T-20/2 (20-30)	Subsoil	0.13	1651	0.4	119.9	43.3	1.3	5.6	2.7	0.003	0.2	53	0.1	112
T-20/3 (20-30)	Subsoil	0.07	1546	0.5	55.1	31.4	0.6	3.8	3.2	<0.001	0.2	38	<0.1	75
T-20/4 (20-30)	Subsoil	0.17	2091	0.7	103.4	53.6	0.2	7.2	5.3	0.006	1.0	79	<0.1	115
T-21/1 (20-30)	Subsoil	0.36	893	0.2	170.9	36.5	0.1	4.9	2.4	0.003	0.1	32	<0.1	75
T-21/2 (20-30)	Subsoil	0.07	743	0.4	140.3	43.6	0.2	4.3	3.6	0.003	0.2	41	<0.1	85
T-21/3 (20-30)	Subsoil	0.14	691	0.2	149.1	34.5	0.2	6.0	2.9	0.004	0.1	43	<0.1	80
T-21/5 (20-30)	Subsoil	0.16	1587	0.4	71.3	46.2	1.6	5.5	3.0	0.005	0.3	64	0.1	99
T-21/6 (20-30)	Subsoil	0.07	794	0.3	82.7	39.9	0.3	5.9	4.4	0.003	0.2	41	<0.1	70
T-21/7 (20-30)	Subsoil	0.08	1319	0.3	77.5	25.6	<0.1	4.4	2.9	0.003	0.2	45	<0.1	73
T-21/8 (20-30)	Subsoil	0.07	1735	0.3	40.5	28.5	<0.1	3.4	3.0	<0.001	0.2	34	<0.1	71
T-22/1 (20-30)	Subsoil	0.17	1642	0.7	70.3	57.7	1.2	4.1	6.3	0.005	0.2	33	<0.1	96
T-22/2 (20-30)	Subsoil	0.48	793	0.4	106.3	34.6	0.6	3.5	2.8	<0.001	0.2	<2	<0.1	79
T-22/3 (20-30)	Subsoil	0.18	1193	0.4	158.0	46.9	0.5	5.5	3.4	0.003	0.2	39	<0.1	105

Sample	Material	Mg	Mn	Mo	Ni	Pb	Sb	Sc	Th	Ti	Tl	V	W	Zn
T-22/4 (20-30)	Subsoil	0.28	1225	0.5	179.5	81.0	1.9	5.4	2.5	0.003	0.1	41	0.1	173
T-22/6 (20-30)	Subsoil	0.13	1189	0.4	123.7	59.6	1.1	6.3	3.6	0.004	0.2	47	<0.1	113
T-22/7 (20-30)	Subsoil	0.10	771	0.3	217.6	53.1	0.3	4.8	2.3	0.003	0.2	34	<0.1	121
T-22/8 (20-30)	Subsoil	0.12	2288	1.2	232.5	67.2	0.8	9.2	6.6	0.007	0.4	89	<0.1	147
T-24/1 (20-30)	Subsoil	0.39	1248	0.6	84.1	46.6	1.0	4.1	3.8	0.003	0.2	26	<0.1	91
T-24/2 (20-30)	Subsoil	0.32	1562	0.7	104.5	71.6	2.5	4.6	3.5	0.005	0.3	38	<0.1	126
T-24/4 (20-30)	Subsoil	0.31	1762	0.6	177.0	65.1	2.2	6.4	5.0	0.003	0.3	51	0.1	138
T-24/5 (20-30)	Subsoil	0.26	1472	0.5	160.2	62.4	0.4	6.0	3.7	0.004	0.4	49	0.1	143
T-24/6 (20-30)	Subsoil	0.14	1775	0.7	94.6	60.1	0.7	4.6	4.5	0.005	0.2	40	<0.1	108
T-25/1 (20-30)	Subsoil	0.48	1950	0.5	138.7	64.8	0.9	5.3	4.3	0.004	0.3	38	<0.1	146
T-26/1 (20-30)	Subsoil	0.46	1004	0.6	74.9	36.3	1.0	3.6	2.8	0.002	0.2	21	<0.1	79
T-26/2 (20-30)	Subsoil	0.31	2236	1.0	86.8	75.3	3.6	5.0	4.3	0.005	0.3	38	0.1	124
T-26/4 (20-30)	Subsoil	0.27	1968	0.7	99.2	75.9	2.3	5.2	4.6	0.004	0.3	39	0.1	116
T-26/5 (20-30)	Subsoil	0.51	981	0.3	115.7	33.7	0.6	3.5	2.0	0.002	0.2	21	<0.1	83
T-27/1 (20-30)	Subsoil	0.38	901	0.4	59.9	34.4	0.9	3.3	3.3	0.003	0.2	20	<0.1	82
T-27/2 (20-30)	Subsoil	0.60	1506	0.3	125.4	86.6	1.0	4.3	2.2	0.005	0.3	37	0.1	152
T-27/4 (20-30)	Subsoil	0.36	1832	0.6	75.8	61.5	0.3	4.9	4.1	0.006	0.3	39	<0.1	116
T-27/5 (20-30)	Subsoil	0.31	1589	0.8	61.6	58.5	0.7	4.1	4.6	0.005	0.2	34	<0.1	101
A-15/3 (20-30)	Subsoil	1.01	10000	1.0	69.0	1736.6	15.7	5.1	2.8	0.038	1.9	50	0.6	1782
A-18/3 (20-30)	Subsoil	1.00	6573	2.2	62.7	1371.6	88.2	3.1	2.2	0.023	0.7	58	1.3	1469
A-19/4 (20-30)	Subsoil	1.05	8227	1.1	89.7	936.5	28.1	4.9	2.8	0.033	0.9	37	0.4	1168
A-21/4 (20-30)	Subsoil	0.93	9121	1.3	99.6	828.2	31.1	4.4	2.2	0.026	0.5	51	0.2	765
A-22/5 (20-30)	Subsoil	0.84	5673	0.9	103.8	396.2	22.6	3.7	2.0	0.013	0.4	46	0.3	404
A-23 (20-30)	Subsoil	0.95	6093	2.5	95.7	822.8	60.4	3.9	2.4	0.025	0.6	43	1.2	923
A-24/3 (20-30)	Subsoil	0.69	8075	0.9	84.9	446.7	11.8	3.8	2.3	0.024	0.6	36	0.2	448
A-25/2 (20-30)	Subsoil	0.89	6669	1.1	95.5	411.0	23.4	4.0	2.2	0.021	0.5	39	0.3	464
A-26/3 (20-30)	Subsoil	0.78	4874	0.8	109.3	500.3	12.4	4.2	2.4	0.016	0.5	42	0.2	495
A-27/3 (20-30)	Subsoil	0.82	6478	1.7	87.3	518.0	21.6	4.6	3.1	0.023	0.7	29	0.4	797
S-01	S. Sediment	0.70	1361	0.9	66.5	71.7	2.5	2.5	1.9	0.037	0.1	39	0.1	194
S-02	S. Sediment	0.87	1113	0.3	69.0	46.2	1.0	3.7	2.1	0.087	0.1	49	0.1	151
S-03	S. Sediment	0.76	1094	0.3	61.7	61.3	1.3	2.9	2.2	0.020	0.1	26	0.1	118
S-04	S. Sediment	0.76	1059	0.2	53.0	91.7	1.9	2.7	2.0	0.035	0.1	29	0.1	134
S-06	S. Sediment	0.69	1010	0.4	49.4	121.2	2.6	2.4	1.8	0.037	0.1	26	0.1	125
S-07	S. Sediment	1.06	1348	0.5	53.0	157.7	5.7	3.4	1.8	0.066	0.1	37	0.1	172
S-09	S. Sediment	1.06	1784	0.7	48.8	342.6	21.4	3.6	1.9	0.068	0.3	37	0.1	228
S-11	S. Sediment	1.17	2472	1.4	60.2	571.7	38.9	3.9	1.9	0.063	0.3	42	0.3	383
S-13	S. Sediment	1.48	2105	1.1	125.5	395.1	20.5	4.0	1.8	0.058	0.3	44	0.3	293
S-15	S. Sediment	1.19	1399	0.8	88.2	219.7	11.3	3.0	2.1	0.030	0.2	35	0.3	240
S-17	S. Sediment	1.23	2117	1.1	116.5	245.4	18.5	3.2	1.9	0.032	0.2	40	0.5	274
S-18	S. Sediment	1.10	2153	1.3	92.2	252.3	17.7	3.1	1.9	0.033	0.2	35	0.7	285
S-20	S. Sediment	1.10	3342	1.6	94.6	421.2	28.6	3.1	1.9	0.029	0.3	49	0.7	389
S-22	S. Sediment	1.16	3474	1.2	87.2	455.7	30.4	3.5	1.7	0.017	0.3	40	0.4	467
S-23	S. Sediment	1.00	2348	1.0	84.9	191.6	13.8	3.1	2.0	0.026	0.2	30	0.4	282
S-26	S. Sediment	0.81	1499	0.6	87.2	157.2	9.2	2.7	1.1	0.014	0.2	38	0.3	264
S-27	S. Sediment	0.82	2398	1.0	78.4	291.3	15.5	2.8	1.5	0.012	0.2	30	0.3	393
P-01/2	Attic Dust	0.48	1478	1.6	43.1	260.4	12.7	1.6	0.2	0.022	0.3	36	0.7	606
P-02/1	Attic Dust	0.58	1212	3.8	83.1	142.6	11.6	1.9	0.7	0.020	0.1	27	0.6	274
P-02/3	Attic Dust	0.56	1087	1.3	38.2	230.3	9.7	0.9	0.2	0.006	0.2	23	1.1	543
P-05/1	Attic Dust	0.81	1646	2.6	42.9	516.3	28.1	2.2	1.0	0.020	0.5	29	1.5	795
P-06/5	Attic Dust	0.99	2106	2.8	70.4	776.9	32.2	2.7	0.9	0.023	0.6	41	1.7	989
P-08/4	Attic Dust	0.80	1527	2.8	65.5	482.9	19.5	1.3	0.2	0.009	0.3	36	1.3	1055
P-09/2	Attic Dust	0.52	4793	11.3	134.1	2130.1	53.7	2.9	1.8	0.036	1.1	52	9.7	5286
P-10	Attic Dust	0.54	6242	16.9	117.2	2767.7	67.9	2.6	1.7	0.032	2.5	47	15.5	7124
P-11/4	Attic Dust	0.68	6033	13.5	148.2	2596.0	78.9	3.1	1.4	0.031	1.7	64	10.3	5434
P-15/2	Attic Dust	0.45	1862	3.4	65.9	1144.5	35.8	2.2	1.2	0.014	0.9	44	2.9	1160
P-16/1	Attic Dust	0.61	913	3.9	61.8	381.8	18.8	2.0	1.0	0.013	0.3	41	2.4	496
P-19/2	Attic Dust	0.62	1091	1.4	60.0	184.7	9.2	2.8	1.1	0.015	0.3	42	0.9	413
P-19/3	Attic Dust	0.75	822	4.0	83.7	303.3	16.5	1.6	0.4	0.014	0.4	47	1.9	699
P-20/3	Attic Dust	0.42	587	1.3	36.1	161.8	4.3	1.2	0.4	0.006	0.8	20	0.6	656
P-22/4	Attic Dust	0.68	907	2.1	135.5	228.0	8.8	2.7	1.1	0.017	0.4	42	1.4	1445

Appendix E: Estimates values of standard materials (E) and their analyzing values (accuracy estimation);Values of Al, Fe, Mg and Ti are in %, remaining elements in mg/kg

Sample	Ag	Al	As	Ba	Bi	Cd	Co	Cr	Cu	Fe	Ga	Hg	La
DS7 (E)	**0.9**	**0.96**	**48.2**	**370**	**4.5**	**6.4**	**9.7**	**179**	**109.0**	**2.39**	**5.0**	**0.20**	**12**
DS7	0.9	1.00	50.3	410	4.5	6.0	9.5	221	108.5	2.41	5.0	0.18	13
DS7	0.7	0.99	50.8	382	4.6	5.4	9.0	195	103.0	2.27	5.0	0.17	13
DS7	0.8	0.95	48.5	390	4.7	5.9	8.6	185	102.3	2.26	5.0	0.19	13
DS7	0.8	0.99	52.3	403	4.5	6.2	9.2	199	97.8	2.32	4.0	0.18	12
DS7	0.8	1.00	52.6	400	5.0	6.4	9.8	193	105.5	2.37	5.0	0.18	13
DS7	0.9	1.09	54.2	427	4.4	6.5	10.4	240	121.9	2.52	5.0	0.18	13
DS7	0.7	1.03	52.0	407	4.7	6.4	9.9	173	116.3	2.42	5.0	0.19	13
OREAS45PA (E)	**0.3**	**3.34**	**4.2**	**187**	**0.2**	**0.1**	**104.0**	**873**	**600.0**	**16.56**	**16.8**	**0.03**	**16**
OREAS45PA	0.3	3.43	4.3	182	0.2	<0.1	106.3	786	615.9	16.04	16.0	0.03	15
OREAS45PA	0.2	3.27	4.6	184	0.2	<0.1	108.0	799	598.9	16.13	16.0	0.02	16
OREAS45PA	0.2	2.99	4.3	178	0.2	0.1	99.3	764	546.7	15.42	15.0	0.03	15
OREAS45PA	0.2	2.84	4.0	279	0.2	0.1	101.8	781	557.5	16.39	17.0	0.03	16
OREAS45PA	0.2	2.94	4.0	176	0.2	0.1	107.5	767	572.1	16.57	16.0	0.02	15
OREAS45PA	0.3	3.27	4.8	179	0.2	0.1	110.2	771	559.2	16.53	16.0	0.02	15
OREAS45PA	0.2	3.16	4.5	183	0.2	<0.1	106.5	741	534.4	15.99	16.0	0.02	15
DS8 (E)	**1.7**	**0.93**	**26.0**	**279**	**6.7**	**2.4**	**7.5**	**115**	**110.0**	**2.46**	**4.7**	**0.19**	**15**
DS8	1.8	1.00	25.5	305	6.7	2.3	7.7	118	112.2	2.55	5.0	0.21	18
DS8	1.6	0.90	25.1	293	6.4	2.6	7.5	120	110.4	2.44	4.0	0.18	13
DS8	1.9	0.95	25.4	292	6.1	2.3	7.5	118	109.0	2.59	5.0	0.20	14
DS8	1.7	0.97	25.6	303	6.7	2.4	7.7	126	110.7	2.57	5.0	0.19	16
DS8	2.0	0.92	24.6	285	6.6	2.4	7.8	117	115.6	2.38	5.0	0.18	16
OREAS45CA (E)	**0.3**	**3.59**	**3.8**	**164**	**0.2**	**0.1**	**92.0**	**709**	**494.0**	**15.69**	**18.4**	**0.03**	**16**
OREAS45CA	0.2	3.93	3.5	165	0.2	<0.1	88.6	640	510.7	16.49	19.0	0.04	17
OREAS45CA	0.3	3.45	3.8	159	0.2	<0.1	87.2	687	484.5	15.83	18.0	0.02	16
OREAS45CA	0.3	3.52	4.0	155	0.2	<0.1	84.7	695	481.7	16.25	17.0	0.03	16
OREAS45CA	0.3	3.89	4.1	163	0.2	<0.1	86.3	724	490.6	16.48	18.0	0.04	16
OREAS45CA	0.2	3.74	3.5	153	0.2	0.1	85.5	710	493.4	15.80	19.0	0.04	16

Sample	Mg	Mn	Mo	Ni	Pb	Sb	Sc	Th	Ti	Tl	V	W	Zn
DS7 (E)	**1.05**	**627**	**20.5**	**56.0**	**70.6**	**4.6**	**2.5**	**4.4**	**0.124**	**4.2**	**84**	**3.4**	**411**
DS7	1.00	638	20.0	56.8	64.3	5.8	2.5	4.1	0.134	4.0	80	3.6	377
DS7	1.01	581	20.2	55.5	70.6	6.2	2.2	4.4	0.120	4.0	75	3.5	397
DS7	0.97	579	20.3	52.5	75.4	6.3	2.1	4.9	0.116	4.1	78	3.5	389
DS7	0.98	619	20.6	52.2	62.2	6.1	2.3	4.5	0.121	4.1	79	3.5	375
DS7	1.02	572	20.6	58.0	76.8	6.6	2.2	5.1	0.121	4.6	78	3.3	402
DS7	1.07	646	21.9	63.5	67.7	6.0	2.5	4.5	0.140	4.3	91	3.8	422
DS7	0.98	632	22.3	58.4	65.8	5.7	2.4	4.5	0.139	4.2	87	3.7	383
OREAS45PA (E)	**0.10**	**1130**	**0.9**	**281.0**	**19.0**	**0.1**	**43.0**	**6.0**	**0.124**	**0.1**	**221**	-	**119**
OREAS45PA	0.11	1077	1.2	288.7	18.0	<0.1	43.3	6.0	0.146	<0.1	204	<0.1	121
OREAS45PA	0.10	1074	1.2	280.7	19.3	0.1	39.9	6.5	0.143	<0.1	207	<0.1	123
OREAS45PA	0.09	1060	1.3	270.6	16.7	<0.1	38.3	5.7	0.124	<0.1	193	<0.1	111
OREAS45PA	0.09	1070	1.4	267.9	19.1	<0.1	40.9	6.5	0.131	<0.1	202	<0.1	116
OREAS45PA	0.10	1038	1.4	288.9	18.9	<0.1	41.8	6.4	0.124	<0.1	194	<0.1	114
OREAS45PA	0.11	1078	1.4	296.9	17.2	0.1	40.7	6.0	0.144	<0.1	218	<0.1	115
OREAS45PA	0.10	1057	1.4	287.8	17.6	0.1	38.9	6.1	0.153	<0.1	210	<0.1	110
DS8 (E)	**0.60**	**615**	**13.4**	**38.1**	**123.0**	**4.8**	**2.3**	**6.9**	**0.113**	**5.4**	**41**	**3.0**	**312**
DS8	0.68	622	13.8	36.0	126.3	5.2	2.3	7.2	0.126	5.6	43	3.0	321
DS8	0.62	617	13.6	38.3	120.5	4.8	1.9	6.3	0.108	5.3	43	2.6	308
DS8	0.63	638	14.1	36.9	129.2	5.5	2.1	6.1	0.118	5.6	42	2.8	323
DS8	0.64	627	13.4	39.8	124.2	4.7	2.2	6.6	0.115	5.5	45	2.4	322
DS8	0.62	596	14.0	37.7	119.1	4.9	2.3	6.7	0.111	5.3	44	2.3	313
OREAS45CA (E)	**0.14**	**943**	**1.0**	**240.0**	**20.0**	**0.1**	**39.7**	**7.0**	**0.128**	**0.1**	**215**	-	**60**
OREAS45CA	0.16	896	0.8	247.6	19.8	<0.1	36.2	7.0	0.145	<0.1	198	<0.1	66
OREAS45CA	0.13	875	0.9	228.7	20.3	0.1	34.0	6.8	0.113	<0.1	198	<0.1	60
OREAS45CA	0.13	935	0.9	227.3	20.8	<0.1	35.6	6.9	0.133	<0.1	196	<0.1	60
OREAS45CA	0.14	904	0.7	246.7	20.9	<0.1	35.5	7.0	0.118	<0.1	198	<0.1	61
OREAS45CA	0.13	899	0.9	232.1	19.9	<0.1	37.7	6.7	0.104	<0.1	191	<0.1	60

Appendix F: Results of the analysis of duplicate samples (precision estimation);Values of Al, Fe, Mg and Ti are in %, remaining elements in mg/kg

Sample	Ag	Al	As	Ba	Bi	Cd	Co	Cr	Cu	Fe	Ga	Hg	La
T-01/3 (20-30)	0.1	2.11	12.5	101	0.3	0.2	21.0	44	28.9	3.56	6.0	0.09	7
T-01/3 (20-30) - R	0.1	2.07	13.0	104	0.3	0.2	20.7	44	28.6	3.51	6.0	0.09	7
T-02/3 (0-5)	<0.1	1.64	11.7	157	0.4	0.4	12.2	28	21.5	2.54	5.0	0.08	2
T-02/3 (0-5) - R	<0.1	1.77	12.7	168	0.4	0.4	13.0	30	23.6	2.81	5.0	0.09	3
T-04/4 (0-5)	0.1	2.30	5.0	207	0.3	0.6	21.8	52	19.5	3.67	6.0	0.09	9
T-04/4 (0-5) - R	0.1	2.43	5.0	206	0.2	0.6	21.0	53	18.8	3.59	6.0	0.09	9
T-06/6 (20-30)	0.4	2.35	12.5	239	0.6	0.3	13.9	29	25.2	3.05	7.0	0.13	26
T-06/6 (20-30) - R	0.4	2.28	12.0	246	0.6	0.3	13.6	28	22.8	3.07	6.0	0.13	26
T-07/3 (0-5)	1.1	1.53	46.6	1197	0.6	2.1	15.0	26	34.1	3.45	5.0	0.17	10
T-07/3 (0-5) - R	1.1	1.43	45.5	1109	0.6	2.1	14.7	25	33.6	3.43	5.0	0.17	9
T-11/6 (20-30)	0.1	2.14	29.8	149	0.3	0.5	33.8	214	33.0	3.54	6.0	0.08	14
T-11/6 (20-30) - R	0.1	2.14	30.6	154	0.3	0.6	33.5	216	33.1	3.48	6.0	0.07	15
T-16/1 (0-5)	0.1	1.71	30.1	139	0.5	0.9	20.8	59	67.6	3.10	6.0	0.11	20
T-16/1 (0-5) - R	0.1	1.64	29.0	131	0.4	0.9	20.7	53	66.4	2.99	6.0	0.08	19
T-16/2 (20-30)	0.1	2.24	79.2	207	0.5	0.8	16.9	49	35.5	2.84	6.0	0.11	23
T-16/2 (20-30) - R	0.2	2.32	77.6	210	0.5	1.0	17.3	54	35.7	3.14	6.0	0.09	23
T-17/1 (0-5)	0.1	1.62	37.9	100	0.4	0.4	25.3	69	42.7	3.19	5.0	0.06	21
T-17/1 (0-5) - R	<0.1	1.58	38.0	98	0.4	0.4	24.0	71	40.6	3.20	5.0	0.07	21
T-25/1 (0-5)	0.1	2.18	39.8	262	0.5	0.6	23.8	64	45.2	3.34	7.0	0.11	14
T-25/1 (0-5) - R	0.2	2.20	40.4	276	0.5	0.6	22.9	61	40.6	3.39	6.0	0.12	15
A-22/5 (0-5)	2.3	1.29	38.3	835	0.8	1.2	16.5	80	89.0	3.67	3.0	0.99	9
A-22/5 (0-5) - R	2.3	1.17	37.7	858	0.9	1.2	16.1	77	88.3	3.81	2.0	1.08	9
A-23 (20-30)	5.3	1.39	49.3	1302	1.3	2.5	16.8	81	161.8	4.74	3.0	1.94	13
A-23 (20-30) - R	4.8	1.39	46.8	1240	1.4	2.6	14.8	77	157.6	4.59	2.0	1.92	12
A-27/3 (20-30)	4.7	1.50	41.3	263	1.5	1.8	14.8	68	129.1	4.30	3.0	1.53	13
A-27/3 (20-30) - R	4.8	1.53	41.4	483	1.3	1.8	14.6	64	120.1	4.41	2.0	1.36	15
S-18	1.4	1.05	17.8	827	0.4	0.7	13.8	85	81.6	3.40	3.0	0.75	6
S-18 - R	1.3	1.07	18.3	819	0.4	0.8	13.8	83	80.3	3.45	3.0	0.71	6
P-11/4	7.4	1.29	92.9	69	10.1	7.6	27.8	126	261.2	15.63	5.0	1.50	9
P-11/4 - R	7.4	1.22	78.1	50	10.2	7.1	25.9	123	262.0	15.00	5.0	1.54	10

Sample	Mg	Mn	Mo	Ni	Pb	Sb	Sc	Th	Ti	Tl	V	W	Zn
T-01/3 (20-30)	0.36	2177	0.6	39.4	39.5	1.0	2.6	2.3	0.007	0.2	55	<0.1	80
T-01/3 (20-30) - R	0.36	2163	0.6	37.8	38.4	0.8	2.6	2.4	0.007	0.2	57	<0.1	84
T-02/3 (0-5)	0.41	1505	0.5	29.2	48.0	0.8	1.7	1.6	<0.001	0.1	25	<0.1	151
T-02/3 (0-5) - R	0.43	1660	0.6	32.7	52.6	0.7	1.7	1.6	<0.001	0.1	31	<0.1	170
T-04/4 (0-5)	1.29	1455	0.3	71.7	69.2	0.6	4.1	0.5	0.086	0.2	63	<0.1	131
T-04/4 (0-5) - R	1.27	1422	0.2	71.4	67.5	0.5	4.4	0.5	0.092	0.1	61	<0.1	132
T-06/6 (20-30)	0.66	1234	0.5	27.3	137.1	2.5	2.3	4.6	0.001	0.3	30	0.1	235
T-06/6 (20-30) - R	0.66	1201	0.5	25.8	141.0	2.1	2.2	4.8	0.001	0.2	30	0.1	216
T-07/3 (0-5)	0.38	3253	1.1	28.6	313.0	3.1	3.6	2.4	0.004	1.0	32	0.1	662
T-07/3 (0-5) - R	0.37	3275	0.9	28.3	308.0	3.0	3.3	2.0	0.003	1.0	29	0.1	663
T-11/6 (20-30)	1.37	1354	0.4	240.1	50.8	1.3	4.8	2.9	0.004	0.4	59	<0.1	128
T-11/6 (20-30) - R	1.38	1369	0.3	241.2	51.9	1.2	4.8	3.0	0.004	0.4	59	<0.1	130
T-16/1 (0-5)	0.17	2246	0.5	89.9	59.3	1.3	5.4	3.6	0.002	0.3	56	0.1	108
T-16/1 (0-5) - R	0.17	2070	0.4	92.6	57.3	1.2	5.4	3.3	0.002	0.3	52	0.1	105
T-16/2 (20-30)	0.42	1017	0.6	74.2	74.5	3.0	3.8	4.0	0.008	0.5	40	0.1	153
T-16/2 (20-30) - R	0.43	1133	0.6	73.3	75.2	3.0	4.0	4.2	0.009	0.5	45	0.1	155
T-17/1 (0-5)	0.17	1474	0.7	95.0	43.6	0.4	4.9	3.2	0.002	0.2	52	0.1	88
T-17/1 (0-5) - R	0.18	1556	0.6	96.5	42.7	0.4	5.2	3.3	0.003	0.2	55	<0.1	90
T-25/1 (0-5)	0.47	1639	0.5	126.3	60.0	1.0	4.4	3.7	0.002	0.3	28	<0.1	143
T-25/1 (0-5) - R	0.45	1624	0.6	121.6	62.4	1.0	4.4	3.6	0.004	0.3	33	<0.1	139
A-22/5 (0-5)	0.83	4984	1.1	97.7	440.3	23.0	3.6	1.8	0.014	0.3	41	0.5	491
A-22/5 (0-5) - R	0.85	5049	1.2	101.5	420.5	23.2	3.6	1.8	0.015	0.3	44	0.4	486
A-23 (20-30)	0.95	6093	2.5	95.7	822.8	60.4	3.9	2.4	0.025	0.6	43	1.2	923
A-23 (20-30) - R	0.89	5855	2.6	92.7	793.2	53.8	3.9	2.5	0.024	0.5	38	1.2	936
A-27/3 (20-30)	0.82	6478	1.7	87.3	518.0	21.6	4.6	3.1	0.023	0.7	29	0.4	797
A-27/3 (20-30) - R	0.84	6630	2.0	85.1	541.7	23.0	4.6	3.0	0.029	0.5	35	0.8	763
S-18	1.10	2153	1.3	92.2	252.3	17.7	3.1	1.9	0.033	0.2	35	0.7	285
S-18 - R	1.12	2104	1.1	96.1	266.4	18.4	3.1	1.8	0.032	0.2	33	0.6	292
P-11/4	0.68	6033	13.5	148.2	2596.0	78.9	3.1	1.4	0.031	1.7	64	10.3	5434
P-11/4 - R	0.62	5655	12.8	135.7	2656.5	81.0	3.1	1.5	0.029	1.8	57	10.5	4841